SURVIVAL PATHWAYS SUPPORTING BRCA1 FUNCTION

By Elizabeth Jennifer Anthony

A thesis submitted to the University of Birmingham for the degree of

DOCTOR OF PHILOSOPHY

Institute of Cancer and Genomic Sciences

College of Medical and Dental Sciences

University of Birmingham

January 2024

Abstract

The Breast cancer susceptibility protein 1 (BRCA1) is a tumour suppressor protein that functions in the DNA damage response and in replication. In DNA double-strand break repair BRCA1 functions within the pathway homologous recombination, mainly in the regulation of DNA resection. Its roles in replication, including the protection of stalled replication forks and the suppression of single-stranded DNA (ssDNA) post-replicative gaps, are poorly understood. BRCA1 forms a heterodimeric complex with BRCA1 associated RING domain 1 (BARD1), forming an active E3 ubiquitin ligase, the cellular roles of which remain controversial. A method of further understanding the functional role(s) of BRCA1 is to investigate the pathways supporting cell survival when some of those functions are disabled.

A synthetic lethal interaction between DNA polymerase θ (Polθ) loss in BRCA1-mutated cells has been identified, yet the mechanisms underlying this relationship remain to be fully elucidated. In this thesis, we have determined that BRCA-RAD51 interactions suppress cell sensitivity to Polθ loss using *Brca1*$^{C61G/C61G}$ *53bp1*$^{-/-}$ mouse embryonic fibroblasts (MEFs) as our *Brca1*-mutated model. In addition, we find that RAD52 underlies the synthetic lethal relationship between *Brca1/53bp1* deficiencies and Polθ depletion. We identified that Polθ limits RAD52-mediated suppression of ssDNA gap fill-in during G2/M.

We also investigated a potential ligase-defective murine allele, *Bard1*$^{R93E/R93E}$. *Bard1*$^{R93E/R93E}$ cells are proficient in homologous recombination yet form ssDNA gaps behind replication forks. We found that the *Bard1*$^{R93E/R93E}$ cells exhibited sensitivity to the loss of ubiquitin-specific protease 1 (USP1). These *Bard1*-mutant cells have

provided preliminary findings surrounding the role of USP1 in DNA damage tolerance (DDT) mechanisms in our cells. Overall, the findings in this thesis increase our understanding of survival pathways supporting BRCA1 function.

Acknowledgements

I would first like to express my sincere gratitude to my supervisor Jo Morris for all of her support, guidance and advice to help me improve as a scientist over the past three years. I would also like to thank my APR supervisors Aga Gambus and Andrew Turnell for their assistance throughout the process. I would like to thank the MIBTP and BBSRC for funding my PhD and for helping me become a well-rounded student. I would also like to thank the “C61G club” George, Kas and Liza for helping me learn and be inspired by their postdoc wisdom whilst working on the paper and on my project.

I would like to give a massive thank you to everyone in the Morris group. A very special thank you goes to Ruth for all her support in the lab but also as an amazing listening ear when I needed it. I couldn’t have gotten through my PhD without a special mention to these amazing humans at Birmingham and Warwick who I have spent so much time with, inside and outside of the lab: Yara, Katie, Lanz, Lauren, Matt M, Rosie, Ciara, Matt S, Izzy and Nicole. Especially Yara and Katie who have been my absolute rocks, my fellow slugs who I am so grateful for.

Outside of the lab I would like to thank Lydia for being there for me especially when I first started at Birmingham. I couldn’t have done it without my best friend Sim, who has been there for me since we were 18 in Jack Martin, helping each other through the lows and highs of our PhDs. Shopping and cocktail nights always helped us get

through. I am also eternally grateful for my best friend Phoebe, who has helped me more than she knows this past year: DnB, Guinness, raccoons and all, especially with the final few months of the thesis living with you. I would also like to thank my girls Amelia and Megan, “the Elite” my travel buddies who have helped me not only through my PhD but for the many years leading up to it. They have supported me from the beginning and I am so grateful.

And a special thank you to my boyfriend Richard who has been my biggest supporter from helping me revising for my exams back in first year to reading my thesis, I could not have done it without his love and support. Finally, I would like to especially thank my family, my parents Julia and Stuart, and brother Harry who have listened to and read all my work even if they don’t know much about it. Their continuous love and support especially through the tough times has been invaluable. I honestly couldn’t have gotten through it without my mum/therapist who has helped me more than she realises.

Table of Contents

List of Tables

List of Figures

Abbreviations

[6-4] PPs	(6-4) pyrimidine-pyrimidone photoproducts
5-hmC	5-hydroxymethyl-cytosine
53BP1	p53-Binding protein 1
9-1-1 complex	RAD9-RAD1-HUS1
AEP	Archaeo-eukaryotic primase
ANK	Ankyrin repeat domain
ANOVA	Analysis of Variance
AP site	Apurinic/apyrimidinic site
ATM	Ataxia Telangiectasia Mutated
ATR	Ataxia Telangiectasia and Rad3-related
BARD1	BRCA1-Associated RING Domain Protein 1
BCDX2 complex	RAD51B, RAD51C, RAD51D, XRCC2
BER	Base excision repair
BFP	Blue fluorescent protein
BIR	Break-Induced Replication
BLM	Bloom syndrome protein
BRCA1	Breast cancer associated gene 1
BRCA1-P	BRCA1-PALB2-BRCA2-RAD51 complex
BRCA2	Breast Cancer Susceptibility Protein 2
BRCT	BRCA1 C-Terminus
BrdU	5'-bromo-2'-deoxyuridine
CAF-1	Chromatin Assembly Factor 1
CDKs	Cyclin-dependent kinases

CDT1	Chromatin licensing and DNA replication factor 1
CIP2A	Cancerous inhibitor of protein phosphatase 2A
CldU	5-chloro-2'-deoxyuridine
CPDs	Cyclobutene pyrimidine dimers
CRISPR	Clustered regularly interspaced short palindromic repeats
CtIP	Ct-BP Interacting protein
CTRB	C-terminal RAD51 Binding
CX3 complex	RAD51C, XRCC3
D-loop	Displacement loop
DDK	DBF4-dependent kinase
DDR	DNA damage response
DDT	DNA damage tolerance
dHJ	Double Holliday junction
DMEM	Dulbecco's Modified Eagle Media
DMSO	Dimethyl Sulfoxide
DNA	Deoxyribonucleic acid
DNA-PKcs	DNA-dependent protein kinase catalytic subunit
DNA2	DNA replication helicase/nuclease 2
DSBs	Double strand breaks
dsDNA	Double stranded DNA
DUB	De-ubiquitinating enzyme
DYNLL1	Dynein light chain LC8 type 1
E1	Ubiquitin-activating enzyme
E2	Ubiquitin-conjugating enzyme
E3	Ubiquitin ligase enzyme

EEPD1	endonuclease/exonuclease/phosphatase family domain containing 1
EtOH	Ethanol
EV	Empty vector
FA	Fanconi Anaemia
FANCM	Fanconi Anaemia complementation group M
FBS	Foetal Bovine Serum
FEN1	Flap structure-specific endonuclease 1
GEN1	Holliday junction 5'flap endonuclease
H1	Histone 1
HBOC	Hereditary breast and ovarian cancer
HLTF	Helicase Like Transcription Factor
hmdU	5-hydroxymethyl-2'-deoxyuridine
HR	Homologous recombination
HU	Hydroxyurea
ICL	Inter-strand crosslinks
IdU	5-iodo-2'-deoxyuridine
IR	Ionising radiation
Ku	Ku70-80 heterodimer
L3MBTL2	Lethal malignant brain tumour-like 2
MCM	Mini-chromosome maintenance
MDC1	Mediator of DNA damage checkpoint protein 1
MEFs	Mouse embryonic fibroblasts
MK2	MAPK-activated protein kinase 2
MiDAS	Mitotic DNA synthesis pathway
MMEJ	Microhomology-mediated end joining

MMR	Mismatch repair
MRE11	Meiotic recombination 11
MRN	MRE11-RAD50-NSB1
MUS81	MUS81 structure specific endonuclease subunit
NBS1	Nijmegan breakage syndrome 1
NCP^{Ub}	Nucleosome core particle
NER	Nucleotide excision repair
NHEJ	Non-homologous end joining
NTC	Non-targeting control
OFP	Okazaki fragment processing
ORC	Origin replication complex
PALB2	Partner and localiser of BRCA2
PARP1	Poly (ADP-ribose) polymerase 1
PARPi	(poly-ADP) ribose-polymerase inhibitor
PCNA	Proliferating cell nuclear antigen
PI3K	Phosphoinositide 3-kinase
PIN1	Peptidylprolyl Cis/Trans Isomerase, NIMA-Interacting 1
PIP box	PCNA-interacting peptide box
PLA	Proximity ligation assay
PLK1	Polo-like kinase 1
POLK	DNA polymerase kappa
Polθ	DNA polymerase θ
pre-RC	Pre-replication complex
PRIMPOL	The human Primase and DNA-directed polymerase
PRR	Post-replicative repair

PTIP	PAX transcription activation domain interacting protein
RAD52	Radiation sensitive 52
RER	Ribonucleotide excision repair
RFC	Replication factor C
RFWD3	Ring Finger and WD Repeat Domain 3
RHINO	RAD9-HUS1-RAD1 Interacting Nuclear Orphan 1
RIF1	Replication timing regulatory factor 1
RING	Really Interesting New Gene
Rmi1	RECQ-mediated genome instability protein 1
RPA	Replication protein A
SCD	Serine cluster domain
SCJ	Sister-chromatid junction
SDS-PAGE	SDS Polyacrylamide Gel Electrophoresis
Sgs1	Slow growth suppressor 1
siRNA	Small interfering RNA
SLX4	SLX4 structure-specific endonuclease subunit
SMARCAD1	SWI/SNF-Related, Matrix-Associated Actin-Dependent Regulator Of Chromatin, Subfamily A, Containing DEAD/H Box 1
SMART	Single Molecule Analysis of Resection Tracks
SSA	Single strand annealing
SSBs	Single strand breaks
ssDNA	Single-stranded DNA
TLS	Translesion synthesis
TMEJ	Polymerase θ-mediated end joining
Top3	Topoisomerase 3

TOPBP1	Topoisomerase II Binding Protein 1
TS	Template switching
TULIP	Targets of Ubiquitin Ligases Identified by Proteomics
Ub	Ubiquitin
UBM	Ubiquitin-binding motifs
UBQLN4	Ubiquilin 4
UBZ	Ubiquitin-binding zinc fingers
UDR	Ubiquitylation-dependent recruitment motif
UHRF1	Ubiquitin like with PHD and ring finger domains 1
USP1	Ubiquitin-specific peptidase 1
USP48	Ubiquitin specific peptidase 48
UV	Ultra-violet
VUS	Variant of unknown significance
WRN	Werner syndrome protein
XLF	XRCC4-like factor
Zn^{2+}	Zinc ion
ZRANB3	Zinc finger RANBP2-type containing 3

1. Introduction

1.1. The DNA damage response

DNA damage and genome instability are important factors that result in the development of cancer. DNA is continuously damaged by endogenous replication stress and exogenous genotoxic compounds such as during DNA replication, by ultra-violet (UV) damage, ionising radiation (IR), chemicals that induce crosslinks, base adducts and disruptive topoisomerase function. The detection, signalling and subsequent repair of these breaks is known as the DNA damage response (DDR) (Ciccia and Elledge, 2010; Jackson and Bartek, 2009; Blackford and Jackson, 2017; Zhao et al., 2019). DNA damage can range from single-strand breaks (SSBs), double-strand breaks (DSBs), base mismatches, insertions and deletions, bulky adducts and base alkylation events (Hoeijmakers, 2001). DSBs are the most toxic DNA lesions and can result in genomic instability and cell death if unrepaired (Jeggo et al., 2011). Familial and sporadic cancers can arise due to mutations within the DDR machinery which can no longer repair stalled replication forks and cells pass through the cell cycle with unrepaired DNA damage resulting in mutagenesis and ultimately tumorigenesis (Bartkova et al., 2006).

The major regulators of the DDR are Ataxia Telangiectasia Mutated (ATM) and RAD3-related (ATR) kinases, which are members of the phosphoinositide 3-kinase (PI3K)-related protein kinase family, that sense alterations to the structure of DNA and activate a downstream DDR (Suzuki et al., 1999; Ünsal-Kaçmaz et al., 2002). Also, the cell

cycle checkpoint kinases CHK1, CHK2 and MAPK-activated protein kinase 2 (MK2) are phosphorylated in an ATM and ATR-dependent manner (Matsuoka et al., 1998; Liu et al., 2000; Reinhardt et al., 2007). ATM kinase activation in response to DSBs is regulated by its interaction with the MRE11-RAD50-NSB1 (MRN) complex which localises ATM to chromatin facilitating the DDR signalling cascade (van den Bosch et al., 2003; Uziel et al., 2003; Lee and Paull, 2005).

ATM, ATR and the non-homologous end joining (NHEJ) repair factor DNA-dependent protein kinase catalytic subunit (DNA-PKcs) both phosphorylate a conserved serine residue (S139) on the C-terminus of the histone variant H2AX within regions of chromatin bearing DSBs (Falck et al., 2005; Stiff et al., 2004; Rogakou et al., 1999). Phosphorylation of the histone variant is termed *γ*-H2AX, which formulates a scaffold to modulate the recruitment of further DDR factors (Rogakou et al., 1998; Celeste et al., 2003). In immunofluorescence assays *γ*-H2AX forms nuclear foci in response to its phosphorylation and is used as a DNA damage marker due to its primary cellular response to DSBs (Mah et al., 2010).

Gamma-H2AX interacts with mediator of DNA damage checkpoint protein 1 (MDC1) by forming a docking site for the BRCT domain of MDC1 (Stucki et al., 2005). The N-terminal phosphorylation of the SDT repeats of MDC1 retains Nijmegan breakage syndrome 1 (NBS1) (NBN component of the MRN complex) and MDC1 interacts with ATM via its FHA domain thus facilitating the retention of the MRN-ATM complex forming a positive feedback loop and amplification of MDC1 spreading on chromatin (Chapman and Jackson, 2008; Melander et al., 2008; Spycher et al., 2008; Wu et al., 2008a; Goldberg et al., 2003). ATM-dependent phosphorylation of MDC1 recruits the RING-type E3 ubiquitin (Ub) ligase RNF8, which ubiquitylates histone 1 (H1) and lethal

malignant brain tumour-like 2 (L3MBTL2) to promote the ubiquitin-dependent localisation of the E3 ligase RNF168 (Mailand et al., 2007; Kolas et al., 2007; Thorslund et al., 2015; Nowsheen et al., 2018). The ubiquitin pathway encompasses the ubiquitin activating enzyme (E1), a ubiquitin-conjugating enzyme (E2) and a ubiquitin ligase (E3), with the E3 facilitating the formation of mono- and poly-ubiquitin chains to transfer ubiquitin onto certain targets linked by isopeptide bonds (Hershko and Ciechanover, 1998; Pickart and Eddins, 2004; Wu et al., 2008b). Subsequently, RNF168-mediated monoubiquitylation of H2A and the formation of K63-linked ubiquitin chains on K13/15 (H2AK13-Ub and H2AK15-Ub) generates a scaffold for the recruitment of proteins such as the p53-binding protein 1 (53BP1) (Pinato et al., 2009; Mattiroli et al., 2012; Gatti et al., 2012; Stewart et al., 2009; Doil et al., 2009).

53BP1 interacts directly with RNF168-mediated H2AK15-Ub via its ubiquitylation-dependent recruitment (UDR) motif and recognises di-methylated H4K20 (H4K20me2) via its Tudor domain (Fradet-Turcotte et al., 2013; Botuyan et al., 2006). 53BP1 is important for regulating DSB repair pathway choice by associating with PAX transcription activation domain interacting protein (PTIP) and replication timing regulatory factor 1 (RIF1) to recruit the Shieldin complex (REV7, SHLD1, SHLD2 and SHLD3) to sites of damage (Noordermeer et al., 2018; Zimmermann et al., 2013; Escribano-Díaz et al., 2013; Feng et al., 2013; Chapman et al., 2013; Ghezraoui et al., 2018; Dev et al., 2018).

The breast cancer type 1 susceptibility protein (BRCA1) is a tumour suppressor that mediates DSB pathway choice by facilitating homologous recombination (HR) by interacting with CtIP and displacing the 53BP1-RIF1 complex to mediate DNA end resection in a cell cycle dependent manner (Cao et al., 2009; Chapman et al., 2013;

Escribano-Díaz et al., 2013). BRCA1 counteracts the 53BP1-mediated block on DNA end resection as the loss of 53BP1 rescues genomic instability in *BRCA1*-deficient cells (Bouwman et al., 2010; Bunting et al., 2010). DSB pathway choice between NHEJ and HR is cell cycle dependent with the 53BP1-RIF1 complex inhibiting BRCA1 recruitment in G1 phase and BRCA1-CtIP restricts RIF1 recruitment during S/G2 phase (Escribano-Díaz et al., 2013).

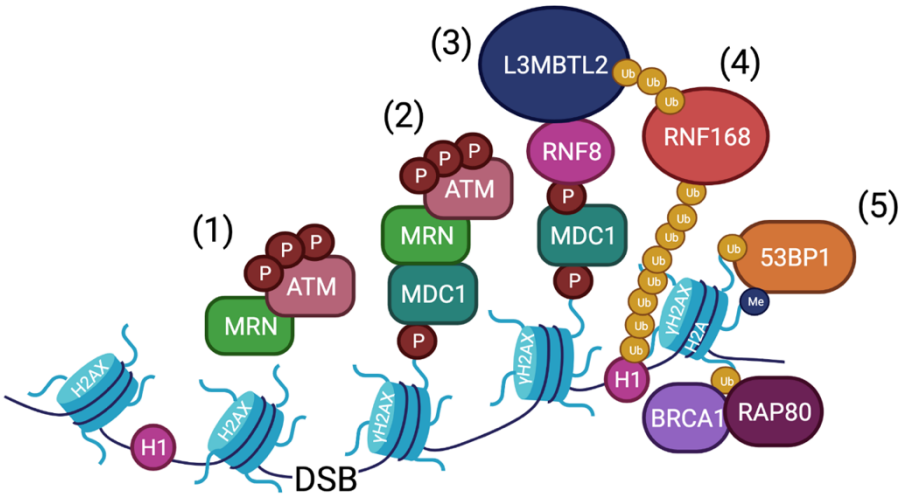

Figure 1.1 – DNA damage response pathway. The MRN complex recruits ATM to DSBs and ATM phosphorylates itself and proteins such as H2AX. γH2AX associates with MDC1 which amplifies the recruitment of ATM-MRN to sites of damage. The phosphorylation of MDC1 recruits the E3 ubiquitin ligase RNF8 which ubiquitinates H1 and L3MBTL2 to recruit RNF168 (Stewart et al., 2009). RNF168 ubiquitinates histone H2A to recruit 53BP1 and RNF8-dependent ubiquitination of H1 recruits RAP80 which interacts with the BRCT domain of BRCA1 (Doil et al., 2009; Mattiroli et al., 2012; Fradet-Turcotte et al., 2013). Based on (Adamowicz, 2018) (Created using *BioRender.com*).

1.2. Breast cancer type 1 susceptibility protein (BRCA1)

BRCA1 is essential for maintaining genomic stability, consequently *BRCA1* mutations are detrimental to cell survival and genomic viability (Eyfjord and Bodvarsdottir, 2005). In 1994, heterozygous germline *BRCA1* was sequenced and cloned, shortly followed by breast cancer susceptibility protein 2 (*BRCA2)* in 1995 (Rahman and Stratton, 1998; Miki et al., 1994). Mutations in the *BRCA1* gene predispose individuals to an increased risk of developing hereditary breast and ovarian cancer (HBOC), harbouring a lifetime risk of up to 40-65% for developing ovarian cancer and >80% for breast cancer (Rahman and Stratton, 1998; King et al., 2003; Li et al., 2022; Petrucelli et al., 2017). Germline mutations of the *BRCA1* gene are also associated with a predisposition to prostate, stomach, pancreatic, laryngeal, and fallopian tube cancer at lower frequencies (Roy et al., 2012; Foulkes, 2008; Li et al., 2022). BRCA1 achieves genomic stability through pleiotropic functions such as its integral role within the DNA damage repair pathway, transcription, cell cycle checkpoint activation, protection of stalled replication forks from nucleolytic degradation, mRNA splicing and preventing of single-stranded DNA (ssDNA) gaps (Scully et al., 1997; Schlacher et al., 2012; Yarden et al., 2002; Savage et al., 2014; Panzarino et al., 2021).

1.2.1. BRCA1 functional domains and binding partners

Human *BRCA1* is located on chromosome 17q21.3 and is made up of 24 exons encoding an 1863 amino acid protein and is 220 kDa in size (Miki et al., 1994; Savage and Harkin, 2015).

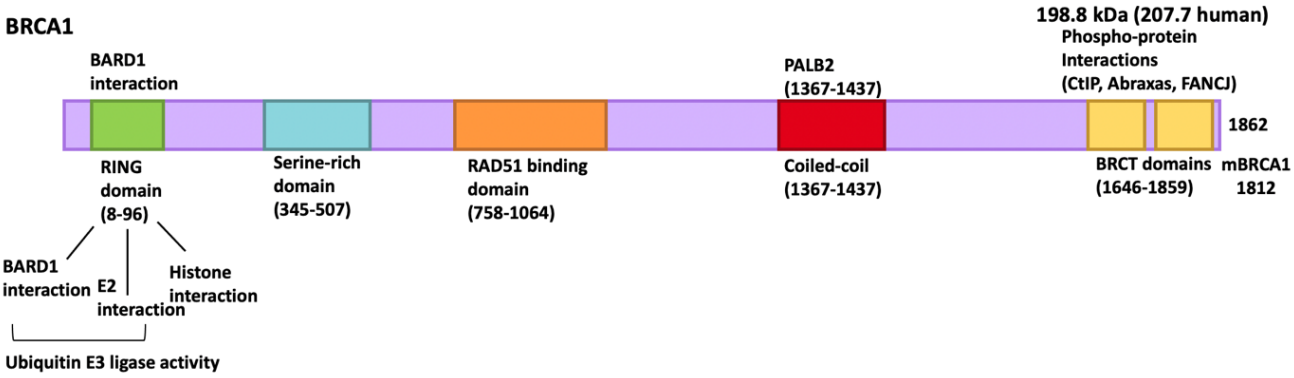

Figure 1.2 – Functional domains of BRCA1. The BRCA1 N-terminus contains a RING domain to associate with its obligate binding partner BARD1. BRCA1 has a RAD51 binding domain and a coiled-coil domain that interacts with PALB2. 60% of the BRCA1 protein consists of exon 11. The C-terminal BRCT domains interact with phosphoproteins such as CtIP.

1.2.1.1. BRCA1 RING domain

The BRCA1 protein contains an amino-terminal RING (Really Interesting New Gene) domain that has E3 ubiquitin ligase activity which is augmented when the N-terminal domain of BRCA1 is associated with its binding partner and localiser, BRCA1-associated RING domain protein 1 (BARD1) (Wu et al., 1996; Roy et al., 2012). BRCA1/BARD1 binds to 10 E2 ubiquitin conjugating enzymes with the products generated depending on the specific partnered E2 (Stewart et al., 2017).

The RING domain is located at exons 2-7 (amino acids 1-109) and is made up of a RING finger and two flanking α-helices that align perpendicular to the RING finger, containing a core three strand β-sheet (Brzovic et al., 2001b; Meza et al., 1999). The conserved RING motif consists of seven cysteine residues and one histidine residue

forming two Zn^{2+} binding sites, Site I and Site II (Borden and Freemont, 1996; Brzovic et al., 2001a). Site I consists of four cysteine residues and Site II encompasses three cysteine residues and one histidine residue (Fig.1.3) (Clark et al., 2012). The RING structure is made stable by the coordination of the two Zn^{2+} atoms by the RING finger (Bienstock et al., 1996).

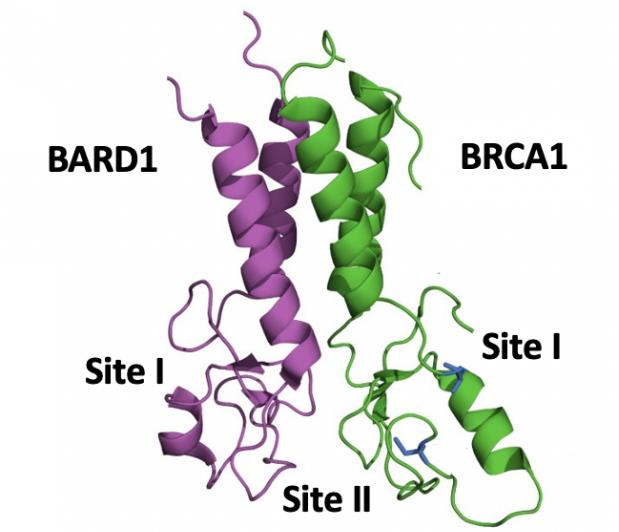

Figure 1.3 – BRCA1/BARD1 Nuclear magnetic resonance (NMR) structure. Structure of the BRCA1 and BARD1 RING domains forming a heterodimeric complex. (Adapted from (Elia and Elledge, 2012)).

BRCA1 and BARD1 form a stable heterodimeric complex and during S-phase of the cell cycle co-localise within nuclear foci (Jin et al., 1997). The BRCA1/BARD1 heterodimer consists of a four helix bundle where the BRCA1 N-terminal alpha helix is antiparallel to the C-terminal alpha helix of BARD1 and vice versa, which stabilises the complex by forming a hydrophobic region that is buried (Fig. 1.3) (Clark et al., 2012). The BRCA1 RING finger interacts with the E2 ubiquitin conjugating enzyme UbcH5 and alternative E2 enzymes to facilitate downstream signalling by producing K6-linked polyubiquitin chains (Nishikawa et al., 2004). Cancer predisposing mutations located

within the Zn^{2+} -ligand residues can abolish the E3 ubiquitin ligase activity of the BRCA1/BARD1 heterodimer (Brzovic et al., 2001a). For example, the C61G-BRCA1 missense mutation is located within the zinc RING finger domain and so disrupts BRCA1/BARD1 heterodimer formation and abrogates E3 ubiquitin ligase activity (Brzovic et al., 1998; Mallery et al., 2002; Hashizume et al., 2001).

BRCA1 exons 11-13 contain numerous binding domains such as for RAD51, partner and localiser of BRCA2 (PALB2) (scaffold protein for BRCA2), a nuclear localisation signal (NLS) as well as a serine cluster domain (SCD) (Clark et al., 2012). The coiled-coil domain of BRCA1 associates with the N-terminal coiled-coil domain of PALB2 which subsequently interacts with BRCA2 via its C-terminus (Zhang et al., 2009a, 2009b; Oliver et al., 2009). The interaction between BRCA1-PALB2-BRCA2 is essential for RAD51 loading onto replication protein A (RPA)-bound ssDNA during HR (Xia et al., 2006). Variants of unknown significance (VUS) have been identified in the coiled-coil domain of BRCA1 that binds to PALB2, which include M1400V, L1407P and M1411T (Anantha et al., 2017; Bouwman et al., 2013; Sy et al., 2009a). For example, the L1407P mutation can disrupt the interaction between BRCA1 and PALB2 and therefore impair DSB repair by HR. The SCD is phosphorylated by the ATM/ATR kinases at serines 1189, 1457, 1524, and 1542 and mutations at these residues could alter the localisation of BRCA1 to sites of DSBs (Traven and Heierhorst, 2005; Cortez et al., 1999).

1.2.1.2. BRCA1 BRCT domain

The BRCA1 carboxyl terminal (BRCT) domains occur as a tandem repeat (amino acids 1650-1863) (BRCT1 and BRCT2) connected by a 22-amino acid linker, and enables its association with proteins that have been phosphorylated by the two kinases ATM and ATR (Leung and Glover, 2011; Clark et al., 2012; Williams et al., 2001). The BRCT1 and BRCT2 domains are oriented in a head-to-tail position and the hydrophobic interface between the BRCT domains is generated by α2 (BRCT1) and α'1 and α'3 (BRCT2) and a linking helix αL between the domains, adjacent to α'3 (Williams et al., 2001; Shiozaki et al., 2004; Wu et al., 2015a). The BRCA1 BRCT domains bind phosphorylated proteins that have the pSXXF sequence motif and interact with proteins such as CtIP, BRIP1/BACH1, and ABRAXAS as well as DNA and poly(ADP-ribose) (PAR) (Rodriguez et al., 2003; Manke et al., 2003; Yu et al., 2003; Pleschke et al., 2000). However, interactions that do not include phosphorylated proteins have been revealed, for example, the interaction between BRCA1-BRCT domains and DNA-PKcs (Davis et al., 2014).

1.2.2. BRCA1-associated RING-domain protein 1 (BARD1)

The obligate binding partner of BRCA1, BARD1 was isolated through a yeast and mammalian two-hybrid screen (Wu et al., 1996). BRCA1 forms a heterodimeric complex with BARD1 via their N-terminal RING domains (Brzovic et al., 2001b). In response to genotoxic compounds, BARD1 can chaperone BRCA1 to form DDR co-localising foci and performs as an E3 ubiquitin ligase in tandem with BRCA1 (Hashizume et al., 2001). Despite both BRCA1 and BARD1 having a RING domain, BRCA1 but not BARD1 has a direct interaction with E2 conjugating enzymes (Brzovic

et al., 2003). Mice deficient in either *Brca1* or *Bard1* are embryonic lethal and display genomic instability, indicating that BARD1 is as fundamental for cell viability as the tumour suppressor BRCA1 (McCarthy et al., 2003; Irminger-Finger and Jefford, 2006). BARD1 interacts with RAD51 to mediate the assembly of the presynaptic complex for DNA joint formation and this interaction is indispensable for enhancing strand invasion by RAD51 during HR (Zhao et al., 2017a).

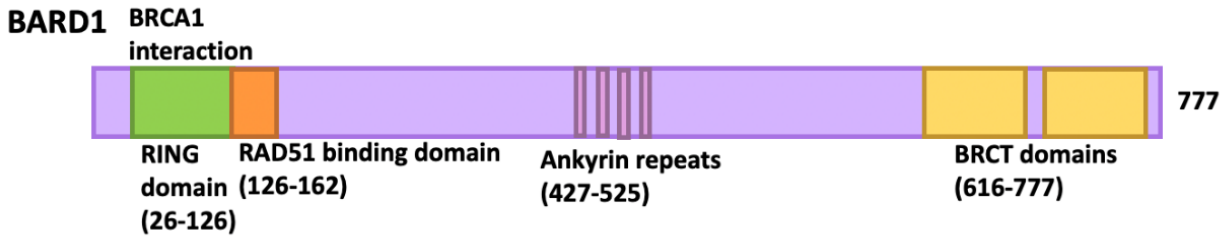

Figure 1.4 – BARD1 structure and functional domains. BARD1 contains a RING domain, RAD51 binding domain, ankyrin repeats and two BRCT domains.

BARD1 harbours four tandem ankyrin motifs that recognise histone H4 unmethylated at lysine 20 (H4K20me0) on new histones initiating BRCA1/BARD1 localisation to post-replicative chromatin, allowing for the available sister chromatid (S/G2 phases) to be used for HR, counteracting the function of 53BP1 (Nakamura et al., 2019; Saredi et al., 2016). Mutations within the BARD1 ankyrin repeat domain (ANK) can abrogate H4K20me0 recognition disrupting BRCA1 localisation to sites of DNA damage, therefore resulting in surplus 53BP1 accumulation during S and G2 phase (Nakamura et al., 2019).

Moreover, BARD1 contains two tandem BRCT repeats that interact with phosphorylated proteins (Billing et al., 2018). However, proteins that bind the BARD1 BRCT phosphate-binding pocket have yet to be explored in great depth (Billing et al.,

2018). The BRCT domain is fundamental for BRCA1/BARD1 recruitment to DSBs via poly(ADP-ribose) (PAR) recognition and binding (Li and Yu, 2013). BARD1-mediated early BRCA1 recruitment to DSBs via its BRCT domain involves the interaction with PAR via C645 and V965, and three BARD1 mutations identified at the same position: C645R, V695L and S761N predispose individuals to breast, ovarian and uterine cancers (Li and Yu, 2013; Thai et al., 1998; Ishitobi et al., 2003; Laufer et al., 2007; Choudhary et al., 2018). The inter-β2′–β3' loop of BARD1 is termed BUDR (BRCT-associated ubiquitin-dependent recruitment motif) and can bind to RNF168-generated mUb-H2A, recruiting the BRCA1-PALB2-BRCA2-RAD51 (BRCA1-P) complex to DSBs (Becker et al., 2021; Krais et al., 2021).

1.2.3. BRCA1 complex formation and recruitment to DSBs

BRCA1 is a member of four complexes: the BRCA1-A, B, C and P complexes. The BRCA1-A complex is made up of receptor-associated protein 80 (RAP80) (UIMC1), ABRAXAS (CCDC98), BRCC36, BRCC45 (BRE), BRCA1, BARD1, and MERIT40 (NBA1) (Liu et al., 2007; Kim et al., 2007a; Wang et al., 2007; Yan et al., 2007; Feng et al., 2009; Wang et al., 2009; Kim et al., 2007b). RNF8 and RNF168-generation of K63-linked ubiquitin chains recruits RAP80 via its ubiquitin-interacting motifs (UIMs) (Wang et al., 2007; Kim et al., 2007a). Subsequently, RAP80 recruits BRCA1 via ABRAXAS to DSBs forming the BRCA1-RAP80 complex which encompasses the BRCC36 enzyme (Sobhian et al., 2007). The BRCA1-A complex mediates BRCA1 recruitment to DSBs, with ABRAXAS interacting with the BRCA1-BRCT domain (Hu et al., 2011; Castillo et al., 2014). Additionally, the BRCA1-A complex localises PALB2 to DSBs, as the BRCA1 BRCT interaction with ABRAXAS and RAP80 coincidingly permits the coiled-coil domain of BRCA1 to interact with PALB2 (Zhang et al., 2012).

The BRCA1-B complex is comprised of BRCA1, TOPBP1 and BACH1 (FANCJ/BRIP1) which are important for inter-strand crosslink repair and DNA replication cell cycle checkpoint control to maintain genomic stability during S-phase (Gong et al., 2010; Xu et al., 2002). BACH1 is a part of the DEAH Box DNA helicase family and is phosphorylated at serine 990 in a cell cycle dependent manner and interacts with the BRCA1-BRCT domain (Kumaraswamy and Shiekhattar, 2007; Yu et al., 2003; Yu and Chen, 2004). In response to replication stress, BACH1 and DNA topoisomerase II binding protein 1 (TOPBP1) are necessary to extend ssDNA and RPA loading replication checkpoint activation (Gong et al., 2010). Moreover, the BRCA1-B complex loads the replication-licensing factor CDC45L for DNA replication initiation (Greenberg et al., 2006; Van Hatten et al., 2002; Hashimoto and Takisawa, 2003). Overall, as reviewed in Huen *et al* (2010) the BRCA1-B complex is important for replication checkpoint activation in the presence of stalled replication forks (Huen et al., 2010).

The BRCA1-C complex is made up of BRCA1, CtIP and the MRN complex and is important for DNA end resection to generate ssDNA for DSB repair by HR (Chen et al., 2008). CtIP is phosphorylated at serine 327 which is then bound to BRCA1 C-terminal BRCT domains (Yu and Chen, 2004; Wong et al., 1998; Yu et al., 1998; Yu hello and Baer, 2000). A study has shown that the interaction between BRCA1 and CtIP is not necessary for tumour suppression or HR (Reczek et al., 2013), yet other studies have suggested that BRCA1-CtIP modulates the processivity of end resection (Cruz-García et al., 2014).

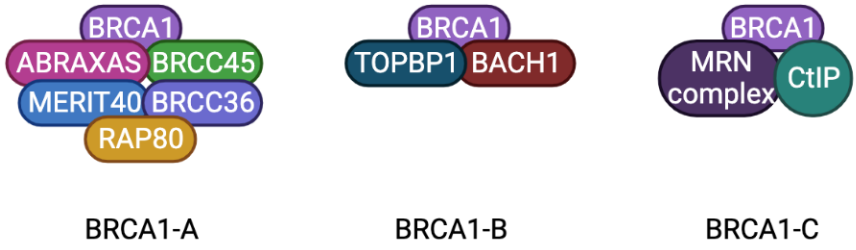

Figure 1.5 – BRCA1-A, B, C complexes. The BRCA1-A complex recruits BRCA1 to DSB sites. The BRCA1-B complex is important for DNA replication cell cycle checkpoint control and inter-strand crosslink repair. The BRCA1-C complex is involved in HR-mediated DNA end resection.

1.3. Double strand break repair pathways

Two major DNA damage repair pathways mend DSBs: non-homologous end joining (NHEJ) and homologous recombination (HR). NHEJ is an error-prone pathway that is active throughout the cell cycle that protects DNA ends from resection prior to re-ligation, however insertions, deletions and translocations can form (Mao et al., 2008; Lieber et al., 2014). Whereas, HR functions at S/G2 phase of the cell cycle and is more precise because of its use of the undamaged sister chromatid as its template, resulting in the restoration of the original sequence (Kim et al., 2001; Prakash et al., 2015).

1.3.1. Non-homologous end joining

The primary pathway for DSB repair that takes place throughout the cell cycle is the NHEJ pathway. Firstly, the Ku70-80 heterodimer (Ku) recognises the DSB and binds to the ends of the damaged DNA, behaving as a scaffold to enable the recruitment of additional NHEJ factors, both directly and indirectly (Davis and Chen, 2013). The NHEJ factors recruited to DSBs include the DNA-dependent protein kinase catalytic subunit DNA-PKcs, DNA Ligase IV, XRCC4, XRCC4-like factor (XLF), a paralogue of XRCC4

and XLF and aprataxin and PNK-like factor (APLF) (Mari et al., 2006; Davis and Chen, 2013; Nick McElhinny et al., 2000). Ku70/80 recruits DNA-PKcs directly leading to the activation of the kinase activity of the DNA-PKc complex, forming a DNA-PK holoenzyme (Gottlieb and Jackson, 1993). Ku70/80 protects the DNA ends from non-specific processing which could result in genomic instability (Pang et al., 1997). It is thought that APLF functions to assemble and retain DNA Ligase IV, XRCC4, and XLF at DSBs (Yano et al., 2009).

The DNA-PKc complex becomes a 5'- and 3'-endonuclease when bound to a DSB DNA end and is likely to form a synaptic complex (Cary et al., 1997; Weterings and Van Gent, 2004; Davis and Chen, 2013). The XRCC4-XLF complex generates a filament to bridge DNA ends, with a potential role in stabilising DNA ends (Malivert et al., 2010; Hammel et al., 2010). There are numerous enzymes involved in DNA end processing, depending on the nature of the break, including APLF, DNA polymerases μ and λ, Werner (WRN), and Ku (Davis and Chen, 2013). The Ku-XRCC4 scaffold is thought to have recruited these DNA end processing enzymes to DSBs (Lieber, 2008; Davis and Chen, 2013). In NHEJ, DNA end resection is carried out by Artemis, WRN and APLF. Artemis has endonuclease activity which is activated when phosphorylated by DNA-PKcs (Ma et al., 2002; Povirk et al., 2007). WRN interacts with XRCC4 and the Ku heterodimer to initiate 3' to 5' exonuclease activity (Cooper et al., 2000; Kusumoto et al., 2008). Finally, APLF performs DNA end resection as a 3' to 5' exonuclease and an endonuclease, but is not stimulated by an NHEJ core element (Kanno et al., 2007). Gap filling of the DNA is undertaken by DNA polymerases μ and λ, followed by DSB ligation by DNA Ligase IV (Moon et al., 2007; Gu et al., 2007). XRCC4 stabilises DNA Ligase IV by adenylation, XLF promotes ligation of mismatched

DNA ends by XRCC4, and APLF initiates ligation yet only when Ku70/80 is present (Grawunder et al., 1997; Lu et al., 2007; Davis and Chen, 2013; Grundy et al., 2013).

1.3.2. Homologous recombination

1.3.2.1. DNA end resection and pathway choice

HR, also known as homology-directed repair, is an error-free DSB repair pathway that uses a homologous sequence (Moynahan and Jasin, 2010; Daley et al., 2015). Repair pathway choice is reliant on the antagonistic relationship between the chromatin binding protein 53BP1 and BRCA1 (Daley and Sung, 2014). During HR, ATM phosphorylates CtIP which subsequently recognises and binds to the BRCA1 BRCT domain, which in turn is mediated by CDK2 and facilitated by meiotic recombination 11 (MRE11) (Buis et al., 2012). BRCA1-CtIP functions in conjunction with the MRN complex (BRCA1-C complex) to form short 3' ssDNA overhangs by nucleolytic degradation of the 5' DNA strand in a process called 5'-3' DNA end resection (Huertas and Jackason, 2009; Yun and Hiom, 2009; Lamarche et al., 2010). The repair of DSBs by NHEJ cannot take place as the 5' overhangs necessary for this error-prone pathway are removed by resection forming the 3' overhangs (Daley et al., 2005, 2015).

However, longer 3' ssDNA is required for RPA coating, therefore newly formed ssDNA undergoes additional elongation by MRN-mediated recruitment of exonuclease 1 (EXO1) performing 5' to 3' exonuclease and 5'-flap exonuclease functions (Shim et al., 2010; Cannavo et al., 2013; Anand et al., 2016). Additionally, extensive resection is carried out by the DNA helicase (DNA2) which also undertakes 5'- and 3' exonuclease functions alongside the DNA unwinding RecQ helicase bloom syndrome protein (BLM) (Levikova et al., 2017; Zhou et al., 2015; Sturzenegger et al., 2014; Pinto et al., 2016;

Bernstein et al., 2010). The RecQ helicase WRN functions in tandem with BLM in extensive resection (Bernstein et al., 2010). Yet, extensive resection performed by the aforementioned nucleases and helicases cannot take place without the prior generation of the short 3'ssDNA overhang by the CtIP-MRN complex (Symington, 2016; Nimonkar et al., 2011). Whereas, 53BP1 stimulates NHEJ via the recruitment of RIF1 by inhibiting resection involving CtIP, BLM, and EXO1, therefore limiting the accumulation of BRCA1/BARD1 to sites of DNA damage (Zimmermann et al., 2013). HR is abrogated as BRCA1-CtIP mediated end resection and RAD51 loading are halted (Zhao et al., 2020; Zimmermann and De Lange, 2014). BRCA1 can counteract 53BP1-mediated block on resection by recruiting the E3 ubiquitin ligase ubiquitin like with PHD and ring finger domains 1 (UHRF1), via its BRCT domain, which prevents the recruitment of RIF1 and therefore abrogates the interaction between 53BP1 and RIF1, subsequently promoting end resection (Zhang et al., 2016). *BRCA1*-deficient cells which exhibit compromised HR are restored by the removal of 53BP1 and therefore removing this block (Cao et al., 2009). However, 53BP1 deletion did not impact checkpoint responses or proliferation arrest in *BRCA2*-deficient cells, indicating that the effects of 53BP1 loss are BRCA1 specific (Bouwman et al., 2010).

SHLD1/SHLD2/SHLD3 plus REV7 (MAD2L2) form the "Shieldin" (SHLD1/2/3) complex, which functions as a downstream effector of 53BP1/RIF1/MAD2L2 in order to facilitate DSB end-joining (Dev et al., 2018). Shieldin counteracts HR and restricts DSB resection by antagonising BRCA2/RAD51 loading in *BRCA1*-deficient cells (Dev et al., 2018). The 53BP1-RIF1-Shieldin (SHLD1-SHLD2-SHLD3-REV7-CST) complex is recruited where it restricts BRCA1/BARD1 retention (Densham and Morris, 2019). SHLD2 carries 3 oligonucleotide/oligosaccharide-binding (OB) folds which interact with

ssDNA of >50 nucleotides in order to promote 53BP1 in NHEJ promotion (Gao et al., 2018). The Shieldin complex recruits DNA Polα leading to the priming of DNA synthesis to fill in resected DNA ends, which in turn prevents long range resection and facilitates NHEJ repair (Barazas et al., 2018). These data highlight that BRCA1 is critical for overcoming the 53BP1-mediated block on resection (Bunting et al., 2010; Bouwman et al., 2010; Densham and Morris, 2019).

Besides BRCA1/CtIP, Dynein light chain LC8 type 1 (DYNLL1) facilitates NHEJ over HR by associating with MRE11, inhibiting end resection as well as mediating 53BP1 loading and oligomerisation (He et al., 2018; Becker et al., 2018; West et al., 2019). Also, ATM phosphorylates Ubiquilin 4 (UBQLN4) which promotes MRE11 degradation and its overexpression amplifies NHEJ (Jachimowicz et al., 2019). Furthermore, PTIP antagonises DNA end resection by inhibiting DNA2 facilitated resection, whereas the Shieldin complex antagonises end resection mediated by EXO1 (Callen et al., 2020). Also, 53BP1-PTIP recruits Artemis which exhibits both endonuclease function and digests resected ssDNA to promote NHEJ over HR (Wang et al., 2014).

The current targets of BRCA1 E3 ubiquitin ligase have been identified as histones H2A, H2AX, CtIP, NPM1, TFIIE, RNA polIII, tubulin, claspin, ER-α and others (Wu et al., 2008b; Witus et al., 2021b). In relation to the DDR, BRCA1 harbours BRCA1-dependent conjugation sites on the C-terminus of H2A at positions K125/127/129 (Zhu et al., 2011; Kalb et al., 2014). Densham *et al* (2016) determined that there was an association between 53BP1 positioning away from the DSB site and E3 ubiquitin ligase proficiency (Densham et al., 2016). The disruption of BRCA1 or its ligase function results in long-range DNA end resection, indicating that the ubiquitin ligase activity of

BRCA1/BARD1 repositions 53BP1 on damaged chromatin (Densham et al., 2016; Shibata et al., 2011; Alagoz et al., 2015; Drost et al., 2016).

SWI/SNF-Related, Matrix-Associated Actin-Dependent Regulator Of Chromatin, Subfamily A, Containing DEAD/H Box 1 (SMARCAD1) has been implicated in DSB end resection to load repair and checkpoint proteins (Chen et al., 2012, 2016; Costelloe et al., 2012). The chromatin remodeller SMARCAD1 harbours ubiquitin-binding CUE domains that are necessary for BRCA1/BARD1 function in HR (Costelloe et al., 2012; Chen et al., 2012). BRCA1/BARD1-mediated ubiquitination of H2A-K125/127/129ub is recognised by SMARCAD1 CUE domains and facilitates the interaction between SMARCAD1 and damage-proximal nucleosomes (Densham et al., 2016; Densham and Morris, 2019). BRCA1/BARD1 ligase transforms chromatin which results in the accrual and function of SMARCAD1, leading to 53BP1 mobilisation to finalise resection (Densham et al., 2016; Densham and Morris, 2017). BRCA1 loss reduces the circumference of 53BP1 localisation, positioning it in the centre of foci, therefore BRCA1 localises 53BP1 away from the break core in S-phase cells (Kakarougkas et al., 2013a; Wu et al., 2008b). However, it is E3 ligase proficiency rather than BRCA1 occupation itself linking to 53BP1 repositioning because cells complemented with ligase defective BRCA1/BARD1 co-locate with 53BP1 to the core and are no longer situated at the periphery (Densham and Morris, 2017). However, Chakraborty *et al* (2018) reveal that SMARCAD1 is recruited to DSBs by ATM-dependent phosphorylation and recruits BRCA1 at break sites, and that the polycomb group protein ring finger protein 1 (RING1) and not BRCA1/BARD1 is the E3 ligase that ubiquitinates SMARCAD1 at K905 (Chakraborty et al., 2018).

The ubiquitin specific peptidase 48 (USP48) is a de-ubiquitinating enzyme (DUB) specific for nucleosomal-H2A modified at the BRCA1 K125/K127/K129 sites, and DNA resection lengths are regulated by levels of USP48 (Uckelmann et al., 2018). Overexpression leads to constrained resection, in contrast to diminished USP48 levels resulting in 53BP1 mobilisation away from the DSB, increasing BRCA1 and SMARCAD1 dependent DNA end resection (Densham and Morris, 2019; Uckelmann et al., 2018). This antagonistic relationship ensures genomic stability by restricting excess resection and toxic DSB repair by RAD52-mediated single-strand annealing (SSA) (Uckelmann et al., 2018).

1.3.2.2. BRCA1-P complex recruitment and RAD51 loading

The 3' ssDNA tails generated by DNA end resection are coated by the ssDNA binding protein RPA, made up of RPA 70, RPA 32 and RPA14 subunits, removing secondary structures and stabilising the ssDNA (Wold, 1997). BRCA1 recruits BRCA2 via its interaction with the coiled-coil domain of PALB2 to displace loaded RPA with the recombinase protein RAD51 (Zhang et al., 2009b, 2009a; Sy et al., 2009a). BRCA1-PALB2-BRCA2-RAD51 form the BRCA1-P complex that mediates RAD51 accumulation at DSBs followed by RAD51 filament formation (Zhang et al., 2009b). Nacson *et al* (2018) revealed that the loss of 53BP1 to induce HR is dependent on the *BRCA1* mutant, as post end resection hypomorphic BRCA1 proteins can facilitate RAD51 loading (Nacson et al., 2018). Using the *Brca1*$^{\Delta C}$ allele, which failed to form a detectable BRCA1 protein, RAD51 foci did not form and cells were sensitive to (poly-ADP) ribose-polymerase inhibition (PARPi) and so elicited sub-optimal HR (Nacson et al., 2018). Also, Chen *et al* (2020) demonstrated that knocking out 53BP1 can partially

rescue embryonic lethality of total BRCA1 knock-out mice but cannot retore HR deficiency (Chen et al., 2020).

BRCA2 recruits RAD51 to ssDNA and displaces RPA via its BRC1-8 repeats and its C-terminal domain that binds RAD51 (Zhao et al., 2015; Esashi et al., 2005; Wong et al., 1997). BRCA2 contains a DNA binding domain consisting of three OB folds (OB1, OB2, OB3), and so BRCA2 can enhance the assembly of RAD51 presynaptic filaments on ssDNA coated with RPA via its two BRC repeats and the DNA binding domain (Jensen et al., 2010; Liu et al., 2010). As BRCA2 cannot directly bind to RPA, the BRCA2-associated DSS1 protein (70 amino acids) facilitates RPA-RAD51 strand exchange (Crackower et al., 1996; Ignatius et al., 1996; Ma et al., 2013; Rezano et al., 2013; Jensen et al., 2010; Zhao et al., 2015). DSS1 interacts with the BRCA2 OB1 domain in order to undertake RAD51 presynaptic filament formation by binding to RPA and functioning as a DNA mimic mediating RPA-RAD51 strand exchange. (Yang et al., 2002; Zhao et al., 2015). The BRCA2-DSS1 interaction is fundamental for RAD51 loading as the L2431P pathogenic BRCA2 Fanconi Anaemia (FA) mutant which abrogates this interaction is sensitive to genotoxic agents and is HR-deficient (Biswas et al., 2011). Cells deficient of DSS1 show elevated chromosomal aberrations and reduced RAD51 focal accumulations (Gudmundsdottir et al., 2004; Kojic et al., 2003). Although, the BRCA2-DSS1 association is dispensable when loading RAD51 in the case that the homologous DNA is near the DNA damage site (Mishra et al., 2022). DSS1 can also directly bind to RAD52, modifying its ability to bind DNA by changing its oligomeric conformation so that RAD52 can function within the SSA and break-induced replication (BIR) pathways (Stefanovie et al., 2020).

RAD51 loading onto ssDNA generates a nucleoprotein complex called the presynaptic filament which invades the homologous duplex to form a heteroduplex DNA, collectively termed the displacement loop (D-loop) (Ira and Haber, 2002; West, 2003; Sung et al., 2003). The assembly of the synaptic complex is a pre-requisite for D-loop formation, and data suggests that BRCA1/BARD1 functions with the RAD51 presynaptic filament to form the complex. BRCA1 and BARD1 bind the D-loop directly, though BARD1 showed a higher affinity for substrate binding (Zhao et al., 2017b). Additionally, the BARD1 mutant (AAE-BARD1 (F133A, D135A, and A136E)) disrupts the binding between BRCA1/BARD1 and RAD51 without impacting DNA binding (Zhao et al., 2017a). The AAE-BARD1 mutant cannot facilitate RAD51-mediated synaptic complex assembly and D-loop generation and these cells are sensitive to the PARP inhibitor olaparib and mitomycin C and are defective in HR but still form RAD51 foci (Zhao et al., 2017a). Therefore, BRCA1/BARD1 have a direct role with RAD51 in the mediation of synaptic complex assembly and D-loop generation (Zhao et al., 2017b; Tarsounas and Sung, 2020).

Paralogues of PALB2, RAD54 and RAD51 have been identified: RAD51B, RAD51C, RAD51D, XRCC2, and XRCC3 which ameliorate RAD51 strand exchange and D-loop formation (Serra et al., 2013; Wiese et al., 2007; Dray et al., 2010; Suwaki et al., 2011; Chun et al., 2013). RAD51 paralogues form the BCDX2 complex (RAD51B, RAD51C, RAD51D, XRCC2) and CX3 complex (RAD51C, XRCC3). BCDX2 and CX3 are both capable of binding to ssDNA and partial duplex DNA (Bonilla et al., 2020; Masson et al., 2001a, 2001b; Yokoyama et al., 2004). The loss of RAD51 paralogues has been associated with cancer predisposition and FA and the RAD51 paralogues are fundamental for early functions during HR (Garcin et al., 2019; Chun et al., 2013;

Somyajit et al., 2013; Nagaraju et al., 2006, 2009). Also, RAD51 paralogues have been implicated in the reversal of replication forks to promote the restart of stalled forks (Somyajit et al., 2015; Saxena et al., 2019; Longo et al., 2023; Berti et al., 2020b; Saxena et al., 2018). Guh *et al* (2023) highlighted that *in vitro* BCDX2 and CX3 function in fork protection with BCDX2 synergising with RAD51 to protect forks from MRE11 and EXO1-mediated digestion (Guh et al., 2023).

RAD51 filament formation can require the alternative recruitment of PALB2/BRCA2 via RNF168-mediated chromatin ubiquitylation, performing redundantly with BRCA1 (Zong et al., 2019). It's thought that 53BP1 antagonises RNF168-driven RAD51 filament formation in addition to blocking resection (Zong et al., 2019). One of the pathways involved in the localisation of the BRCA1-P complex to sites of DNA damage includes the RNF168 signalling pathway as BARD1 is recruited by RNF168-generated mUb-H2A via the BUDR domain of BARD1 (Krais et al., 2021; Becker et al., 2020).

The extended D-loop is resolved by one of three mechanisms: synthesis-dependent strand annealing (SDSA), a double Holliday junction (dHJ) or by dissolution to finally restore the DNA sequence (Fig.1.6) (Moynahan and Jasin, 2010; Rosen, 2013; Daley et al., 2014). In SDSA a homologous strand is created from DNA synthesis that is identical to the broken DNA end and so the two strands anneal once the extended D-loop has unwound, without forming Holliday junctions and producing non-crossover products only (Heyer et al., 2010; Wright et al., 2018). A Holliday junction is the generation of a four-way junction between the strands and Holliday junctions are resolved by the following proteins: MUS81 structure specific endonuclease subunit (MUS81) or Holliday junction 5'flap endonuclease (GEN1) alongside the scaffold protein SLX4 structure-specific endonuclease subunit (SLX4) (Schwartz and Heyer,

2011; Rass, 2013; Hromas et al., 2017). The dissolution of Double Holliday junctions involves the function of the dissolvasome which encompasses a type IA topoisomerase termed topoisomerase III (Top3/TopoIIIα) and the RecQ helicase BLM with the OB fold protein Rmi1 (Wu and Hickson, 2003; Fu et al., 1994; Plank et al., 2006; Cejka et al., 2010; Wu et al., 2005).

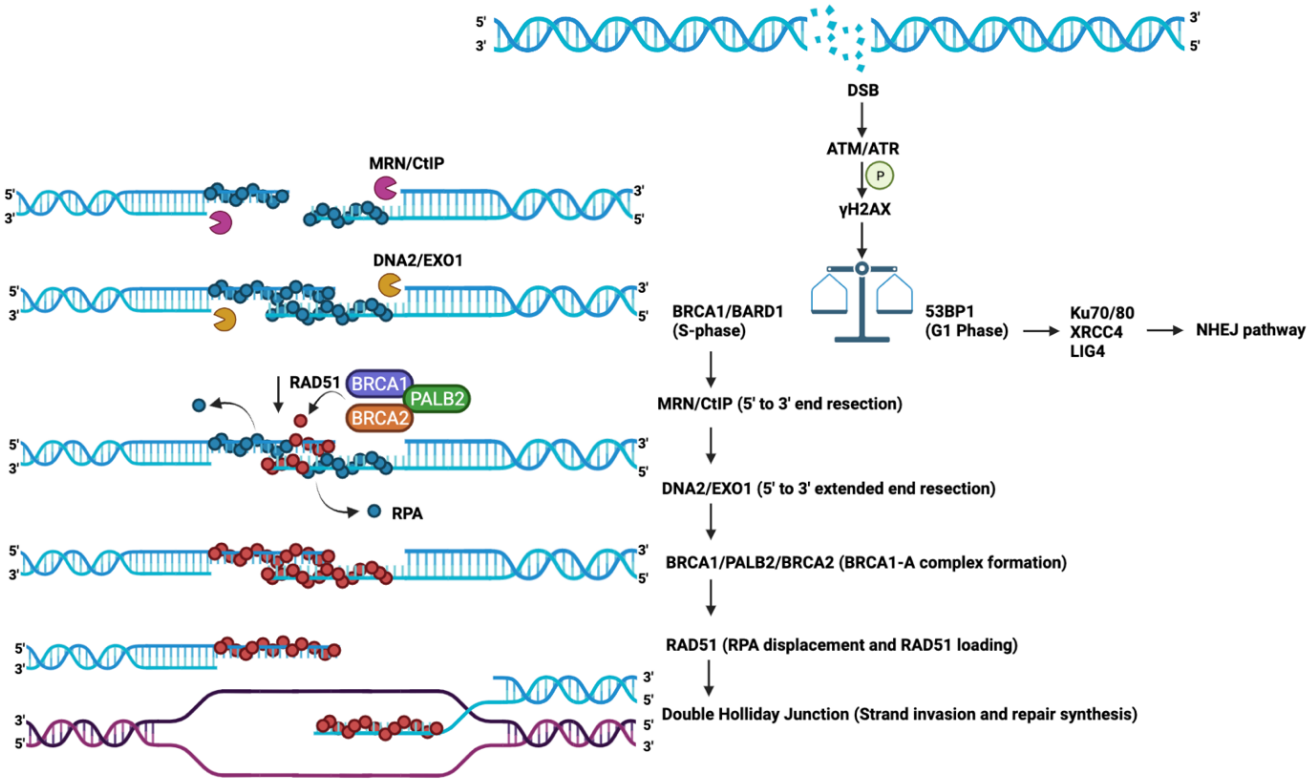

Figure 1.6 – Homologous recombination. Homologous recombination (HR), also known as homology-directed repair, is the main error-free DNA DSB repair pathway. DNA end resection is an early determinant of pathway choice, demonstrated by the antagonistic relationship between BRCA1 (HR) and 53BP1 (NHEJ). BRCA1 interacts with PALB2 and subsequently recruits BRCA2 to function within the later steps of HR. BRCA2 mediates RAD51 filament formation on the 3' single strands, followed by strand invasion, D-loop formation, and DNA repair synthesis. (Created using *BioRender.com*, inspired by (Orhan et al., 2021)).

1.3.3. Theta-mediated end joining

Originally termed alternative end joining (alt-EJ) or microhomology-mediated end joining (MMEJ), the DSB repair pathway is also characterised as polymerase θ-mediated end joining (TMEJ) (Boulton and Jackson, 1996; Kabotyanski et al., 1998; Sfeir and Symington, 2015; Koole et al., 2014). HR and TMEJ both require resected DNA ends and compete for 3' ssDNA overhangs (Truong et al., 2013), as the inhibition of HR factors such as BRCA1 or RPA can amplify TMEJ-mediated mutagenesis implying that HR-related proteins suppress TMEJ (Ahrabi et al., 2016). TMEJ is preferred over NHEJ because the 3' overhangs generated by the CtIP/MRN complex have undergone increased resection, producing elongated overhangs of 30-70 nucleotides (Wyatt et al., 2016). Poly (ADP-ribose) polymerase 1 (PARP1) is recruited to resected DNA ends and initiates TMEJ by recruiting DNA Polymerase θ (Polθ) (Audebert et al., 2004; Truong et al., 2013; Wang et al., 2006). The A-family polymerase Polθ (*POLQ)* is an error-prone translesion synthesis enzyme that harbours an N-terminal conserved super-family helicase domain, a central domain and a DNA polymerase domain at the C-terminus (Black et al., 2019; Newman et al., 2015). Polθ recruitment to DSBs is reduced in *PARP1*-deficient cells or in cells treated with PARP inhibitors, indicating that PARP1 inhibition reduces TMEJ (Mansour et al., 2010; Wang et al., 2006). Additionally, Kais *et al* (2016) showed that FA complementation group D2 (FANCD2) as well as PARP1 can mediate Polθ and CtIP recruitment to sites of DNA damage (Kais et al., 2016).

Polθ binds to long 3' ssDNA overhangs generated by exonuclease-mediated 5'-3' resection of DSBs (Truong et al., 2013; Chan et al., 2010). RPA is bound to resected 3' ssDNA and antagonises TMEJ by preventing the annealing of overhangs and

subsequently promotes HR (Deng et al., 2014). Ceccaldi *et al* (2015) demonstrated that the Polθ helicase domain contains 3 RAD51 binding domains and that in *BRCA1*-deficient cells, the helicase domain suppresses toxic RAD51 filament formation by restricting RAD51-ssDNA binding (Ceccaldi et al., 2015). Yet, Mateos-Gomez *et al* (2017) revealed that mutating this identified RAD51 binding site had no impact on cell viability in *BRCA1*-deficient cells (Mateos-Gomez et al., 2017). Mateos-Gomez *et al* (2017) revealed that in mammalian cells, the Polθ helicase function enables RPA removal from DSB ends using its ATP hydrolysis energy to mediate strand annealing by TMEJ (Mateos-Gomez et al., 2017). The removal of the helicase domain led to an inability to remove RPA and showed diminished chromosomal TMEJ (Mateos-Gomez et al., 2017). Moreover, the Polθ helicase functions in a similar way to RecQ type SF2 helicases as it unwinds DNA with 3'-5' polarity (Ozdemir et al., 2018).

During TMEJ, the polymerase domain undertakes fill-in synthesis and tethers DNA ends. The Polθ-polymerase domain extends ssDNA overhangs with 2-6 base pairs of microhomology but lacks proof reading activity as it bypasses thymine glycols and abasic sites (Seki et al., 2004; Hogg et al., 2012, 2011; Kent et al., 2015b; Ahrabi et al., 2016). The Polθ polymerase domain encompasses three insertion loops that aid in bypassing these bulky lesions as well as facilitate dimerisation (Brambati et al., 2020). Polθ is promiscuous as it undertakes template-dependent and template-independent DNA synthesis (Kent et al., 2016; Hogg et al., 2012). After Polθ undertakes strand displacement synthesis, which can form displaced ssDNA 5' flaps, these flaps are then repaired by flap structure-specific endonuclease 1 (FEN1) prior to ligation by DNA Ligase III/XRCC1 or Ligase I (Liang et al., 2005; Sharma et al., 2015; Kent et al., 2015b; Lu et al., 2016; Simsek et al., 2011; Liang et al., 2008).

A study revealed that BRCA2 and RAD52 inhibit the polymerase function of Polθ prior to mitosis by binding to ssDNA to delay its function until the onset of mitosis to ensure that one-ended DSBs are converted into two-ended DSBs (Llorens-Agost et al., 2021). Also, studies have shown that repair by Polθ cannot be inhibited by mitotic kinases, implying that TMEJ is the main form of repair during mitosis when HR and NHEJ are greatly reduced (Orthwein et al., 2015). Evidence for the repair of DSBs during mitosis by TMEJ has come to light. The 9-1-1 complex (RAD9-RAD1-HUS1) interacts with RAD9-HUS1-RAD1 Interacting Nuclear Orphan 1 (RHINO) and the phosphorylation of RHINO by Polo-like kinase 1 (PLK1) activates the localisation of Polθ to DSBs during mitosis to carry out TMEJ (Brambati et al., 2023). Also, PLK1 has been shown to directly stimulate Polθ recruitment to DSBs during M-phase (Gelot et al., 2023). On that account, during M-phase MDC1-Cancerous inhibitor of protein phosphatase 2A (CIP2A)-TOPBP1 complex facilitate the tethering of broken chromosomes to be pulled to centrosomes during anaphase and carried through mitosis to be repaired in G1 (De Marco Zompit et al., 2022; Leimbacher et al., 2019; Adam et al., 2021).

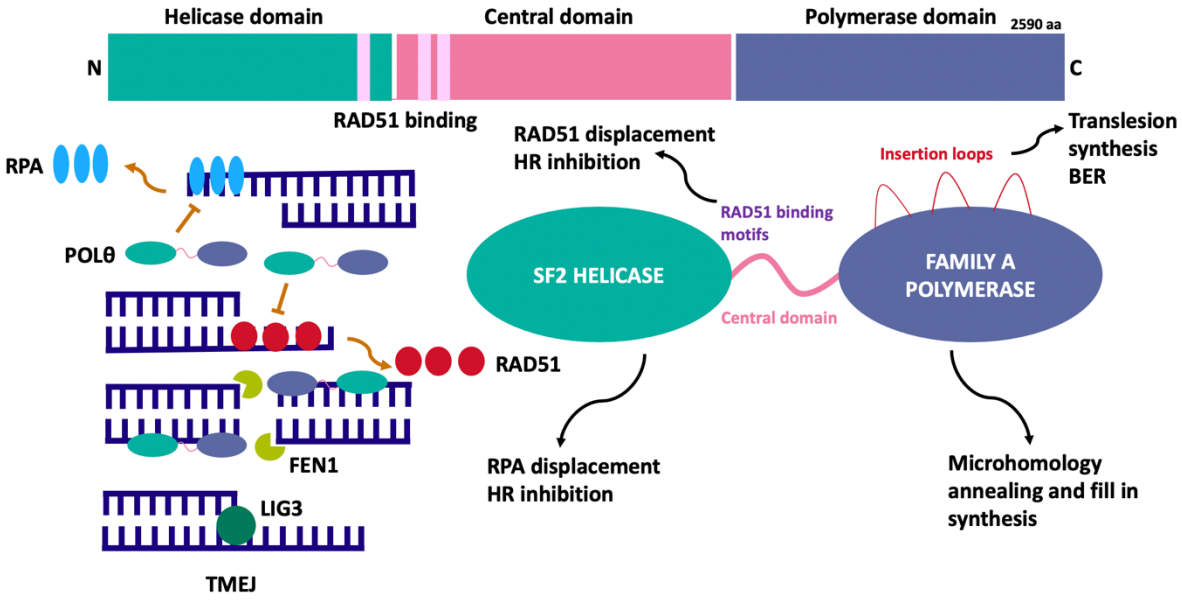

Figure 1.7 – Human Polθ domains showing the structures of the helicase, central domain and the family-A polymerase domain. The helicase domain functions to remove RPA to facilitate TMEJ and counteract HR as well as mediating dimerisation. Polθ contains 3 RAD51 binding motifs to suppress excessive RAD51 filament formation. The polymerase domain encompasses three insertion loops and extends ssDNA overhangs. (Based on (Schrempf et al., 2021; Brambati et al., 2020)).

1.3.4. Single strand annealing

Another error prone DSB repair pathway is the single strand annealing (SSA) pathway that has a pre-requisite for more extensively resected DNA. (Bhargava et al., 2016; Bennardo et al., 2008; Mortensen et al., 1996). RAD52 is the predominant protein involved in SSA and is a ssDNA-annealing protein that forms a heptameric ring (Stasiak et al., 2000). The N- and C-terminal structures of each monomer generates a positively charged ssDNA binding groove (Gottifredi and Wiesmüller, 2020). The human RAD52 N-terminal domain is important for DNA binding and multimerisation and the C-terminal domain encompasses RPA and RAD51-binding regions (Lloyd et al., 2005; Shen et al., 1996; Park et al., 1996). RAD52 binds to resected DNA ends

and mediates the annealing of homologous sequences of ssDNA (Hanamshet et al., 2016). After the annealing of ssDNA ends by RAD52, ERCC1 in complex with XPF binds to RAD52 to impede SSA (Motycka et al., 2004). The non-homologous 3'ssDNA tails are then removed by nucleolytic cleavage carried out by the RAD52-ERCC1-XPF complex (Symington, 2002; Rothenberg et al., 2008; Motycka et al., 2004). Then gap filling is mediated by DNA polymerases to form substrates to be ligated, however the specific proteins involved in this stage remain elusive (Bhargava et al., 2016; Blasiak, 2021). SSA can lead to copy number alterations and deletions making it a mutagenic repair pathway (Stark et al., 2004; Sugawara et al., 2004; Scully et al., 2019).

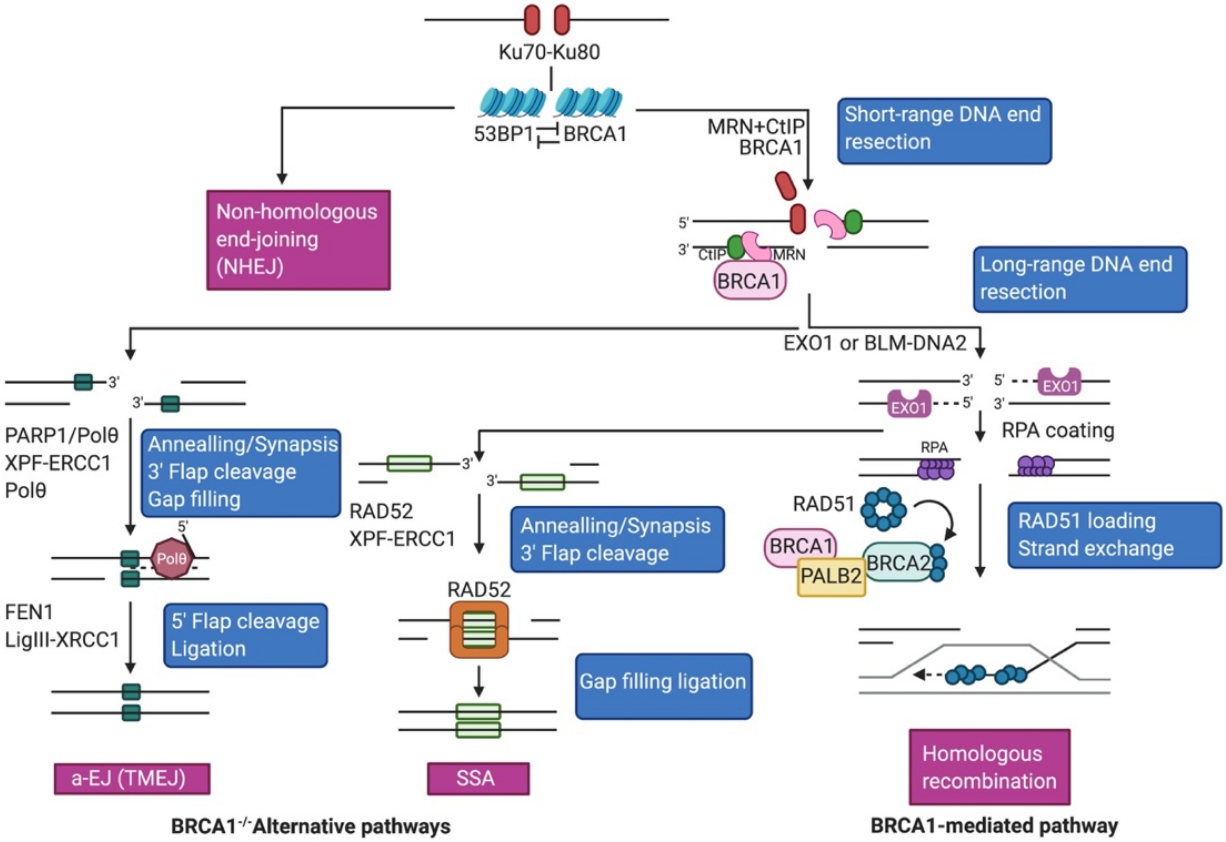

Figure 1.8 – Canonical and non-canonical double-strand break (DSB) repair pathways. Pol θ mediated end-joining (TMEJ) is an error prone pathway that facilitates the synapsis of opposing ends, then identifying and annealing internal microhomologies. Single-strand annealing (SSA) requires RAD52, although is a mutagenic form of repair that induces large

deletions between homologous repeats. (Created using *BioRender.com* based on (Trenner and Sartori, 2019)).

1.3.5. Additional DNA damage repair pathways

As well as the DNA damage repair pathways mentioned above, there are three more DDR pathways that are active throughout the cell cycle, which include base excision repair (BER), nucleotide excision repair (NER) and mismatch repair (MMR). BER repairs damaged DNA from alkylation, oxidation and deamination that does not extensively distort the structure of the DNA alpha helix (Lindahl, 1993). Depending on the DNA lesion, one of the 11 damage-specific DNA glycosylases are stimulated to remove the damaged uracil base and forms an abasic site (AP-site) (Loeb and Preston, 1986; Higgins et al., 1987; Krokan and Bjørås, 2013). BER is divided into either short-patch repair or long-patch repair which encompasses base excision, incision by the endonuclease APEX1, end processing, followed by repair synthesis and gap filling by POLB and finally by Ligase III which catalyses phosphodiester bond formation (Fig.1.9) (Krokan and Bjørås, 2013; Robertson et al., 2009).

NER facilitates the removal of bulky adducts and lesions that distort the DNA alpha helix induced by exposure to UV and cisplatin (Sancar, 2016; Pettijohn and Hanawalt, 1964; Rasmussen and Painter, 1964). The mammalian NER pathway is essential for repairing DNA damage caused by UV, which is reinforced by the fact that people harbouring NER gene mutations such as Xeroderma pigmentosum (Cleaver, 1968) are photosensitive and predisposed to developing skin cancers (Giordano et al., 2016; Robu et al., 2020). NER uses over 30 proteins to locate the DNA lesion, remove the

impaired nucleotides and synthesise a novel strand using the undamaged strand as a template followed by gap filling (Fig.1.9) (Marteijn et al., 2014).

MMR is highly conserved and is important for repair during recombination or due to external sources generating mismatched nucleotides (Kunkel, 2009). These insertions/deletions are repaired by the heterodimers MSH2-MSH6 and MSH2-MSH3 and subsequent recruitment of proteins involved in excision and resynthesis of the DNA strand (Fig.1.9) (Graham et al., 2018; Kleczkowska et al., 2001). The daughter strand containing the mismatched area is cut by the exonuclease EXO1 and annealed by DNA polymerase accessory proteins including proliferating cell nuclear antigen (PCNA) (Kadyrov et al., 2009). Inherited mutations in genes within the MMR pathway can cause hereditary Lynch syndrome, predisposing individuals to cancers such as early-onset colorectal cancers (Heinen, 2016; Pino et al., 2009).

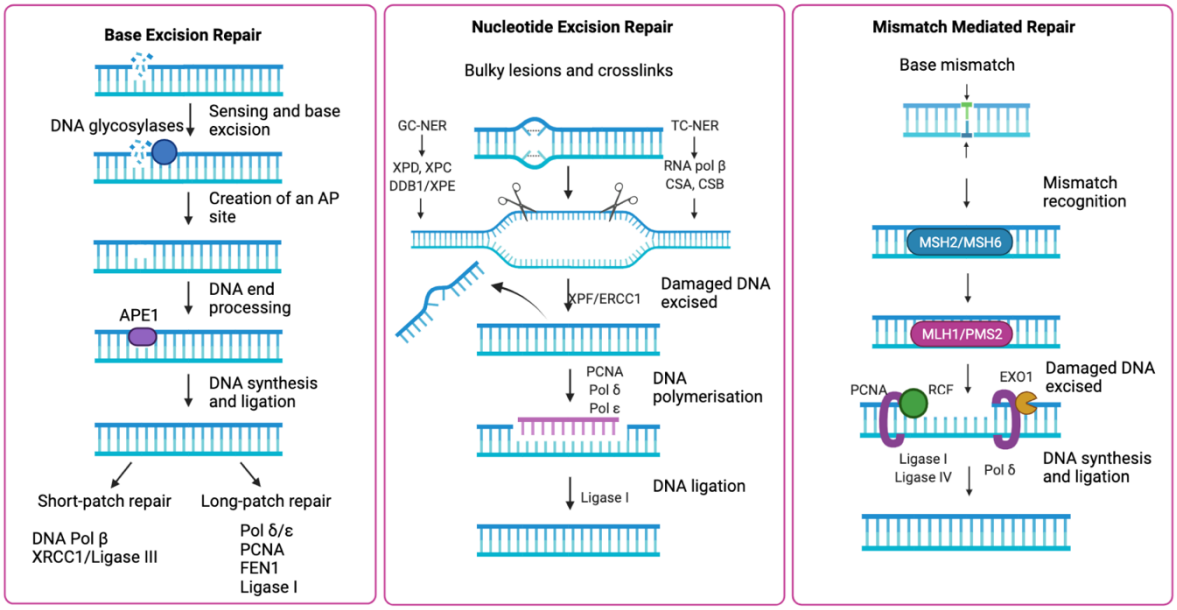

Figure 1.9 – Single-strand DNA repair pathways. Base damages and bulky adducts are generated by depurination and deamination repaired by base excision repair (BER). Bulky adducts such as UV radiation induced pyrimidine dimers are repaired by nucleotide excision repair (NER). Spontaneous base-base mismatches during DNA replication are repaired by mismatch repair (MMR). (Created using *BioRender.com* based on (Shadfar et al., 2023)).

1.4. DNA replication

During S-phase of the cell cycle, DNA synthesis takes place, which is facilitated by the replisome containing numerous proteins working in coordination to synthetise DNA at the replication origins (Aze and Maiorano, 2018; Alabert and Groth, 2012). DNA replication origins are activated at the start of M-phase, throughout G1-phase and are completed at S-phase prior to the start of DNA replication to guarantee that the entire genome is replicated prior to cell division as reviewed in Fragkos *et al* (2015) (Fragkos et al., 2015).

The sequential DNA replication licensing system ensures that no genome re-replication takes place (Blow and Laskey, 1988; Shreeram and Blow, 2003). During licensing, the pre-replication complex (pre-RC) is formed by the binding of specific proteins, such as the replicative helicase mini-chromosome maintenance (MCM2-7) complex (Hyrien, 2016; Remus et al., 2009; Tanaka and Diffley, 2002). Subsequently, DNA synthesis is activated during a stage called origin firing (Yeeles et al., 2015; Marheineke and Hyrien, 2004). Firstly, the origin replication complex (ORC) made up of ORC1-6 is localised and bound to chromatin at replication origins, with the subsequent binding of the CDC6 ATPase and CDC10-dependent transcript 1 (CDT1) (Maiorano et al., 2004; Aze and Maiorano, 2018). Both CDC6 and CDT1 recruit MCM2-7. The MCM2-7 double hexamer is fundamental for unwinding DNA and becomes activated by S-phase kinases (Masai et al., 2010; Aze and Maiorano, 2018; Remus et al., 2009). All together, these proteins make up the pre-RC (Fragkos et al., 2015). During S-phase pe-licensing is restricted so that chromosomes are only replicated once during the cell cycle (Blow and Gillespie, 2008).

The activation of replication origins involves the phosphorylation of MCM helicase complex subunits by DBF4-dependent kinase (DDK) and by cyclin-dependent kinases (CDKs), involving ATP and ATPase motifs (Kang et al., 2014; Tanaka et al., 2007). DDK binds to chromatin which subsequently phosphorylates the MCM complex, which leads to the recruitment of the CMG complex, consisting of CDC45, the MCM complex and the GINS complex, which goes on to form the pre-initiation complex (pre-IC) (Ilves et al., 2010). CDKs phosphorylate treslin (SId3 in yeast) to facilitate its association with (TOPBP1, Dpb11 in yeast), to activate CMG helicase which unwinds double-stranded DNA (Kumagai et al., 2010; Boos et al., 2011). DDK and CDKs phosphorylate numerous replication factors including MCM2-7 residues ultimately leading to the initiation of DNA unwinding by helicases (Ilves et al., 2010). The double MCM hexamer is dissociated into two active MCM hexamers generating two replisomes. These replisomes unwind the DNA to form two replication forks at each DNA replication origin (Heller et al., 2011; Fragkos et al., 2015).

The stimulation of helicase function initiates the recruitment of proteins such as replication factor C (RFC), PCNA, and RPA that transitions the pre-IC to two replication forks moving bidirectionally away from the origin (Kelch, 2016; Arbel et al., 2021; Ellison and Stillman, 2003; Cai et al., 1996; Bylund and Burgers, 2005). PCNA functions as a sliding clamp wrapped around DNA (Krishna et al., 1994; Gulbis et al., 1996), RFC loads PCNA onto DNA (Arbel et al., 2021; Bylund and Burgers, 2005; Bowman et al., 2004) and at 3'ss/double-stranded (dsDNA) junctions RPA mediates the loading of PCNA and RFC (Hayner et al., 2014). DNA unwinding allows for the replicative polymerases (α, δ, and ε) to synthesise the nascent DNA strands. The DNA polymerases function in the 3' to 5' direction, therefore the leading strand synthesises

in the direction of the replisome, whereas the lagging strand undergoes discontinuous replication in the opposite direction to the replisome, generating numerous Okazaki fragments (Burgers and Kunkel, 2017; Okazaki et al., 1968). RNA primers stimulate Okazaki fragment formation eventually forming one daughter duplex that is ligated together (Georgescu et al., 2014). Pol ε specifically synthesises the leading strand and Pol δ synthesises the lagging strand (Kunkel and Burgers, 2008). Progression of the replisome can be hindered by genotoxic stress such as DNA damage and interstrand crosslinks, with termination of the leading strand having more of an impact than cessation of the lagging strand which is more easily bypassed and tolerated (Guilliam, 2021; Zeman and Cimprich, 2014). This is because stalling of one Okazaki fragment does not impact the subsequent fragments (Fu et al., 2011).

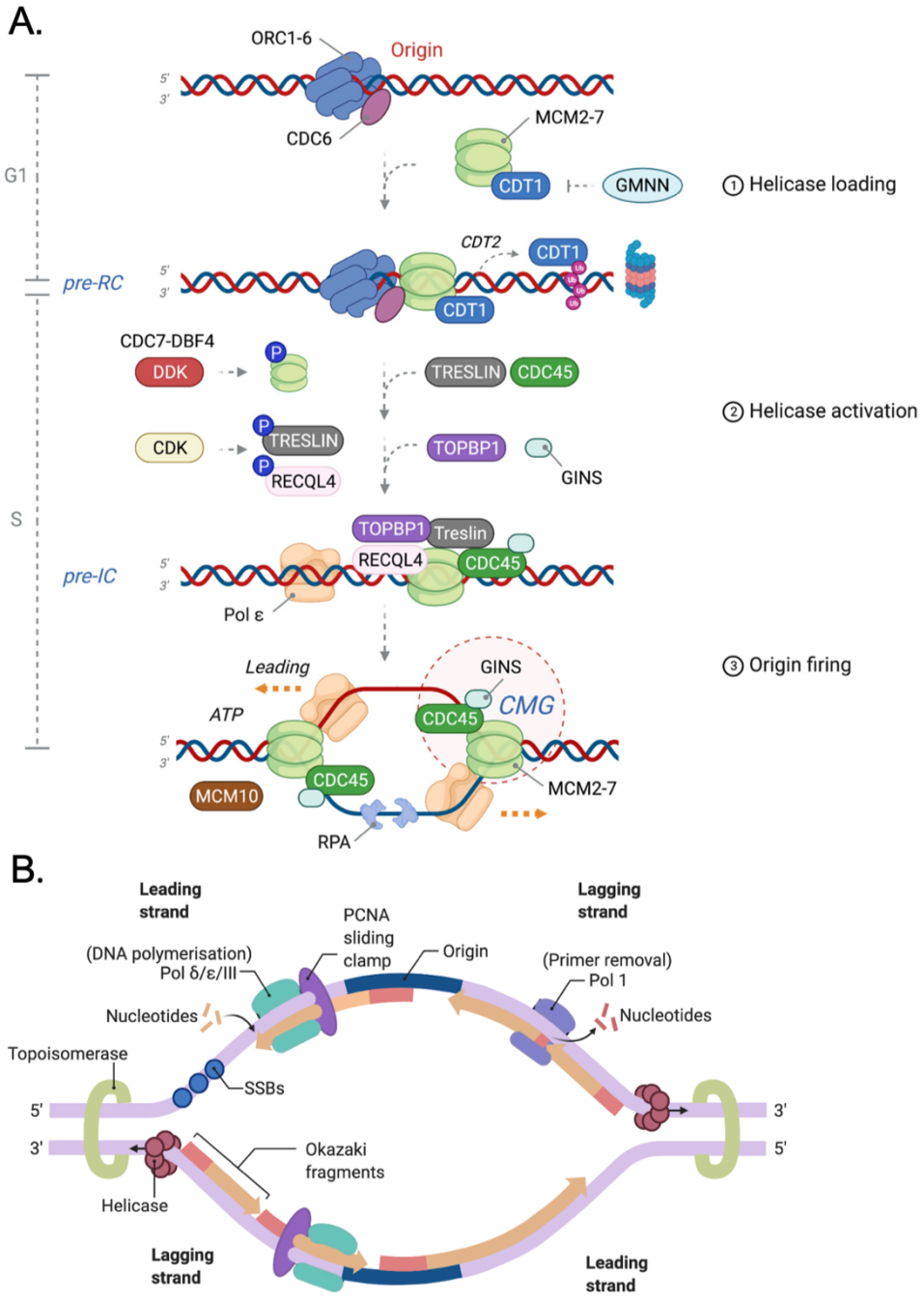

Figure 1.10 – Eukaryotic replisome formation during DNA replication. (A) Replication origin licensing and activation. OCR1-6 recruits CDC6 to load MCM2-7/CDT1 generating the pre-RC. CDT1 and GEMININ interact to restrict licensing to G1. The Pre-IC complex is formed by the phosphorylation of MCM2-7 by DDK (CDC7-DBF4) facilitating the binding of TRESLIN and RECQL4 which is subsequently phosphorylated by CDKs to mediate the formation of the CMG (CDC45-MCM2-GINS) helicase complex with Pol ε. The pre-IC associates with MCM10 to unwind dsDNA by the CMG complex and RPA protects the ssDNA generated. Two active

replication forks are formed and synthesise nascent DNA in the 5' to 3' direction. (B) Double-stranded DNA is unwound by helicase enzymes to allow for nascent DNA strand generation by the replicative polymerases (*α*, *δ*, and *ε*). The leading strand is synthesised in the 5' to 3' direction and the lagging strand is synthesised in the opposite direction forming discontinuous Okazaki fragments (Adapted from *BioRender.com* and (Saldanha et al., 2023)).

1.4.1. Replication fork stalling and reversal

The disruption to replication fork progression can be due to endogenous DNA lesions, collisions between replication and transcription machineries and because of challenging areas to replicate resulting in replication fork slowdown or stalling (García-Muse and Aguilera, 2016; Liao et al., 2018). To limit genomic instability, cells harbour replication fork protection mechanisms, such as fork stabilisation and restart which are fundamental for reducing the likelihood of DSB formation (Liao et al., 2018).

The accumulation of ssDNA is a hallmark of stress and is induced by the uncoupling of helicase-polymerase or nucleolytic processing (Sabatinos and Forsburg, 2015). RPA functions as a first responder at ssDNA sites and is loaded onto exposed ssDNA to avert secondary structure formation (Chen and Wold, 2014). RPA-ssDNA binding recruits the replication stress response protein SWI/SNF-related matrix-associated actin-dependent regulator of chromatin subfamily A-like protein 1 (SMARCAL1), catalysing regression of the stalled replication fork and promoting Holliday junction branch migration (Bétous et al., 2012). ATR and DNA-PKcs phosphorylate RPA bound to ssDNA to mediate DNA synthesis repair rather than replication and ATR and CDK-cyclin B phosphorylation of RPA recruits BRCA2 and PALB2 to promote fork stalling (Vassin et al., 2004; Liu et al., 2012; Murphy et al., 2014). Additionally, in response to fork stalling, RPA is ubiquitinated on chromatin by the E3 ligase Ring Finger and WD

Repeat Domain 3 (RFWD3) which facilitates HR repair and fork restart (Elia et al., 2015; Duan and Pathania, 2020). The intracellular RPA pool is finite and requires ATR/CHK1-dependent checkpoint activation which limits origin firing and the DDI1/2-RTF2 pathway limits surplus ssDNA at stalled forks, targeting ubiquitinated substrates for proteasomal degradation to prevent genome instability (Shechter et al., 2004; Petermann et al., 2010; Kottemann et al., 2018; Nowicka et al., 2015). The RPA-ssDNA interaction is subsequently displaced by RAD51 which facilitates replication fork reversal (Liao et al., 2018). DNA replication forks are remodelled into a four-way junction, also known as a 'chicken foot' by the simultaneous unwinding and annealing of parental and nascent DNA strands, forming a regressed arm (Neelsen and Lopes, 2015; Zellweger et al., 2015; Tye et al., 2020). Fork reversal temporarily disables fork progression to allow for the repair of DNA lesions to take place (Neelsen and Lopes, 2015).

RAD51 and the SNF2-family DNA translocases SMARCAL1, Zinc Finger RANBP2-Type Containing 3 (ZRANB3) and Helicase Like Transcription Factor (HLTF), as well as the FBH1 helicase facilitate fork reversal (Achar et al., 2011; Bétous et al., 2012; Taglialatela et al., 2017; Vujanovic et al., 2017; Fugger et al., 2015). Fork reversal is fundamental to prevent surplus ssDNA accumulation and convert DNA lesions to dsDNA for repair (Joseph et al., 2020). SMARCAL1 is recruited to stalled forks by interacting with RPA and is restrained at forks by RAD52 (Malacaria et al., 2019). ZRANB3 is associated with polyubiquitinated PCNA and harbours DNA translocase activity to catalyse fork reversal once RPA has been removed (Vujanovic et al., 2017; Ciccia et al., 2012). The E3 ligase HLTF polyubiquitinates PCNA and has dsDNA translocase activity to mediate fork regression but can also facilitate strand invasion

and D-loop formation (Burkovics et al., 2014; Bai et al., 2020; Motegi et al., 2008). HLTF-mediated polyubiquitination of PCNA can recruit ZRANB3 to forks (Ciccia et al., 2012; Tye et al., 2020). Also, RFWD3 promotes the polyubiquitination of PCNA to mediate fork reversal in a ZRANB3-dependent manner (Moore et al., 2023). In *BRCA1/2*-deficient cells, the inactivation of the SNF2-family DNA translocases salvages fork protection stability by protecting stalled forks from degradation by MRE11 as these fork remodellers facilitate MRE11-dependent nascent DNA degradation (Taglialatela et al., 2017). Fork reversal can also be facilitated by Fanconi Anaemia complementation group M (FANCM), RAD54, BLM, Werner syndrome protein (WRN) and RECQL5 (Tye et al., 2020; Machwe et al., 2006; Yan et al., 2010; Bugreev et al., 2011). Also, the strand-exchange activity of RAD51 is important for fork reversal without the need to unload the replication machinery thus maintaining the helicase in a position to resume DNA synthesis. Yet, RAD51 is not required if the CMG helicase is displaced from forks (Liu et al., 2023).

1.4.2. Replication fork protection and restart

Stalled replication forks are vulnerable to nucleolytic degradation by nucleases such as MRE11, DNA2, CtIP and EXO1 (Lemaçon et al., 2017; Thangavel et al., 2015). The stabilisation of RAD51, when bound to ATP, is a major factor in fork protection from degradation (Van der heijden et al., 2007). In *BRCA2*- and *FANCD2*-deficient cells treated with hydroxyurea (HU), the overexpression of RAD51 or the presence of the RAD51 mutant RAD51-K133R (defective ATPase activity) can rescue replication fork degradation (Schlacher et al., 2012; Tye et al., 2020). Whilst patients that harbour the following RAD51 mutations: T131P and A293T (forming unstable nucleoprotein filaments) displayed features of FA, termed FA-RAD51 mutations (Ameziane et al.,

2015). Zadorozhny *et al* (2017) used *Xenopus laevis* egg extracts to demonstrate that the FA-RAD51 mutations cannot protect stalled forks from MRE11 exonuclease activity by destabilising RAD51 nucleofilaments due to defective ATP-binding (Zadorozhny et al., 2017). FANCD2 has been identified as a stabiliser of RAD51 nucleofilaments, as the loss of FANCD2 leads to reduced RAD51 foci numbers and a lowered interaction with PCNA (Sato et al., 2016).

BRCA1 and BRCA2 function to suppress MRE11-mediated degradation as the loss of these tumour suppressor proteins results in fork degradation and genome instability (Taglialatela et al., 2017). BRCA2 is fundamental at stalled replication forks as it facilitates RAD51 nucleofilament formation when exposed to stress which protects the fork from MRE11 (Schlacher et al., 2011; Ying et al., 2012). This role of BRCA2 is independent from its role in DSBs, reinforced by the discovery of a conserved C-terminal site which is fundamental for RAD51 filament stabilisation but not for RAD51 loading onto ssDNA (Schlacher et al., 2011). Replication fork protection via BRCA2-PALB2 is independent of BRCA1, unlike during HR and is thought to be facilitated by RNF168, ATR and phosphorylated RPA (Daza-Martin et al., 2019; Yazinski et al., 2017; Murphy et al., 2014; Luijsterburg et al., 2017). An additional recruitment is that PALB2 might directly bind to chromatin and that the WD40 domain can bind to RAD51 and RAD51C (Sy et al., 2009b; Belotserkovskaya et al., 2020; Park et al., 2014; Tye et al., 2020). Also a recruitment mechanism of BRCA2 has been demonstrated that is independent of PALB2; an interaction between BRCA2 and the cohesion cofactor PDS5 (Brough et al., 2012). Furthermore, the phosphorylation-directed peptidylprolyl Cis/Trans Isomerase, NIMA-interacting 1 (PIN1) induces a conformational change of the BRCA1/BARD1 heterodimer increasing the complexes' affinity for RAD51,

protecting the replication fork from MRE11-mediated degradation (Daza-Martin et al., 2019). Mutating the interaction face between BARD1-RAD51 and the phosphorylation site on BRCA1 eliminates the ability of the heterodimer to protect replication forks, despite still functioning normally during HR (Daza-Martin et al., 2019). This conformational change is facilitated by CDK1-mediated or CDK2-mediated phosphorylation of BRCA1 (Daza-Martin et al., 2019).

Replication fork restart is essential to avoid a build-up of replication intermediates and involves the conversion from a four-way junction back to a three-way DNA junction (Liptay et al., 2020). The helicase RECQ1 associates with replication origins and is involved in priming branch migration and mediates fork restart at reversed replication forks (Thangavel et al., 2010; Sharma et al., 2007). Furthermore, replication forks can be restarted by nascent strand unwinding in regressed arms by WRN and DNA2 (Murfuni et al., 2012). The ATM and ATR kinases mediate WRN recruitment and activity at replication forks. ATR phosphorylates WRN at its C-terminus controlling the formation of WRN nuclear foci formation and co-localisation with RPA, whereas ATM-mediated phosphorylation of WRN mediates RAD51 nuclear foci generation to allow for efficient recovery of collapsed forks (Ammazzalorso et al., 2010). Additionally, the dual helicase and exonuclease functions of WRN restrict HU-treated fork breakage by MUS81 (Ammazzalorso et al., 2010). DNA2 functions with WRN to degrade reversed forks and mediate replication restart following HU treatment (Thangavel et al., 2015). Therefore, genomic maintenance is aided by replication fork restart by RecQ1 and DNA2/WRN in S-phase (Berti et al., 2013; Liptay et al., 2020). Overall, cells have adapted numerous replication restart mechanisms as aberrant replication fork restart can lead to developmental defects and cancer (Li et al., 2020b; Scully et al., 2021).

1.5. DNA damage tolerance pathways

To prevent continuous fork stalling and facilitate timely fork progression, cells elicit DNA damage tolerance (DDT) pathways so that replication can continue despite the presence of DNA damage by performing fork reversal (covered in section 1.4.1), template switching (TS), translesion synthesis (TLS), and replication fork repriming (Saldanha et al., 2023; Quinet et al., 2021).

1.5.1. Template switching

TS is active during S-phase and is an error-free DDT pathway that is activated by the poly-ubiquitination of PCNA by SNF2 histone linker PHD RING helicase (SHPHR) or HLTF to localise to the Rad6/Rad18 complex (Xu et al., 2015). Also, INO80 promotes the addition of K63-linked poly-ubiquitin chains to PCNA by SHRPH and HLTF (Falbo et al., 2009). The 9-1-1 complex binds to the gap on nascent DNA at the 5' end and stimulates the recruitment of Exo1 (Karras et al., 2013). On the template strand, a Rad51-ssDNA presynaptic filament forms, stabilised by Rad55/Rad57, and the filament works in conjunction with Rad54 and Rad52 to mediate a homology search and carry out strand invasion of the sister chromatid (Vanoli et al., 2010; Zhang and Lawrence, 2005; Ler and Carty, 2022). The invading strand and the homologous template undergo complementary base-pairing and DNA polymerase δ mediates DNA synthesis to form a D-loop and a sister-chromatid junction (SCJ) (Vanoli et al., 2010; Symington, 2002; Branzei, 2011; Bi, 2015; Ler and Carty, 2022). Successively, the slow growth suppressor 1 (Sgs1)/DNA topoisomerase 3 (Top3)/RECQ-mediated genome instability protein 1 (Rmi1) (Sgs1/Top3/Rmi1) complex resolves the SCJ to

complete the process (Giannattasio et al., 2014; Cejka et al., 2012; Bernstein et al., 2009; Ler and Carty, 2022).

1.5.2. Translesion synthesis

TLS is activated by the mono-ubiquitination of PCNA at lysine 164 by the RAD6-RAD18 E2-E3 ubiquitin ligase complex to mediate the transition from error-free replicative polymerases (δ or ε) to error-prone TLS polymerases (Chang and Cimprich, 2009; Stelter and Ulrich, 2003; Kannouche et al., 2004). In humans TLS polymerases are made up of the Y-family (Polη, Polι, Polκ and REV1), the B-family (Polζ (REV3/REV7)), the A-family (Polθ) and the archaeo-eukaryotic primase (AEP) family Primase and DNA directed polymerase (PRIMPOL) (Lehmann et al., 2007; Bienko et al., 2005; Guo et al., 2009; Friedberg et al., 2002). Mono-ubiquitinated PCNA can interact directly to Y-family polymerases Polη and Polκ via their ubiquitin-binding zinc fingers (UBZ) and to Polι and REV1 via their ubiquitin-binding motifs (UBM) (Ma et al., 2020; Bienko et al., 2005). PCNA can also bind to Polη, Polι, Polκ via the PCNA-interacting peptide (PIP) boxes and to REV1 via its N-terminal BRCT domain (Pustovalova et al., 2013; Guo et al., 2006a; Ma et al., 2020; Prakash et al., 2005).

TLS can take place via two mechanisms: one involving a single polymerase and the other encompassing multiple. Either one polymerase inserts a nucleotide at the lesion followed by extension past the site or two polymerases act: one inserting the nucleotide opposite the lesion and the other mediates primer extension across the site (Quinet et al., 2018; Yang and Gao, 2018; Livneh et al., 2010). PCNA acts as a TLS polymerase “tool belt” to coordinate the insertion of a nucleotide at the lesion site by TLS polymerases such as Polη or Polκ, followed by extension by a specific polymerase typically Polζ, subsequently transitioning back to a replicative polymerase (Masutani

et al., 1999; Zhao et al., 2012; Masutani, 2000; Huang et al., 2003; Zhang et al., 2000a; Nayak et al., 2021). TLS can also be activated independently of PCNA ubiquitination by a REV1 scaffold domain “bridge” that can associate with multiple TLS polymerases, which is termed “on-the-fly” bypass (Powers and Washington, 2018; Boehm et al., 2016; Edmunds et al., 2008). The Y-family TLS polymerases lack replication fidelity because of absent 3’ to 5’ proofreading exonuclease activity and a larger, more open active site that incorporates altered bases (McCulloch and Kunkel, 2008; Sale et al., 2012; Biertümpfel et al., 2011; Temprine et al., 2020). Moreover, TLS polymerases have been shown to be upregulated in numerous cancers, such as the overexpression of Polκ in the tumour tissue of lung cancer and glioblastoma patients and increased expression of Polη in head and neck squamous cell carcinoma (Zhou et al., 2013; Bostian et al., 2016; O-Wang et al., 2001; Peng et al., 2016). Numerous cancers have gained TLS as an adaptation to mediate lesion bypass and avoid replication barriers, which augments mutability, forming TLS-specific mutational signatures (Alexandrov et al., 2013; Nayak et al., 2021).

1.5.3. Repriming

PRIMPOL is a member of the AEP superfamily and the enzyme functions as TLS polymerase and a primase mutually, localised to both the nucleus and mitochondria (García-Gómez et al., 2013; Wan et al., 2013; Mourón et al., 2013; Bianchi et al., 2013). Exogenous and endogenous toxic lesions such as G-quadruplexes, R-loops, chain terminating nucleotides and UV lesions result in a replication hindrance, so PRIMPOL binds to RPA to carry out fork restart and utilises its DNA primase function to form a DNA primer (Mourón et al., 2013; Saldanha et al., 2023). The recruitment of PRIMPOL to ssDNA behind the CMG complex requires the interaction between PRIMPOL’s RPA

binding motifs and RPA70 (Guilliam et al., 2017). The polymerase activity extends the primer beyond the lesion, assisted by polymerase-delta interacting protein 2 (PolDIP2), prior to the restriction of further extension by the interaction between the PRIMPOL zinc finger domain and RPA. Subsequently, PRIMPOL dissociates from the template strand allowing for the re-association of the replicative polymerase to complete DNA replication (Guilliam et al., 2017). Yet, a ssDNA gap is generated that needs to be filled-in by post-replicative repair (PRR) (Mourón et al., 2013).

PRIMPOL-generated ssDNA gaps are resolved either by additional resection followed by HR or PRR through TLS via the REV1/POLζ complex (Piberger et al., 2020; Tirman et al., 2021b; Taglialatela et al., 2021). PRIMPOL exhibits limited processivity with regards to DNA synthesis and is unlikely to incorporate more than four nucleotides on template DNA (Keen et al., 2014; Quinet et al., 2021). PLK1 phosphorylates PRIMPOL at conserved RPA binding motifs and this modification is altered throughout the cell cycle to ensure correct localisation of PRIMPOL to chromatin (Bailey et al., 2021). PRIMPOL-dependent repriming acts on the leading strand, yet, it should not be discounted that PRIMPOL could act on the lagging strand, however this would be redundant due to the action of pol α-primase (Bainbridge et al., 2021; Díaz-Talavera et al., 2022)

In situations where fork reversal is inactivated by the removal of HLTF or SMARCAL1, PRIMPOL repriming can rescue stalled replication forks (Bai et al., 2020; Quinet et al., 2020). Also, *BRCA1*-deficient cells treated with several doses of cisplatin prevent replication fork reversal and activates PRIMPOL-mediated repriming to limit excess reversed fork degradation in the absence of BRCA1/2 (Quinet et al., 2020). BRCA2 associates with MCM10 to prevent error-prone PRIMPOL-mediated repriming and gap

formation (Kang et al., 2021). In addition, *Brca2*-mutated mouse embryonic fibroblasts (MEFs) that lack RAD51 stabilisation elicit elevated PRIMPOL-mediated repriming and ssDNA gap generation (Lim et al., 2023). PRIMPOL is not essential for cell viability as human and mice knock-out cell lines are viable (Bianchi et al., 2013; Quinet et al., 2020; Bailey et al., 2019; González-Acosta et al., 2021; Mourón et al., 2013), yet cells lacking PRIMPOL elicit reduced proliferation and restart, form elevated yH2AX and RPA foci, and generate micronuclei and increased sister chromatid exchanges in the presence of genotoxic stress (Wan et al., 2013; Mourón et al., 2013; Bailey et al., 2019; González-Acosta et al., 2021). Overall, the DDT pathway choice is regulated by different factors such as the nature of DNA damage, the genetic background, the extent of fork stalling and the post-translational modifications of the “tool belt” PCNA (Saldanha et al., 2023).

On the lagging strand repriming is undertaken by the Polα-primase complex which forms ssDNA gaps which are formed in *BRCA1/2*-deficient cells in the presence of replication stress. In *BRCA1/2*-deficient cells Polα-generated lagging strand gaps result in the retention of Chromatin Assembly Factor 1 (CAF-1) and so cannot be recycled (Thakar et al., 2022). Therefore, there is a reduced availability of CAF-1 at ongoing forks resulting in fork degradation (Thakar et al., 2022). Also, Mann *et al* (2022) revealed that RAD51 and Polθ bind to DNA on lagging strands to protect replication forks from MRE11-dependent endo-nucleolytic fork cleavage (Mann et al., 2022).

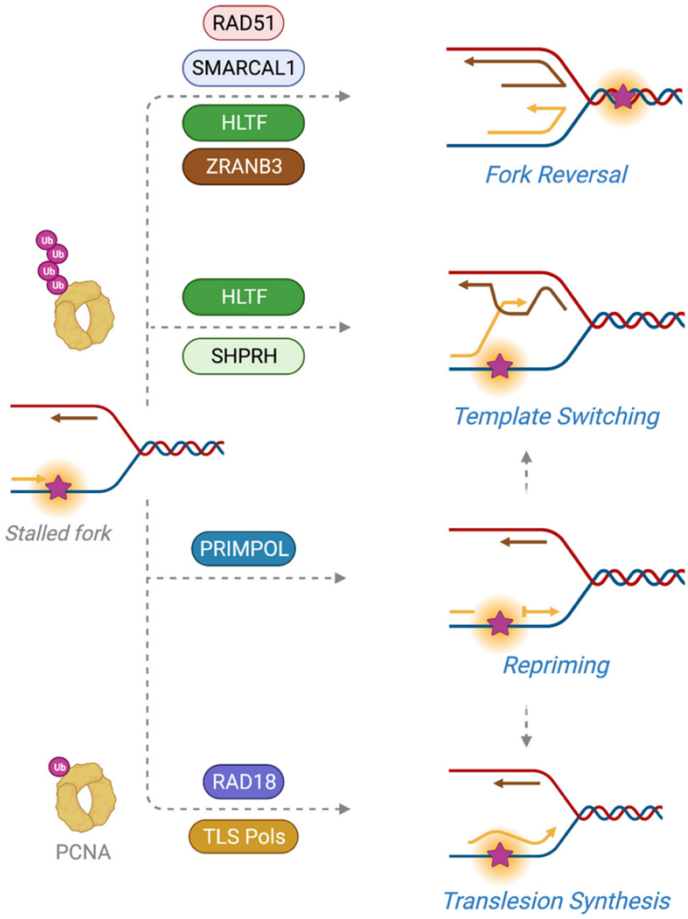

Figure 1.11. DNA damage tolerance pathways. Stalled replication forks can respond to DNA damage using different DNA damage tolerance (DDT) pathways. Fork reversal involves the formation of a four-way chicken foot structure, followed by DNA stabilisation for fork restart which is facilitated by RAD51 and fork remodellers (SMARCAL1, ZRANB3, HLTF). HLTF and SHPRH-mediated poly-ubiquitination of PCNA instigates error-free template switching (TS) using the nascent daughter strand on the sister chromatid. PRIMPOL-dependent repriming can bypass a DNA lesion to allow DNA replication to continue beyond the lesion, forming a ssDNA gap to be repaired by post-replicative repair (PRR). Mono-ubiquitination of PCNA by RAD18 activates translesion synthesis (TLS), involving the transition from replicative polymerases to error-prone TLS polymerases for lesion bypass. PRR can be undertaken by either TS or TLS. (Adapated from (Saldanha et al., 2023)).

1.5.4. Replication ssDNA gaps and DNA synthesis gap fill-in

Replication fork repriming results in leading strand unreplicated ssDNA gaps as DNA synthesis takes place downstream of the toxic lesion, requiring post-replicative gap filling of the ssDNA gap (Bianchi et al., 2013; García-Gómez et al., 2013; Mourón et al., 2013; Wan et al., 2013). ssDNA replication gaps are thought to underlie the BRCA1/2 cancer phenotype as *BRCA1/2*-deficient cells generate ssDNA gaps due to insufficient replication restraint, rendering cells sensitive to genotoxic stress (Panzarino et al., 2021). In *BRCA1/2*-mutated tumours, the restoration of fork restraint and DNA synthesis gap fill-in led to therapy resistance, uncoupled from HR and fork protection restoration when ssDNA gaps are present (Cong et al., 2021; Panzarino et al., 2021; Simoneau et al., 2021; Nayak et al., 2020). Also, Paes Dias *et al* (2021) stated that the loss of Ligase III enhanced cell susceptibility to PARPi by encouraging MRE11-mediated post-replicative ssDNA gaps in *BRCA1/53BP1*-deficient cells (Paes Dias et al., 2021).

ssDNA gaps formed behind the replication fork are filled by PRR which is facilitated by TLS as well as an alternative HR pathway involving RAD51 which can perform gap fill-in opposite a bulky lesion or abasic site (Adar et al., 2009; Piberger et al., 2020; Tirman et al., 2021b). Temporally distinct mechanisms of PRR have been identified: the PCNA poly-ubiquitination factor UBC13 and RAD51 stimulate PRR during S-phase, whilst RAD18-mediated mono-ubiquitination of PCNA activates PRR by the REV1-POLζ complex during G2, which can also function during S-phase (Tirman et al., 2021b). Additionally, BRCA1/2 can function in both S and G2 phase to mediate DNA synthesis gap fill-in by preventing MRE11 nuclease activity (Tirman et al., 2021b).

In keeping with this, the A-family polymerase Polθ has been shown to be involved in the sealing of post-replicative ssDNA gaps. Belan *et al* (2022) showed that in BRCA1 hypomorphs and BRCA2-depleted cells Polθ limits ssDNA gap formation by performing microhomology-mediated gap skipping to prevent genome instability (Belan et al., 2022). Likewise, Mann *et al* (2022) demonstrated that the polymerase domain of Polθ extends stalled Okazaki fragments and its helicase domain subsequently removes them to prevent ssDNA gap accumulation on lagging strands in the absence of functional RAD51 for fork reversal (Mann et al., 2022). Also, Polθ prevents the MRE11-mediated endo-nucleolytic cleavage of unprotected ssDNA gaps leading to asymmetric single-ended DSBs (Mann et al., 2022). Finally, Schrempf *et al* (2022) agree that in *BRCA1*-deficient cells Polθ functions in replication gap filling to extend ssDNA gaps and enable fork progression (Schrempf et al., 2021). Polθ is known to be recruited by PARP1 (Mateos-Gomez et al., 2015), but there is evidence for Polθ-mediated recruitment by ubiquitinated PCNA and so Polθ could also be localised by TLS signalling (Yoon et al., 2019). Overall, DDT mechanisms allow for the continuation of replication in the face of toxic lesions to reduce genome instability (Ler and Carty, 2022).

1.6. Synthetic lethal interactions with *BRCA1*-deficiency

BRCA1-mutated cells are reliant on non-canonical pathways for support, making the proteins involved potential therapeutic targets. An effective therapeutic approach for treating *BRCA1*-deficient tumours is synthetic lethality, which is the simultaneous disruption of two genes leading to cell or organismal death, yet the perturbation of either gene alone remains viable (O'Neil et al., 2017; Topatana et al., 2020). It is

therefore important to improve our understanding of the function of BRCA1 using synthetic lethal approaches.

1.6.1. Poly(ADP-ribose) polymerase 1 (PARP1)

The poly(ADP-ribose) polymerase (PARP) proteins such as PARP1 facilitate PARylation of substrate proteins involved in the DNA damage response and PARP1 is able to detect SSBs which are repaired by BER (Caldecott, 2008; Dantzer et al., 1999, 2000). PARP1 deficient cells or the inhibition of PARP1 show hypersensitivity to DNA damaging agents that create base lesions (Ménissier De Murcia et al., 1997; Wang et al., 1997). *BRCA1*-deficient tumour cells are hypersensitive to PARPi (D'Andrea, 2018; Bryant et al., 2005; Farmer et al., 2005). The synthetic lethal interaction between PARPi and *BRCA1/2*-deficiency has shown success in the clinic, with several FDA-approved PARPi available for treating numerous cancers (Yi et al., 2019; Lord and Ashworth, 2017; Mateo et al., 2019). Patients harbouring *BRCA1* germline mutations demonstrate a better prognosis when treated with PARPi including Olaparib, Rucaparib and Niraparib (He et al., 2018; Yang et al., 2011; Farmer et al., 2005).

There are numerous mechanisms of action of PARPi including: the disruption of PARP1 induced transcription of proteins such as those involved in cancer cell survival, inhibition of SSB repair, initiation of NHEJ, replication fork stalling and PARP trapping and the more recent discovery of the induction of aberrant processing of Okazaki fragments (Rose et al., 2020). Originally it was perceived that the presence of PARPi leads to PARP1 inactivation and trapping, elevating the cytotoxic impact of the drug, which can be resolved in HR-proficient cells with a functional DSB repair pathway (Pommier et al., 2012). Therefore, in HR-deficient cells, these PARP trapping blocks

cannot be surpassed and this results in cell death of HR-deficient tumours (Bryant et al., 2005; Noordermeer and van Attikum, 2019). In keeping with this, it was been proposed that replication fork collision induces DSBs with *BRCA1* mutations harbouring defects in fork protection, thereby leading to chemoresistance when fork protection is restored (Feng and Jasin, 2017; Schlacher et al., 2012; Lomonosov et al., 2003).

Replication ssDNA gaps have become a determinant of the PARPi/BRCA1 synthetic lethality (Hanzlikova et al., 2018; Kolinjivadi et al., 2017a; Panzarino et al., 2021; Cong et al., 2021). Olaparib accelerates DNA replication rather than slowing or stalling replication as previously thought, but is in agreement with PARP1 inducing replication fork reversal (D'Andrea, 2018; Pommier et al., 2012; Michelena et al., 2018; Maya-Mendoza et al., 2018; Ray Chaudhuri and Nussenzweig, 2017). Therefore, it is unconstrained replication that is inducing DSBs in the presence of PARPi (Maya-Mendoza et al., 2018; Quinet and Vindigni, 2018). PARPi create ssDNA breaks, gaps and nicks which are likely due to Okazaki fragment processing (OFP) or disrupted PARPi-mediated ssDNA repair (Lord and Ashworth, 2012; van Wietmarschen and Nussenzweig, 2018; Hanzlikova et al., 2018; Leppard et al., 2003; Cong et al., 2021). PARP has been shown to be a "back-up" pathway in OFP in the absence of FEN1 or LIG1, so PARPi are thought to abrogate OFP forming lagging strand ssDNA gaps (Azarm and Smith, 2020; Hanzlikova and Caldecott, 2019; Hanzlikova et al., 2018; van Wietmarschen and Nussenzweig, 2018).

BRCA1/2 are essential to prevent DNA replication ssDNA gaps as well as carry out HR and fork protection (Panzarino et al., 2021; Kolinjivadi et al., 2017b, 2017a; Schlacher et al., 2011; Somyajit et al., 2021). It is thought that replication gaps could

be causing under-replication in *BRCA1*-deficient cells with the HR protein RAD51 being important for replication gap suppression and so cells deficient of BRCA1 and RAD51 could harbour excess gaps when treated with PARPi (Kolinjivadi et al., 2017a; Panzarino et al., 2021). Defects in OFP leads to RPA pool exhaustion so sensitises cells to PARPi. yet in *BRCA1*-deficient cells with defective OFP, the loss of 53BP1 can rescue this impairment by initiation the PARP1-XRCC1-Ligase III lagging strand ligation pathway, therefore implying that lagging strand gaps are a biomarker of PARPi response in these *BRCA1*-mutated cancers (Panzarino et al., 2021; Hanzlikova et al., 2018; Arakawa and Iliakis, 2015; Kumamoto et al., 2021). Recent studies have deduced that ssDNA replication gaps underlie *BRCA*-deficiency and therapy response as opposed to HR and fork protection (Panzarino et al., 2021; Cong et al., 2021).

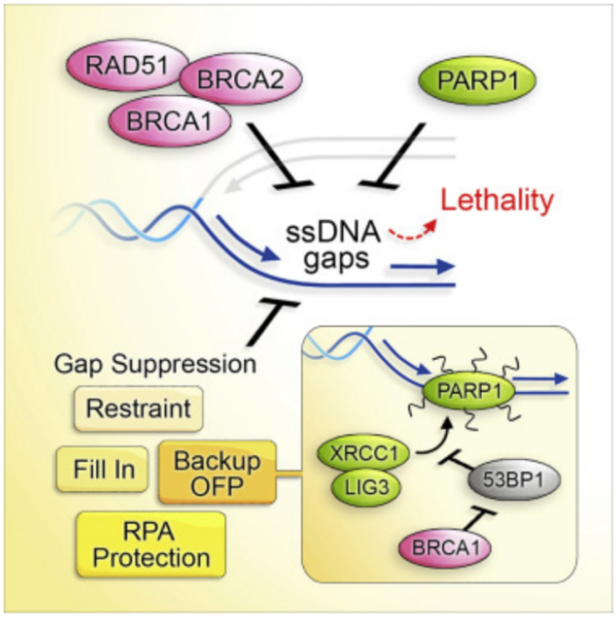

Figure 1.12 - The synthetic lethality between PARP1 and BRCA1 and ssDNA replication gaps. There is an association between the formation of ssDNA gaps and sensitivity to PARPi and so suppressing these gaps can re-sensitise cells to PARPi. In *BRCA1*-deficient cells, the impairment of Okazaki fragment processing (OFP) is the cause behind these replication gaps and OFP disruption can be rescued by inhibiting 53BP1 (Cong et al., 2021).

De novo and acquired resistance is a common clinical barrier and therapy response can vary between *BRCA1* mutations (Wakefield et al., 2019). The core mechanisms of PARPi resistance include: reactivation and suboptimal HR, the abundance of PAR chains, PARP1 mutations, DNA end resection, RAD51 filament formation, PARylation restoration, reversion mutations, replication fork protection, the availability of the inhibitor within the cell (elevated drug efflux) and most recently replication gap suppression (Rottenberg et al., 2007, 2008; Pettitt et al., 2018; Barber et al., 2013; Gornstein et al., 2018; Kondrashova et al., 2017; Kolinjivadi et al., 2017b; Su et al., 2008). Unfortunately, more than 40% of patients with *BRCA1/2* mutations do not respond to PARPi, therefore alternative strategies are required to overcome resistance and amplify PARPi sensitivity (Fong et al., 2010; Audeh et al., 2010).

1.6.2. RNF168

RNF168 loss is synthetically lethal with *BRCA1*-deficient cells (Zong et al., 2019; Krais et al., 2020; Patel et al., 2021a; Bohgaki et al., 2013). RNF168 acts redundantly with BRCA1 to facilitate PALB2-BRCA2-RAD51 loading onto 3' ssDNA, but the removal of RNF168 in *Brca1* heterozygous mice predisposed them to cancer (Zong et al., 2019). Removing RNF168, thus disrupting the chromatin ubiquitylation pathway in *BRCA1*-deficient cells resulted in genomic instability and cell death as the pathway is essential for HR in the absence of BRCA1 (Krais et al., 2020; Zong et al., 2019). RNF168-mediated mono-ubiquitination of H2A at K13/15 can also localise BARD1 via its BUDR BRCT domain to localise the BRCA1-P complex to DSBs via the BRCA1-PALB2 coiled-coil domain interaction (Krais and Johnson, 2021). The abrogation of the BARD1 BUDR domain renders cells susceptible to PARPi by disrupting the ability to

carry out HR reiterating the importance of RNF168-mediated recruitment of the BRCA1-P complex (Becker et al., 2021).

Also, Patel *et al* have demonstrated that RNF168 deletion leads to the accumulation of R-loops in *BRCA1/2*-deficient cells as usually BRCA1/2 would suppress these DNA:RNA hybrid structures, subsequently reducing cell viability (Patel et al., 2021a). RNF168 ubiquitinates DHX9, a helicase, facilitating the localisation and removal of R-loops and so the loss of RNF168 disables DHX9-mediated elimination of cytotoxic R-loops (Patel et al., 2021a). The RNA helicase DHX9 plays an important role in HR by forming a complex with BRCA1 that interacts with the RNA Pol II holoenzyme via RNA for the promotion of DNA end resection (Chakraborty and Hiom, 2021).

1.6.3. POLθ

Polθ loss is synthetic lethal in HR-deficient cancers, such as in *BRCA1/2*-mutated cancers rendering Polθ a promising target for cancer therapy, with the development of Polθ inhibitors entering Phase I/II clinical trials (NCT04991480) (Schrempf et al., 2021). Polθ is the predominant protein in TMEJ (section 1.3.3) which is an error-prone DNA repair pathway and can introduce mutational signatures including microhomology-flanked deletions and templated insertions, with the depletion of HR factors elevating TMEJ mutational signatures (Sallmyr and Tomkinson, 2018; Schimmel et al., 2019; Ahrabi et al., 2016). The removal of Polθ disrupts TMEJ which leads to reduced cell viability in HR-deficient cells and elevated cell death in the presence of mitomycin C (MMC), cisplatin and PARPi (Ceccaldi et al., 2015; Patel et al., 2021b). Moreover, Brambati *et al* (2023) revealed a role for TMEJ during mitosis to repair DSBs formed during S-phase and accounts for the synthetic sickness between Polθ and BRCA2 (explained in section 1.3.3) (Brambati et al., 2023).

As well as during TMEJ Polθ is important for translesion synthesis bypassing abasic sites and bases damaged by UV, BER and replication repair (Seki et al., 2004, 2003; Yoon et al., 2014). Human cells depleted of Polθ treated with HU harbour disrupted replication fork restart and lowered replication speed (Ceccaldi et al., 2015). Polθ also functions to prevent replication fork collapse, genome instability and tumorigenesis by performing mutagenic replication via UV lesions (Yoon et al., 2019). UV exposure is responsible for producing covalent links between two adjacent pyrimidines generating cyclobutene pyrimidine dimers (CPDs) and (6-4) pyrimidine-pyrimidone photoproducts ([6-4] PPs) (Mak and Fix, 2008; Yoon et al., 2000; You et al., 2001). Polθ is essential for mutation-prone TLS opposite (6-4) PPs and mutagenic replication via CPDs (Yoon et al., 2019). However, Yoon *et al* (2019) have demonstrated that the error-prone TLS Polθ protects against tumorigenesis and chromosomal instability in skin exposed to sun as shown by an increased prevalence of skin cancers in Polθ$^{-/-}$ mice (Yoon et al., 2019).

Finally, the function of Polθ in the PRR of ssDNA gaps provides a broader role for the polymerase that is distinct from DSB repair and provides further insight into the possible mechanisms underlying Polθ inhibition in *BRCA1/2*-mutated cancers (Schrempf et al., 2021; Mann et al., 2022; Belan et al., 2022). Polθ seals post-replicative ssDNA gaps in *BRCA1/2*-mutated cells and Polθ inhibitors can be used synergistically with PARPi with the combination of the Polθ inhibitor ART4215 and the PARPi Talazoparib in Phase I/IIa clinical trials (NCT04991480) (Zatreanu et al., 2021). In the absence of Polθ and BRCA2/RAD51, ssDNA gaps are exposed to MRE11 endo-nucleolytic cleavage forming single-ended forks resulting in fork breakage and DSBs (Mann et al., 2022). The role of Polθ in microhomology-mediated gap skipping could

contribute towards the Polθ-specific genomic scars generated in HR-deficient cancers and provide an insight into the Polθ/BRCA1/2 synthetic lethal relationship (Schrempf et al., 2021; Mann et al., 2022; Belan et al., 2022).

Recently, Polθ small molecule inhibitors have been identified that specifically kill HR-deficient cells (Zatreanu et al., 2021). For example, Zatreanu *et al* (2021) studied the ART558 compound which inhibits Polθ polymerase activity which is synthetic lethal with *BRCA1*-deficient cells but also is synthetic lethal with the PARPi resistant 53BP1/Shieldin complex (Zatreanu et al., 2021). Additionally, the antibiotic novobiocin (NVB) was identified as an inhibitor of Polθ which abrogates its ATPase activity by binding to the helicase domain causing the impairment of TMEJ (Zhou et al., 2021). Not only does NVB kill HR-deficient tumours, but also potentiates the cytotoxicity of PARPi and so can eliminate PARPi-resistant tumour cells, making the antibiotic an effective therapeutic avenue for overcoming acquired PARPi resistance (Zhou et al., 2021). An additional potent, selective, and orally bioavailable Polθ polymerase domain inhibitor called RP-6685 was published by Bubenik *et al* (2022). RP-6685 could successfully reduce tumour growth in *BRCA2*$^{-/-}$ murine xenograft models (Bubenik et al., 2022).

1.6.4. RAD52

Increasing evidence has shown that RAD52 is necessary for cell survival in *BRCA1*-deficient cells, therefore targeting RAD52 is seen as a popular potential therapy (Cramer-Morales et al., 2013; Kumar et al., 2016; Lok et al., 2013). Suppressing RAD52 in *BRCA1/2*-proficient cells has no detrimental impact on HR, but in *BRCA1/2*- and *PALB2*-deficient cells that exhibit impaired RAD51 loading, these cells cannot survive in the absence of RAD52. (Stark et al., 2004; Bennardo et al., 2008). Yeast

cells are reliant on Rad52 mediated loading of Rad51 onto RPA-coated ssDNA, whereas in mammalian cells, BRCA2 loads RAD51 onto ssDNA (Sugiyama et al., 1998). In yeast that harbour impaired Rad52, there are defects for example in HR and meiotic recombination, whereas in *Rad52*-deficient mice there is only a minor impact on HR and no observable phenotype (Rijkers et al., 1998; Jalan et al., 2019). However, in *BRCA1/2*-deficient human cells RAD52 can interact directly with RAD51 and RPA (Stefanovie et al., 2020). The N-terminal domain of RAD52 undergoes RNA/DNA pairing functions and the C-terminal domain can bind RAD51 and RPA (Hanamshet et al., 2016; Kwon and Sung, 2017; Park et al., 1996; Shen et al., 1996). RAD52 interacts with RAD51 to initiate strand invasion and homologous pairing and RAD52 loss in *BRCA2*-deficient cells provides evidence that RAD52 is necessary for HR through RAD51 foci, gene conversion assays and cell viability (Feng et al., 2011; Lok et al., 2013; McIlwraith et al., 2000). However, only the N-terminal domain appears important for maintaining cell viability in *BRCA1*-deficient cells via RAD52-mediated HR and SSA (Hanamshet and Mazin, 2020).

Further evidence for the role of RAD52-mediated RAD51 loading during HR in *BRCA1*-deficient cells is the relationship between the 5' endonuclease/exonuclease/phosphatase family domain containing 1 (EEPD1) and *RAD52* and *BRCA1*-deficiency (Hromas et al., 2017). EEPD1 initiates 5'end resection by EXO1 in the absence of BRCA1, enabling the formation of 3'ssDNA for RAD52 to load RAD51 (Chun et al., 2016; Wu et al., 2015b; Kim et al., 2017b). We already know that depleting both BRCA1 and RAD52 induces synthetic lethality as RAD52-mediated HR is compromised, but EEPD1 depletion can rescue the synthetic lethality of these cells as inhibiting EEPD1 and RAD52 simultaneously removes chromosomal defects

and facilitates replication fork restart (Hromas et al., 2017). These data imply that EEPD1 is involved in generating these mitotic aberrations during DNA replication (Hromas et al., 2017).

Directly targeting RAD52 in *BRCA1/2*-deficient cells sensitises them to genotoxic compounds without impacting healthy HR-proficient cells (Toma et al., 2019). Therefore, small molecule inhibitors of RAD52 have been designed to trigger synthetic lethality in *BRCA1/2*-depleted cells (Cramer-Morales et al., 2013; Chandramouly et al., 2015). For example 6-Hydoxy-DL (6-OH-dopa) (6-OHD) is an allosteric inhibitor of RAD52 that exhibits a detrimental effect on *BRCA1/2*-deficient cells treated with PARPi (Sullivan-Reed et al., 2018). 6-OHD functions by perturbing the heptameric ring as well as RAD52 recruitment and recombination activities and so disrupts RAD52-mediated repair of DSBs when BRCA1 is not functional (Chandramouly et al., 2015). The compound D-I03 was identified as a selective RAD52 inhibitor that blocks RAD52-mediated single-strand annealing and D-loop formation, abrogates RAD52 foci formation and diminishes cell viability of *BRCA1/2*-deficient cells (Huang et al., 2016). Also, phenylalanine 79 within the RAD52 binding domain (RAD52-phenylalanine 79) (F79) was identified as a synthetic lethal target in *BRCA1/2*-deficient carcinomas and leukaemias (Cramer-Morales et al., 2013). Disrupting F79 using a small peptide aptamer abrogates the association between RAD52 and DNA leading to DSB formation in tumour cells over healthy cells (Cramer-Morales et al., 2013). Treatment of *BRCA1/2*-deficient cells with Olaparib alongside either 6-OHD, F79 aptamer or D-I03 demonstrated a clear reduction in cell viability making RAD52 inhibitors alongside PARPi an effective therapeutic approach (Sullivan-Reed et al., 2018).

As well as DSB repair, during pro-metaphase RAD52 functions within the BIR-facilitated lengthening of telomeres and during G2-phase RAD52 mediates the spontaneous elongation of telomeres (independent of the SLX4 nuclease) (Verma et al., 2019; Zhang et al., 2019). RAD52 harbours a DSB-independent role which involves limiting replication fork reversal and protecting nascent DNA strand degradation (Gottifredi and Wiesmüller, 2020). Furthermore, in checkpoint deficient CHK1 depleted cells, RAD52 converts replication forks into a structure that can be cleaved by MUS81 and subsequently repaired by BIR (Murfuni et al., 2013; Jalan et al., 2019).

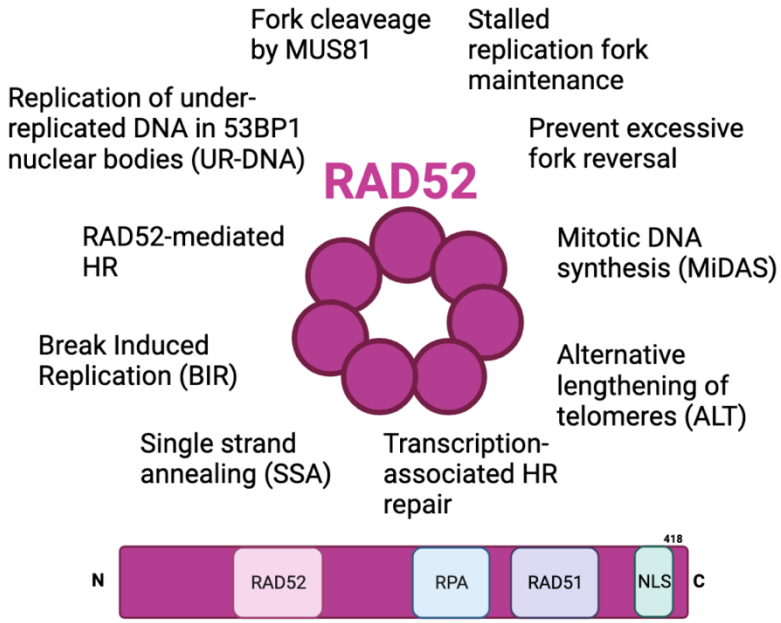

Figure 1.13 – The roles of RAD52 in double-strand break repair and DNA replication. RAD52 repairs breaks by single-strand annealing (SSA) and break-induced repair (BIR) at single-ended DSBs. RAD52 is involved in the alternative lengthening of telomeres by mediating spontaneous telomere synthesis in G2 and during metaphase facilitates telomere elongation by BIR. During MiDAS and in Chk1-depleted cells, RAD52 is involved in MUS81-mediated DSB formation. RAD52 restricts unchecked fork reversal but during fork reversal RAD52 is involved in the degradation of nascent DNA by MRE11.

1.6.5. USP1

There have been numerous synthetic lethal partners of BRCA1/2 identified that act within replication fork protection such as USP1, EXD2 and CtIP (Patel et al., 2021b). The ubiquitin-specific peptidase 1 (USP1) is a DUB required for the survival of HR-deficient cancers such as *BRCA1/2*-deficient cancers, making the inhibition of USP1 a promising therapeutic target. USP1 is also overexpressed in numerous cancers such as in colorectal and gastric cancers (Xu et al., 2019; Meng and Li, 2022). *USP1* encodes a 785 amino acid protein within the largest family of DUBs containing approximately 50 USPs (Faesen et al., 2011; Cohn et al., 2007). USP1 forms a heterodimeric complex with the WD40 repeat-containing protein UAF1 which functions to de-ubiquitinate targets such as PCNA and FANCD2 (Cohn et al., 2007; Huang et al., 2006; Nijman et al., 2005; Sims et al., 2007).

USP1 is fundamental for the regulation of TLS by reversing PCNA-ubiquitination by RAD18 and counteracting the transition from replicative polymerases to TLS polymerases for DNA damage bypass to limit persistent TLS activation (Hoege et al., 2002; Stelter and Ulrich, 2003). In *BRCA1*-deficient cells, USP1 is recruited to the replication fork to stabilise and protect the fork in the absence of BRCA1 and the synthetic lethal relationship between USP1 and BRCA1 can be undone by the loss of the PCNA ubiquitin ligase RAD18 or the TLS polymerase Polκ (Lim et al., 2018). A potential mechanism explaining the USP1/BRCA1 synthetic lethal relationship is that the loss of USP1 drives persistent PCNA mono-ubiquitination leading to replication fork degradation and instability (Lim et al., 2018; Coleman et al., 2022). In addition, the inhibition of USP1 has been shown to cause aberrant mono- and poly-ubiquitination of PCNA leading to PCNA protein degradation, whereas the loss of RAD18 or UBE2K

diminished USP1 inhibitor sensitivity and retained PCNA expression levels (Simoneau et al., 2023a). Nusawardhana *et al* (2024) suggest that USP1 drives ssDNA gap accumulation by promoting ssDNA bidirectional expansion in the 3'-5' direction by MRE11 and in the 5'-3' direction by EXO1 and counteracts gap filling by TLS (Nusawardhana et al., 2024). Whereas, others have shown that in *BRCA1*-deficient cells, the loss of USP1 and elevated TLS induces ssDNA gaps (Lim et al., 2018). Likewise, Nayak *et al* (2023) indicated that USP1 inhibition using a novel small molecule inhibitor KSQ-4279 resulted in ssDNA gap generation resulting in replication fork degradation and the loss of PCNA eventually leading to DSB formation (Nayak et al., 2023).

The USP1-UAF1 inhibitor ML323 is a potent, selective, allosteric and reversible inhibitor (Dexheimer et al., 2010). ML323 binds to and disrupts part of the hydrophobic core of USP1 which induces a conformational change resulting in minor changes to the active site, rather than the inhibitor directly binding with the active site or on the surface of USP1 (Rennie et al., 2022; Dexheimer et al., 2010; Coleman et al., 2022). ML323 has shown success in suppressing ovarian cancer progression by targeting the USP1-regulated cell cycle (Song et al., 2022). An additional potent and selective inhibitor of the USP1-UAF1 complex is I-138 which is structurally related to ML323 (Liang et al., 2014; Simoneau et al., 2023a). I-138A treatment in BRCA1-deficient ovarian cancer cells resulted in replication fork instability and the development of ssDNA gaps, whereas this was not apparent in I-138A resistant *BRCA1*-deficient cells (Da Costa et al., 2023). The loss of RAD18 in *BRCA1*-deficient cells led to reduced PCNA mono-ubiquitination, the suppression of ssDNA gaps and resistance to I-139A treatment (Da Costa et al., 2023). ISM3091 is a novel and selective inhibitor of USP1

that could sensitise HR-deficient and proficient cancers and the synergistic treatment of ISM3091 and PARPi could sensitise HR-deficient cancers further (Li et al., 2023). TNG348 is a highly potent, allosteric oral inhibitor of USP1 that induces loss of cell survival in *BRCA1/2*-mutated cell lines and is currently in clinical trials with and without the combination of PARPi to treat patients harbouring *BRCA1/2*-mutated cancers (NCT06065059) (Simoneau et al., 2023b). Overall, USP1 inhibitors are a powerful tool for treating HR-deficient cancers and can be used in synergy with PARPi (Simoneau et al., 2023a).

1.7. BRCA1/BARD1 mutations and mouse models

Mutant mouse models have thoroughly enriched our understanding of the tissue-specific tumour suppressor functions of BRCA1 and highlighted the applications for therapeutic treatment and cancer prevention (Dine and Deng, 2013). Murine *Brca1* encodes a 1812-amino acid protein with significant homology to the human protein that is 1863 amino acids in length (Lane et al., 1995). Numerous *Brca1* mutant alleles induce embryonic lethality, although mouse mutants die at different stages during development, demonstrating that mutant alleles have alternative impacts on BRCA1 function. BRCA1 possesses many different functional domains and posttranslational modifications varying in size and so understanding this further will provide information on the contribution of certain domains to function (Liu and Lu, 2020; Yueh et al., 2024).

1.7.1. Mutant mouse models that rescue embryonic lethality

When BRCA1 is impaired, the removal of 53BP1 mediates the release of the block on DNA end resection and thus facilitates HR (Bunting et al., 2010; Li et al., 2016). In mice

homozygous for *Brca1* $^{\Delta 11/\Delta 11}$ and *Brca1* $^{\Delta 2/\Delta 2}$, the knock-out (KO) of 53BP1 can fully rescue embryonic lethality in these mice (Cao et al., 2009; Li et al., 2016; Bunting et al., 2010). These mice harbour proficient HR, have an elevated life span and lack tumour development, likely due to retaining a hypomorphic BRCA1 protein that maintains the BRCT domain required for protein localisation to DSBs and the coiled-coil domain necessary for its interaction with PALB2 (Chen et al., 2020). 53BP1 knockout can also rescue embryonic lethality in *Brca1* $^{\Delta C/\Delta C}$ mice, albeit with a reduced life span and HR and genomic stability are not restored to full capacity (Nacson et al., 2018). *Brca1* $^{\Delta C/\Delta C}$ mice should not have a functional BRCT nor coiled-coil domain but still produce a truncated protein, although no protein could be detected (Chen et al., 2020). Despite this, it is theorised that the *Brca1*$^{\Delta C}$ protein is expressed at undetectable levels, and therefore explain the survival of these mice in the absence of 53BP1 (Chen et al., 2020).

Table 1.1 – A selection of *Brca1* mutant mouse alleles.

MGI allele ID	Mutant mouse allele	Embryonic lethality	Phenotype	Reference
RING domain mutations				
MGI:5307254 Brca1$^{tm1.1Jon}$	*Brca1*^{C61G}	Embryonic lethal Die between E9.5 and E12.5	-Disrupts BRCA1:BARD1 interaction. -Prevents ubiquitin E3 ligase function. - Impaired DNA damage ability. -Mice become therapy resistant	(Drost et al., 2011; Mylavarapu et al., 2018)

			(PARPi and cisplatin) suggesting a hypomorphic activity.	
MGI:5494435 Brca1$^{tm3.1Thl}$	*Brca1^{I26A}*	Viable embryos	-Disrupts E3 ubiquitin ligase activity due to its interrupted association with the E2 conjugating enzyme UbcH5c but thought to retain residual activity with other E2 conjugating enzymes. - Maintains BRCA1:BARD1 heterodimer structure. -Does not impact HR repair or cell survival.	(Reid et al., 2008; Stewart et al., 2017)
MGI:5823771 Brca1^{tm2Jjon}	*Brca1^{185stop}*	Embryonic lethal Die between E9.5 to E13.5	-Rapidly develops therapy resistance to PARPi and cisplatin. - Mimics the common *BRCA1* founder mutation within the Ashkenazi Jewish population. - *Brca1^{185stop}* mice predisposed to	(Drost et al., 2016)

			tumour development.	
MGI:5494435 Brca1$^{tm3.1Thl}$	Brca1$^{FH-I26A}$	Viable embryos	-Disrupts E3 ubiquitin ligase activity due to its interrupted association with the E2 conjugating enzyme UbcH5c but thought to retain residual activity with other E2 conjugating enzymes. - Mutation is indispensable for tumour suppression. -Allows assembly of the BRCA1/BARD1 heterodimer. - Mice have smaller testes, sterile and have a decreased body weight.	(Shakya et al., 2011)
MGI:1930613 Brca1^{tm1Arge}	Brca1^{ex2}	Embryonic lethal Die between E6.5 and E9.5 Fully viable on a *p53*$^{-/-}$ *53bp1*$^{-/-}$ or *Rnf168*$^{-/-}$	- Genomic instability and replication fork stability defect. - Deletion of 53BP1 rescues embryonic lethality. -Cisplatin sensitivity.	(Ludwig et al., 1997; Li et al., 2016; Zong et al., 2019; Bunting et al., 2012)

		background	- BRCA1 protein isoform is RING-less.	
MGI:1858108 Brca1^{tm1Mak}	*Brca1*$^{\Delta 5\text{-}6}$	Die before E7.5 Partial rescue prolonging survival to E9.5 on a *p53*$^{-/-}$, *p21*$^{-/-}$ null background. Viable on a *53bp1-/-* background, but. a shorter life span, HR deficient and increased TMEJ.	-Null *Brca1* mouse allele. -Homozygous embryos have no BRCA1. -Embryos die at E7.5 but develop normally prior to implantation. -Defects in HR repair. -Embryos show epiblast cell proliferation defects.	(Hakem et al., 1996, 1997; Chen et al., 2020)
Exon 11 mutations				
MGI:2182470 Brca1$^{tm2.1Cxd}$	*Brca1*$^{\Delta 11}$	Die between E12.5 and 18.5 with some viable embryos. Fully viable when on *53bp1*$^{-/-}$,	-Is a hypomorphic allele as it interacts with BARD1 and PALB2 and localises to sites of DNA damage. - Embryos survive longer than *Brca1* null alleles. - Reduced DNA damage generated phosphorylation	(Xu et al., 1999; Huber et al., 2001; Cao et al., 2006, 2009; Callen et al., 2020)(Krais et al., 2023)

		53bpp1$^{S25A/S25A}$, *Chk2*$^{-/-}$ *or* *Atm*$^{-/-}$, p53$^{-/-}$ Partially viable on a *Chk2*$^{+/-}$ *or Atm*$^{+/-}$ background *Brca1*$^{\Delta 11}$, *Polq*$^{-/-}$; *53bp1*$^{-/-}$ is lethal.	of *Brca1*$^{\Delta 11}$ compared to *Brca1* full-length. - Deletion of *53Bp1*$^{-/-}$ rescues embryonic lethality and development mammary glands. - *Brca1*$^{\Delta 11}$ MEFs exhibit disrupted G2/M cell cycle checkpoint and show genomic instability.	
MGI:1857931 Brca1^{tm1Bhk}	*Brca1*$^{\Delta 223-763}$	Die between E8.5 to E13.5	-Compromised HR repair. -Homozygous *Brca1*$^{\Delta 223-763}$ ES cells are viable. -Hypersensitive to MMC. - Homozygous *Brca1*$^{\Delta 223-763}$ ES cells showed chromosome exchanges.	(Gowen et al., 1996; Reid et al., 2008; Cressman et al., 1999)
MGI:1858107 Brca1^{tm1Whl}	*Brca1*$^{\Delta 300-361}$	Die before E7.5	-Embryos homozygous for the allele die very early with defects	(Liu et al., 1996)

			displaying from E4.5-5.5. -Unable to form egg cylinders at E5.5-E6.5.	
MGI:1930612 Brca1^{tm1Cxd}	*Brca1*$^{11-}$	Die between E7.5 and E9.5 Extended survival for 2 days on a p53$^{-/-}$ background	-Show chromosomal aberrations and growth retardation post-implantation. -Sensitive to IR.	(Shen et al., 1998)
MGI:2177209 Brca1^{tm2Arge}	*Brca1*^{tr}	Largely viable embryos	-Develop mammary tumours. -Hypomorphic allele. -Homozygous mice are viable but this depends on the genetic background.	(Ludwig et al., 2001)
Coiled-coil domain mutations				
MGI:6281370 Brca1^{em1Njo}	*Brca1*$^{\Delta C}$	Embryonic lethal Fully viable on a *53Bp1*$^{-/-}$ background	-Deficient in HR and exhibit genomic instability. -Forms a truncated protein without the coiled-coil domain and the BRCT in homozygous	(Chen et al., 2020; Nacson et al., 2018)

			mice, although no truncated protein is detected so close to BRCA1 null mice. -Hypersensitive to PARPi. - *Brca1*$^{\Delta C/\Delta C}$ mice on a *53Bp1*$^{-/-}$ background develop thymic lymphoma after 7 months. -RAD51 loading is impaired but proficient in end resection, developing FA-like phenotypes.	
N/A	*Brca1*^{L1363P}	Lethal	-Embryonic lethal but depending on mouse strain FA phenotypes can form.	(Pulver et al., 2021; Park et al., 2020)
BRCT domain mutations				
MGI:5494434 Brca1$^{tm2.1Th1}$	*Brca1*^{S1598F} *(Brca*$^{(SF)}$*)*	Viable embryos Crossed on an *Atm-/-* background, die E9.5. Crossed on an *Atm-/-*, *53bp1+/-*, *53bp1-/-* background forming	-Loss of genomic integrity by ablation of stalled fork protection and HR. -Murine *Brca1* shows basal-like triple-negative mammary tumours in mice. -The interaction between BRCA1 and the BRCT phospho-ligands	(Billing et al., 2018; Chen et al., 2017; Shakya et al., 2011)

		viable embryos.	are disrupted by the mutation. -The mutation disrupts the phosphorylated protein binding pocket but not affecting protein stability. -Deficient in HR repair.	
MGI:2178447 $Brca1^{tm1Rfo}$	$Brca1^{1700T}$	Embryonic lethal Die between E9.5-E10.5	-Embryos die due to apoptosis throughout the embryo and show delayed embryonic lethality in contrast to *Brca1 null* alleles. -The mutation disrupts the p53-specific co-activation domain. -Low level truncated BRCA1ΔBRCT proteins are thought to be present in these cells due to the reduced severity of embryonic lethality compared to *Brca1* null alleles.	(Hohenstein et al., 2001)

MGI:5823772 Brca1^{tm3Jjon}	Brca1^{5382stop}	Embryonic lethal Die between E9.5 and E.12.5	- Low level truncated BRCA1ΔBRCT proteins are thought to be present in these cells due to the reduced severity of embryonic lethality compared to *Brca1* null alleles. -Truncated proteins with folding defects undergo proteasomal degradation. -Predisposed to mammary tumour development. -Develop therapy resistance.	(Drost et al., 2016; Mgbemena et al., 2017)
MGI:3706167 Brca1^{tm1Aash}	Brca1^{F22-24}	Viable embryos	-Develops basal-triple-negative type mammary cancers in combination with *p53* haploinsufficiency . Tumours resemble those seen in *BRCA1* carriers. -Has a complete loss of protein expression resulting in a null mutation. -Deletion of exons 22-24	(Diaz-Cruz et al., 2010; McCarthy et al., 2007)

			removing the final BRCT domain by Cre-mediated incision.	
Phosphorylation sites				
MGI:4418211 Brca1$^{tm5.1Cxd}$	*Brca1*^{S1152A}	Viable embryos	-The phosphorylation site (ATM in exon 11) is disrupted but embryos are viable, insinuating that embryonic development does not require CHK2 and ATM-dependent phosphorylation of BRCA1. -36% of homozygous mice show phenotypes relating to age such as growth retardation, delayed mammary gland morphogenesis, skin abnormalities and elevated apoptosis.	(Kim et al., 2009)
MGI:3513253Brca1^{tm3Cxd}	*Brca1*^{S971A}	Viable embryos	-Homozygous mice showed a moderately increased risk of developing tumours and most of the female mice developed ovarian abnormalities and	(Kim et al., 2004)

			uterus hyperplasia. -After treatment with γ-irradiation, homozygous cells show a reduced ability to activate the G2/M cell cycle checkpoint.	

Table 1.2 – A selection of *Bard1* mutant mouse alleles.

MGI allele ID	Mutant mouse allele	Embryonic lethality	Phenotype	Reference
MGI:2668394 $Bard1^{tm1Thl}$	$Bard1^{-}$ Extended survival to E9.5 days on a $p53^{-/-}$ background	Embryonic lethal Die between E7.5 and E8.5	-Cell proliferation impaired and show genomic instability. - Chromosomal instability in *Bard1*$^{-/-}$, *p53*$^{-/-}$ mice.	(McCarthy et al., 2003)
MGI:6399949 $Bard1^{tm1.1Rjbr}$	$Bard1^{S563F}$, $Bard1^{SF}$	Viable embryos	-Not tumour prone. -Disrupt BRCA1:BARD1 recruitment to stalled replication forks by poly(ADP)ribose. -Replication fork degradation and chromosomal aberrations. -Bard1 BRCT phosphor-recognition is not required for HR but is	(Billing et al., 2018)

			needed for stalled fork protection. -Normal embryonic development but males are sterile. -MEFs are hypersensitive to MMC and Olaparib. -Little to no sensitivity to IR.	
MGI:6399951 $Bard1^{tm2.1Rjbr}$	$Bard1^{K607A}$, $Bard1^{KA}$	Viable embryos	-Not tumour prone. -Disrupt BRCA1:BARD1 recruitment to stalled replication forks by poly(ADP)ribose. -Replication fork degradation and chromosomal aberrations. -Bard1 BRCT phosphor-recognition is not required for HR but is needed for stalled fork protection. -MEFs are hypersensitive to MMC and Olaparib. -Little to no sensitivity to IR.	(Billing et al., 2018)
MGI:3790742 $Bard1^{tm2Thl}$	$Bard1^{flex1}$	Viable embryos	-Healthy, fertile and have a normal lifespan compared to nullizygous embryos.	(Shakya et al., 2008)

MGI:6399953 Bard1$^{tm3.1Rjbr}$	Bard1^{Q552X}	Embryonic lethal. Die between E7.5 and E8.5	-Mimics a patient BARD1 nonsense mutation. -Protein product is not stably expressed.	(Ratajska et al., 2012)
MGI:6399957 Bard1$^{tm4.1Rjbr}$	Bard1^{co}	Embryonic lethal	-Conditional null allele. -Lacks first coding exon.	(Billing et al., 2018)
MGI:6399960 Bard1$^{tm4.2Rjbr}$	Bard1$^{co\text{-}rec}$	Embryonic lethal	-Conditional null allele (Cre-recombinase product). -Loss of *Bard1* coding exon 1.	(Billing et al., 2018)

1.8. Summary

In the introduction we have covered the important roles that the tumour suppressor BRCA1 has for facilitating DSB repair by HR and its involvement in the protection of stalled replication forks from nucleolytic degradation (Ghimenti et al., 2002; Moynahan et al., 1999; Daza-Martin et al., 2019; Schlacher et al., 2012). We have covered the fundamental role of BRCA1 in the suppression of replication-associated ssDNA gaps (Panzarino et al., 2021). The two predominant DSB pathways include NHEJ which modifies damaged DNA ends to promote their direct ligation and repairs the majority of DSBs (Lieber, 2008), whereas HR is restricted to S and G2 cell cycle phases because of the requirement for an intact sister chromatid for repair (Lieber et al., 2014; Jasin and Rothstein, 2013). During S-phase BRCA1 facilitates the removal of 53BP1 to promote resection and HR (Bunting et al., 2010). However, non-canonical DSB repair pathways can be upregulated in *BRCA1*-mutated cells, such as TMEJ that uses

microhomologies of approximately 20 base pairs and SSA that acts on extended resected DNA (Kent et al., 2015b; Bhargava et al., 2016). The predominant proteins for the alternative repair pathways TMEJ and SSA include Polθ and RAD52 respectively, so the disruption of either protein in *BRCA1*-mutated cancers cause synthetic lethality (Kelso et al., 2019). Targeting synthetic lethal interactions in *BRCA1*-deficient cancers has become fundamental in the emergence of novel clinical therapeutics. However, for example the mechanisms surrounding the synthetic lethal interaction between Polθ and BRCA1 remains elusive with increasing reports stating that Polθ promotes DNA synthesis ssDNA gap fill-in in the absence of functional BRCA1/BRCA2/RAD51 proteins (Mann et al., 2022; Belan et al., 2022; Schrempf et al., 2022).

Accordingly, in the absence of BRCA1, replication forks are stabilised by the DUB USP1, however the loss of USP1 in *BRCA1*-deficient cells results in the loss of fork protection and cell death due to the aberrant mono-ubiquitination of PCNA and recruitment of error-prone TLS polymerases making USP1 inhibitors an essential avenue to explore (Lim et al., 2018; Simoneau et al., 2023a). Also, in *BRCA1*-mutant tumours spontaneous PRIMPOL-dependent ssDNA gaps arise that can be repaired by gap filling by the DDT TLS pathway, more specifically the REV1-Polζ complex (Taglialatela et al., 2021). These findings reiterate the importance of understanding mechanisms underlying the survival pathways supporting BRCA1 function and how they can be targeted.

1.9. Project Aims

1) To further understand the synthetic lethal relationship between *Brca1* and *53bp1* deficiencies and Polθ targeting.
2) To identify what factors are driving the synthetic lethal interaction between *Brca1/53bp1* deficiencies and Polθ loss and inhibition.
3) To characterise the *R93E-Bard1* mutation.
4) To further understand the synthetic lethal interaction between USP1 and BRCA1 using $Bard^{R93E/R93E}$ cells.

2. Materials and Methods

2.1. Cell Biology

2.1.1. Cell line maintenance

Immortalised Mouse Embryonic Fibroblasts (MEFs) and HEK293 Platinum E cells were grown in Dulbecco's Modified Eagle Media (DMEM) (*Merck*) supplemented with 10% Foetal Bovine Serum (FBS) (*Gibco*) and 100 U/ml Penicillin and 100 µg/ml Streptomycin (P/S) (*Gibco*) in T75 flasks (Corning) at 37 °C 5 % CO_2. Cells were passaged at 80 % confluency by removing DMEM media, washing cells in 1 x PBS and incubated in 1 x Trypsin-EDTA at 37 °C 5 % CO_2 to detach from the surface of the flask. DMEM media was added to neutralise the trypsin, and cells were split 1:10 in T75 flasks (Corning). For long term storage, cells at a 90-95 % confluency were washed in 1 x PBS and trypsinised with Trypsin-EDTA. Cells were centrifuged at 200 x g for 5 minutes and pelleted followed by resuspension in DMEM media (10 % Dimethyl Sulfoxide (DMSO) for freezing) and divided into cryovials, 1 ml per cryovial. Cells were frozen down using a *Thermo Scientific*™ Mr. Frosty™ Freezing Container at a rate of -1 °C/minute and stored at -80 °C or for long-term storage in liquid nitrogen.

2.1.2. Generation of Mouse Embryonic Fibroblasts (MEFs)

The uterine horns were prepared by the animal house and placed in a 50 ml falcon tube (*Corning*) containing ice-cold PBS. The uterine horns were dissected and washed in Ethanol (EtOH) and twice in 1 x PBS. Using fine scissors and forceps the extraembryonic membranes were dissected. Each embryonic sac was cut open and embryos placed into designated 6 cm *(Corning)* dishes containing 1 x PBS. Using

forceps, the tail of the embryo was removed and placed into a 96-well plate to be sent for genotyping. Using forceps, the soft organs and viscera were dissected, and the top of the head (eye and above) was cut away. The remaining carcass was placed into a labelled 10 cm dish (*Corning)* containing 1 ml 1 x Trypsin-EDTA. The embryo was minced with a scalpel until homogenous and resuspended in 1 ml 1 x Trypsin-EDTA and transferred to labelled 15 ml falcon tubes (*Corning*). An additional 1 ml 1 x PBS was added to take up the remaining tissue suspension. The tissue suspension was added to 15 ml falcon tubes (*Corning)* in a 37 °C water bath for 15 minutes, resuspended and then incubated for a further 20 minutes. Cells were resuspended in 5 ml DMEM media and added to a T75 flask (*Corning*), an additional 8 ml DMEM media was added to resuspend the tissue suspension and added to the T75 flask. The tissue suspension was incubated for 2-3 days at 37 ^{o}C, 5 % CO_2 until very confluent (95 – 100 % confluency). Cells were trypsinised and transferred to a T175 flask and grown to extreme confluency (100 % confluent) and frozen using a *Thermo Scientific*™ Mr. Frosty™ Freezing Container (~ 9 vials/flask). For immortalisation, MEFs were seeded in 6-well plates, and after 24 hours transduced with the SV40 large T antigen (pBsSVD2005, AdGene) using FuGENE (1:8 ratio) (*Promega)* according to manufacturer's protocol. Cells were expanded until completely immortalised.

2.1.3. HEK293 Platinum E Viral Packaging and Retroviral infection

2 x 10^6 HEK293 Platinum E cells were seeded in 10 cm dishes (*Corning)* and incubated for 24 hours at 37 °C 5 % CO_2. Cells were transfected with pMSCV-IRES-GFP containing BARD1 variants / RPA fusions / H2A fusions using FuGENE-6 (*Promega*) according to manufacturer's instructions. Cells were incubated at 37 °C 5 % CO_2 for 48 hours and the viral supernatant was harvested and subsequently filtered through a

0.45 µm filter. MEFs were seeded in 24-well plates and retroviral supernatant containing media were added to appropriate wells with 4 µg/ml Hexadimethrine Bromide (polybrene) (*Sigma)*. MEFs were infected by spinoculation and centrifuged at 2200 RPM for 1 hour. Retroviral supernatant was removed and DMEM media was added. The RPA70 constructs were designed based on the BRCA2 paper from (Saeki et al., 2006).

NLS-BRC4-RPA70-FLAG BRC4:EKIKEPTLLGFHTASGKKVKIAKESLDKVKNLFDE (human BRCA2 residues 1,514-1,548).

NLS-Ex27-RPA-FLAG:

$BRCA2_{Exon\ 27}$:ALDFLSRLPLPPPVSPICTFVSPAAQKAFQPPRSCG (human BRCA2 residues 3,270-3,305).

H2A fusions were cloned in frame with an N-terminal HA tag in pMSCV-IRES-GFP II by GenScript.

2.1.4. Small interfering RNA (siRNA) transfection and Colony Survival assay

Cells were seeded in a 6-well plate (7.5 x 10^4 cells per well) or in a 24-well plate (15 x 10^3 cells per well) in DMEM media and grown at 37 °C 5 % CO_2. At 40-60% confluency, cells were treated with appropriate drugs/inhibitors (Table 2.8) or transfected with siRNA (0.25 nM) (*Dharmacon)* following manufacturer's instructions (Table 2.6) and incubated at 37°C 5% CO_2 for 72 hours. Cells were trypsinised in 100 µl 1 x Trypsin and resuspended in 900 µl of DMEM media. Appropriate limiting dilutions were added to 3 x wells in a 6-well plate to give triplicates and incubated at 37 °C 5 % CO_2 for 7 days. DMEM media was replaced with either 1 % methylene blue in 50 % ethanol or 0.5 % crystal violet *(BDH chemicals)* in 50 % methanol and colonies were counted.

Results were normalised to untreated controls for each condition. Graphs labelled “% cell viability” where no treatment other than knockdown is applied, otherwise graphs are labelled “% survival”.

2.1.5. Immunofluorescence Staining

Cells were seeded on circular coverslips (13-mm diameter) (*epredia)* in 24-well plates (~60% confluency). Depending on the experiment, cells were treated with siRNA for 72 hours prior to fixing. Depending on the experiment, cells were incubated with EdU (10 μM) (*Sigma*) for 10 minutes followed by irradiation at 2 Gy and incubated at 37 °C 5 % CO_2. Cells were pre-extracted with 0.5 % ice-cold Triton X-100 in 1 x PBS for 5 minutes and fixed with 4 % Paraformaldehyde (PFA) for 10 minutes. 1 x PBS was added, and cells could be stored short term at 4 °C wrapped in parafilm. Cells were permeabilised with 0.5 ml 0.5% Triton X-100 in 1 x PBS for 30 minutes and blocked with 5% FBS in 1 x PBS for 30-60 minutes. Cells were then incubated in primary antibody (Table 2.5) diluted in 5 % FBS in 1 x PBS overnight/ 1 hour depending on the antibody and stored at 4 °C. Cells were washed 3 x for 5 minutes in 1 x PBS and then incubated in secondary antibody (1:1000) (Table 2.5) diluted in 5 % FBS in 1 x PBST (1 X PBS + 0.1 % Tween® 20 detergent) for at least 1 hour and protected from the light using a fluoroshield. Cells were washed 3 x in PBST and then treated with a Click-IT reaction (EdU Imaging Kit). Click-IT reaction master mix was made fresh (1 ml master mix) (40 mM TBS pH 7.6, 4 mM Copper Sulphate, 0.125% Alexa-Fluor Azide 647, 100 mM Sodium ascorbate) and 250 μl of the reaction mix was added per well. Cells were washed 3 x in PBST for 5 minutes each and stained with Hoescht (1:50,000) for 5 minutes and cells were washed twice with 1 x PBS. Immunomount mounting media was added to Snowcoat slides and the coverslips were mounted onto the slides and

stored at 4°C until required. Immunofluorescent staining was viewed and imaged using the Leica DM6000B microscope.

2.1.6. DNA fibre labelling and spreading

Cells were seeded in 6-well plates at approximately 50-80 % confluency and treated with DNA damaging agents as appropriate. Cells were pulse labelled with two thymidine analogues CldU and IdU depending on the DNA fibre assay (Table 2.8). To monitor fork protection cells were incubated at 37 °C with 25 μM CldU for 20 minutes, followed by the incubation with 250 μM IdU for 20 minutes and 5 mM HU for 3 hours to deplete cells of dNTPs. After incubation with thymidine analogues, cells were washed with 2 x ice-cold 1 x PBS for 5 minutes and trypsinised. Cells were centrifuged at 500 x g for 3 minutes and resuspended in 1 x PBS to a final concentration of 50-70 x 10^4 cells / ml PBS and kept on ice. 2 μl of cell suspension was added to each Snowcoat slide (3 slides per condition) for 3-7 minutes until slightly dry. Then 7 μl of spreading buffer (200 mM Tris pH7.4, 50 mM EDTA, 0.5% SDS) was added, mixed with a pipette tip, and incubated for 2 minutes. Snowcoat slides were tilted at a 25-40 ° angle to spread the sample to the bottom of the slide and were left to dry. Snowcoat slides were fixed with 3:1 Methanol: Acetic acid fixative for 10 minutes and air-dried for 10 minutes, then stored at 4°C until immunostaining.

2.1.7. DNA Fibre Immunostaining

Snowcoat microscope slides were washed 2 x in distilled H_2O followed by 2.5 M HCl, and then DNA spreads were denatured with 2.5 M HCl for 1 hour 15 minutes (denaturation step is skipped when doing the SMART assay). Slides were washed 2 x in 1 x PBS and in blocking solution (1 x PBS, 1% BSA, 0.1% Tween® 20 detergent) for 5 minutes, then incubated for 1 hr in blocking solution. 115 μl of primary antibody

(Table 2.5) in blocking solution was added: Rat α-BrdU (*Abcam*) at 1:2000 to detect CldU and Mouse α-BrdU (*Becton Dickinson*) at 1:250 to detect IdU. Large coverslips were added and incubated at room temperature for 1 hour. Microscope slides were washed 3 x in 1 x PBS and fixed in 4 % PFA for 10 minutes. Slides were rinsed 3 x in 1 x PBS and incubated in blocking solution for 1, 5 and 30 minutes. Slides were then incubated in 115 µl of secondary antibodies (α-Rat AlexaFluor 555 and α-Mouse AlexaFluor 488, 1:500 each) and covered with large coverslips to avoid drying and incubated between 1.5 – 2 hours. Slides were then rinsed 2 x with 1 x PBS and 3 drops of mounting media was added and coverslips were mounted onto the slide and air-dried for 5-10 minutes. Slides were stored at -20 °C until visualisation. Immunofluorescent staining was viewed and imaged using the Leica DM6000B/ Zeiss AxioObserver. Z1 Apotome 2 microscopes.

2.1.8. S1 nuclease-modified fibre assay

Cells were seeded in 6-well plates and were treated with 25 µM CldU for 20 minutes and 250 µM IdU for 40 minutes. Cells were then permeabilised with CSK100 buffer ((100 mM NaCl, 10 mM MOPS, 3 mM $MgCl_2$, 300 mM sucrose, 0.5% triton X-100, pH 7.0) for 10 minutes. Exposed nuclei were treated with either S1 buffer (30 mM sodium acetate, 10 mM zinc acetate, 5% glycerol, 50 mM NaCl, pH 4.6) or S1 buffer containing 20 U/ml S1 endonuclease (Invitrogen 18001016) for 30 min at 37 °C. Nuclei were subsequently harvested by scraping and kept on ice prior to spreading. Fibres were spread and stained as described in the fibre labelling and spreading (2.1.7), and fibre immunostaining (2.1.8) sections.

2.1.9. Single-molecule analysis of resection tracks (SMART) assay

Cells were seeded in 6-well plates and then treated with 20 μM BrdU for 48 hours to label the entire genome. DNA was harvested and fibres were spread as described in the fibre labelling and spreading (2.1.7) section. Native DNA fibres were stained following the fibre immunostaining (2.1.8) section but avoiding the denaturation stage with HCl and stained with mouse α-BrdU (1:500) for 1.5 hours, fixed with 4 % PFA, and incubated with α-mouse AlexaFluor 488 for 1.5 – 2 hours.

2.1.10. Post Replicative Repair (PRR) assay

Cells were seeded in 6-well plates and treated with appropriate siRNA/compounds (Table 2.6, 2.8) 72 hours prior to treatment with 250 μM IdU for 1 hour at 37 °C. Cells were washed 2 x with 1 x PBS and replaced with DMEM media containing 200 ng/ml nocodazole for 16-24 hours. During the final 4 hours of nocodazole treatment, 20 μM CldU was added to be incorporated during post-replicative repair. DNA fibres were harvested and spread as explained in the fibre labelling and spreading (2.1.7), and fibre immunostaining (2.1.8) sections, apart from secondary antibodies were alternated to visualise green IdU tracts and red CldU dots representing PRR activity (α-Rat AlexaFluor 488 and α-Mouse AlexaFluor 555).

2.1.11. DNA fibre analysis

DNA fibre tracts were measured using Image J. For quantification of fork protection, the ratio of IdU/CldU tract lengths were plotted and a lower ratio is indicative of a loss of fork protection. Fork speeds were calculated by measuring IdU and CldU tract lengths and calculating the kb/min from μm/min. To quantify ssDNA gap formation the length of bi-labelled CldU and IdU tracks were measured and S1-dependent shortening of IdU tracks are indicative of ssDNA gap generation in nascent DNA. For the quantification of PRR events, IdU tracts containing at least one CldU dot were

measured using image J and lengths were converted into kilobases (1 μm = 2.59 kilobases). PRR density was calculated by dividing CldU dot density against IdU tract length. ssDNA lengths using SMART were calculated by measuring lengths of green labelled native DNA converted into μm.

2.2. Molecular Biology

2.2.1 CRISPR/Cas9 Homologous Recombination assay (George Ronson)

Adapted from (Nacson et al., 2018). Cells (2×10^6 per condition) were electroporated using the 100 μl Neon electroporation system (1350 V, 30 ms, 1 pulse) to introduce 10 μg of pX459 V2.0 containing Cas9 and a gRNA targeting Rosa26 locus, and 10 μg of pUC57 containing a Rosa26 HR template with a 4 bp edited sequence. Cells were plated into antibiotics free DMEM media to recover. After 72 hours, cells were harvested and the DNEasy Blood and Tissue kit was used to isolate genomic DNA, as per manufacturer's instructions. PCR was prformed using the GoTaq Green 2 x master mix (*Promega*) followed by agarose gel electrophoresis. Image J was used to quantify the HR specific band intensities which were normalised to a HR-independent PCR product at the Rosa26 locus. In other cases, PCR using the PfU DNA polymerase (*Promega*) was performed, and products were purified by the AMPure XP magnetic beats (*Beckman Coulter*), as per manufacturer's instructions. PCR products were barcoded, pooled and sequenced using a LSK109 library preparation kit on a single R.9.4.1 MinION flowcell (Oxford Nanopore Technologies) for 4 hours.

Raw FAST5 files were base called with Guppy 5 to produce raw FASTQ files. These files then underwent read correction using Canu 2.2 (Sergey et al., 2017) using the –correctReads parameter. Reads were aligned to the mm10 mouse reference genome

using minimap2 (version 2.24 (Li, 2018)) using the parameters: *ax map-ont*. CRISPResso2 (https://crispresso.pinellolab.partners.org/submission)(Clement et al., 2019) was then run targeting the Rosa26 locus of the mm10 genome. If matching the template sequence, each read was assigned as an HR outcome, or a TMEJ/NHEJ outcome if matching those specific sequences. TMEJ predictions were carried out using MEDJED (http://www.genesculpt.org/medjed/). For a full list of primers, template and gRNA sequences see (Ronson et al., 2023).

2.2.2. Polymerase Chain Reaction (PCR)

DNA amplification reaction was carried out using the reagents in Table 2.1 and primers in Table 2.7.

Table 2.1. PCR reaction mixture.

Component	Stock Concentration	Volume (µl)
dNTPs (*Bioline*)	10 mM	2 µl
Forward primer (*Sigma*)	10 µM	1.5 µl
Reverse primer (*Sigma*)	10 µM	1.5 µl
DNA	150 ng/ µl	1 µl
Pfu buffer	10 x	2.5 µl
Pfu polymerase (*Promega*)	3 U/ µl	0.5 µl
Nuclease free dH_2O	-	Up to 25 µl

Table 2.2. Site-directed mutagenesis PCR.

Step	Temperature (°C)	Time	Cycles

Initial denaturing	95	1 minute	1
Denaturing	95	30 seconds	25
Annealing	60	1 minute	25
Extension	72	14 minutes	25
Final extension	72	5 minutes	1
Hold	4	-	-

2.2.3. Restriction Enzyme Digest

1 µl of restriction enzyme was added using the reagent mixture volumes in Table 2.3 and incubated at 37 °C for 1 hr. Appropriate NEB enzymes and buffers were used according to DNA and plasmids to be cut.

Table 2.3. Restriction enzyme digest mixture.

Component	**Volume (µl)**
10 x buffer	1 µl
BSA	1 µl
DNA	1 µl
Enzyme 1	1 µl
Enzyme 2	1 µl
H_2O	Up to 10 µl

2.2.4. Agarose Gel Electrophoresis

PCR product was digested using 1 µl DpNI restriction enzyme (20,000 U/ml) *(New England Biolabs)* for 1 hour at 37 °C. 1 % Agarose gels were made using 1 x TAE with the addition of Ethidium Bromide (1:100,000). Gels were added to an electrophoresis

tank (*Biorad)* containing 1 x TAE buffer. 5 µl of DNA ladder (*Thermofisher* Hyperladder 1kb) was added to the first lane and 6 µl of the PCR products together were loaded (*QIAGEN* loading dye added) and run at 120 V for 40 minutes. Agarose gels were visualised using a UV transilluminator (*Syngene*).

2.2.5. Bacterial Transformation

Competent *Escherichia coli (E. coli)* DH5α (*Bioline*) were thawed on ice. 10 µl of DH5α cells were added to 1-100 ng of plasmid DNA for 30 minutes on ice and heat shocked for 30 seconds at 42 °C and transferred to ice for 2 minutes. 950 µl of Luria-Bertani (LB) broth (*Melford*) was added to the DH5α competent cells and incubated at 37°C for 1 hour. 100-200 µl was plated onto LB agar plates containing Ampicillin (50 µl/ml). LB agar plates were incubated at 37 °C overnight.

2.2.6. Plasmid DNA Purification and Quantification

Bacterial colonies were selected from Ampicillin (50 µl/ml) LB agar plates and grown in 5 ml LB Ampicillin (50 µl/ml) cultures at 37 °C at 200 RPM overnight. 4 ml of cultures were added to 500 ml LB Ampicillin cultures at 37 °C at 200 RPM overnight for Maxipreps. Bacterial cultures were centrifuged at 4,000 x g for 10 minutes forming a bacterial pellet and supernatant was discarded. DNA purification was performed using *Thermofisher* Maxiprep kit as per manufacturer's instructions. Purified DNA was quantified by adding 1 µl of DNA sample to the Nanodrop 2000/2000c (*Thermofisher*) spectrophotometer, which was previously blanked using 1 µl of dH_2O, and then stored at -20 °C.

2.2.7. DNA sequencing

Quantified DNA was diluted to 10-100 ng/µl in 10 µl nuclease-free H_2O and sent to *Source Biosciences* for sequencing and analysis was carried out using *SeqMan* Pro 15 software.

2.3. Protein biology

2.3.1. SDS Polyacrylamide Gel Electrophoresis (SDS-PAGE)

Samples were prepared by adding 4 x loading buffer directly to lyse the cells. Loading buffer samples were sonicated at 50 % intensity for 10 seconds, then boiled for 5-10 minutes at 95 °C. Samples were then centrifuged at 13,000 x g for 5 minutes before loading. SDS-PAGE protein gels were prepared to different percentages of acrylamide depending on the molecular weight of the protein of interest (Table 2.4). Once set, the gels were transferred to a *Biorad* tank containing 1 x Running Buffer (*Geneflow*). The first lane was loaded with 5 µl Spectra Broad Range/ PageRuler™ Prestained Protein Ladder/ HiMark™ Pre-stained Protein Standard (*Thermofisher*) and subsequent wells were loading with sample containing 4 x loading buffer. Protein samples were separated by SDS-PAGE protein gels running at 250 V for 45 minutes.

2.3.2. Western blotting

The gel was transferred onto a methanol activated PVDF Immunobillon membrane (*Sigma*) in 1 x Transfer Buffer *(Geneflow).* Transfer cassettes were arranged by the following: *Biorad* Trans-blot cassettes containing a sponge and 2 x Whatman filter paper (*Cytvia*) either side of the membrane and SDS-PAGE gel. The transfer cassette was placed in a tank containing 1 x Transfer buffer (20 % v/v methanol, 0.19 M glycine and 0.05 M Tris) for 1.5-22 hours at 100 V/25 V depending on protein size at 4 °C. Following the transfer, membranes were blocked in 5 % skimmed dried milk *(Marvel)*

in 1 x PBST for 30-60 minutes. Membranes were then incubated in primary antibody (Table 2.5) diluted in 3 ml 5 % skimmed dried milk either at room temperature for up to 6 hours or incubated overnight at 4 °C on a roller. Membranes were washed 3 x for 5 min in 1 x PBST and incubated in secondary antibody (Table 2.5) (1:10,000) conjugated to horse-radish peroxidase (HRP) diluted in 5 ml 5 % skimmed dried milk for a minimum of 1 hour on a roller at room temperature. Membranes were washed 3 x for 5 min in 1 x PBST, followed by probing in 1:1 chemiluminescent EZ-ECL mix (*Biological Industries* or ECL prime (*Cytvia*)) for 5 minutes. Excess ECL was removed from the membrane and placed in a plastic wallet secured within a cassette. A single X-ray film (*SIS Scientific laboratory supplies*) was placed within the cassette for a selected exposure time and developed via a *Konica SRX101A* developer in a dark room. ImageJ was used to perform densitometry calculations. For a full list of antibodies see Table 2.5.

Table 2.4. Resolving and stacking gel components.

Component	**Resolving gel (ml)**			**Stacking gel (ml)**
-	4%	6%	8%	5%
H_2O	4	5.3	4.6	3.4
30% Acrylamide	1.35	2	2.7	0.83
1.5M Tris pH 8.8	2.5	2.5	2.5	-
1.0M Tris pH 6.8	-	-	-	0.65
10% SDS	0.1	0.1	0.1	0.05
10% APS	0.01	0.1	0.1	0.05

TEMED	0.01	0.01	0.01	0.005
Final Volume (ml)	10	10	10	5

Table 2.5. Antibodies.

Antibody (clone)	Host	Cat. number	Supplier	Technique	Concentration
53BP1	Rabbit	Ab36823	Abcam	WB	1:1000
Murine BARD1 (1734p)	Rabbit	N/A	Gift from R. Baer	WB/IF	1:1000
Murine BRCA1 (56E)	Rabbit	N/A	Gift from R. Baer	IF	1:1000
Murine BRCA1	Rabbit	AF6288	Affinity Bioscience	WB	1:300
Murine BRCA1 (287.12)	Mouse	Sc-135732	Santa Cruz	WB/IF	1:1000
CldU (BrdU)	Rat	Ab6326	Abcam	IF/Fibres	1:2000
DNA2	Rabbit	Ab96488	Abcam	WB	1:1000
Flag (M2)	Mouse	347580	Sigma	WB	1:1000
GAPDH	Mouse	Ab8245	Abcam	WB	1:10000
H2A	Rabbit	Ab18255	Abcam	WB	1:1000
H2A-Ub (E6C5)	Mouse	05-678	Sigma	WB	1:500
γH2AX	Mouse	Ab22551	Abcam	IF	1:2000
γH2AX	Rabbit	Ab2893	Abcam	IF	1:2000

HA.11	Mouse	901501	Biolegend	IF	1:1000
IdU (BrdU)	Mouse	347580	BD Biosciences	IF/Fibres	1:250/500
MRE11	Rabbit	NB100-142	Novus Biologicals	WB	1:1000
PCNA	Mouse	PC-10	Santa Cruz	WB	1:1000
POLK	Rabbit	PA5-99004	Thermofisher	WB	1:500
Polθ	Rabbit	MBS9612322	MyBiosource	WB	1:500
RAD18	Mouse	H00056852-M01	Novus Biologicals	WB/IF	1:1000
RAD51 (Ab-1)	Rabbit	PC130	Calbiochem	IF	1:1000
RAP80	Rabbit	PA5-77181	Thermofisher	WB	1:1000
RNF168	Sheep	A301.246A	Bethyl	WB	1:1000
RPA70	Mouse	Abcam	Abcam	WB	1:1000
SMARCAD1	Rabbit	A301-593A	Bethyl	WB	1:1000
USP1	Mouse	66069-1-Ig	Proteintech	WB	1:1000
USP48	Rabbit	Ab72226	Abcam	WB	1:1000
Vinculin (EPR8185)	Rabbit	Ab129002	Abcam	WB	1:5000
Donkey α Mouse Alexa Fluor 488	Donkey	A21202	Life technologies	IF	1:1000
Donkey α Rabbit Alexa Fluor 488	Donkey	A21206	Life technologies	IF	1:1000

Donkey α Mouse Alexa Fluor 555	Donkey	A31570	Life technologies	IF	1:1000
Donkey α Rabbit Alexa Fluor 555	Donkey	A31572	Life technologies	IF	1:1000
Rabbit α Mouse HRP	Rabbit	P0161	Dako	WB	1:10000
Swine α Rabbit HRP	Swine	P0217	Dako	WB	1:10000

Table 2.6. siRNA sequences.

siRNA	siRNA sequences	Supplier
Luciferase (NTC)	Sense: CUUACGCUGAGUACUUCGA[dT][dT] Antisense: [Phos]UCGAAGUACUCAGCGUAA G[dT][dT]	Sigma Aldrich
mBRCA1	Sense: GGAUUUAUCUGCCGUCCAA [dT][dT] Antisense: [Phos] UUGGACGGCAGAUAAAUCC[[dT][dT] Sense: GAACAGAGCAACUUGAAAC [dTdT] Antisense: [Phos] AUUGUCUGUAUAGUCCACAGG [dT][dT]	Sigma Aldrich
mRAD52	Sense: UUGAAGGUCAUCGGGUAAUUA [dT][dT] Antisense: [Phos]UAAUUACCCGAUGACCUUCAA [dT][dT] Sense: ACUAUCUGAGGUCACUAAAUA [dT][dT] Antisense: [Phos] UAUUUAGUGACCUCAGAUAGU [dT][dT]	Sigma Aldrich
mRNF168	Sense: CCUUGGCUUCUCCUUUGAGUU [dT][dT] Antisense: [Phos] AACUCAAAGGAGAAGCCAAGG [dT][dT]	Sigma Aldrich
mPOLQ	Sense: CCAGACUAAGAGUUCUCAUAA [dT][dT] Antisense:[Phos] UUAUGAGAACUCUUAGUCUGG [dT][dT] Sense: CCAGGAAUCAAAGACGACAAU [dT][dT] Antisense:[Phos] AUUGUCGUCUUUGAUUCCUGG [dT][dT]	Sigma Aldrich

	Sense: CACGGAAGAAAGCGUUGUUUA [dT][dT] Antisense:[Phos] UAAACAACGCUUUCUUCCGUG [dT][dT]	
mUSP48	Sense: AUUCCUUUGUGGGCUUGACUA[dT][dT] Antisense: [Phos]UAGUCAAGCCCACAAAGGAAU[dT][dT] Sense: AUUCUGGCCACUACAUCGCAC[dT][dT] Antisense: [Phos]GUGCGAUGUAGUGGCCAGAAU[dT][dT]	Sigma Aldrich
mSMARCAD1	Sense: CCAGUAUUACACACCUGAGAA[dT][dT] Antisense: [Phos]UUCUCAGGUGUGUAAUACUGG[dT][dT]	Sigma Aldrich
hRAP80 (works in mouse)	Sense: CCAUUGCUGAAAGCCUGAAUA[dT][dT] Antisense: [Phos]UAUUCAGGCUUUCAGCAAUGG[dT][dT]	Sigma Aldrich
mUSP1	Sense: CAGUGACCAAACAGGCGUUAA[dT][dT] Antisense:[Phos]UUAACGCCUGUUUGGUCACUG[dT][dT	Horizon
mSMUG1	Sense: GCACUGCUUUGUCCACAAUCU[dT][dT] Antisense: [Phos]AGAUUGUGGACAAAGCAGUGC[dT][dT]	Sigma Aldrich
mPRIMPOL	Sense: CGGAAGAAUUACUGGUUUAUU[dT][dT] Antisense: [Phos]UAAACCAGUAAUUCUUCCGUU[dT][dT]	Horizon
mPOLK	Sense: CCGGAAUUUGAACAAUACCAU[dT][dT] Antisense: [Phos]AUGGUAUUGUUCAAAUUCCGG[dT][dT] Sense: GCCCUUAGAAAUGUCUCAUAA[dT][dT] Antisense:[Phos]UUAUGAGACAUUUCUAAGGGC[dT][dT]	Sigma Aldrich
53BP1 smartpool	Dharmacon product code: L042290-01	Horizon

Table 2.7. Primer sequences.

Gene	Point mutation (human)	Point mutation (murine)	Sequences (5'-3-)	Supplier
BARD1	L44R	L38R	Forward: GCTTGCCCGCCGGGAGAAGCT GCTG Reverse: ACTGGGCATCCTGAGCCAACA CAG	Sigma Aldrich

F133A/D135A/A136E (AAE)	F125A/D127A/A128E (AAE)	Forward:CATTTTTATTGAATTCTTCTTCCTTTCTTCAGCACCAGCTAAACTTGCCCTAGATGTGTTGTCTTTTGAAT Reverse:ATTCAAAAGACAACACATCTAGGGCAAGTTTAGCTGGTGCTGAAGAAAGGAAGAAGAATTCAATAAAAATG	Sigma Aldrich
A460T	A448T	Forward: CGGTGTCCATCCAGTATGGTCTTTAACATTTGGGT Reverse: ACCCAAATGTTAAAGACCATACTGGATGGACACCG	Sigma Aldrich
D712A	D700A	Forward: GATGGTCTGAGTCACAGCACTGTCTGGCTTGGG Reverse: CCCAAGCCAGACAGTGCTGTGACTCAGACCATC	Sigma Aldrich

Table 2.8. Drug treatments and inhibitors.

Agent	Target	Cat. number	Concentration	Supplier
BrdU	Thymidine analogue	B5002	10 μM	Sigma
EdU	Thymidine analogue	A10044	10 μM	Thermofisher
CldU	Thymidine analogue	C6891	250 μM	Sigma
IdU	Thymidine analogue	I7125	25 μM	Sigma
Hydroxyurea (HU)	Ribonucleoside reductase	H8627	0.1-10 mM	Sigma
6-OH-DL-DOPA	RAD52	H2380	0.15-5 μM	Sigma
ART558	Polθ	N/A	2.5-30 μM	Artios
Olaparib	PARP	S1060	1-25 μM	Selleckchem

Mirin	MRE11	J67462	2.5-5 μM	Alfa Aesar
Nocodazole	B-tubulin	SML-1665-1ML	200 ng/ml	Sigma
JH-RE-06	REV1	SML2993-5MG	1-10 μM	Sigma

2.4. Statistical analysis

Statistical tests were undertaken using a two-tailed Student's *t*-Test, two-way ANOVA (Analysis of Variance) and Mann-Whitney test, and p-values were generated. Ns = not significant. p>0.05, "*" =p ≤0.05, "**" =p ≤ 0.01, "***" =p ≤ 0.001, "****" =p ≤ 0.0001. The number of biological repeats is shown (n).

Table 2.9. Antibiotics.

Antibiotic	Stock concentration	Working concentration
Penicillin/Streptomycin	100 X	1 X
Ampicillin	10 gm/ ml in H_2O	10 μg/ ml

2.5. Buffers

PBS

1 tablet (*Sigma)* in 200 ml H_2O.

Methylene Blue stain

1% Methylene Blue powder, 50% Ethanol.

Crystal Violet Stain

0.5% crystal violet, 50% methanol, 49.5% H_2O.

Fibre Spreading Buffer

200 mM Tris pH 7.4, 50 mM EDTA, 0.5% SDS

Fibre Fixative

3:1 Methanol, Acetic Acid

CSK100 buffer

100 mM NaCl, 10 mM MOPS, 3 mM $MgCl_2$, 300 mM sucrose, 0.5% triton X-100, pH 7.0

S1 buffer

30 mM sodium acetate, 10 mM zinc acetate, 5% glycerol, 50 mM NaCl, pH 4.6

LB Broth

10 g LB Broth powder (*Sigma)* in 500 ml H_2O.

LB agar

1 x LB agar capsule (*Thermofisher*) in 500 ml H_2O.

4 x SDS Loading Buffer

0.25 M Tris pH 6.8, 8% SDS, 40% Glycerol, 6 M Urea, 10% β-Mercaptoethanol

1 x SDS Running Buffer

10% 10 x Tris/Gycine/SDS in 90% H_2O.

1 x Transfer Buffer

10% 10 x Tris/Glycine, 20% Methanol, 80% H_2O.

3. BRCA-RAD51 interactions suppress cell sensitivity to Polθ loss and inhibition

3.1. Preface

Chapter 3 is adapted from our published study:

Ronson GE*, Starowicz K*, **Anthony EJ**, Piberger AL, Clarke LC, Garvin AJ, Beggs AD, Whalley CM, Edmonds MJ, Beesley JFJ, Morris JR. Mechanisms of synthetic lethality between BRCA1/2 and 53BP1 deficiencies and DNA polymerase theta targeting. Nat Commun. 2023 Nov 29;14(1):7834. doi: 10.1038/s41467-023-43677-2. PMID: 38030626; PMCID: PMC10687250.

3.2. Introduction

BRCA1 is essential for maintaining genome integrity through the repair of DSBs by homologous recombination, via the protection of stalled replication forks, during DNA replication and through the suppression of ssDNA replication gap formation (Panzarino et al., 2021; Schlacher et al., 2012; Moynahan et al., 1999; Chaudhuri et al., 2016). The BRCA1 RING finger contains two zinc finger-like motifs made up of seven cysteine residues and one histidine residue generating the Site I and Site II Zn^{2+} binding sites (Brzovic et al., 2001b; Meza et al., 1999; Borden and Freemont, 1996; Bienstock et al., 1996; Brzovic et al., 1998). Mutations located within the Zn^{2+} binding residues can disrupt BRCA1/BARD1 E3 ubiquitin ligase function (Brzovic et al., 2001a). The N-terminal RING domain mutation C61G-*BRCA1* is one of the most frequently reported missense mutations and is associated with the development of breast and ovarian

cancer (Castilla et al., 1994; Drost et al., 2011; Greenman et al., 1998; Spurdle et al., 2012). The C61G-*BRCA1* mutation destabilises the second Zn^{2+} binding loop which abrogates the BRCA1/BARD1 heterodimer and disrupts its E3 ubiquitin ligase activity (Hashizume et al., 2001; Ruffner et al., 2001; Mallery et al., 2002; Drost and Jonkers, 2014). Genetic mouse models have become an incredibly useful tool to demonstrate *Brca1* function, identify critical protein domains, and determine response to genotoxic agents (Yueh et al., 2024). Mutant mouse models harbouring the homozygous *Brca1*$^{C61G/C61G}$ mutation are embryonic lethal forming no viable pups, only surviving to embryonic day (E) E9.5 and E12.5 (Drost et al., 2011). *Brca1*$^{C61G/C61G}$ mice elicit a developmental phenotype similar to that of *Brca1* null mutants (Drost et al., 2011).

To create a *Brca1* mutant mouse model containing the C61G mutation *Brca1*$^{C61G/+}$ mice were crossed with *53bp1*$^{-/-}$ mice to produce *Brca1*$^{C61G/C61G}$ 53bp1$^{-/-}$ live pups born at expected Mendelian ratios (Ronson et al., 2023). 53BP1 is a DNA damage response factor that is an activator of p53 functioning in NHEJ (Gupta et al., 2014). 53BP1 and BRCA1 exhibit an antagonistic relationship whereby 53BP1 promotes NHEJ and BRCA1 E3 ubiquitin ligase function facilitates the removal of 53BP1 to mediate DNA end resection and thus DNA-damage repair by HR (Daley and Sung, 2014; Feng et al., 2013; Kakarougkas et al., 2013b; Bunting et al., 2010; Densham and Morris, 2017).

Synthetic lethal interactors of BRCA1 have become an attractive treatment for *BRCA1*-mutated cancers (Patel et al., 2021b; Dedes et al., 2011; Helleday, 2011). Synthetic lethality is defined as the loss of two genes causing cell death when the loss of either gene alone has no impact on cell survival (Kaelin, 2005). For example, Polθ elicits synthetic lethality in HR-deficient cancers and augments PARPi efficacy, therefore Polθ inhibitors have become an attractive therapeutic target for HR-deficient cancers

(Zatreanu et al., 2021; Zhou et al., 2021). Polθ is upregulated in numerous cancers and is associated with poor survival in breast cancer (Lemée et al., 2010). Polθ is a large protein that contains an N-terminal helicase domain, a disordered central domain and a C-terminal polymerase domain (Mateos-Gomez et al., 2017). Polθ functions in TMEJ; an alternative DSB repair pathway in the absence of optimal HR (Kent et al., 2015a; Mateos-Gomez et al., 2015; Ceccaldi et al., 2015). Like HR, TMEJ requires short 3'ssDNA overhangs generated by MRN and Ct-BP interacting protein (CtIP) with a pre-requisite for sequence microhomologies (2-6 base pairs) (Truong et al., 2013). Polθ is also important for DDT as a translesion synthesis polymerase and there is evidence that Polθ can seal post-replicative ssDNA gaps (Seki et al., 2003; Belan et al., 2022; Mann et al., 2022; Schrempf et al., 2021).

ssDNA gaps arise due to stress-induced unrestrained DNA replication, and recently has been shown to underlie hypersensitivity of *BRCA*-deficient cells to genotoxic agents such as cisplatin, unlike HR and fork protection (Panzarino et al., 2021). ssDNA gaps can be prevented by appropriate fork restraint by replication fork reversal and protection or by post-replicative repair of gaps (Panzarino et al., 2021; Taglialatela et al., 2017; Kolinjivadi et al., 2017b; Mijic et al., 2017). The RAD51 recombinase is characterised as a major guardian of genome stability with both HR-dependent and independent roles (Wassing and Esashi, 2021). It is well defined that BRCA1 interacts with PALB2 which subsequently recruits BRCA2 to mediate RAD51 nucleofilament assembly on resected DNA, and RAD51 facilitates strand invasion of 3'ssDNA into the homologous template (Jensen et al., 2010; Sy et al., 2009a; Haas et al., 2018). Nevertheless, RAD51 has recently been implicated in limiting ssDNA gap formation (Tirman et al., 2021b). The loss of a functional BRCA1/2-RAD51 pathway leads to

ssDNA gap generation by PRIMPOL repriming and preventing RAD51-mediated post replicative repair of ssDNA gaps (Kang et al., 2021; Taglialatela et al., 2021; Kolinjivadi et al., 2017b; Piberger et al., 2020; Tirman et al., 2021b; Cong et al., 2021). PRIMPOL-generated ssDNA gaps can be repaired by RAD51-mediated HR (Hashimoto et al., 2010; Kolinjivadi et al., 2017b; Zellweger et al., 2015; Piberger et al., 2020). However, more research is necessary to uncover how the BRCA1/2-RAD51 pathway suppresses ssDNA gaps.

The aims of this chapter are to uncover the hierarchy of support mechanisms for HR using the *Brca1*^{C61G} hypomorph and to further understand the synthetic lethal relationship between *Brca1* deficiency, *53bp1* deficiency and Polθ loss. We use modified DNA fibre assays to study replication dynamics which identifies a vulnerability of Polθ loss and inhibition in our *Brca1*^{C61G} model with regards to the PRR of ssDNA gaps, which can be rescued by the reinstatement of the BRCA1/2-RAD51 machinery.

3.3. Results

3.3.1. *Brca1*$^{C61G/C61G}$ *53bp1*$^{-/-}$ cells express a hypomorphic BRCA1 protein

Mutant mouse models harbouring the homozygous *Brca1*$^{C61G/C61G}$ mutation are embryonic lethal forming no viable pups, so were crossed on a *53bp1*$^{-/-}$ background (Drost et al., 2011; Ronson et al., 2023). We derived MEFs from *Brca1*$^{+/+}$ *(WT), Brca1*$^{+/+}$ *53bp1*$^{-/-}$ *(+/+), Brca1*$^{C61G/+}$ *53bp1*$^{-/-}$ (*CG/+)* and *Brca1*$^{C61G/C61G}$ *53bp1*$^{-/-}$ *(CG/CG)* embryos that we subsequently used as our *Brca1*-mutated mouse model. We determined C61G-BRCA1 protein expression by carrying out immunoprecipitation followed by mass spectrometry analysis, revealing that C61G-BRCA1 and BARD1 expression levels were 20% that of cells with WT-BRCA1 (Ronson et al., 2023). The BRCA1 expression levels can be seen between the different genotypes: WT*, Brca1*$^{+/+}$

53bp1$^{-/-}$, *Brca1*$^{C61G/+}$ *53bp1*$^{-/-}$and *Brca1*$^{C61G/C61G}$ *53bp1*$^{-/-}$ using western blot analysis, highlighting that the expression of both BRCA1 and BARD1 is reduced in *Brca1*$^{C61G/C61G}$ *53bp1*$^{-/-}$ MEFs (Fig.3.1A). We then wanted to decipher whether the recruitment of BRCA1 to sites of DNA damage is impaired by analysing the ability of cells to form IR-induced nuclear foci. BRCA1 localisation to foci takes place during S-phase of the cell cycle, so we quantified foci numbers in cells that were positively tagged for the thymidine analogue EdU, highlighting its incorporation into DNA during active DNA synthesis and proliferation (Pereira et al., 2017). We revealed that *Brca1*$^{C61G/C61G}$ *53bp1*$^{-/-}$ cells displayed fewer and weaker IR-induced BRCA1 foci, on average 7 foci per EdU positive cell after 3 hours post IR treatment compared to *Brca1*$^{+/+}$ *53bp1*$^{-/-}$ MEFs at a mean of 20 foci per EdU positive cell (Fig.3.1B). Overall, these data show that *Brca1*$^{C61G/C61G}$ *53bp1*$^{-/-}$ cells elicit reduced BRCA1/BARD1 expression which could explain why BRCA1 recruitment is lowered.

We then wanted to explore whether homozygous *Brca1*$^{C61G/C61G}$ *53bp1*$^{-/-}$ MEFs are proficient in the error-free double strand break repair pathway HR. We noted that *Brca1*$^{C61G/C61G}$ *53bp1*$^{-/-}$ MEFs harbour BRCA1-dependent RAD51 foci formation post IR close to numbers seen in *Brca1*$^{+/+}$ *53bp1*$^{-/-}$ cells (Fig.3.1C), which is a marker for functional HR. BRCA1-depleted cells showed a mean of 7 RAD51 foci per EdU positive cell compared to 14 RAD51 foci per EdU positive cell in *Brca1*$^{C61G/C61G}$ *53bp1*$^{-/-}$ cells without BRCA1 knockdown (Fig.3.1C). Whilst BRCA1-depleted *Brca1*$^{+/+}$ *53bp1*$^{-/-}$ cells showed an average of 10 RAD51 foci per EdU positive cell and a mean of 18 RAD51 foci in untreated cells (Fig.3.1C). The dependency on BRCA1 indicates that RAD51 foci formation is supported by the C61G-BRCA1 protein. The PARPi Olaparib is synthetic lethal with HR-defective *BRCA1/2*-deficient cancers (Farmer et al., 2005;

Bryant et al., 2005), hence we wanted to decipher whether our *Brca1*$^{C61G/C61G}$ *53bp1*$^{-/-}$ MEFs are sensitive to Olaparib. We noted that BRCA1-depleted WT cells showed a significant sensitivity to Olaparib, whereas *Brca1*$^{C61G/C61G}$ *53bp1*$^{-/-}$ cells did not (Fig.3.1D). These results demonstrate that C61G-BRCA1 is hypomorphic but shows phenotypes of proficient HR.

To confirm HR competency in our *Brca1*$^{C61G/C61G}$ *53bp1*$^{-/-}$ cells we performed semi-quantitative PCR to measure HR outcome frequency. HR proficiency was measured with primers specific for the HR outcome at a specific DSB site. Subsequently the HR-specific PCR product band intensities were quantified and normalised to a PCR product at the Rosa26 locus which is HR-independent (Ronson et al., 2023). The quantified HR-specific PCR products identified that there was a significant reduction in relative HR in *Brca1*$^{C61G/C61G}$ *53bp1*$^{-/-}$ cells compared to *Brca1*$^{+/+}$ *53bp1*$^{-/-}$ cells (Fig.3.1E). However, *Brca1*$^{C61G/C61G}$ *53bp1*$^{-/-}$ cells had a higher HR frequency compared to WT cells (Ronson et al., 2023). Yet, there is evidence of sub-optimal HR activity when compared to *Brca1*$^{+/+}$ *53bp1*$^{-/-}$ cells, which also has 53BP1 removed (Fig.3.1E). In summary, the diminished expression of BRCA1/BARD1, abrogated BRCA1 focal formation and reduced HR frequency show that *Brca1*$^{C61G/C61G}$ *53bp1*$^{-/-}$ cells are HR competent albeit suboptimal.

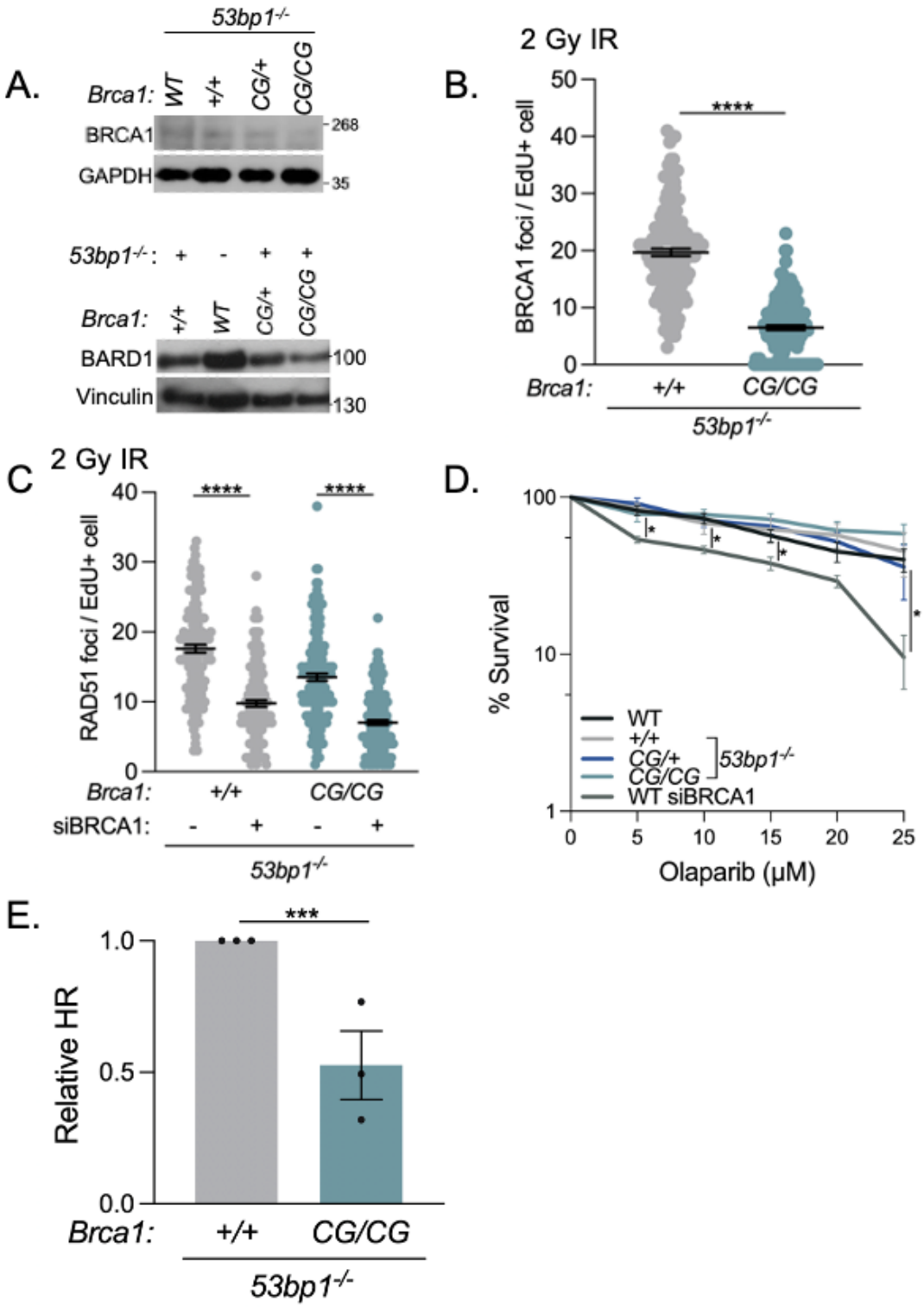

Figure 3.1. Characterisation of Brca1$^{C61G/C61G}$ 53bp1$^{-/-}$ cells to determine HR proficiency.

A. Representative western blot analysis of BRCA1 and BARD1 protein levels in MEFs of genotypes shown. Vinculin and GAPDH were used as loading controls.

B. Quantification of BRCA1 foci in EdU-positive *Brca1*$^{+/+}$ *53bp1*$^{-/-}$ and *Brca1*$^{C61G/C61G}$ *53bp1*$^{-/-}$ cells post 2 Gy irradiation and 3 hr recovery. N=90 cells from 3 biological repeats. Data are mean ± SEM. Statistical analysis performed using a two-tailed Student's *t*-Test; ****= p≤0.0001.
C. Quantification of RAD51 foci in EdU-positive *Brca1*$^{+/+}$ *53bp1*$^{-/-}$ and *Brca1*$^{C61G/C61G}$ *53bp1*$^{-/-}$ cells post 2 Gy irradiation and 3 hr recovery. N=150 cells from 3 biological repeats. Data are mean ± SEM. Statistical analysis performed using a two-tailed Student's *t*-Test; ****= p≤0.0001. *George Ronson/Katarzyna Starowicz.*
D. Colony survival in MEFs of genotypes shown, treated with a dose range of Olaparib for 16 hr. MEFs were plated 24 hr prior to transfection, treated with Olaparib (2 – 10 μM) for 16 hr and re-plated into colonies and grown out for 7 days. N=3. Data are mean ± SEM. Statistical analysis performed using a two-tailed Student's *t*-Test; *= p≤0.05. *George Ronson/Katarzyna Starowicz.*
E. Relative PCR product intensity of HR-specific product in *Brca1*$^{+/+}$ *53bp1*$^{-/-}$ and *Brca1*$^{C61G/C61G}$ *53bp1*$^{-/-}$ cells. n=3 biological repeats. *George Ronson.*

3.3.2. *Brca1*$^{C61G/C61G}$ *53bp1*$^{-/-}$ cells rely on the non-canonical support of Polθ

BRCA1/BARD1 levels in *Brca1*$^{C61G/C61G}$ *53bp1*$^{-/-}$ cells are drastically reduced (Fig.3.1A), therefore we considered whether additional non-canonical mechanisms are required to support HR. Polθ is overexpressed in HR and Shieldin-deficient cancers and evidence suggests that Polθ loss is synthetic lethal in *BRCA1*-deficient cancers (Ceccaldi et al., 2015; Zhou et al., 2021; Zatreanu et al., 2021). Polθ functions in translesion synthesis, TMEJ, and ssDNA gap prevention (Brambati et al., 2020; Mann et al., 2022; Belan et al., 2022; Schrempf et al., 2022; Ceccaldi et al., 2015) and has previously been reported to support cell viability in situations where HR proteins are reduced (Wang et al., 2019; Ceccaldi et al., 2015; Kelso et al., 2019; Feng et al., 2019). We therefore wanted to determine whether *Brca1*$^{C61G/C61G}$ *53bp1*$^{-/-}$ cells are reliant on Polθ for survival.

We demonstrated that Polθ expression levels were raised ~2-fold in *Brca1*$^{C61G/C61G}$ *53bp1*$^{-/-}$ cells compared to *Brca1*$^{+/+}$ *53bp1*$^{-/-}$ cells (Fig. 3.2A, B). Increased Polθ expression is associated with poor cancer prognosis and mutation burden (Wood and Doublié, 2016). Subsequently, we wanted to investigate cell sensitivity of *Brca1*$^{C61G/C61G}$ *53bp1*$^{-/-}$ cells in the absence of Polθ to see whether our cells are reliant on the error-prone mutagenetic Polθ. We carried out colony survival assays on *Brca1*$^{C61G/C61G}$ *53bp1*$^{-/-}$ cells treated with siRNA to Polθ and showed that cell viability was significantly reduced from a mean of 67% survival in *Brca1*$^{C61G/C61G}$ *53bp1*$^{-/-}$ cells compared to an average of 97% survival in *Brca1*$^{+/+}$ *53bp1*$^{-/-}$ cells, which indicates that *C61G* homozygous MEFs require Polθ for cell viability (Fig. 3.2C).

We then considered how Polθ loss impacts RAD51 foci formation in our cells. During HR, exposed resected 3'ssDNA is coated by RPA which is successively displaced by RAD51 (Deng et al., 2014; Ma et al., 2017a; Sugiyama et al., 1997), however the Polθ helicase domain displaces RPA from ssDNA in an ATP-dependent manner as RPA-ssDNA complexes block the annealing of microhomologies. The Polθ central domain binds to RAD51 and the polymerase functions as an anti-recombinase. (Ceccaldi et al., 2015; Mateos-Gomez et al., 2015; Schaub et al., 2022; Mateos-Gomez et al., 2017). In our system, we discovered that Polθ depletion by siRNA induced significantly elevated RAD51 foci formation post IR in our *Brca1*$^{C61G/C61G}$ *53bp1*$^{-/-}$ MEFs (Fig. 3.2E,F). In summary, our data show that Polθ inhibition could be an alternative target for *C61G-BRCA1* mutated cells, yet the mechanism underlying the synthetic lethal relationship between 53BP1, BRCA1 and Polθ remains largely unknown.

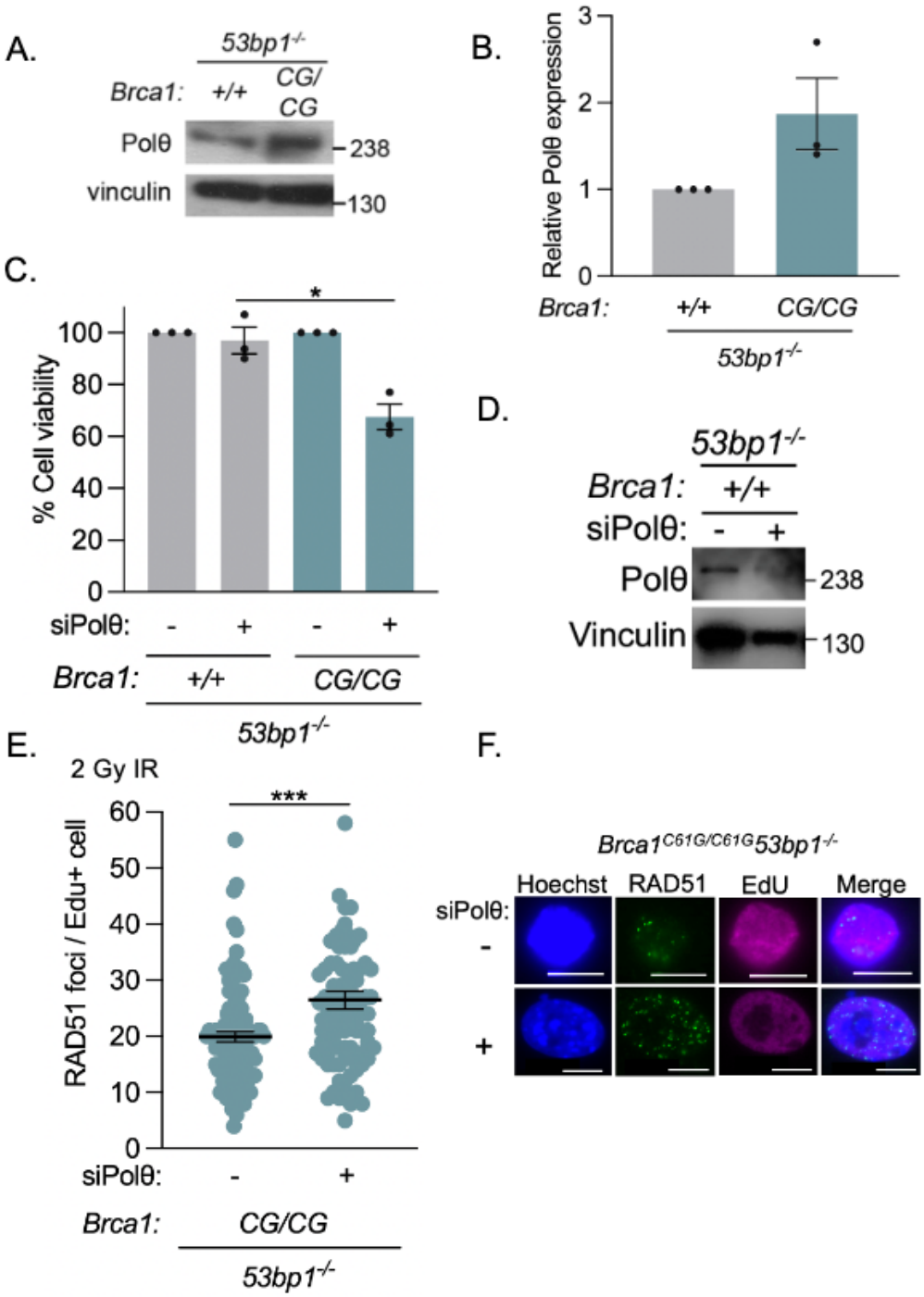

Figure 3.2. Brca1$^{C61G/C61G}$ 53bp1$^{-/-}$ cells rely on the non-canonical support of Polθ for survival.

A. Representative western blot of Polθ expression levels with vinculin as a loading control.
B. Quantification of Polθ protein levels, n=3 biological repeats. Data are mean ± SEM.

C. Colony survival in *Brca1*$^{+/+}$ *53bp1*$^{-/-}$ and *Brca1*$^{C61G/C61G}$ *53bp1*$^{-/-}$ cells treated with non-targeting control (NTC) siRNA (-) or siRNA targeting Polθ (+). n=3 biological repeats. Data are mean ± SEM. Statistical analysis performed using a two-tailed Student's *t*-Test; *= p≤0.05.
D. Representative western blot showing knockdown of Polθ in *Brca1*$^{+/+}$ *53bp1*$^{-/-}$ cells using NTC siRNA (-) or siRNA targeting Polθ. Vinculin was used as a loading control.
E. Quantification of EdU+ RAD51 foci in *Brca1*$^{+/+}$ *53bp1*$^{-/-}$ and *Brca1*$^{C61G/C61G}$ *53bp1*$^{-/-}$ cells, treated with siRNA to Polθ after 3 hours post 2 Gy irradiation. EdU incubated for 10 minutes prior to irradiation. n=150 cells from 3 biological replicates per condition. Statistical analysis performed using a two-tailed Student's *t*-Test; ***= p≤0.001.
F. Representative images of RAD51 foci in *Brca1*$^{C61G/C61G}$ *53bp1*$^{-/-}$ cells with and without Polθ depletion. The scale bar is 10 μm.

Polθ inhibitors are currently being developed and are in Phase II clinical trials (NCT04991480). We were kindly gifted ART558 from Artios Pharma Limited, which is a potent, selective, allosteric inhibitor of Polθ that specifically targets its DNA polymerase activity (Zatreanu et al., 2021). ART558 treatment is synthetic lethal in *BRCA1/2*-deficient cancers and can be used in synergy with PARPis (Zatreanu et al., 2021). Also, it has been reported that there is a synthetic lethal interaction between Polθ and 53BP1 (Wyatt et al., 2016; Feng et al., 2019). We tested a dose range of ART558 inhibitor (5 – 20 μM) on WT, *Brca1*$^{+/+}$ *53bp1*$^{-/-}$ and *Brca1*$^{C61G/C61G}$ *53bp1*$^{-/-}$ MEFs (Fig. 3.3A). We noted that *Brca1*$^{+/+}$ *53bp1*$^{-/-}$ and *Brca1*$^{C61G/C61G}$ *53bp1*$^{-/-}$ cells were more sensitive to ART558 than WT cells. Despite this, there was a noteworthy sensitivity to ART558 in the *Brca1*$^{C61G/C61G}$ *53bp1*$^{-/-}$ cells compared to *Brca1*$^{+/+}$ *53bp1*$^{-/-}$ cells (Fig. 3.3A). DSBs in chromatin facilitate H2AX phosphorylation at serine 139 to generate γH2AX, and γH2AX foci quantification is recognised in the field as a marker of DSBs (Kinner et al., 2008). ART558 treatment elicited increased DNA damage represented by augmented γH2AX foci formation in both *Brca1*$^{+/+}$ *53bp1*$^{-/-}$ and

Brca1$^{C61G/C61G}$ *53bp1*$^{-/-}$ MEFs, albeit with considerably higher numbers in *Brca1*$^{C61G/C61G}$ *53bp1*$^{-/-}$ cells (Fig. 3.3B), reinforcing that our *Brca1*-mutated cells treated with ART558 have a higher DNA damage burden.

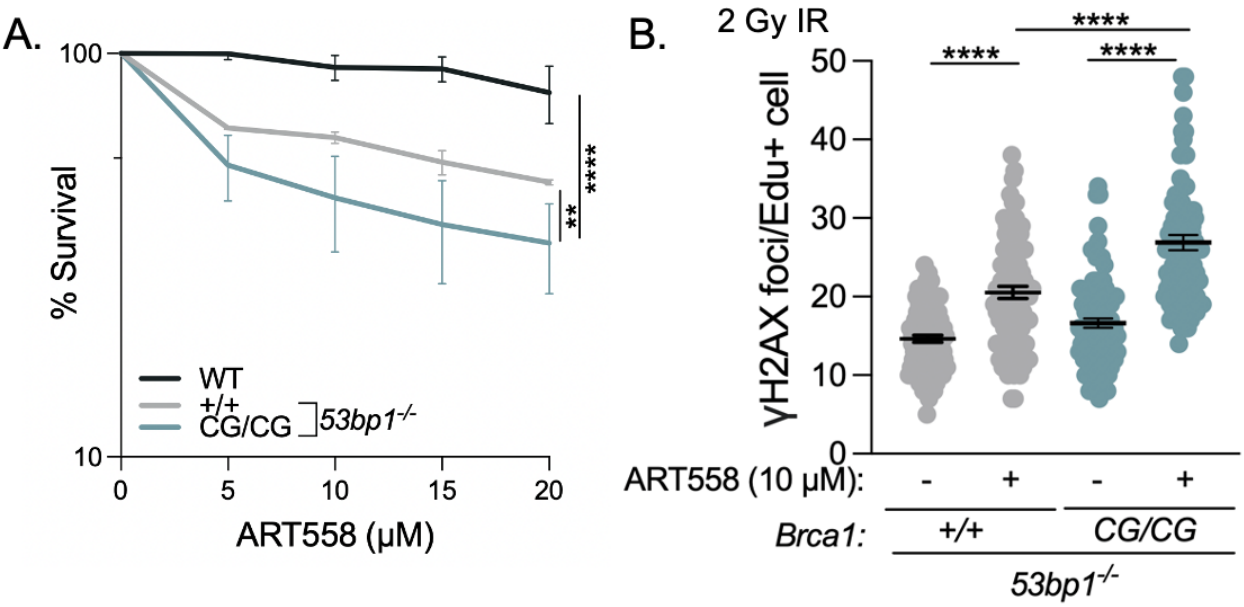

Figure 3.3. Brca1$^{C61G/C61G}$ 53bp1$^{-/-}$ cells are sensitive to the Polθ inhibitor ART558.

A. Colony survival in MEFs shown treated with the Polθ inhibitor ART558. n=3 biological repeats. Data are mean ± SEM. Data are mean ± SEM. Statistical analysis performed using a two-way ANOVA; ****= p≤0.0001; ** = p≤0.05.

B. Quantification of EdU+ γH2AX foci in *Brca1*$^{+/+}$ *53bp1*$^{-/-}$ and *Brca1*$^{C61G/C61G}$ *53bp1*$^{-/-}$ cells, treated with the Polθ inhibitor ART558 after 3 hours post 2 Gy irradiation. n=150 cells from 3 biological replicates per condition. Data are mean ± SEM. Statistical analysis performed using a two-tailed Student's *t*-Test; ****= p≤0.0001.

3.3.3. BARD1 overexpression rescues cell sensitivity to Polθ loss in *Brca1*$^{C61G/C61G}$ *53bp1*$^{-/-}$ cells

We next wanted to address what is driving the sensitivity to the loss of Polθ in our *Brca1*$^{C61G/C61G}$ *53bp1*$^{-/-}$ cells. Previous studies have shown that the overexpression of BARD1 can encourage the localisation of BRCA1 into the nucleus and generate DNA damage induced BRCA1 foci, even in NLS-deficient forms of BRCA1 (Fabbro et al., 2002; Huber et al., 2001). So, we wanted to identify whether BARD1 overexpression can improve C61G-BRCA1 localisation and potentially overcome deleterious impacts of Polθ depletion. A FLAG co-immunoprecipitation undertaken by my lab colleague highlighted that the interaction between C61G-BRCA1 and BARD1 is weakened but not lost (Ronson et al., 2023). Therefore, we considered whether the reduced expression of BRCA1/BARD1 could be rescued in *Brca1*$^{C61G/C61G}$ *53bp1*$^{-/-}$ cells by overexpressing exogenous murine BARD1. We did this by developing retrovirally infected *Brca1*$^{+/+}$ *53bp1*$^{-/-}$ and *Brca1*$^{C61G/C61G}$ *53bp1*$^{-/-}$ cells to exogenously express BARD1 constructs. HEK293T Platinum E cells are a platinum retroviral packaging cell line that contain gag, pol and env genes to promote retroviral packaging via a single plasmid transfection of a cloning vector, in this case pMSCV-IRES-GFP II, containing the gene of interest, *Bard1* (Morita et al., 2000). The ecotropic viral supernatant produced from the HEK293T Platinum E cells can readily infect our MEFs (Morita et al., 2000).

The exogenous expression of retroviral BARD1 could improve BARD1 expression levels in our *Brca1*$^{C61G/C61G}$ *53bp1*$^{-/-}$ cells (Fig.3.4A). As mentioned previously, there were fewer and weaker IR induced C61G-BRCA1 foci in *Brca1*$^{C61G/C61G}$ *53bp1*$^{-/-}$ cells

compared to *Brca1*$^{+/+}$ 53bp1$^{-/-}$ MEFs (Fig.3.1B). Yet, exogenous expression of murine BARD1 significantly elevated C61G-BRCA1 foci formation post IR (Fig.3.4B,C). *Brca1*$^{C61G/C61G}$ *53bp1*$^{-/-}$ cells treated with NTC siRNA had an average of 7 foci per EdU positive cell, but the cells retrovirally infected with BARD1 increased foci numbers to approximately 11 foci per EdU positive cell (Fig.3.4B,C). The overexpression of BARD1 did not alter the number of γH2AX foci, a chromatin mark stimulated by DNA breaks, with an average of 22 foci per EdU positive cell in *Brca1*$^{C61G/C61G}$ *53bp1*$^{-/-}$ cells treated with an empty vector compared to an average of 21 foci per EdU positive cell in *Brca1*$^{C61G/C61G}$ *53bp1*$^{-/-}$ cells treated with BARD1 overexpression (Fig.3.4B,C).

Due to the increase of C61G-BRCA1 to sites of damage, we wanted to determine whether increased localisation could improve cell viability in the absence of Polθ. Consistent with the foci data, exogenous BARD1 expression suppressed cell sensitivity to Polθ loss in *Brca1*$^{C61G/C61G}$ *53bp1*$^{-/-}$ cells back to levels seen in *Brca1*$^{+/+}$ 53bp1$^{-/-}$ MEFs depleted of Polθ, increasing cell viability from approximately 52% to 89% (Fig.3.4D). These data suggest that the overexpression of murine BARD1 can ameliorate *Brca1*$^{C61G/C61G}$ *53bp1*$^{-/-}$ cell dependency on Polθ for survival by improving BARD1 expression and recruitment of the C61G-BRCA1 hypomorphic protein to sites of damage.

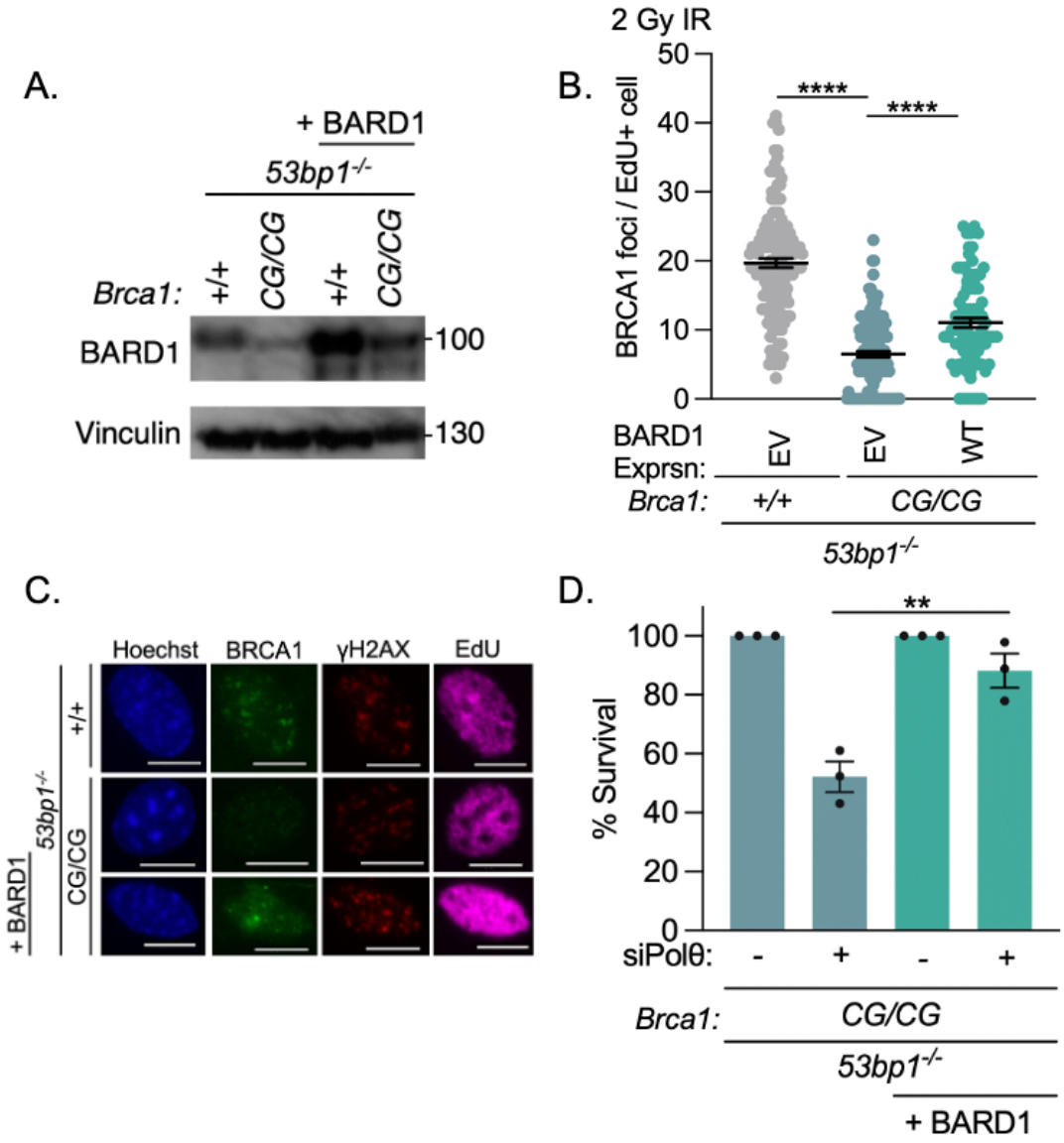

Figure 3.4. BARD1 overexpression rescues cell sensitivity to Polθ loss in Brca1$^{C61G/C61G}$ *53bp1*$^{-/-}$ cells.

A. Western blot of BARD1 expression in *Brca1*$^{+/+}$ *53bp1*$^{-/-}$ and *Brca1*$^{C61G/C61G}$ *53bp1*$^{-/-}$ cells infected with empty vector (EV) or containing BARD1.

B. Quantification of EdU+ C61G-BRCA1 foci post 3 hr 2 Gy IR in *Brca1*$^{+/+}$*53bp1*$^{-/-}$ and *Brca1*$^{C61G/C61G}$ *53bp1*$^{-/-}$ cells infected with empty vector (EV) or containing BARD1. n=90 cells from 3 biological replicates per condition. Data are mean ± SEM. Statistical analysis performed using a two-tailed Student's *t*-Test; ****= p≤0.0001.

C. Representative images of BRCA1 and γH2AX foci in *Brca1*$^{+/+}$ *53bp1*$^{-/-}$ and *Brca1*$^{C61G/C61G}$ *53bp1*$^{-/-}$ cells infected with empty vector (EV) or containing BARD1. The scale bar is 10 μm.

D. Colony survival in *Brca1*$^{C61G/C61G}$ *53bp1*$^{-/-}$ cells infected with empty vector (EV) or containing BARD1 treated with NTC siRNA (-) or siRNA targeting Polθ (+). n=3 biological repeats. Data are mean ± SEM. Statistical analysis performed using a two-tailed Student's *t*-Test; **= p≤0.01.

3.3.4. BRCA1 recruitment through BARD1-RAD51 interactions promotes resistance to Polθ loss

To decipher which domains of BARD1 are important for alleviating defects in *Brca1*$^{C61G/C61G}$ *53bp1*$^{-/-}$ cells, we mutated murine BARD1 using site directed mutagenesis to modify the retroviral construct (Fig.3.5A). Proteins encoded from human *BRCA1* and mouse *Brca1* genes share a high sequence homology forming BRCA1 isoforms consisting of 1863 amino acids for human and 1812 amino acids for mouse, so there exists 51 fewer residues in mouse BRCA1 compared to the human BRCA1 protein (Abel et al., 1995; Yueh et al., 2024).

BARD1 was mutated at position L38R, a mutation known to abrogate BRCA1/BARD1 heterodimer formation in human cells (L44R-BARD1) (Morris et al., 2002). Human L44R-BARD1 is ligase defective and also disrupts heterodimer formation, stability and BRCA1/BARD1 localisation to DSBs (Densham et al., 2016). The exogenous expression of the equivalent mouse mutation L38R-BARD1 in our *Brca1*$^{C61G/C61G}$ *53bp1*$^{-/-}$ MEFs could not improve C61G-BRCA1 foci formation (Fig.3.5B) nor rescue cell sensitivity to Polθ loss (Fig.3.5C). Therefore, the heterodimeric interaction between BRCA1/BARD1 is required for BARD1 overexpression to rescue cellular defects in *Brca1*$^{C61G/C61G}$ *53bp1*$^{-/-}$ cells.

In keeping with BRCA1/BARD1 recruitment to DSBs, we wanted to determine whether the interaction between BRCA1/BARD1 and ubiquitinated nucleosomes, imperative for

its recruitment to sites of damage, is important for this rescue. Becker *et al* (2021) have shown that BARD1 is recruited to sites of DNA damage involving both the ANK and BRCT domains, with ANK being the reader of H4K20me0 and BRCT containing a BUDR domain which binds directly to RNF168-mediated mUb-H2A (Becker et al., 2021; Nakamura et al., 2019; Dai et al., 2021). A460T-BARD1 (A448T in mice) was identified as a missense mutation that disrupts the ANK-H4K20me0 binding interface and is thought to abrogate its interaction with V21 of H4, thus reducing its interaction with the nucleosome core particle (NCP^{Ub}) and exhibits lowered HR activity (Adamovich et al., 2019; Dai et al., 2021). We overexpressed exogenous murine A448T-BARD1 in *Brca1*$^{C61G/C61G}$ *53bp1*$^{-/-}$ cells and discovered that disrupting the BARD1-NCP^{Ub} interaction and therefore the recruitment and retention of BRCA1/BARD1 to nucleosomes could no longer support C61G-BRCA1 foci formation nor improve cell viability in the absence of Polθ like that of WT BARD1 (Fig. 3.5B, C).

The human D712A-BARD1 mutation is located within the inter-B2'-B3' loop of the second BRCT of BARD1 and therefore disrupts the BARD1-BUDR domain necessary for BARD1-dependent BRCA1/BARD1 localisation to DSBs (Becker et al., 2021). The D712A-BARD1 mutation showed reduced RAD51 foci formation post IR and showed hypersensitivity to the PARPi Olaparib (Becker et al., 2021). We overexpressed the equivalent D700A-BARD1 mouse missense mutation in our *Brca1*$^{C61G/C61G}$ *53bp1*$^{-/-}$ cells which revealed no improvement in C61G-BRCA1 foci formation nor enhancement in cell survival in cells treated with siRNA targeting Polθ (Fig. 3.5B, C). Overall, these data show that the overexpression of exogenous BARD1 can only rescue C61G-BRCA1 foci formation and survival in the absence of Polθ if BRCA1/BARD1 recruitment to sites of damage is not hindered.

We then wanted to explore whether the BARD1-RAD51 interaction is important for C61G-BRCA1 foci formation and suppressing cell sensitivity to Polθ loss. The interaction between BARD1-RAD51 is imperative for RAD51-facilitated strand invasion during HR and the protection of stalled replication forks (Zhao et al., 2017b; Daza-Martin et al., 2019). We mutated BARD1 using SDM to alter the conserved F125 and D127 residues to an alanine and the A128 residue to a glutamic acid, termed the AAE mutant, originally designed in human cells (F133A, D135A, A136E) by Zhao *et al* (2017) (Zhao et al., 2017b). The AAE-BARD1 mutant disrupts the BARD1-RAD51 association and hinders D-loop formation plus the assembly of the synaptic complex during HR sans disrupting its DNA binding ability (Zhao et al., 2017b). Overexpression of the BARD1-RAD51 disruptive AAE-BARD1 mutant (F125A, D127A, A128E) could rescue C61G-BRCA1 foci numbers but was less able to promote resistance to the loss of Polθ (Fig. 3.5B, C). We postulated that the BRCA1/BARD1-RAD51 interaction, necessary for D-loop formation and assembly of the synaptic complex as well as fork protection (Zhao et al., 2017b; Daza-Martin et al., 2019), contributes to the suppression of cell toxicity in cells depleted of Polθ.

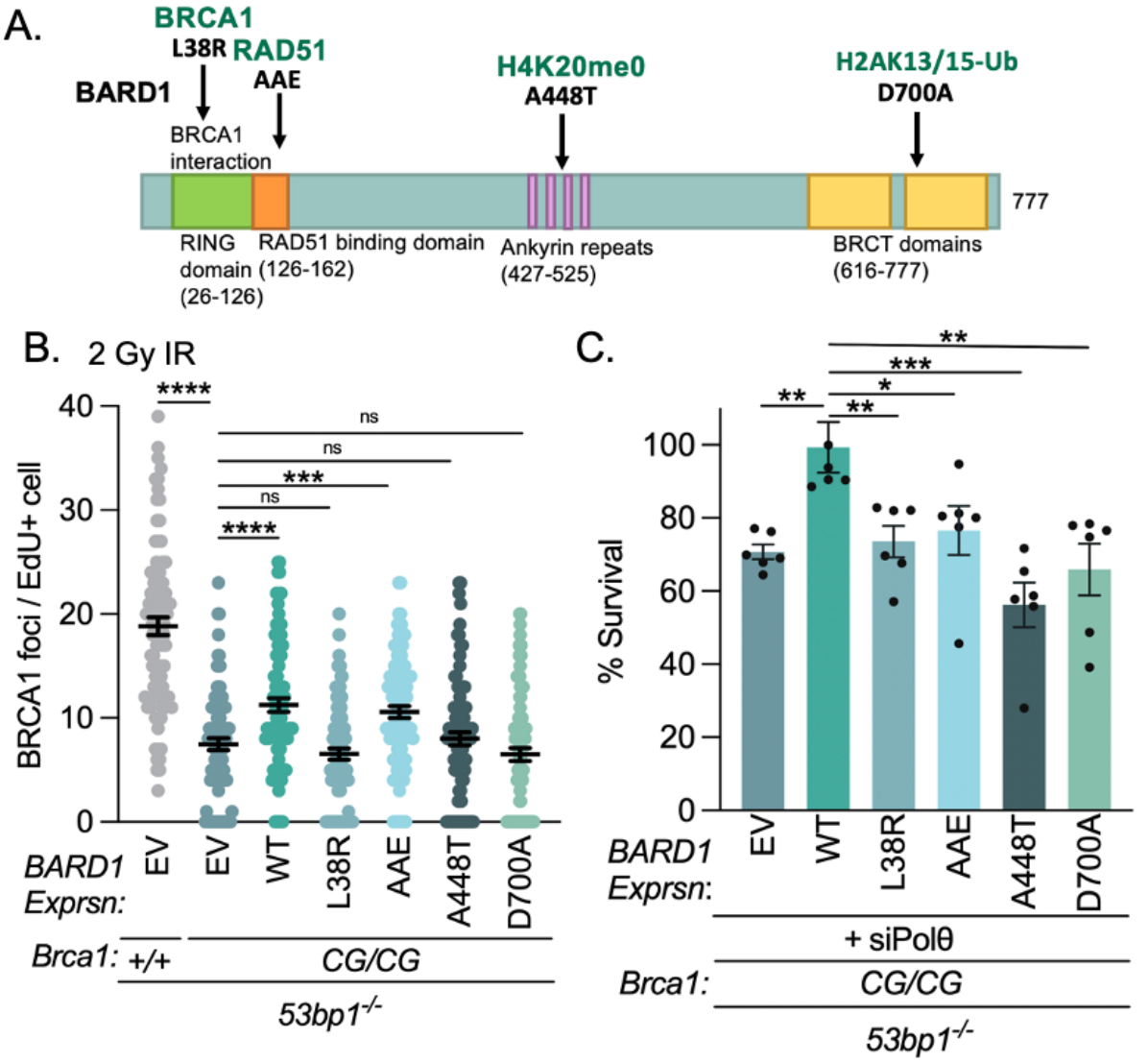

Figure 3.5. BRCA1/BARD1:RAD51 interactions influence Polθ synthetic lethality.

A. Murine BARD1 schematic highlighting the areas of BARD1 selected for site-directed mutagenesis.

B. Quantification of EdU+ C61G-BRCA1 foci post 3 hr 2 Gy IR in *Brca1*$^{+/+}$*53bp1*$^{-/-}$ and *Brca1*$^{C61G/C61G}$ *53bp1*$^{-/-}$ cells infected with empty vector (EV) or containing BARD1 mutants. n=90 cells from 3 biological replicates per condition. Data are mean ± SEM. Statistical analysis performed using a two-tailed Student's *t*-Test; ****= p≤0.0001; ***= p≤0.001; ns = not significant.

C. Colony survival in *Brca1*$^{C61G/C61G}$ *53bp1*$^{-/-}$ cells infected with empty vector (EV) or containing BARD1 mutants treated with siRNA targeting Polθ. n=6 biological repeats.

Data are mean ± SEM. Statistical analysis performed using a two-tailed Student's *t*-Test; ***= p≤0.001; **= p≤0.01; *= p≤0.5.

3.3.5. Overexpression of the BRC4 repeat of BRCA2, important for RPA:RAD51 exchange, evades the reliance on Polθ for survival

We have only looked at Polθ sensitivity in relation to BRCA1 deficiency, therefore we wanted to determine whether BRCA2-depleted cells are reliant on Polθ. My lab colleague treated WT cells with siRNA targeting BRCA2 and witnessed a sensitivity to the loss of Polθ (Ronson et al., 2023) Also, BRCA1 promotes the recruitment of PALB2:BRCA2 to RAD51 to stimulate D-loop formation during HR (Sy et al., 2009a; Zhang et al., 2009b, 2009a). Therefore, we wanted to explore whether the interaction between BRCA2:RAD51 could also overcome the toxicity to Polθ loss. Using the same retroviral system, we expressed two constructs: one containing the BRC4 repeat of BRCA2 fused with RPA70 (Fig. 3.6A, B) and the other with the C-terminal binding region within exon 27 of BRCA2 also fused to RPA70 (Fig. 3.6A, B) (Saeki et al., 2006). BRCA2-BRC4 is important for the exchange of RPA with RAD51 during HR and exon 27 is located on the C-terminus of BRCA2 promoting RAD51 stability and replication fork restart by directly contacting oligomerised RAD51 (Thorslund and West, 2007; Carreira et al., 2009; Kolinjivadi et al., 2017b; Esashi et al., 2007; Davies and Pellegrini, 2007) (Fig.3.6A). The importance of fusing these BRCA2 constructs to RPA70 is to promote its recruitment to ssDNA without the need for BRCA1.

We overexpressed the BRC4-RPA and Ex27-RPA FLAG-tagged constructs in *Brca1*$^{+/+}$ 53bp1$^{-/-}$ and *Brca1*$^{C61G/C61G}$ *53bp1*$^{-/-}$ MEFs, confirmed by FLAG expression (Fig.3.6C). We demonstrated that BRC4-RPA expression restored RAD51 foci formation in cells

depleted of BRCA1, showing that it can bypass BRCA1 for RAD51 recruitment (Ronson et al., 2023). Whereas Ex27-RPA could partially restore RAD51 foci generation in *BRCA1*-depleted cells (Ronson et al., 2023). We then wanted to determine whether the expression of these BRCA2 constructs could rescue sensitivity to Polθ depletion in *Brca1*$^{C61G/C61G}$ *53bp1*$^{-/-}$ cells. Surprisingly, BRC4-RPA was able to improve cell viability in cells treated with siRNA targeting Polθ, whereas Ex27-RPA could not (Fig.3.6D). These data indicate that overexpressing the BRC4 repeat of BRCA2, important for RPA:RAD51 exchange, could overcome the need for Polθ to survive. Whereas the fusion of BRCA2 C-terminal Ex27-RPA, which facilitates RAD51 stability and fork restart, could not promote cell viability without Polθ.

These data provide evidence that BRCA1/BARD1-RAD51 and BRCA2-RAD51 are important for the suppression of cell sensitivity to Polθ loss in *Brca1*$^{C61G/C61G}$ *53bp1*$^{-/-}$ cells. We then wanted to determine whether these constructs can overcome sensitivity to the Polθ inhibitor ART558. We treated *Brca1*$^{C61G/C61G}$ *53bp1*$^{-/-}$ cells expressing empty vector, WT-BARD1, BRC4-RPA and Ex27-RPA with ART558 for 72 hours which were subsequently replated at low densities to form colonies. Our data highlighted that the overexpression of WT-BARD1 and BRCA2 BRC4-RPA could suppress ART558 sensitivity compared to *Brca1*$^{C61G/C61G}$ *53bp1*$^{-/-}$ cells expressing Ex27-RPA and the empty vector (Fig.3.6E), which is in line with the Polθ depletion data in Fig.3.6D. The discrepancies between the two constructs highlights that the exchange of RPA with RAD51 is essential for not only overcoming the requirement for Polθ, but also circumvents ART558-induced toxicity. Overall, these data provide evidence that the overexpression of BRC4-RPA is capable of bypassing the hypomorphic C61G-BRCA1 protein to remove the reliance on Polθ.

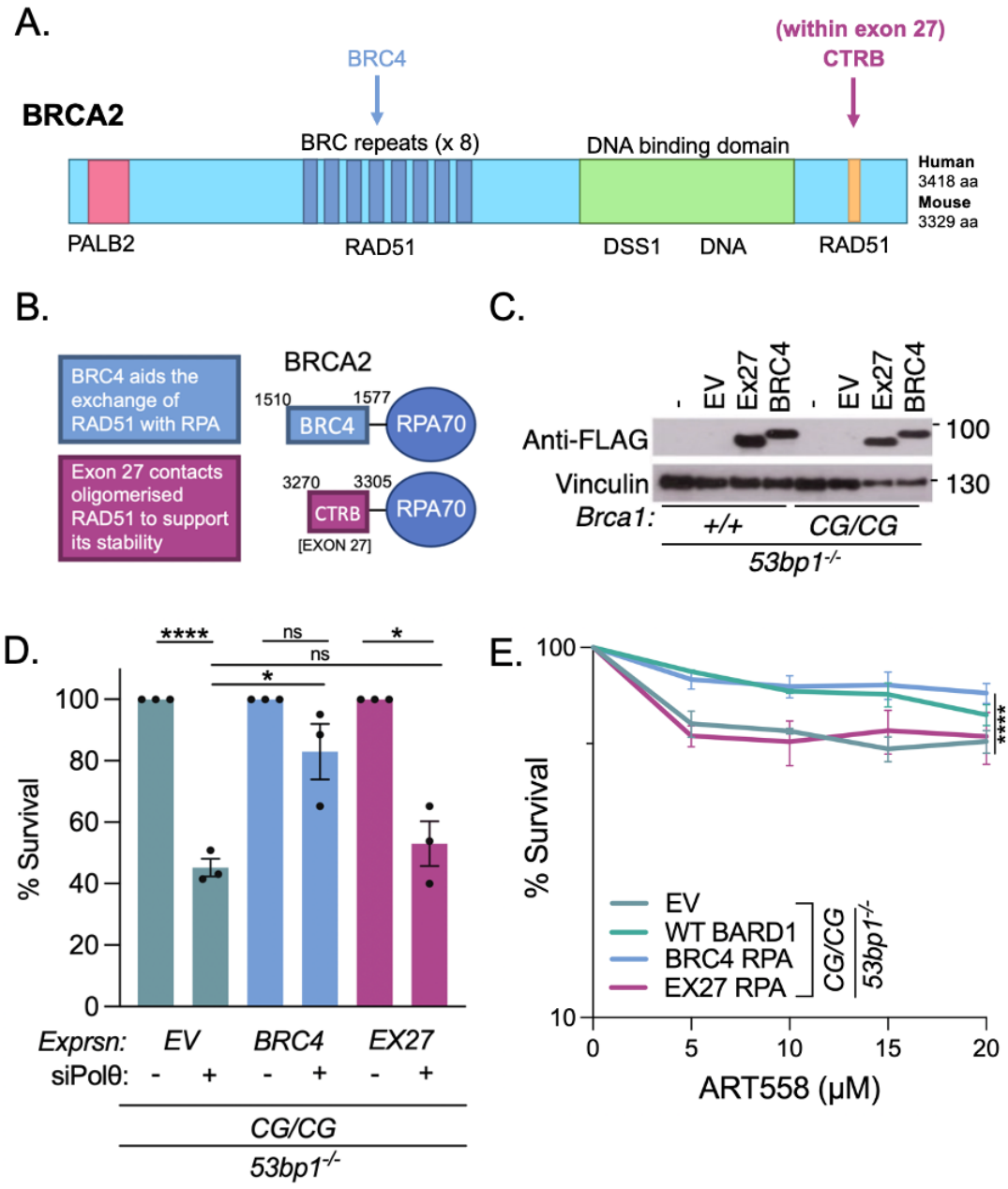

Figure 3.6. Overexpression of the BRC4 repeat of BRCA2, important for RPA:RAD51 exchange, evades the reliance of C61G-BRCA1 on Polθ.

A. Schematic of the functional domains of murine BRCA2. BRCA2 interacts with PALB2 via its N-terminal domain and within the central region has 8 x BRC repeats for its association with RAD51. The BRCA2 C-terminus contains a DNA binding domain encompassing a helical domain, tower domain and three oligonucleotide (OB) domains, important for binding to DNA lesions. The C-terminus also contains 2 x NLS

domains and a TR2 domain and exon 27 encodes the C-terminal Recombinase Binding (CTRB) portion of BRCA2 which binds RAD51.

B. Schematic of BRCA2: BRC4-RPA and Exon 27-RPA.
C. Western blot of cells infected with empty vector (EV) or retrovirus expressing RPA-70-BRCA2-Exon27 (EX27) or RPA-70-BRCA2-BRC4 (BRC4) in *Brca1*$^{+/+}$ *53bp1*$^{-/-}$ and *Brca1*$^{C61G/C61G}$ *53bp1*$^{-/-}$ cells. Vinculin was used as a loading control.
D. Colony survival of cells retrovirally infected with EV or expressing RPA-70-BRCA2-Exon27 (EX27) or RPA-70-BRCA2-BRC4 (BRC4) after NTC (-) or Polθ (+) siRNA treatment in *Brca1*$^{C61G/C61G}$ *53bp1*$^{-/-}$ cells. Data are mean ± SEM. Statistical analysis performed using a two-tailed Student's *t*-Test; ****= p≤0.0001; *= p≤0.05; ns = not significant.
E. Colony survival after EV, BARD1, BRC4 or EX27 retrovirus infection and Polθ inhibitor ART558 treatment in *Brca1*$^{C61G/C61G}$ *53bp1*$^{-/-}$ cells. n=3 biological repeats. Data are mean ± SEM. Statistical analysis performed using a two-way ANOVA; ****= p≤0.0001.

3.3.6. Polθ depletion increases resected ssDNA lengths in *Brca1*$^{C61G/C61G}$ *53bp1*$^{-/-}$ cells

Depleting Polθ on a HR-deficient background produces elevated ssDNA formation (Schrempf et al., 2022; Mann et al., 2022; Belan et al., 2022). Therefore, we used an adapted DNA fibre assay termed Single Molecule Analysis of Resection Tracks (SMART) to visualise ssDNA resection in *Brca1*$^{C61G/C61G}$ *53bp1*$^{-/-}$ cells depleted of Polθ (Altieri et al., 2020). The SMART assay involves treatment with appropriate siRNA/drug treatments for 24 hours followed by the treatment of cells with the pyrimidine analogue Bromodeoxyuridine (BrdU) for 48 hours, which is incorporated into nascent DNA during S-phase. Subsequently cells were lysed and extracted prior to staining. Extracts were treated in non-DNA denaturing conditions (no use of hydrochloric acid) so that the anti-BrdU antibody can recognise BrdU that has been incorporated when DNA is single stranded (Fig. 3.7A). Therefore, long 3' single-strand DNA tails can be visualised and

measured to determine the efficacy of the endogenous resection machinery (Fig.3.7B) (Altieri et al., 2020). Under native conditions, we observed that *Brca1*$^{C61G/C61G}$ *53bp1*$^{-/-}$ cells depleted of Polθ demonstrated elevated native BrdU lengths compared to cells treated with NTC siRNA (Fig.3.7C). We noted a significant elevation in ssDNA lengths from a mean of 2 μm to an average of 3 μm in the absence of Polθ. These data suggest that Polθ acts to restrict aberrant ssDNA formation in *Brca1*$^{C61G/C61G}$ *53bp1*$^{-/-}$ cells.

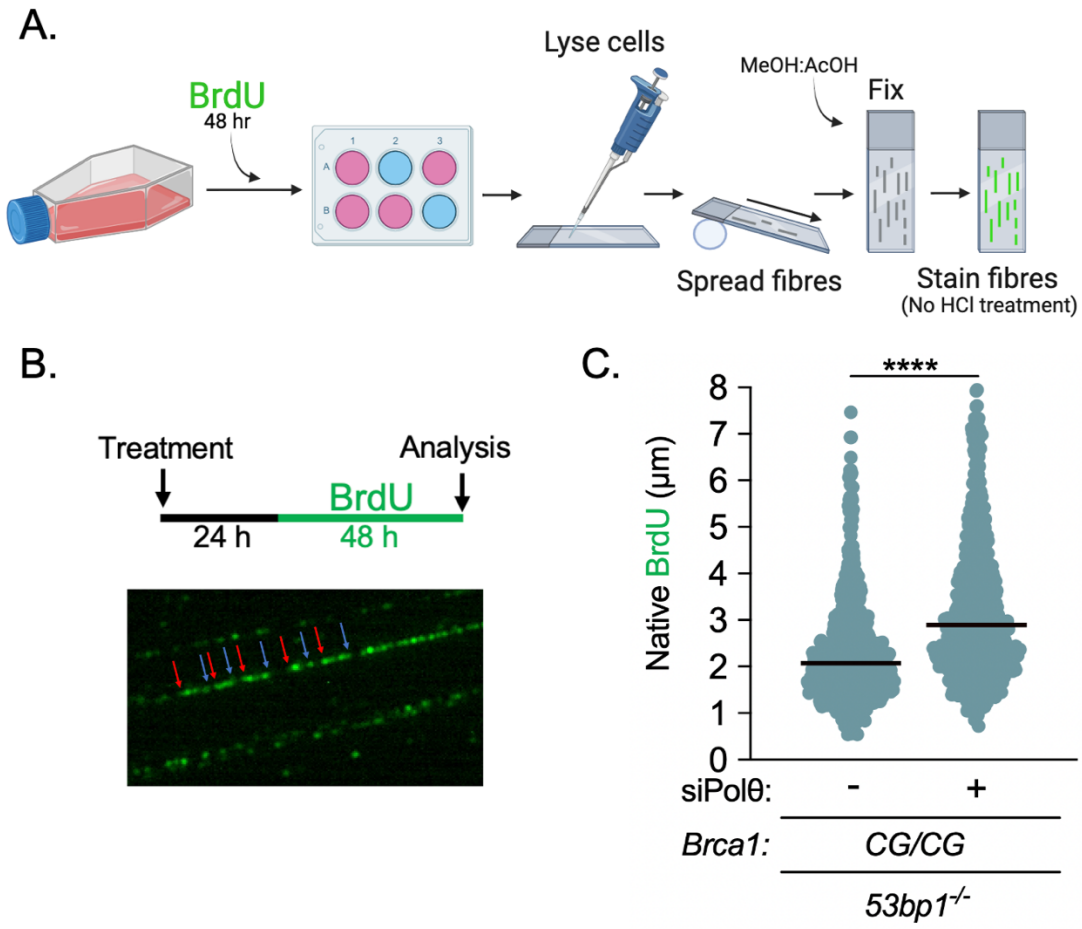

Figure 3.7. Polθ depletion increases resected ssDNA lengths in *Brca1*$^{C61G/C61G}$ *53bp1*$^{-/-}$ cells.

A. Schematic of the Single Molecule Analysis of Resection Tracks (SMART) modified DNA fibre technique.

B. Simplified SMART schematic and a representative image. DNA fibre shown with a red arrow indicating the start and a blue arrow for the end of the dimension analysed DNA tract.
C. Native BrdU tracts after control (-) or Polθ siRNA (+) for 72 hours. n ≥ 750 tracks from 3 biological replicates. Data shown are median. Statistical analysis was performed using a Mann–Whitney test; ****= p≤0.0001.

3.3.7. *Brca1*$^{C61G/C61G}$ *53bp1*$^{-/-}$ cells have nascent ssDNA gaps

Panzarino *et al* (2021) have demonstrated that ssDNA gap accumulation behind the replisome due to unrestrained replication in response to genotoxic stress underlies BRCA1/2 deficiency, and that the repair of ssDNA gaps can be carried out by HR proteins including BRCA1/BRCA2/RAD51 (Panzarino et al., 2021; Cong et al., 2021). Also, inhibiting Polθ generates post-replicative ssDNA gaps in *BRCA1*-deficient hypomorphic cells (Belan et al., 2022; Mann et al., 2022; Schrempf et al., 2021). We sought to identify whether the increased resected DNA generated in Polθ-depleted cells were produced at the replication fork.

Firstly, we wanted to determine whether our untreated *Brca1*$^{C61G/C61G}$ *53bp1*$^{-/-}$ cells harbour ssDNA gaps behind the replisome as *BRCA1*-deficient cells develop ssDNA gaps (Panzarino et al., 2021). We used an adapted DNA fibre assay which involves the incorporation of two nucleotide analogues 5-chloro-2'-deoxyuridine (CldU) and 5-iodo-2'-deoxyuridine (IdU) followed by S1 nuclease incubation, an enzyme that digests ssDNA (Fig.3.8A). If ssDNA gaps are present, S1 nuclease will digest the ssDNA gaps resulting in a reduced IdU tract length (Fig.3.8B) (Quinet et al., 2017; Martins et al., 2022). Under nascent conditions, we observed a decrease in IdU tract length, thus an increase in ssDNA gap generation in *Brca1*$^{C61G/C61G}$ *53bp1*$^{-/-}$ MEFs but not in the *Brca1*$^{+/+}$ *53bp1*$^{-/-}$ cells (Fig.3.8C). These results highlight the importance of functional

BRCA1 for the repression of ssDNA gaps during replication. However, results from my lab colleagues demonstrated that the inhibition of Polθ produced a negligeable increase in ssDNA gap formation in our *Brca1*$^{C61G/C61G}$ *53bp1*$^{-/-}$ MEFs, denoting a limited role for inhibited Polθ for gap-fill in with regards to these cells (Ronson et al., 2023)

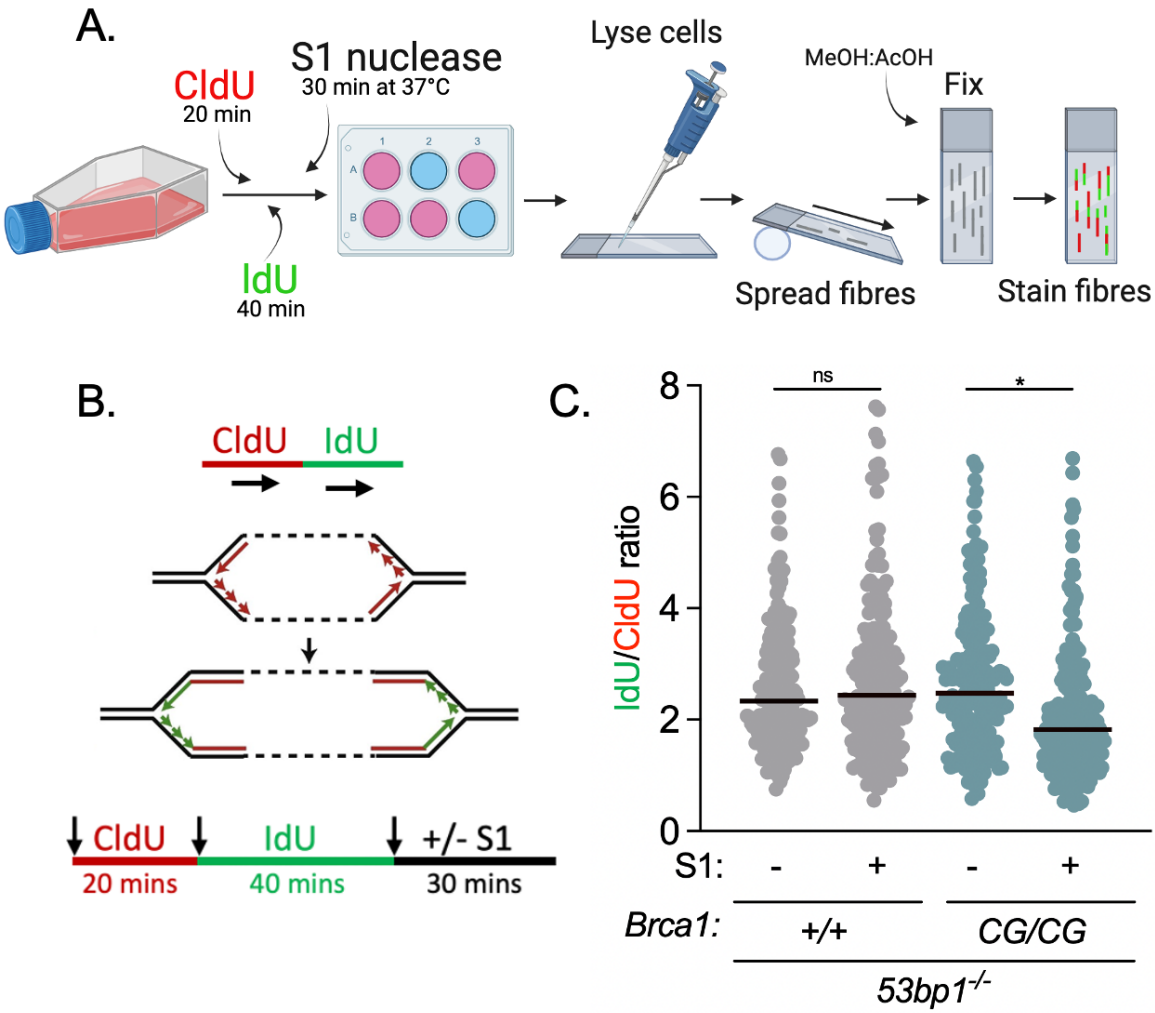

Figure 3.8. *Brca1*$^{C61G/C61G}$ *53bp1*$^{-/-}$ cells exhibit ssDNA gaps.

A. Schematic of the modified S1 nuclease DNA fibre assay. The assay involves the incorporation of two nucleotide analogues CldU for 20 minutes and IdU for 40 minutes followed by S1 nuclease incubation, an enzyme that digests ssDNA, for 30 minutes. If ssDNA gaps are present, S1 nuclease will digest the ssDNA gaps resulting in reduced IdU tract length.
B. Simplified schematic of the modified S1 nuclease assay.

C. S1 nuclease DNA fibre assay in *Brca1*$^{+/+}$*53bp1*$^{-/-}$ and *Brca1*$^{C61G/C61G}$ *53bp1*$^{-/-}$ cells. n ≥ 200 tracks from 2 biological replicates. Data shown are median. Statistical analysis was performed using a Mann–Whitney test; *= p≤0.05; ns = not significant.

3.3.8. BARD1 and BRC4-RPA expression suppress S1-sensitive nascent DNA and support G2/M DNA synthesis fill-in after Polθ loss/inhibition

Previously, we showed that exogenous expression of BARD1 and BRCA2 BRC4-RPA could rescue sensitivity to Polθ depletion and inhibition in *Brca1*$^{C61G/C61G}$ *53bp1*$^{-/-}$ MEFs (Fig.3.4D, 3.6D, E). Ergo, we wanted to explore whether exogenous expression of BARD1 and BRCA2 BRC4-RPA could suppress nascent ssDNA gaps. Remarkably, Fig 3.9A reveals that indeed both exogenous expression of BARD1 and BRC4-RPA can reduce the formation of ssDNA gaps in *Brca1*$^{C61G/C61G}$ *53bp1*$^{-/-}$ cells (Fig.3.9A).

We wanted to determine whether the role of Polθ in DNA synthesis gap fill-in is during G2/M phase. We carried out a post-replicative repair (PRR) assay which is a modified DNA fibre technique that involves the incorporation of IdU followed by overnight treatment with nocodazole, which arrests cells in G2/M, and the subsequent incubation of cells in CldU for 4 hours prior to spreading. CldU dots mark late DNA synthesis which can be calculated by the number of dots per IdU tract divided by the length of the tract to provide the density of PRR events per kilobase of DNA (Fig.3.9B) (Tirman et al., 2021b).

Work from my lab colleagues highlighted that *Brca1*$^{C61G/C61G}$ *53bp1*$^{-/-}$ cells exhibited ssDNA gaps in G2/M phase with a diminished ability to perform PRR which was reduced further upon depletion and inhibition of Polθ (Ronson et al., 2023). We carried out the PRR technique in *Brca1*$^{C61G/C61G}$ *53bp1*$^{-/-}$ cells treated with exogenous BARD1

and BRC4-RPA and uncovered that expression of both constructs supported the ability of the C61G-mutated cells to perform G2/M DNA synthesis gap fill-in post treatment with siRNA to Polθ and ART558 inhibitor (Fig.3.9C,D). Overall, these data demonstrate that expression of BARD1 or BRC4-RPA suppressed Polθ sensitivity, ART558 toxicity, suppressed ssDNA gaps in nascent DNA and facilitated G2/M DNA synthesis fill-in.

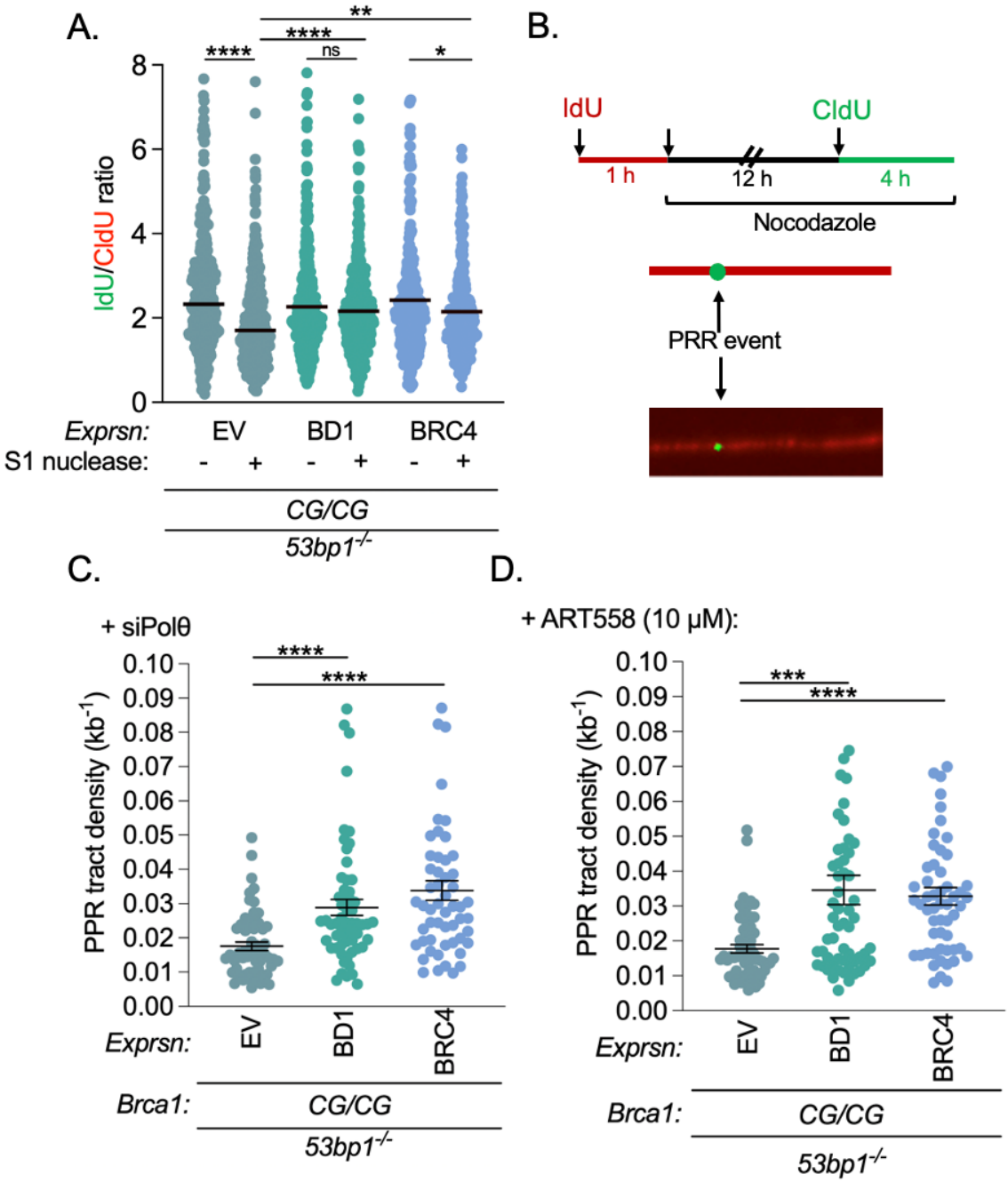

Figure 3.9. BARD1 and BRC4-RPA expression suppress S1-sensitive nascent DNA and support G2/M DNA synthesis fill-in after Polθ loss/inhibition.

A. S1 nuclease DNA fibre assay in *Brca1*$^{C61G/C61G}$ *53bp1*$^{-/-}$ cells infected with empty vector (EV), BARD1 or BRC4-RPA. n ≥ 260 tracks from 3 biological replicates. Data shown are median. Statistical analysis was performed using a Mann–Whitney test; ****= p≤0.0001; **= p≤0.01 *= p≤0.05; ns = not significant. (*With Liza Piberger).*
B. Schematic of the modified post-replicative repair (PRR) DNA fibre assay. Nascent DNA is labelled with IdU for 1 hour, nocodazole is added to arrest cells in G2/M, followed by the addition of CldU for the final 4 hours of nocodazole treatment which is incorporated during DNA synthesis gap fill-in (Tirman et al., 2021b). Below, representative images of a PRR event labelled with CldU on an IdU-labelled tract.
C. PRR density after EV, BARD1 (BD1) or BRC4-RPA retroviral infection and Polθ siRNA. n=60 tracks from 3 biological replicates. Statistical analysis performed using a two-tailed Student's *t*-Test; ****= p≤0.0001.
D. PRR density after EV, BARD1 (BD1) or BRC4-RPA retroviral infection and Polθ inhibitor ART558. n=60 tracks from 3 biological replicates. Statistical analysis performed using a two-tailed Student's *t*-Test; ****= p≤0.0001; ***= p≤0.001.

3.3.9. *Brca1*$^{P62R/P62R}$ cells are reliant on the non-canonical support of Polθ for survival

To further understand the function of the BRCA1 RING domain and how mutations within this region of BRCA1 increase the risk of early-onset breast and ovarian cancer, a variant of unknown significance (VUS) P62R-BRCA1 was selected for investigation (Findlay et al., 2018). The P62R variant (185C>G) is a substitution of proline at position 62 to an arginine, adjacent to the C61G mutation. Mice were crossed to produce *Brca1*$^{P62R/P62R}$ pups that were born at expected Mendelian frequencies (Fig.3.10A). The homozygous *Brca1*$^{P62R/P62R}$ mice did not require the removal of *53bp1* to survive unlike *Brca1*$^{C61G/C61G}$ mice. In addition, mice were crossed to produce *Brca1*$^{C61G/P62R}$ mice, which were unexpectedly viable (unpublished data). We then derived SV40

immortalised MEFs from the following viable *Brca1*$^{P62R/P62R}$ mouse embryos for further investigation. The C61G-BRCA1 mutation destabilises the second Zn^{2+} binding loop, abrogates BRCA1/BARD1 heterodimer stability and loses its ability to function as an E3 ubiquitin ligase (Brzovic et al., 1998; Hashizume et al., 2001). It is unknown whether the P62R-BRCA1 mutation phenocopies C61G-BRCA1, despite the evident discrepancy in embryo viability. A yeast-2-hybrid screen performed by my lab colleague showed that P62R-BRCA1 exhibited defective E3 ubiquitin ligase activity, on a level similar to that of C61G-BRCA1 (unpublished data). However, we were uncertain whether the P62R mutation disrupts the BRCA1 BARD1 heterodimer to the extent of C61G-BRCA1 or whether the P62R mutation acts as a separation of function E3 ligase defective mutant. *Brca1*$^{C61G/C61G}$ *53bp1*$^{-/-}$ cells exhibit reduced BRCA1/BARD1 expression levels compared to *Brca1*$^{+/+}$ *53bp1*$^{-/-}$ cells, therefore we wanted to determine whether our *Brca1*$^{P62R/`P62R}$ MEFs alter BRCA1/BARD1 expression. Western blot analysis demonstrated that *Brca1*$^{P62R/`P62R}$ MEFs had reduced BARD1 expression levels compared to WT and *Brca1*$^{P62R/+}$ cells (Fig.3.10B). Surprisingly, BARD1 expression was further reduced in the double mutant *Brca1*$^{C61G/P62R}$ MEFs (Fig.3.10B).

Brca1$^{C61G/C61G}$ *53bp1*$^{-/-}$ cells showed reduced BRCA1 foci formation 3 hours post IR, indicating that the C61G-BRCA1 mutation impairs BRCA1/BARD1 recruitment to sites of damage (Fig. 3.1B). Likewise, in *Brca1*$^{P62R/P62R}$ MEFs we witnessed a reduction in BARD1 foci following IR treatment, suggesting that localisation to sites of damage is diminished in the homozygous MEFs (Fig.3.10C). Our initial results imply that the P62R-BRCA1 mutation phenocopies C61G-BRCA1 in terms of reduced BARD1 expression and BARD1 foci. Therefore, *Brca1*$^{P62R/P62R}$ cells likely rely on non-canonical

support mechanisms for survival, such as Polθ. Fig.3.10D shows that homozygote *Brca1*$^{P62R/`P62R}$ MEFs are significantly sensitive to the loss of Polθ, however *Brca1*$^{C61G/C61G}$ *53bp1*$^{-/-}$ cells showed a slightly higher toxicity to Polθ loss in comparison (Fig. 3.2C). *Brca1*$^{C61G/C61G}$ *53bp1*$^{-/-}$ cells are on a *53bp1*$^{-/-}$ background, likely enhancing cell susceptibility to Polθ loss compared to *Brca1*$^{P62R/`P62R}$ MEFs.

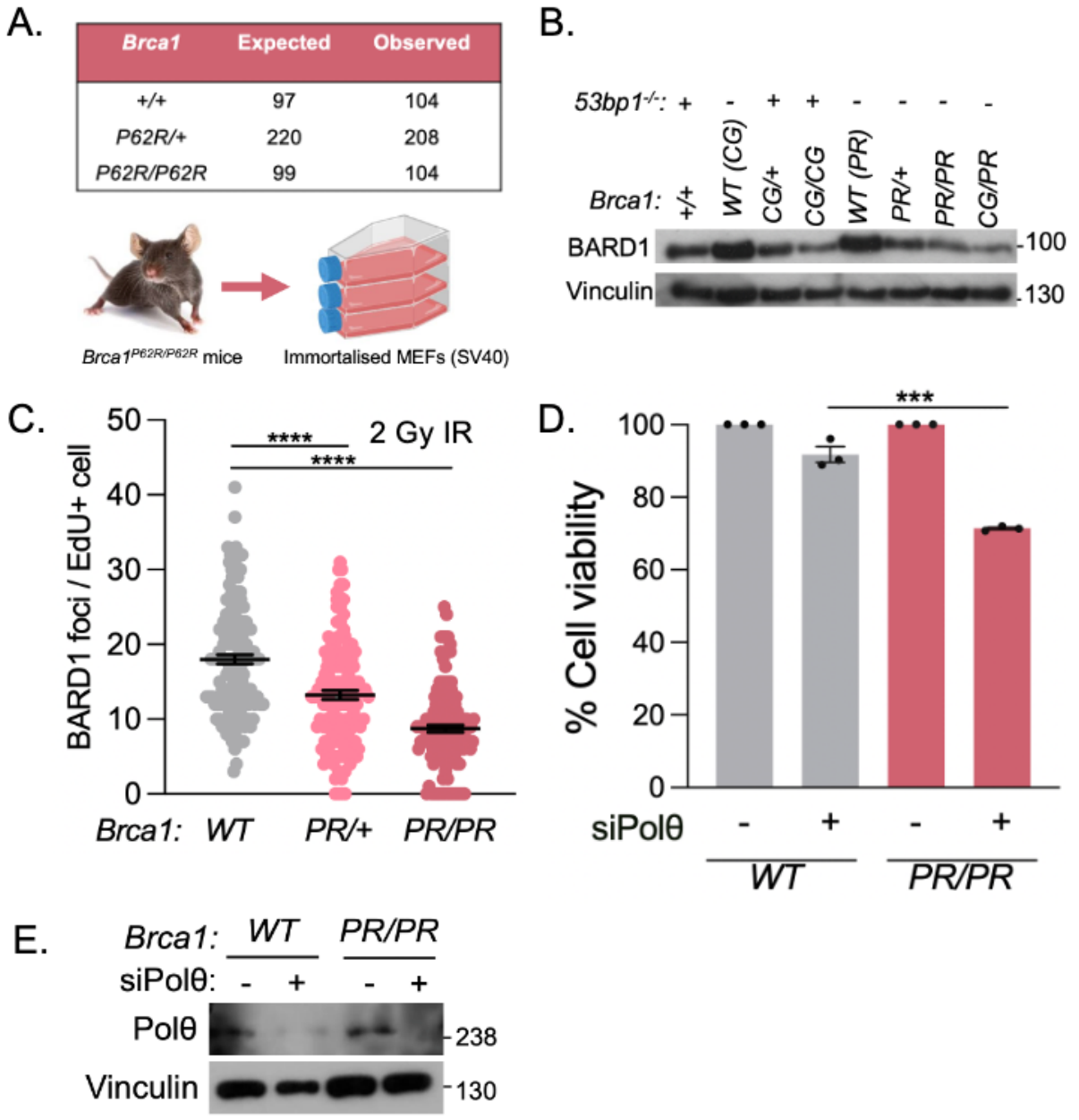

Figure 3.10. *Brca1*$^{P62R/P62R}$ cells are reliant on the non-canonical support of Polθ for survival.

A. The genotypes indicated were inter-crossed demonstrating the expected and observed numbers. A schematic showing the generation of SV40-generated immortalised MEFs from *Brca1*$^{P62R/P62R}$ mice.
B. Representative western blot analysis of BARD1 protein levels in MEFs of genotypes shown. Vinculin was used as a loading control.
C. Quantification of BARD1 foci in EdU-positive *WT, Brca1*$^{P62R/+}$ and *Brca1*$^{P62R/P62R}$ cells post 2 hr irradiation and 3 hr recovery. N=150 from 3 biological repeats. Data are mean ± SEM. Statistical analysis performed using a two-tailed Student's *t*-Test; ****= p≤0.0001.
D. Colony survival in MEFs treated with NTC siRNA (-) or siRNA targeting Polθ (+). n=3 biological repeats. Data are mean ± SEM. Data are mean ± SEM. Statistical analysis performed using a two-tailed Student's *t*-Test; ***= p≤0.001.
E. Representative western blot showing knockdown of Polθ in *Brca1*$^{P62R/P62R}$ cells treated with NTC siRNA (-) and siRNA targeting Polθ (+). Vinculin was used as a loading control.

3.4. Discussion

Here, we have shown a further insight into the synthetic lethal relationship between *Brca1/53bp1* deficiency and Polθ loss and inhibition. A myriad of advancements have been made in the field on the mechanisms underlying the synthetic lethal relationship between Polθ and BRCA1, but there remains a lot to be understood. We used the BRCA1 C61G mutation as our model of BRCA1 dysfunction and derived *Brca1*$^{C61G/C61G}$ *53bp1*$^{-/-}$ MEFs for this study. We identified that *Brca1*$^{C61G/C61G}$ *53bp1*$^{-/-}$ cells are hypomorphic and elicit reduced BRCA1/BARD1 expression (Fig. 3.1A), lowered BRCA1 foci formation (Fig. 3.1B), exhibit BRCA1-dependent RAD51 foci generation post IR (Fig. 3.1C), are resistant to the PARPi Olaparib (Fig. 3.1D) and show competent yet sub-optimal HR function (Fig. 3.1E). Taken together, these results indicate that *Brca1*$^{C61G/C61G}$ *53bp1*$^{-/-}$ cells perform HR competently, albeit show

phenotypes of a hypomorphic mutation. Our data correlates with the results seen in Drost *et al* (2011) who witnessed embryonic lethality in an attempt to generate homozygous C61G mice and showed acquired resistance to PARPi in C61G-*Brca1* tumours, increased γH2AX foci in response to Olaparib and the formation DNA damage-induced RAD51 foci formation (Drost et al., 2011). These data suggest that the hypomorphic C61G-BRCA1 protein is reliant on the support from non-canonical proteins to perform competent HR and led us to targeting the TLS polymerase Polθ.

We identified a significant increase in Polθ expression and reduced cell viability in the absence of Polθ in *Brca1*$^{C61G/C61G}$ *53bp1*$^{-/-}$ cells compared to our control *Brca1*$^{+/+}$ *53bp1*$^{-/-}$ cells (Fig. 3.2A, B,C). In line with our findings, Polθ has been found to be upregulated in numerous cancers, and strikingly high in HR-deficient breast and ovarian cancers that are associated with a poor clinical outcome and show resistance to DSB-inducing agents (Ceccaldi et al., 2015; Lemée et al., 2010; Yousefzadeh et al., 2014; Kent et al., 2015a; Mateos-Gomez et al., 2015; Wyatt et al., 2016). The N-terminal helicase domain of Polθ functions in an ATP-dependent manner to remove RPA and facilitate the annealing of DNA, fundamental for the function of TMEJ (Mateos-Gomez et al., 2017; Schaub et al., 2022). We looked at RAD51 foci formation in *Brca1*$^{C61G/C61G}$ *53bp1*$^{-/-}$ cells treated with NTC siRNA and siRNA targeting Polθ and noted that RAD51 foci formation was significantly increased in the absence of Polθ (Fig. 3.2 E,F). These data correlate with results showing that the Polθ helicase domain displaces RPA from DNA and in Polθ helicase domain ATPase mutants there were elevated RAD51 foci post IR (Mateos-Gomez et al., 2017; Ozdemir et al., 2018; Wyatt et al., 2016; Ceccaldi et al., 2015; Schaub et al., 2022).

In addition, the inhibition of the Polθ helicase domain killed HR-deficient tumour cells reinforcing the importance of Polθ inhibitors to treat HR-defective cancers (Ceccaldi et al., 2015; Mateos-Gomez et al., 2015; Zhou et al., 2021; Feng et al., 2019; Higgins et al., 2010). Yet, Schaub *et al* (2022) suggested that the helicase domain of Polθ can only partially disassemble stabilised RAD51 filaments and had limited clearing activity, unlike others who have demonstrated that helicase-dead Polθ mutants showed increased RAD51 foci (Schaub et al., 2022; Ceccaldi et al., 2015; Mateos-Gomez et al., 2015). However, treatment with the Polθ inhibitor Novobiocin, which targets the helicase domain, could stimulate end resection and augmented non-functional RAD51 loading plus the toxic accumulation of ssDNA intermediates (Zhou et al., 2021).

We treated our different genotypes with increasing doses of ART558 and noted a significant susceptibility to the Polθ inhibitor in both *Brca1*$^{+/+}$*53bp1*$^{-/-}$ and *Brca1*$^{C61G/C61G}$ *53bp1*$^{-/-}$ cells compared to WT cells, albeit with a significant sensitivity in *Brca1*$^{C61G/C61G}$ *53bp1*$^{-/-}$ MEFs (Fig. 3.3A). Hence, we looked at γH2AX foci formation and noted an increase in the number of foci associated with elevated DNA damage in *Brca1*$^{C61G/C61G}$ *53bp1*$^{-/-}$ cells treated with ART558 (Fig. 3.3B). Our data is similar to those shown in Zatreanu *et al* (2021) who have shown that cells harbouring defects in the Shieldin complex are sensitive to Polθ inhibition by ART558 that are otherwise resistant to Olaparib (Zatreanu et al., 2021). In addition, Krais *et al* (2023) demonstrated that MEFs on a *53bp1*$^{-/-}$ background showed a higher sensitivity to ART558 compared to *53bp1*$^{+/+}$ cell lines and that the level of end resection can determine sensitivity to Polθ inhibition (Krais et al., 2023). Next, the reduced but maintained interaction between BRCA1 and BARD1 in our *Brca1*$^{C61G/C61G}$ *53bp1*$^{-/-}$ cells (Ronson et al., 2023) led us to question whether overexpressing BARD1 could alleviate deleterious phenotypes witnessed in

Brca1$^{C61G/C61G}$ *53bp1*$^{-/-}$ cells. Overexpressing exogenous BARD1 using a retroviral system enabled us to significantly increase BARD1 expression (Fig. 3.4A) and improve C61G-BRCA1 foci formation in *Brca1*$^{C61G/C61G}$ *53bp1*$^{-/-}$ cells (Fig. 3.4B, C). Not only this but our findings from Ronson *et al* (2023) highlighted that expression of exogenous BARD1 improved HR outcomes measured by PCR (Ronson et al., 2023) and reduced cell sensitivity to Polθ depletion (Fig. 3.4 D). These results indicate that overexpressing BARD1 circumvents the dependency that *Brca1*$^{C61G/C61G}$ *53bp1*$^{-/-}$ cells have on the non-canonical support of Polθ.

We then tested the expression of BARD1 mutants to determine which domain of BARD1 is important for the increase in C61G-BRCA1 foci and the resistance to Polθ depletion. Overexpression of the L38R-BARD1 mutation (L44R-BARD1 in humans) failed to improve C61G-BRCA1 foci or improve cell survival in the absence of Polθ (Fig. 3.5A,B,C). The L44R-BARD1 mutation has been shown to be HR defective and abrogates BRCA1/BARD1 binding (Morris et al., 2002; Xia et al., 2003; Lee et al., 2015). L44R-BARD1 generates a hydrophilic residue within the BARD1 hydrophobic helical face, thus preventing its interaction with BRCA1 (Morris et al., 2002). Human L44R-BARD1 could not support heterodimer formation or stability, could not localise BRCA1 to IR-induced foci and exhibited reduced ligase activity (Densham et al., 2016). These data are in line with our results showing that murine L38R-BARD1 overexpression could no longer support C61G-BRCA1 foci formation and therefore could not rescue cell sensitivity to Polθ depletion (Fig.3.5. A,B,C). Taken together, these results indicate that the N-terminal interaction between BRCA1/BARD1 is important for the BARD1-mediated rescue of deleterious phenotypes in *Brca1*$^{C61G/C61G}$ *53bp1*$^{-/-}$ cells.

We also looked at BARD1 mutations affecting nucleosomal interactions. The human A460T-BARD1 mutation is located within the ANK domain and is identified as non-functional (Adamovich et al., 2019). Cells expressing A460T-BARD1 are deficient in HR and the mutation is thought to be potentially pathogenic (Lu et al., 2015; Adamovich et al., 2019). This reduced HR activity was explained by the fact that the A460T-BARD1 is located within the ANK-H4K20me0 binding interface (Dai et al., 2021). ANK-BARD1 is a reader of H4K20me0 which facilitates BRCA1/BARD1 localisation to sister chromatids, highlighting the restriction of HR to S and G2 phase of the cell cycle (Nakamura et al., 2019). The location of A460T-BARD1 within the ANK-H4K20me0 binding interface suggests that the mutation is likely disrupting the interaction of the H4 residue V21. Dai *et al* (2021) also showed that A460T-BARD1 diminished binding to the NCP^{Ub} (Dai et al., 2021). We showed that overexpression of murine A448T-BARD1 could no longer improve C61G-BRCA1 foci formation nor promote resistance to Polθ loss (Fig.3.5A,C,B). These results indicate that the ANK-H4K20me0 binding interface, known to be important for histone mark recognition and thus BRCA1/BARD1 recruitment to DSBs is essential for promoting C61G-BRCA1 foci in our cells.

In keeping with this, BARD1 bound to the NCP^{Ub} can recognise the H4K20me0 DNA replication-associated mark as well as the DNA damage-induced mark H2AK15-Ub (Dai et al., 2021). The BUDR motif of BARD1 is a reader of RNF168-mediated ubiquitination of H2AK15-Ub which can subsequently localise the heterodimer to sites of DNA damage for repair by HR (Becker et al., 2020). Human D712A-BARD1 is located within the BUDR motif and the D712 position is important for electrostatic interactions with H2B and so the D712A-BARD1 mutation disrupted the ability of BARD1 to bind the NCP^{Ub} and exhibited HR-deficiency (Dai et al., 2021; Hu et al.,

2021). We overexpressed the mouse equivalent D700A-BARD1 mutation and noted that C61G-BRCA1 foci formation could not be improved, and cells remained sensitive to Polθ depletion (Fig.3.5. A,B,C), reinforcing that the BARD1 recognition of nucleosomes is fundamental for promoting BRCA1/BARD1 recruitment and therefore for mediating C61G-BRCA1 foci in *Brca1*$^{C61G/C61G}$ *53bp1*$^{-/-}$ cells.

However, remarkably we noted that overexpression of the AAE-BARD1 mutant which disrupts the BARD1/RAD51 interaction (Zhao et al., 2017b), could rescue C61G-BRCA1 foci formation but could not suppress cell sensitivity to Polθ loss. Zhao *et al* (2017) designed a triple mutation in humans (F133A, D135A, A136E) termed AAE-BARD1 that disrupts the association between BARD1 and RAD51 and therefore the ability of BRCA1/BARD1-RAD51 to carry out strand invasion with no effect on DNA binding (Zhao et al., 2017b). Cells expressing the AAE-BARD1 mutant are deficient in HR, sensitive to Olaparib and MMC, defective in fork protection, but can still form RAD51 foci (Daza-Martin et al., 2019; Zhao et al., 2017b). The murine equivalent (F125A, D127A, A128E) AAE-BARD1 mutation could improve C61G-BRCA1 foci formation but could not promote resistance to Polθ loss (Fig.3.5. A,B,C). These data suggest that the BARD1/RAD51 interaction is not necessary for localisation of C61G-BRCA1 but is fundamental for the BARD1-mediated rescue of cell viability in the absence of Polθ. Therefore, recruitment of BRCA1 via BARD1 as well as the interaction between BRCA1/BARD1-RAD51 are necessary to overcome the reliance on Polθ in *Brca1*$^{C61G/C61G}$ *53bp1*$^{-/-}$ cells.

Consequently, we considered whether the overexpression of certain domains of BRCA2 fundamental for the interaction with RAD51 could circumvent the reliance on Polθ in *Brca1*$^{C61G/C61G}$ *53bp1*$^{-/-}$ cells. We discovered that exogenous expression of the

BRC4 repeat of BRCA2 fused to RPA70, essential for the exchange of RPA and RAD51 (Thorslund and West, 2007; Carreira et al., 2009), could overcome the need for Polθ for survival and overcome ART558-mediated toxicity (Fig.3.6.D,E). Whereas expression of the C-terminal RAD51 binding region within exon 27 of BRCA2 fused to RPA70, essential for replication fork restart and the stabilisation of RAD51 filaments (Kolinjivadi et al., 2017b; Davies and Pellegrini, 2007; Esashi et al., 2007), could not rescue cell viability in the absence of Polθ or when Polθ is inhibited (Fig.3.6.D,E). Our data is corroborated by the work done by Saeki *et al* (2006) who originally designed the BRC4-RPA fusion. They showed that BRC4-RPA could successfully deliver RAD51 to ssDNA and restored cell viability to DNA damaging agents and RAD51 foci formation (Saeki et al., 2006). Remarkably, they state that only 2% of BRCA2/RPA fusion can overcome defects in *BRCA2*-mutant cells (Saeki et al., 2006). With regards to Ex27-RPA, the C-terminal Recombinase Binding (CTRB) region has been shown to be important for localising oligomeric RAD51 to RPA/ssDNA for presynaptic filament assembly as well as the loading associated RAD51 promoters onto regressed replication forks (Kwon et al., 2023). The C-terminal domain is fundamental for the stabilisation of RAD51 but alone is not capable of overcoming the need for Polθ for cell survival in *Brca1*$^{C61G/C61G}$ *53bp1*$^{-/-}$ cells. Overall, these data show that the BRCA1/BARD1-RAD51 and BRCA2-RAD51 interactions can influence Polθ synthetic lethality.

The loss of Polθ has been shown to increase resection lengths in *BRCA1/2*-deficient cells (Mann et al., 2022; Belan et al., 2022; Schrempf et al., 2022). So, we determined whether the loss of Polθ not only increases RAD51 foci formation (Fig.3.2 E,F) but can increase resected DNA. We visualised 3'ssDNA using the modified DNA fibre SMART

assay and noted a significant rise in BrdU lengths and therefore ssDNA when Polθ is depleted in *Brca1*$^{C61G/C61G}$ *53bp1*$^{-/-}$ cells (Fig 3.7C). Next, we looked at replicative ssDNA gap generation using the S1 nuclease fibre assay and identified significant IdU tract shortening in *Brca1*$^{C61G/C61G}$ *53bp1*$^{-/-}$ cells compared to *Brca1*$^{+/+}$ *53bp1*$^{-/-}$ cells (Fig 3.8C). In keeping with this, Panzarino *et al* (2021) denoted that *BRCA1*-deficient cells are unable to restrain replication in the presence of genotoxic stress resulting in extended regions of ssDNA and ssDNA gaps (Panzarino et al., 2021).

We could overcome ssDNA gap generation in *Brca1*$^{C61G/C61G}$ *53bp1*$^{-/-}$ cells when we overexpressed exogenous BARD1 or BRC4-RPA (Fig. 3.9A), which can remove cell toxicity due to Polθ loss and inhibition. The expression of BARD1 and BRC4-RPA can both bypass C61G-BRCA1 to localise RAD51, therefore we speculate that the enhanced recruitment of RAD51 to ssDNA is potentially limiting the presence of ssDNA gaps. The treatment of siRNA targeting Polθ and Polθ inhibition by ART558 can reduce PRR in *Brca1*$^{C61G/C61G}$ *53bp1*$^{-/-}$ cells, but this phenotype can be reversed upon the expression of BARD1 or BRC4-RPA (Fig.3.9C, D). Therefore, increased BARD1 and therefore BRCA1 and BRC4-RPA localisation to ssDNA is likely promoting gap filling by protecting ssDNA gaps from MRE11-dependent degradation in *Brca1*$^{C61G/C61G}$ *53bp1*$^{-/-}$ cells (Tirman et al., 2021b). BRCA1/2 have been shown to be required for DNA synthesis gap fill-in during S and G2 phase of the cell cycle. The ability of BARD1 and BRC4-RPA overexpression to promote PRR in G2/M is intriguing as RAD51 is thought only to act in gap filling during S phase (Tirman et al., 2021b). These results suggest that the expression of BARD1 and BRC4-RPA are acting in an alternative mechanism for gap suppression in G2.

BRC4 is one of the 8 BRC4 repeats that possesses the largest affinity for RAD51 and is implicated in the RPA:RAD51 exchange (Carreira and Kowalczykowski, 2011; Cole et al., 2017; Wong et al., 1997; Scott et al., 2021; Thorslund and West, 2007; Carreira et al., 2009). Yet, *in vitro* analyses of BRC4 have revealed that in *Xenopus* egg extracts BRC4 disrupts the association between RAD51 and Polα, forming abnormal replication intermediates such as ssDNA gaps and the BRC4 peptide restricts RAD51 oligomerisation (Kolinjivadi et al., 2017b). We have pinpointed a requirement for Polθ in G2/M PRR and recent publications have identified that Polθ-mediated TMEJ takes place during mitosis (Brambati et al., 2023). Overall, we have demonstrated that BARD1 and BRC4-RPA expression can suppress ssDNA gap formation and facilitate G2/M gap fill-in whilst suppressed by Polθ loss and inhibition in *Brca1*$^{C61G/C61G}$ *53bp1*$^{-/-}$ cells.

To further understand the role of the BRCA1 N-terminal domain we derived *Brca1*$^{P62R/P62R}$ MEFs from mice that were surprisingly viable, unlike homozygous *Brca1*$^{C61G/C61G}$ that are embryonic lethal and require a *53bp1*$^{-/-}$ background to survive. It is imperative that future work is undertaken on the further characterisation of *Brca1*$^{P62R/P62R}$ MEFs. A co-immunoprecipitation mass spectrometry experiment would be important to compare the interactions between BRCA1 and BARD1 between *Brca1*$^{C61G/C61G}$ *53bp1*$^{-/-}$ cells and *Brca1*$^{P62R/P62R}$ cells. *Brca1*$^{P62R/P62R}$ MEFs appeared to phenocopy *Brca1*$^{C61G/C61G}$ *53bp1*$^{-/-}$ cells showing reduced BARD1 expression levels (Fig. 3.10B), a reduction in the number of BARD1 foci (Fig. 3.10C) and a sensitivity to the absence of Polθ (Fig. 3.10D). Our data so far indicates that *Brca1*$^{P62R/P62R}$ cells are reliant on Polθ for survival so it would be interesting to explore replication fork dynamics

in the *Brca1*$^{P62R/P62R}$ MEFs such as replication fork speeds, fork protection, S1 nuclease ssDNA gaps, and DNA synthesis gap fill-in.

To summarise, BRCA-RAD51-mediated suppression of ssDNA gaps and the activation of G2/M DNA synthesis gap fill-in is associated with resistance to Polθ loss and inhibition by ART558 in *Brca1*$^{C61G/C61G}$ *53bp1*$^{-/-}$ cells (Fig.3.11). These results increase our understanding of what is driving the synthetic lethal relationship between Polθ and C61G-BRCA1 and are important for future development of Polθ inhibitors for *BRCA1*-mutated cancers.

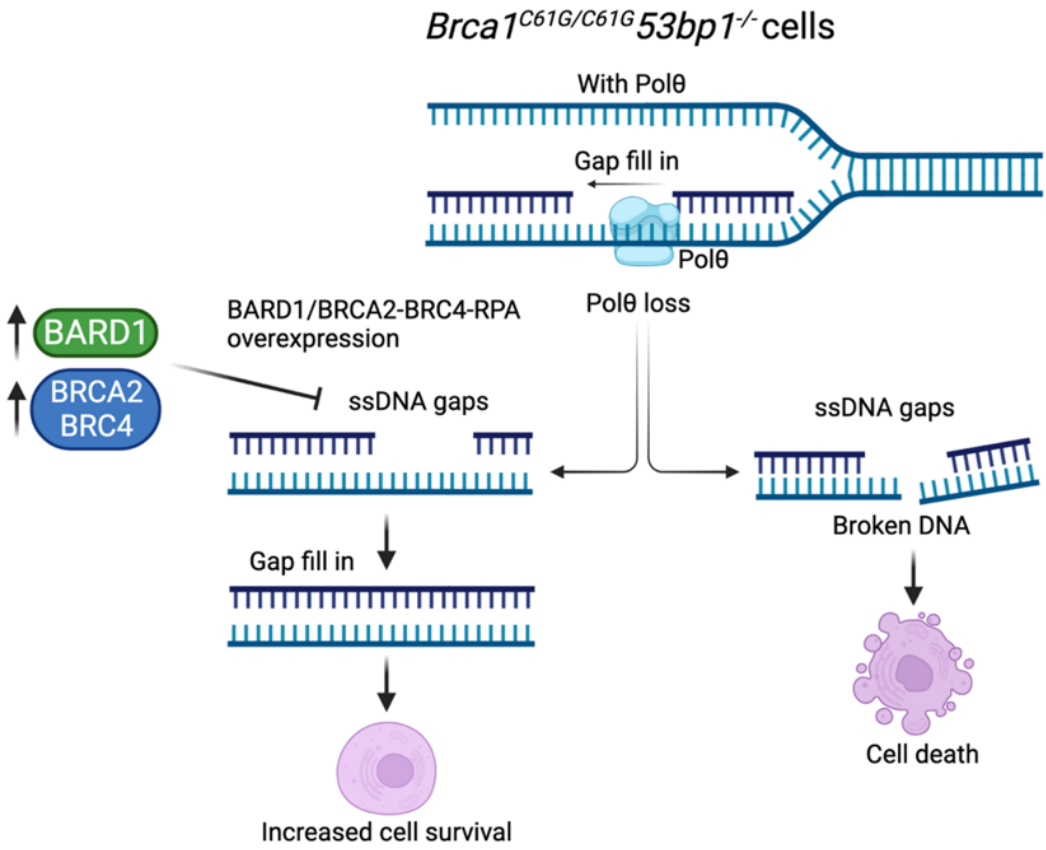

Figure 3.11. BRCA-RAD51 interactions suppress Polθ dependency. BARD1 and BRC4-RPA expression suppress S1-sensitive nascent DNA and support G2/M DNA synthesis fill-in after Polθ loss/inhibition. Created with *BioRender.com*.

4. Polθ prevents RAD52-mediated toxicity in Brca1$^{C61G/C61G}$ 53bp1$^{-/-}$ cells

4.1. Preface

Chapter 4 is adapted from our published study:

Ronson GE*, Starowicz K*, **Anthony EJ**, Piberger AL, Clarke LC, Garvin AJ, Beggs AD, Whalley CM, Edmonds MJ, Beesley JFJ, Morris JR. Mechanisms of synthetic lethality between BRCA1/2 and 53BP1 deficiencies and DNA polymerase theta targeting. Nat Commun. 2023 Nov 29;14(1):7834. doi: 10.1038/s41467-023-43677-2. PMID: 38030626; PMCID: PMC10687250.

4.2. Introduction

In chapter 3 we identified that Polθ supports *Brca1*$^{C61G/C61G}$ *53bp1*$^{-/-}$ cells for survival, however how Polθ functions to support *Brca1*-mutated cells remains to be identified. In this chapter we go onto reveal the mechanisms underlying the synthetic lethal relationship between *Brca1/53bp1* deficiency and Polθ loss. Synthetic lethality has become an essential tool for treating *BRCA1*-deficient cells, resulting in the development of PARP inhibitors, however resistance to PARP inhibition can form due to reasons such as secondary mutations (Lord and Ashworth, 2013). This has stimulated research to identify novel targets to overcome resistance to current treatments. *BRCA1*-deficient cells are reliant on non-canonical pathways for survival, for example RAD52 is synthetic lethal with BRCA1 (Lok et al., 2013). We hypothesise that there could be an association between the mechanism of Polθ/BRCA1 synthetic lethality and the reliance on alternative DNA repair pathways for survival.

That being so, we considered conditional synthetic lethality and driver genes. Non-conditional synthetic lethality is defined as the inhibition of either gene A or B along with a mutation or overexpression of gene A or B leading to synthetic lethality. Whereas conditional synthetic lethality considers intrinsic and extrinsic factors such as genetic background or radiation, indicating that without these factors, mutations in genes A or B do not affect survival. Also, it is important to note that the synthetic lethal relationship between gene A and B could be dependent on gene C. (Li et al., 2020a). An example of conditional synthetic lethality is that the removal of 53BP1 can abolish the synthetic lethal relationship between *BRCA1/2*-mutated tumours and PARP inhibitors, leading to resistance (Bouwman et al., 2010; Bunting et al., 2010; Jaspers et al., 2013). So, taking into account that synthetic lethality can be context dependent, we explored alternative DNA damage pathways and proteins that could explain the synthetic lethal relationship between Polθ and BRCA1.

We considered whether the following proteins could be involved in driving the synthetic lethal relationship between Polθ and BRCA1: RNF168, RAD52, MRE11 and RPA. The E3 ligase RNF168, which mono-ubiquitinates H2A at K13/15, creates a binding molecule for DDR proteins (Doil et al., 2009; Mattiroli et al., 2012; Stewart et al., 2009). Also, RNF168-mediated mono-ubiquitination of H2A can directly bind to BARD1 through its BRCT BUDR domain to recruit the BRCA1-P complex to DSBs (Becker et al., 2020; Krais et al., 2021). So, the disruption of either H2A ubiquitination by RNF168 or mutations located within the BUDR region of BARD1 disrupt BRCA1-P complex recruitment (Krais et al., 2021). Additionally, RNF168 acts redundantly to load PALB2 to support HR (Zong et al., 2019). In the absence of functional BRCA1, RNF168 can promote BRCA1-independent RAD51 loading via PALB2/BRCA2 and the deletion of

RNF168 results in BRCA1 haploinsufficiency, which can be circumvented by increased PALB2 loading (Zong et al., 2019). The loss of RNF168 disrupts the ability of 53BP1 removal to rescue the synthetic lethality of *BRCA1*-deficiency (Zong et al., 2019). Therefore, an alternative mechanism involving RNF168 could be mitigating cell viability in *Brca1*$^{C61G/C61G}$ *53bp1*$^{-/-}$ cells depleted of Polθ and will be explored further in the following chapter.

Another protein to investigate is RAD52, which is synthetic lethal in *BRCA1*-deficient cells and is thought to be a potential therapeutic target for HR-deficient cancers (Liu and Heyer, 2011; Lok et al., 2013). In the absence of BRCA1, RAD52-dependent HR can take place which is facilitated by RPA hyperphosphorylation to promote RAD52-dependent recruitment of RAD51 for loading onto resected DNA (Carley et al., 2022). Also, the error-prone SSA repair pathway, which involves RAD52, is an alternative pathway to HR. SSA requires long resected DNA and the homologous sequences are annealed by RAD52 with DNA ends sealed by ligase I (Bhargava et al., 2016; Motycka et al., 2004; Hanamshet et al., 2016).

Not only this, but RAD52 is involved in pathways such as BIR and in the protection and processing of stalled replication forks (Mijic et al., 2017; Taglialatela et al., 2017; Malacaria et al., 2019). Stalled replication forks are repaired by BIR which involves ATAD5-RLC-like complex mediated removal of PCNA for RAD51 recruitment and protection of the fork, but in situations of damage that is beyond the capability of RAD51, the RAD52-dependent BIR pathway restarts collapsed replication forks (Park et al., 2019; Mason et al., 2019; Mijic et al., 2017; Taglialatela et al., 2017). In the absence of functional BRCA2, RAD52 becomes an essential factor for the repair of collapsed replication forks via the BIR pathway (Sotiriou et al., 2016; Lemaçon et al.,

2017). Likewise, RAD52-mediated BIR has been observed during mitotic DNA synthesis pathway (MiDAS) to promote the repair of difficult to replicate regions of DNA and fragile sites, and RAD52 has been implicated in ALT telomere synthesis (Bhowmick et al., 2016; Claussin and Chang, 2016; Zhang et al., 2019; Verma et al., 2019). A relationship between RAD52 and Polθ has already been established showing that Polθ-mediated TMEJ is restricted until mitosis by RAD52 in BRCA2 mutants by inhibiting the Polθ polymerase function (Llorens-Agost et al., 2021). Hence, RAD52 is a critical factor worth exploring to further understand the relationship between *Brca1* and *53bp1* deficiencies and Polθ targeting.

Evidence has shown that *BRCA1/2*-deficient cells depleted of Polθ accumulate ssDNA gaps (Mann et al., 2022; Schrempf et al., 2022; Belan et al., 2022). A prominent factor involved in the bidirectional expansion of ssDNA gaps is MRE11, which extends gaps in the 3' to 5' direction and functions alongside EXO1 in the 5' to 3' direction, which is then cleaved by the MRE11 endonuclease to form a DSB. This expansion process is restricted by the BRCA1/2 pathway (Hale et al., 2023). In addition, in *BRCA1/2*-deficient cells, the inhibition of the MRE11 exonuclease activity limits the accumulation of ssDNA gaps (Tirman et al., 2021b; Dhoonmoon et al., 2022). Mann *et al* (2022) demonstrated that the endo-nucleolytic function of MRE11 cleaves replication forks in the absence of RAD51 which is prevented by Polθ (Mann et al., 2022). Interestingly, depleting the nucleases/helicases EXO1, DNA2 and BLM in *53bp1/Brca1*-mutated cells reversed the toxicity to Polθ-mediated inhibition by ART558 (Zatreanu et al., 2021). Also, the short-term inhibition of MRE11 was able to relieve cell toxicity in *BRCA1*-deficient cells depleted of Polθ by reducing ssDNA cleavage and processing carried out by the MRN complex (Schrempf et al., 2022). Therefore, MRE11 is a

fundamental component underlying the relationship between BRCA1 and Polθ and could be important with regards to Polθ toxicity in our *Brca1*$^{C61G/C61G}$ *53bp1*$^{-/-}$ cells.

Finally, we explored whether limiting RPA could alleviate the toxicity created by the absence of Polθ in *Brca1*$^{C61G/C61G}$ *53bp1*$^{-/-}$ cells. In Chapter 3, Fig.3.7C, we showed that the removal of Polθ leads to increased native BrdU lengths and thus increased ssDNA, which has also been confirmed in literature (Mann et al., 2022; Belan et al., 2022; Schrempf et al., 2021). We reasoned that elevated ssDNA and thus increased RPA/ssDNA binding could promote raised RPA-RAD52 interactions as the formation of the RPA-RAD52 complex is necessary for RAD52 to carry out RAD51-dependent HR (Deng et al., 2009; Park et al., 1996; Jackson et al., 2002). Furthermore, previous findings have shown that the Polθ helicase domain functions to strip RPA from ssDNA. (Mateos-Gomez et al., 2017; Mann et al., 2022; Schrempf et al., 2021; Belan et al., 2022).

Overall, the mechanisms and proteins underlying the synthetic lethality between BRCA1/53BP1/Polθ still remain largely unknown. In the following chapter we reveal that the toxic activity of RAD52/RPA/MRE11 in our *Brca1*$^{C61G/C61G}$ *53bp1*$^{-/-}$ cells depleted of Polθ go some way to explain the synthetic lethal relationship between *Brca1* deficiency, *53bp1* loss and Polθ loss. However, we also show that there appears to be alternative mechanisms of action between Polθ loss and inhibition between *Brca1*$^{+/+}$*53bp1*$^{-/-}$ and *Brca1*$^{C61G/C61G}$ *53bp1*$^{-/-}$ cells. Surprisingly, we show that reducing RAD52 and its toxic accumulations can alleviate cell defects in our *Brca1*$^{C61G/C61G}$ *53bp1*$^{-/-}$ cells and could be important for future treatments and patient stratification regarding Polθ inhibitor treatment.

4.3. Results

4.3.1. RNF168 is important for survival and BARD1 foci formation in *Brca1*$^{C61G/C61G}$ *53bp1*$^{-/-}$ cells

We have shown that *Brca1*$^{C61G/C61G}$ *53bp1*$^{-/-}$ cells are reliant on Polθ, potentially through the PRR of ssDNA gaps (Chapter 3). However, the mechanism of how Polθ supports this function remains unknown. Data in Chapter 3 suggests that *Brca1*$^{C61G/C61G}$ *53bp1*$^{-/-}$ cells are also dependent on additional support mechanisms to promote HR for survival as our cells have reduced HR frequency (Fig.3.1E) and BRCA1/BARD1 protein levels compared to *Brca1*$^{+/+}$ *53bp1*$^{-/-}$ cells (Fig.3.1A). Fig. 3.1B from Chapter 3 highlighted that BRCA1 foci numbers were reduced in *Brca1*$^{C61G/C61G}$ *53bp1*$^{-/-}$ cells, which implies that there's a reduction in BRCA1 recruitment. This led us to investigate the role of RNF168-mediated support in our cells. Krais *et al* (2021) revealed a role for RNF168 in promoting the recruitment of the BRCA1-P complex via the BUDR domain of BARD1 (Krais et al., 2021; Sherker et al., 2021). Therefore, we wanted to decipher whether *Brca1*$^{C61G/C61G}$ *53bp1*$^{-/-}$ cells are reliant on the support of RNF168 for survival.

We treated both *Brca1*$^{+/+}$ *53bp1*$^{-/-}$ and *Brca1*$^{C61G/C61G}$ *53bp1*$^{-/-}$ cells with siRNA targeting RNF168 and discovered that the loss of RNF168 significantly reduced cell survival in *Brca1*$^{C61G/C61G}$ *53bp1*$^{-/-}$ cells compared to *Brca1*$^{+/+}$ *53bp1*$^{-/-}$ cells (Fig.4.1A). The removal of RNF168 lowered cell viability to approximately 50% in *Brca1*$^{C61G/C61G}$ *53bp1*$^{-/-}$ MEFs, compared to 91% survival in *Brca1*$^{+/+}$ *53bp1*$^{-/-}$ cells (Fig.4.1A). These data highlight that *Brca1*$^{C61G/C61G}$ *53bp1*$^{-/-}$ cells are reliant on the E3 ligase RNF168 for survival. We also demonstrated that heterozygous *Brca1*$^{C61G/+}$ *53bp1*$^{-/-}$ cells are equally sensitive to RNF168 loss, unlike Polθ depletion which only sensitises homozygous *Brca1*$^{C61G/C61G}$ *53bp1*$^{-/-}$ MEFs (Ronson et al., 2023) We highlighted that RNF168 depletes RAD51 foci

formation, a marker for HR, indicating that RNF168 is likely important for mediating RAD51 loading and HR in *Brca1*$^{C61G/C61G}$ *53bp1*$^{-/-}$ cells (Ronson et al., 2023). Overall, these data imply that *Brca1*$^{C61G/C61G}$ *53bp1*$^{-/-}$ cells require the non-canonical support of RNF168 to promote HR and cell viability.

The C61G-BRCA1 protein disrupts BRCA1/BARD1 heterodimerisation leading to decreased stability of both proteins (Brzovic et al., 1998) and we have already seen that *Brca1*$^{C61G/C61G}$ *53bp1*$^{-/-}$ MEFs form fewer and weaker IR-induced BRCA1 foci (Chapter 3, Fig. 3.1B). So, we wanted to determine whether the loss of RNF168 influences BARD1 foci formation in both *Brca1*$^{+/+}$ *53bp1*$^{-/-}$ cells and *Brca1*$^{C61G/C61G}$ *53bp1*$^{-/-}$ MEFs. We treated the cells with siRNA to RNF168 and quantified BARD1 focal accumulation (Fig.4.1B,C). There was a significant reduction in BARD1 foci numbers in untreated *Brca1*$^{C61G/C61G}$ *53bp1*$^{-/-}$ MEFs compared to *Brca1*$^{+/+}$ *53bp1*$^{-/-}$ cells, reinforcing that the N-terminal interaction between BRCA1 and BARD1 is important for proficient BARD1 foci formation and recruitment to DSBs. Depleting RNF168 diminished BARD1 foci numbers in *Brca1*$^{+/+}$ *53bp1*$^{-/-}$ cells from an average of 22 foci per cell to 14 foci per cell, compared to *Brca1*$^{C61G/C61G}$ *53bp1*$^{-/-}$ MEFs which reduced BARD1 foci from a mean of 6 foci per cell to 4 foci per cell post 2 Gy IR (Fig.4.1B,C). Additionally, the loss of RNF168 increased the formation of γH2AX foci in both cell lines from an average of 24 foci per cell to 34 foci per cell in *Brca1*$^{+/+}$ *53bp1*$^{-/-}$ cells, and from an average of 35 foci per cell to 43 foci per cell in *Brca1*$^{C61G/C61G}$ *53bp1*$^{-/-}$ cells (Fig.4.1C). In summation, these data denote that RNF168 is not only fundamental for cell survival but is imperative for the localisation of BARD1 to sites of damage.

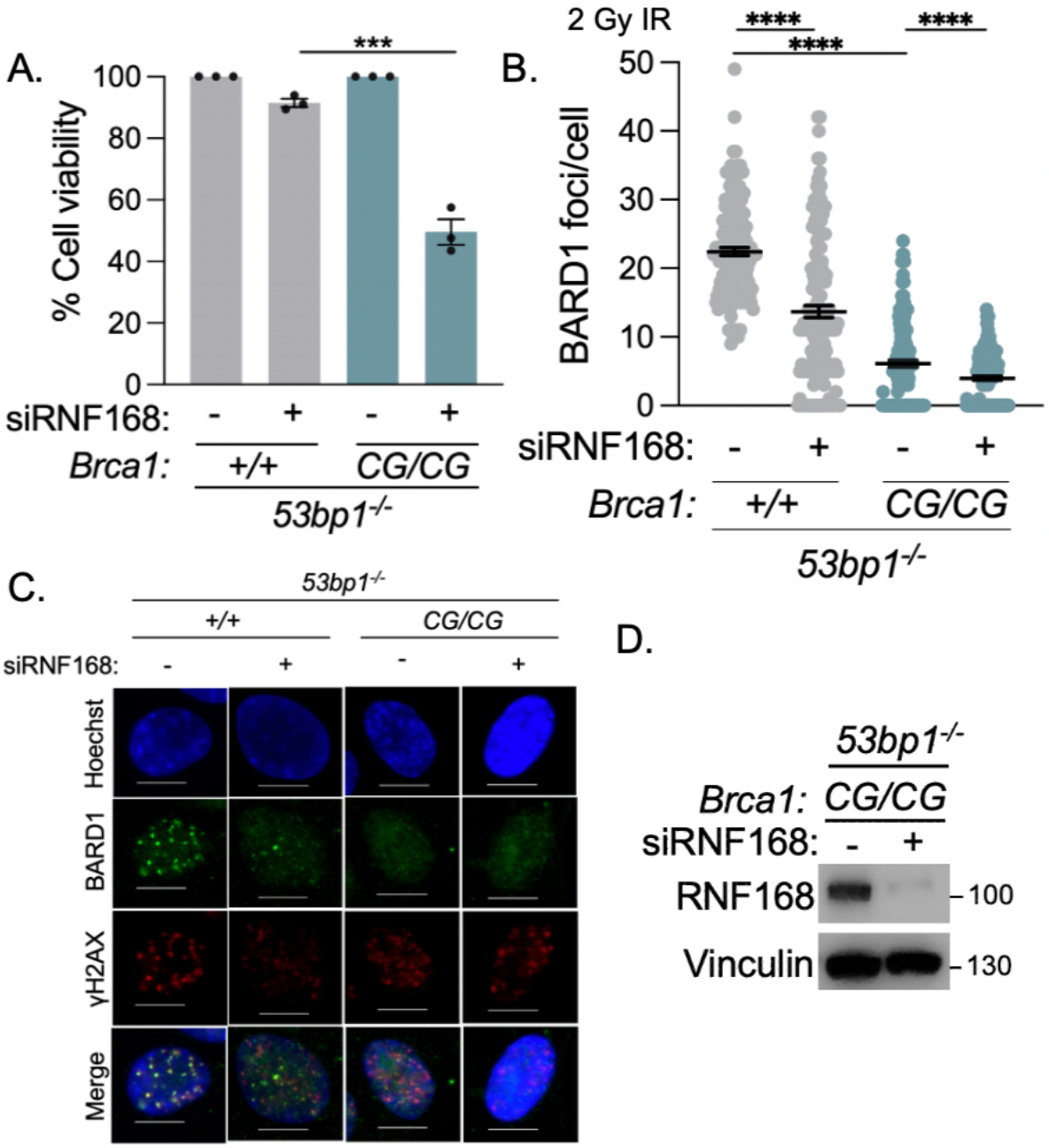

Figure 4.1. RNF168 is important for survival and BARD1 foci formation in *Brca1$^{C61G/C61G}$ 53bp1$^{-/-}$* cells.

A. Colony survival in MEFs of genotypes shown after treatment with non-targeting control (NTC) siRNA (-) or RNF168 siRNA (+) and re-plated into colonies and grown out for 7 days. n=3 biological repeats. Data are mean ± SEM. Statistical analysis performed using a two-tailed Student's *t*-Test; ***= p≤0.001.

B. Quantification of BARD1 foci in asynchronous *Brca1$^{+/+}$ 53bp1$^{-/-}$* and *Brca1$^{C61G/C61G}$ 53bp1$^{-/-}$* cells post 2 Gy irradiation and 3 hr recovery. N=150 cells from 3 biological

repeats. Data are mean ± SEM. Statistical analysis performed using a two-tailed Student's *t*-Test; ****= p≤0.0001.

C. Representative images of BARD1 and γH2AX foci in the genotypes shown with and without RNF168 depletion. The scale bar is 10 μm.
D. Western blot analysis of RNF168 protein levels following NTC (−) or RNF168 (+) targeting siRNA treatment. Vinculin was used as a loading control.

4.3.2. RAD52 is essential for cell viability in *Brca1*$^{C61G/C61G}$ *53bp1*$^{-/-}$ cells

Another protein fundamental for the non-canonical support of *BRCA1/2*-deficient cells is RAD52. The loss of RAD52 is synthetic lethal in *BRCA1*-deficient cells as in the absence of functional BRCA1, RAD52 promotes RAD51-dependent HR, the error-prone repair pathway SSA and functions in the restart of stalled replication forks among other roles (Feng et al., 2011; Lok et al., 2013; Cramer-Morales et al., 2013; Sotiriou et al., 2016; Lemaçon et al., 2017). To assess the importance of RAD52 in *Brca1*$^{C61G/C61G}$ *53bp1*$^{-/-}$, we transfected the cells with siRNA targeting RAD52 and analysed cell survival using colony survival assays. Depleting RAD52 in *Brca1*$^{C61G/C61G}$ *53bp1*$^{-/-}$ cells reduced cell viability to 60% survival compared to 90% survival in *Brca1*$^{+/+}$ *53bp1*$^{-/-}$ cells (Fig.4.2A). Therefore, it appears that *Brca1*$^{C61G/C61G}$ *53bp1*$^{-/-}$ cells are reliant on RAD52 for survival.

In 2015 the first small molecule inhibitor of RAD52 6-Hydroxy-*D*L-DOPA (6-OHD) was developed which can specifically inhibit RAD52-mediated SSA and not impact other DNA damage pathways such as HR (Chandramouly et al., 2015). We wanted to determine whether the inhibition of RAD52 can specifically target *Brca1*$^{C61G/C61G}$ *53bp1*$^{-/-}$ cells over *Brca1*$^{+/+}$ *53bp1*$^{-/-}$ cells. 6-OHD disbands the oligomeric ring structures of RAD52 into dimers preventing binding to ssDNA (Fig.4.2B) (Chandramouly et al., 2015). We used the highest concentration of 6-OHD from an initial dose range which

is toxic to both cell lines, but *Brca1*$^{C61G/C61G}$ *53bp1*$^{-/-}$ cells were significantly more sensitive to 6-OHD compared to *Brca1*$^{+/+}$ *53bp1*$^{-/-}$ cells, diminishing cell viability to approximately 33% survival in contrast to 63% survival (Fig.4.2C). Overall, both RNF168 and RAD52 are important to support cell viability in *Brca1*$^{C61G/C61G}$ *53bp1*$^{-/-}$ cells that have sub-optimal HR function.

To determine whether the synthetic lethal relationship between Polθ and C61G-BRCA1 is facilitated by either RNF168 or RAD52, we explored whether there was an increased recruitment of either protein in the absence of Polθ in our *Brca1*$^{C61G/C61G}$ *53bp1*$^{-/-}$ cells. We treated *Brca1*$^{C61G/C61G}$ *53bp1*$^{-/-}$ cells with siRNA to Polθ and quantified the number of FLAG-tagged RAD52 foci. We did not have a working RAD52 antibody in MEFs that could be used for immunofluorescence, so we monitored FLAG foci formation to recapitulate RAD52 foci generation. On observation we noted that *Brca1*$^{C61G/C61G}$ *53bp1*$^{-/-}$ cells had a higher baseline level of FLAG-RAD52 compared to *Brca1*$^{+/+}$ *53bp1*$^{-/-}$ cells, with a mean of 3 foci per cell compared to 1 focus per cell (Fig.4.2D). Upon depletion of Polθ, we observed a significant increase in FLAG-RAD52 foci, enhanced to a mean of 7 foci per cell compared to only 2 foci per cell in *Brca1*$^{+/+}$ *53bp1*$^{-/-}$ cells (Fig.4.2D). Therefore, the loss of Polθ led to an accumulation of FLAG-RAD52 recruitment in *Brca1*$^{C61G/C61G}$ *53bp1*$^{-/-}$ cells which could be important for driving the synthetic lethal relationship between Polθ and C61G-BRCA1.

As well as increased FLAG-RAD52 in the absence of Polθ, we saw elevated co-localisation of FLAG-RAD52 with γH2AX foci, which is a marker for DSBs (Ronson et al., 2023). So, not only are RAD52 numbers increasing when Polθ is depleted, but there is an augmented recruitment of RAD52 to DSBs. These results indicate that RAD52 accumulation in *Brca1*$^{C61G/C61G}$ *53bp1*$^{-/-}$ cells devoid of Polθ is negatively

impacting the cells. In Ronson *et al* (2023) we also looked at whether RNF168 foci were increased in Polθ-depleted *Brca1*$^{C61G/C61G}$ *53bp1*$^{-/-}$ cells and witnessed a negligible effect on RNF168 foci numbers (Ronson et al., 2023). We therefore wanted to determine whether the suppression of RNF168 or RAD52 could alleviate the synthetic lethal relationship between Polθ and C61G-BRCA1. My lab colleagues explored whether titrating the concentration of siRNA targeting RNF168 or RAD52 in Polθ-depleted *Brca1*$^{C61G/C61G}$ *53bp1*$^{-/-}$ cells could reduce the number of recombination intermediates namely RAD51 foci numbers brought about by Polθ loss. Titrating the concentration of siRNA to RNF168 or RAD52 in *Brca1*$^{C61G/C61G}$ *53bp1*$^{-/-}$ cells devoid of Polθ could significantly reduce the number of IR-induced RAD51 foci (Ronson et al., 2023). So far, these data elicit that RAD52 could be mediating the toxicity seen in the synthetic lethal relationship between Polθ and C61G-BRCA1.

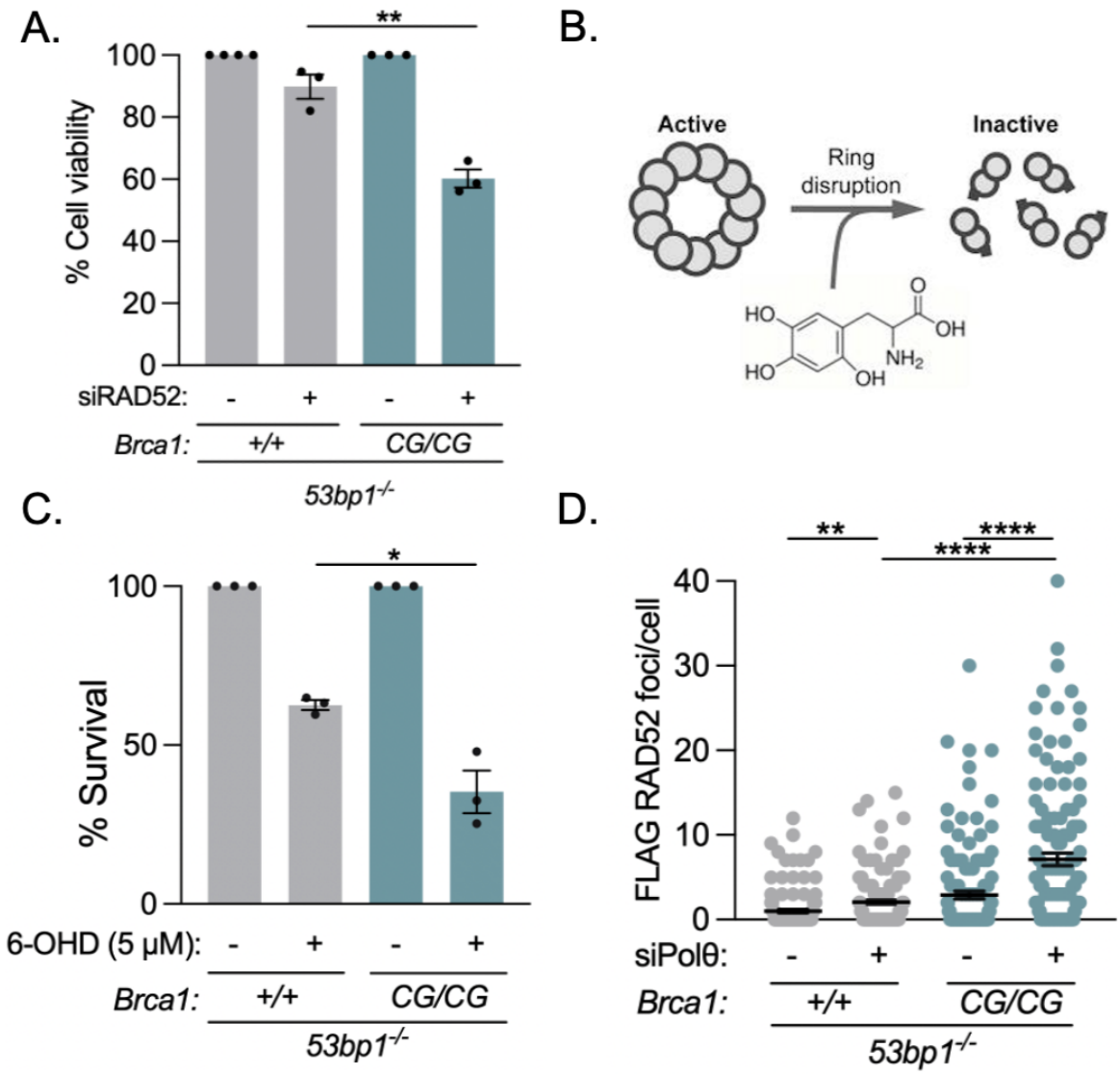

Figure 4.2. *Brca1*$^{C61G/C61G}$ *53bp1*$^{-/-}$ cells are reliant on RAD52, and Polθ loss elevates RAD52 accumulations.

A. Colony survival in *Brca1*$^{+/+}$ *53bp1*$^{-/-}$ and *Brca1*$^{C61G/C61G}$ *53bp1*$^{-/-}$ cells treated with NTC siRNA (−) or siRNA to RAD52 (+). N=3 biological repeats. Data are mean ± SEM. Statistical analysis performed using a two-tailed Student's *t*-Test; **= p≤0.01.

B. Schematic showing 6-OHD transformation of RAD52 from undecamer rings to dimers, disrupting RAD52 recruitment and activity. Adapted from (Chandramouly et al., 2015).

C. Colony survival in *Brca1*$^{+/+}$ *53bp1*$^{-/-}$ and *Brca1*$^{C61G/C61G}$ *53bp1*$^{-/-}$ cells treated with DMSO (-) or 6-OHD (+). N=3 biological repeats. Data are mean ± SEM. Statistical analysis performed using a two-tailed Student's *t*-Test; *= p≤0.05.

D. Quantification of FLAG-RAD52 foci in asynchronous cells with NTC siRNA (-) or Polθ siRNA (+) siRNA. N=120 cells from 3 biological repeats. Data are mean ± SEM. Statistical

analysis performed using a two-tailed Student's *t*-Test; ****= p≤0.0001; **= p≤0.01 *George Ronson.*

4.3.3. Polθ mitigates RAD52-mediated toxicity, and RAD52 suppression rescues cellular defects caused by Polθ loss

We consequently wanted to explore whether there is a functional relationship between RAD52/RNF168 and Polθ in *Brca1*$^{C61G/C61G}$ *53bp1*$^{-/-}$ cells by determining whether titrating the concentration of siRNA to RNF168 or RAD52 could improve cell survival in the absence of Polθ. We repeated the titration of siRNA to RAD52 in Polθ-depleted *Brca1*$^{C61G/C61G}$ *53bp1*$^{-/-}$ cells and strikingly noted an improvement in cell viability, however this was not the case when titrating siRNA to RNF168 under the same conditions (Ronson et al., 2023).

To confirm that RAD52 suppression is specifically driving the toxicity caused by Polθ loss in *Brca1*$^{C61G/C61G}$ *53bp1*$^{-/-}$ cells, we titrated the RAD52 inhibitor 6-OHD. We titrated the RAD52 inhibitor 6-OHD to considerably lower concentrations (0.15 μM – 1.2 μM) compared to 5 μM which was used to elicit the RAD52/C61G-BRCA1 synthetic lethal relationship, to determine whether RAD52 accumulations in the absence of Polθ is driving cell toxicity. Surprisingly, the lowest concentration of 0.15 μM 6-OHD was able to rescue cell survival in *Brca1*$^{C61G/C61G}$ *53bp1*$^{-/-}$ cells treated with Polθ siRNA from 63% to 93% survival (Fig. 4.3A). We then wanted to see whether the effective dose of 0.15 μM 6-OHD could suppress RAD52 accumulations at this concentration and remarkably we witnessed a decreased mean number of FLAG-tagged RAD52 foci (Ronson et al., 2023). These data suggest that RAD52 is involved in driving the toxicity caused by the absence of Polθ in *Brca1*$^{C61G/C61G}$ *53bp1*$^{-/-}$ cells.

It is noteworthy that RAD52 appears to mediate several toxic effects produced from Polθ loss in our *C61G-Brca1* mutated cells. So, we looked at whether the cellular toxicity of Polθ inhibition by ART558 could be rescued by low concentrations of the RAD52 inhibitor 6-OHD, like Polθ loss by siRNA. Single dose treatment of 10 μM ART558 was selected as this concentration clearly separated the sensitivity to Polθ inhibition between WT, *Brca1*$^{+/+}$ *53bp1*$^{-/-}$ and *Brca1*$^{C61G/C61G}$ *53bp1*$^{-/-}$ cells (Chapter 3, Fig.3.3A). We treated *Brca1*$^{C61G/C61G}$ *53bp1*$^{-/-}$ cells with 10 μM ART558 alongside low concentrations of the RAD52 inhibitor 6-OHD (0.15 μM – 1.2 μM) and could not rescue cell viability in *Brca1*$^{C61G/C61G}$ *53bp1*$^{-/-}$ cells (Fig.4.3B). We altered the dose range of ART558 as well as the concentrations of 6-OHD and could not relieve cell toxicity. Therefore, it is likely that the mechanism of action is different between Polθ depletion by siRNA and Polθ inhibition by ART558.

Although the loss of Polθ in *Brca1*$^{+/+}$ *53bp1*$^{-/-}$ cells made little impact compared to *Brca1*$^{C61G/C61G}$ *53bp1*$^{-/-}$ cells (Chapter 3, Fig.3.2C), the *53bp1*$^{-/-}$ background sensitised cells to ART558 compared to WT cells (Chapter 3, Fig.3.3A). We considered whether Polθ sensitivity by ART558 could be rescued by low doses of 6-OHD in our *Brca1*$^{+/+}$*53bp1*$^{-/-}$ cells. Hence, we repeated the experiment from Figure 4.3B and we treated *Brca1*$^{+/+}$*53bp1*$^{-/-}$ cells with 10 μM ART558 as well as low concentrations of the RAD52 inhibitor 6-OHD. Unlike *Brca1*$^{C61G/C61G}$ *53bp1*$^{-/-}$ cells, ART558 sensitivity could be rescued by co-treatment with 1.2 μM 6-OHD in *Brca1*$^{+/+}$*53bp1*$^{-/-}$ cells (Fig.4.3C). These results show that suppressing RAD52 can rescue Polθ inhibition in *Brca1*$^{+/+}$ *53bp1*$^{-/-}$ cells and that Polθ engagement is different between *Brca1*$^{+/+}$ *53bp1*$^{-/-}$ and *Brca1*$^{C61G/C61G}$ *53bp1*$^{-/-}$ cells. Low concentrations of the RAD52 inhibitor could rescue toxic Polθ inhibition by ART558 in *Brca1*$^{+/+}$ *53bp1*$^{-/-}$ cells, albeit making no change to

cell viability in *Brca1*$^{C61G/C61G}$ *53bp1*$^{-/-}$ cells. So far, we have shown that Polθ mitigates RAD52-mediated toxicity in *Brca1*$^{C61G/C61G}$ *53bp1*$^{-/-}$ cells, and that the suppression of RAD52 rescues cellular defects caused by Polθ loss.

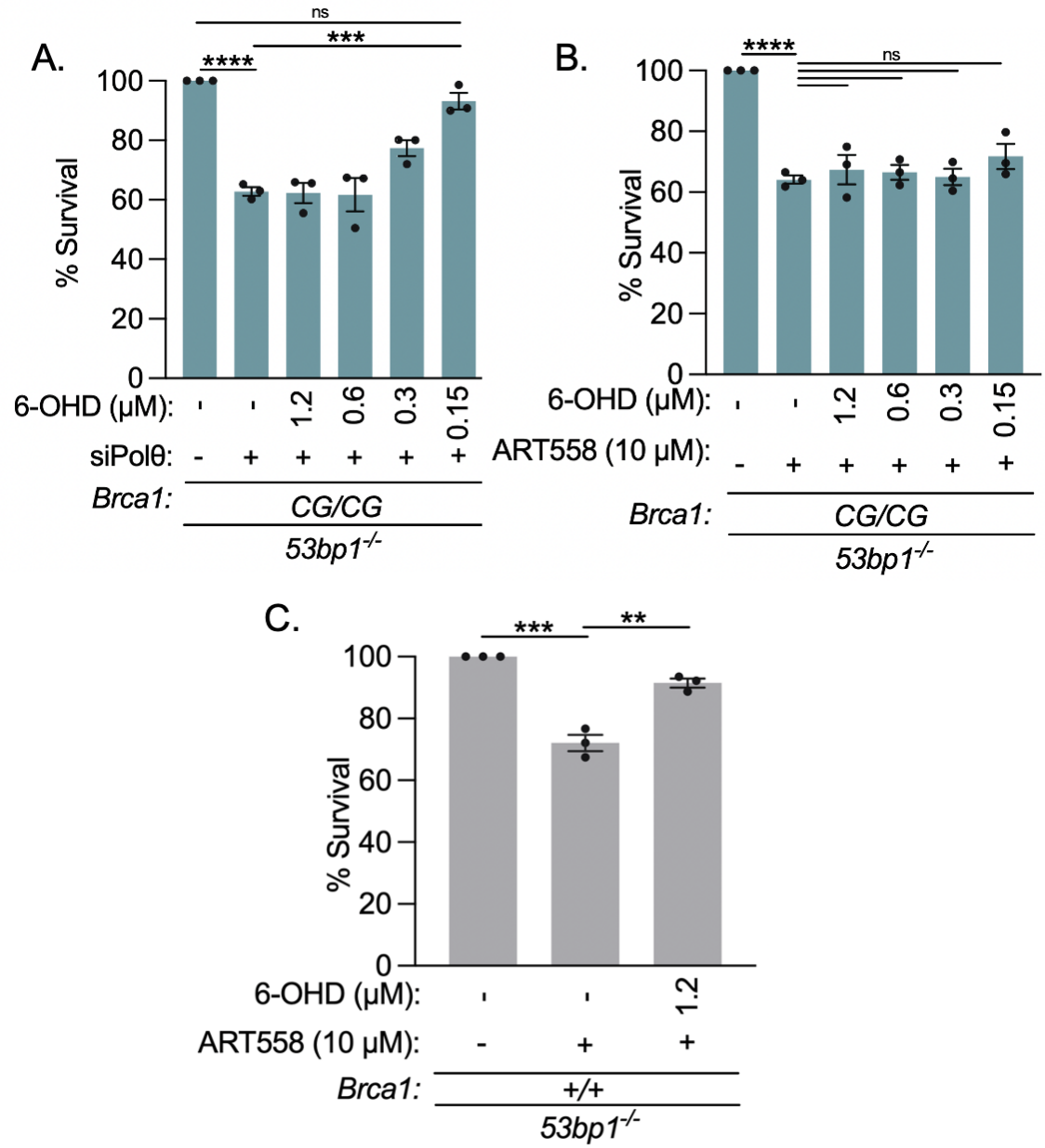

Figure 4.3. Polθ mitigates RAD52-mediated toxicity and RAD52 suppression rescues cellular defects caused by Polθ loss.

A. Colony survival of *Brca1*$^{C61G/C61G}$ *53bp1*$^{-/-}$ cells treated with NTC (-) or siRNA to Polθ (+) and RAD52 inhibitor 6-OHD (different doses as indicated). N=3 biological repeats.

Data are mean ± SEM. Statistical analysis performed using a two-tailed Student's *t*-Test; ****= p≤0.0001; ***= p≤0.001; ns = not significant.

B. Colony survival of *Brca1*$^{C61G/C61G}$ *53bp1*$^{-/-}$ cells treated with DMSO (-) or 10 μM Polθ inhibitor ART558 (+) or RAD52 inhibitor 6-OHD (different doses as indicated). N=3 biological repeats. Data are mean ± SEM. Statistical analysis performed using a two-tailed Student's *t*-Test; ****= p≤0.0001; ns = not significant.

C. Colony survival of *Brca1*$^{+/+}$ *53bp1*$^{-/-}$ cells treated with DMSO (-) or 10 μM Polθ inhibitor ART558 (+) or RAD52 inhibitor 6-OHD. N=3 biological repeats. Data are mean ± SEM. Statistical analysis performed using a two-tailed Student's *t*-Test; ***= p≤0.001; **= p≤0.01.

4.3.3. BARD1 and BRC4-RPA exogenous expression can overcome RAD52-depleted toxicity

In Chapter 3 Fig.3.4D we demonstrated that overexpressing the BRCA1 binding partner BARD1 could improve cell viability in *Brca1*$^{C61G/C61G}$ *53bp1*$^{-/-}$ cells treated with siRNA targeting Polθ, therefore we wanted to determine whether the same could be applied to cells depleted of RAD52. We treated *Brca1*$^{C61G/C61G}$ *53bp1*$^{-/-}$ cells containing an empty vector and those infected retrovirally with exogenous BARD1 and subjected the cells to siRNA targeting RAD52. We noted that the loss of RAD52 reduced cell viability in *Brca1*$^{C61G/C61G}$ *53bp1*$^{-/-}$ cells containing the empty vector to an average of 58% viability, yet we confirmed that exogenous expression of BARD1 could elevate cell viability to a mean of 84% cell survival in the absence of RAD52 (Fig.4.4B). As explained in Chapter 3, we saw that HR outcomes measured by PCR could be improved by the exogenous expression of BARD1 (Ronson et al., 2023). Taken together, these results indicate that the overexpression of BARD1 negate the requirement of RAD52 to support HR in *Brca1*$^{C61G/C61G}$ *53bp1*$^{-/-}$ cells.

Likewise, we wanted to decipher whether exogenous expression of the BRCA2 constructs BRC4-RPA and Ex27-RPA could rescue RAD52 sensitivity in *Brca1*$^{C61G/C61G}$ *53bp1*$^{-/-}$ cells. To explore the interactions between BRCA2 and RAD51, we retrovirally expressed one of the BRCA2 BRC repeats BRC4 or the C-terminal RAD51 binding region of BRCA2 fused to RPA70 (Saeki et al., 2006; Esashi et al., 2007; Davies and Pellegrini, 2007).

Saeki *et al* (2006) originally designed the BRC4-RPA construct to gain an insight into the function of BRCA2 and discovered, like ourselves, that these constructs could bypass the requirement for BRCA1/PALB2/BRCA2 for RAD51 focus formation (Saeki et al., 2006; Ronson et al., 2023) We found that Ex27-RPA could form RAD51 foci in the absence of BRCA1, albeit at a lesser extent than in cells infected with the BRC4-RPA construct (Ronson et al., 2023). The BRC4 repeat of BRCA2 is important for the exchange of RPA:RAD51 whereas the BRCA2 binding region of RAD51 is key for the stabilisation of the nucleofilament by interacting with oligomerised RAD51 (Fig. 4.4A) (Kolinjivadi et al., 2017b; Davies and Pellegrini, 2007; Esashi et al., 2007). Subsequently, we treated *Brca1*$^{C61G/C61G}$ *53bp1*$^{-/-}$ cells expressing either the empty vector or the BRC4-RPA or Ex27-RPA constructs with siRNA targeting RAD52 and tested cell viability using colony survival assays. We found that expression of BRC4-RPA, important to aid in the exchange of RPA with RAD51, improved cell survival in the absence of RAD52, whereas Ex27-RPA, important for RAD51 stability, could not (Fig. 4.4C). BRC4-RPA expression in *Brca1*$^{C61G/C61G}$ *53bp1*$^{-/-}$ cells can form RAD51 foci in the presence of siRNA targeting BRCA1 (Ronson et al., 2023), mediating the recruitment of BRCA2 BRC4 to ssDNA independently of BRCA1 and thus bypass the need for RAD52 to support cell survival by HR.

Consequently, we wanted to determine whether the exogenous expression of either BARD1 or BRC4-RPA could limit RAD52 accumulations in the presence of Polθ inhibition. In line with the results in Figure.4.4B,C, my lab colleague showed that BARD1 and BRC4-RPA exogenous expression could reduce the number of FLAG-RAD52 foci in Polθ inhibitor-treated *Brca1*$^{C61G/C61G}$ *53bp1*$^{-/-}$ cells (Ronson et al., 2023). These data highlight that the accumulation of RAD52 is no longer necessary in retrovirally infected BARD1 and BRC4-RPA *Brca1*$^{C61G/C61G}$ *53bp1*$^{-/-}$ cells treated with ART558. We also revisited the AAE-BARD1 construct from Chapter 3 which disrupts BARD1 binding with RAD51, important for D-loop formation, synaptic complex assembly and fork protection (Zhao et al., 2017b; Daza-Martin et al., 2019). My lab colleague identified that the retroviral expression of AAE-BARD1 could no longer reduce FLAG-RAD52 foci numbers back down in ART558-treated *Brca1*$^{C61G/C61G}$ *53bp1*$^{-/-}$ cells unlike the overexpression of WT BARD1 (Ronson et al., 2023). The interaction between BARD1/RAD51 is necessary to attenuate the toxic accumulation of RAD52 in Polθ inhibited *Brca1*$^{C61G/C61G}$ *53bp1*$^{-/-}$ cells. These data allude to a role of Polθ in suppressing RAD52-mediated toxicity that is redundant in the presence of functional BRCA1/BARD1-RAD51 and BRC4-RPA. RAD52 is driving cell toxicity when Polθ is lost/inhibited but the mechanism and location surrounding this toxicity remains to be uncovered.

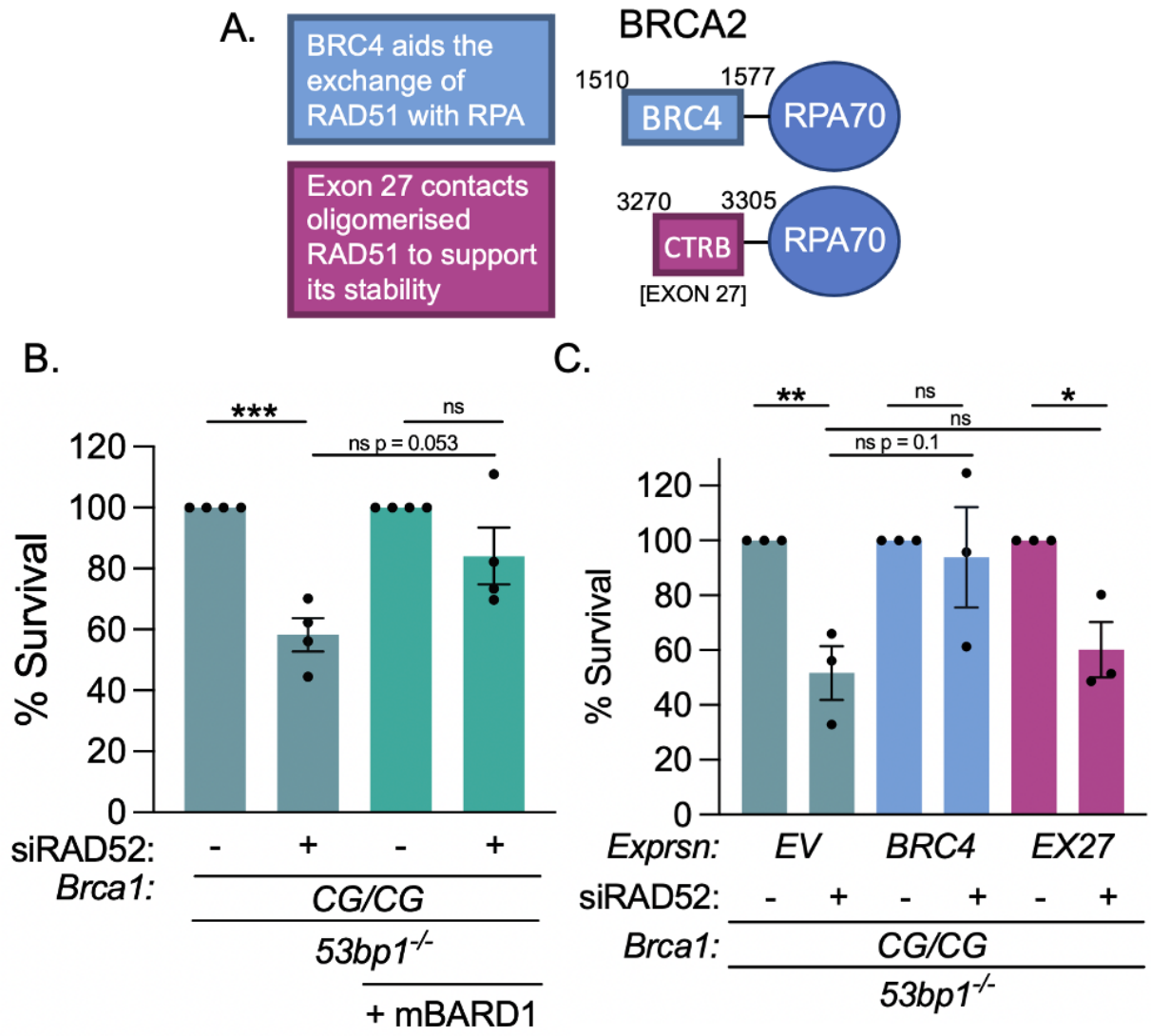

Figure 4.4. BARD1 and BRC4-RPA exogenous expression can overcome RAD52-depleted toxicity in *Brca1*$^{C61G/C61G}$ *53bp1*$^{-/-}$ cells.

A. Schematic of BRCA2: BRC4-RPA and Exon 27-RPA.

B. Colony survival in *Brca1*$^{C61G/C61G}$ *53bp1*$^{-/-}$ cells treated with NTC siRNA (-) or RAD52 siRNA (+) and infection with empty vector (EV) or BARD1 containing vector. N=4 biological repeats. Data are mean ± SEM. Statistical analysis performed using a two-tailed Student's *t*-Test; ***= p≤0.001; ns = not significant.

C. Colony survival in *Brca1*$^{C61G/C61G}$ *53bp1*$^{-/-}$ cells treated with NTC siRNA (-) or RAD52 siRNA (+) and infection with EV or those containing RPA constructs: BRC4-RPA and EX27-RPA. N=3 biological repeats. Data are mean ± SEM. Statistical analysis performed using a two-tailed Student's *t*-Test; **= p≤0.01; *= p≤0.05; ns = not significant.

4.3.4. RAD52 functions with MRE11 to promote toxicity in the absence of Polθ

To further understand the relationship between Polθ and RAD52 in *Brca1*$^{C61G/C61G}$ *53bp1*$^{-/-}$ cells, we explored shared features between the two proteins. We have already seen raised ssDNA formation in *Brca1*$^{C61G/C61G}$ *53bp1*$^{-/-}$ MEFs treated with siRNA targeting Polθ (Chapter 3, Fig.3.7C). Also, RAD52-mediated SSA requires resected homologous ssDNA as a template for repair (Ceccaldi et al., 2016; Hanamshet et al., 2016) and binds directly to RPA and RAD51, with the RAD52-RPA complex having a high affinity for ssDNA (Shinohara et al., 1998; Hanamshet and Mazin, 2020; Shen et al., 1996; Mazina et al., 2017; Park et al., 1996; Jackson et al., 2002). Also, nucleases such as MRE11 can digest nascent DNA, thus limiting cell survival in *BRCA1/2*-deficient cells depleted of Polθ (Belan et al., 2022; Mann et al., 2022; Schrempf et al., 2022). Therefore, we explored whether abnormally extended ssDNA generation in Polθ depleted *Brca1*$^{C61G/C61G}$ *53bp1*$^{-/-}$ MEFs could be deleterious. Then we looked at whether extended ssDNA lengths could be reversed by the suppression of RAD52 and/or MRE11.

Consequently, we visualised resected ssDNA using the SMART DNA fibre assay (explained in Chapter 3, Fig.3.7A,B) (Altieri et al., 2020). We observed extended resection lengths in *Brca1*$^{C61G/C61G}$ *53bp1*$^{-/-}$ MEFs treated with siRNA targeting Polθ which were MRE11 dependent as shown by co-treatment with 5 μM of the MRE11 exonuclease inhibitor mirin bringing native BrdU lengths back down (Fig.4.5A). Polθ-depleted extended resection was also suppressed when co-treated with 0.15 μM

RAD52 inhibitor 6-OHD, the same concentration which could alleviate cell toxicity (Fig.4.5A). Although, treatment with 0.15 μM 6-OHD alone increased ssDNA lengths, which did not affect cell viability, suggesting that excessive ssDNA formation was unlikely the reason behind the Polθ/RAD52 relationship. What's more, treatment with siRNA to Polθ as well as 0.15 μM 6-OHD and 5 μM MRE11 together reduced native BrdU lengths to the same extent suggesting that RAD52 and MRE11 potentially work within the same pathway. With regards to cell survival, treatment with 2.5 μM mirin was able to restore cell viability in Polθ-depleted *Brca1*$^{C61G/C61G}$ *53bp1*$^{-/-}$ cells (Fig.4.5B).

Despite significant amelioration in cell viability when treating Polθ-depleted *Brca1*$^{C61G/C61G}$ *53bp1*$^{-/-}$ cells with 2.5 μM mirin, we discovered that this concentration was not sufficient to reduce FLAG-RAD52 accumulations which have been deemed toxic thus far (Ronson et al., 2023). Therefore, MRE11 does not aid cell survival through the suppression of RAD52, hence we looked at whether RAD52 encourages MRE11 recruitment (Mijic et al., 2017). My lab colleague discovered that MRE11 acts downstream of RAD52 in the absence of Polθ in *Brca1*$^{C61G/C61G}$ *53bp1*$^{-/-}$ cells (Ronson et al., 2023). This was done by analysing the proximity of MRE11 to ssDNA using the proximity ligation assay (PLA) which entails the observation of discrete spots formed when two proteins are in close proximity to one another (< 40 nm) (Bagchi et al., 2015). *Brca1*$^{C61G/C61G}$ *53bp1*$^{-/-}$ cells depleted of Polθ were grown in the presence of BrdU over 48 hours; BrdU can only become exposed and bind to anti-BrdU antibodies in ssDNA under non-denaturing conditions (Fowler and Tyler, 2022). Treatment of siRNA to Polθ in *Brca1*$^{C61G/C61G}$ *53bp1*$^{-/-}$ cells increased the proximity between MRE11 and ssDNA, yet co-treatment of Polθ loss and 0.15 μM 6-OHD reduced the detection of

MRE11:BrdU proximity (Ronson et al., 2023). These data highlight that MRE11 functions downstream of RAD52 in *Brca1*$^{C61G/C61G}$ *53bp1*$^{-/-}$ cells lacking Polθ, and that RAD52 facilitates the proximity between MRE11:ssDNA which drives the toxicity witnessed in Polθ-depleted *Brca1*$^{C61G/C61G}$ *53bp1*$^{-/-}$ cells (Ronson et al., 2023).

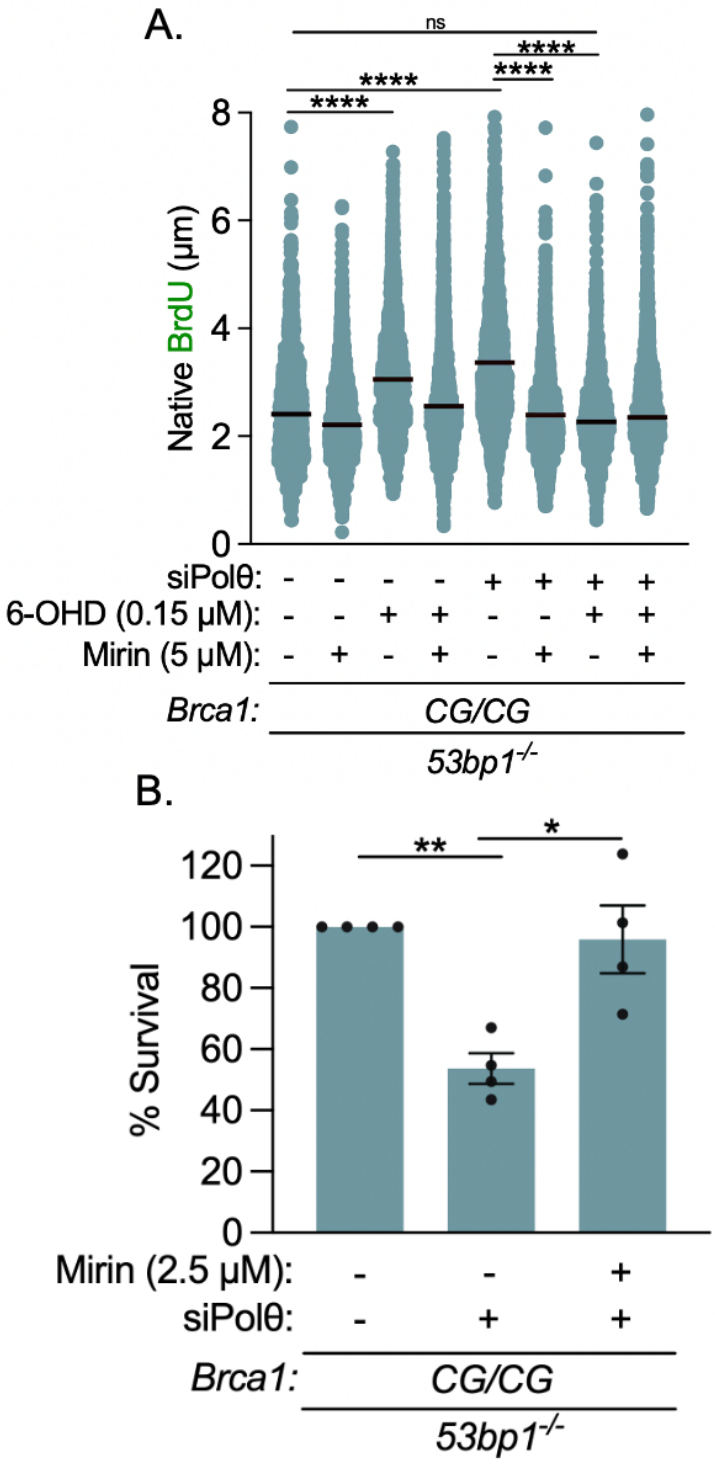

Figure 4.5. Suppression of RAD52 reduces MRE11/ssDNA-mediated toxicity caused by Polθ depletion in *Brca1*$^{C61G/C61G}$ *53bp1*$^{-/-}$ cells.

A. Native BrdU tracts in *Brca1*$^{C61G/C61G}$ *53bp1*$^{-/-}$ cells after control (-) or Polθ siRNA (+) and 0.15 μM RAD52 inhibitor 6-OHD (+) and/or 5 μM mirin (+) for 72 h. n ≥ 1400 tracks from n=3 biological replicates. Statistical analysis performed using Mann-Whitney test. ****= p≤0.0001; ns = not significant. *(with Liza Piberger).*
B. Colony survival of *Brca1*$^{C61G/C61G}$ *53bp1*$^{-/-}$ cells treated with NTC siRNA (-), Polθ siRNA (+) and 2.5 μM MRE11 exonuclease inhibitor mirin (+). N=4 biological repeats. Data are mean ± SEM. Statistical analysis performed using a two-tailed Student's *t*-Test; **= p≤0.01; *= p≤0.05.

4.3.5. Reducing RPA improves cell viability in Polθ-depleted *Brca1*$^{C61G/C61G}$ *53bp1*$^{-/-}$ cells

The promotion of MRE11:ssDNA by RAD52 facilitates the toxicity to Polθ loss in *Brca1*$^{C61G/C61G}$ *53bp1*$^{-/-}$ cells, so we wanted to determine whether limiting the ssDNA binding protein RPA could alleviate cell toxicity in the absence of Polθ. The formation of the RAD52-RPA complex and the phosphorylation of RPA is necessary for the association of RAD52 with RAD51 for RAD52-mediated HR in cells that lack functional BRCA1/2 proteins (Carley et al., 2022; Park et al., 1996). RPA is indispensable and integral to virtually all DNA metabolic pathways (Zou et al., 2006; Dodson et al., 2004), therefore we titrated siRNA to RPA32 and RPA70 to very low concentrations and remarkably we discovered that 0.15 – 0.07 nM siRNA could rescue cell sensitivity to Polθ loss in *Brca1*$^{C61G/C61G}$ *53bp1*$^{-/-}$ MEFs (Fig.4.6A). In addition, we wanted to decipher whether the very low RPA siRNA concentrations of 0.15 and 0.07 nM could suppress FLAG-RAD52 foci generation. My lab colleague witnessed FLAG-RAD52 foci suppression in the face of 0.15 or 0.07 nM siRNA targeting RPA in *Brca1*$^{C61G/C61G}$ *53bp1*$^{-/-}$ cells depleted of Polθ (Ronson et al., 2023).

We then wanted to determine whether reducing the concentration of RPA could limit resection lengths in *Brca1*$^{C61G/C61G}$ *53bp1*$^{-/-}$ cells lacking Polθ. We used the doses of siRNA to RPA (0.15 and 0.07 nM) effective for improving cell viability and noted that these concentrations were sufficient to reduce BrdU lengths in Polθ-depleted *Brca1*$^{C61G/C61G}$ *53bp1*$^{-/-}$ cells (Fig. 4.6B). Previous findings have also shown that lessening RPA concentrations will reduce resection by limiting the action of MRE11 on nascent DNA (Nimonkar et al., 2011; Chen et al., 2013). However, the results from Fig.4.6B do not take into account that RAD52 could still be the driver of cell toxicity in the absence of Polθ. My lab colleague thereby generated two siRNA resistant constructs: WT FLAG-RAD52 and FLAG-RAD52 missing the RPA binding domain (Δ aa 254 – 286) (Grimme et al., 2010). We noted that expression of the WT FLAG-RAD52 construct suppressed the survival advantage brought about by low concentrations of siRNA to RAD52 in the Polθ depleted *Brca1*$^{C61G/C61G}$ *53bp1*$^{-/-}$ cells, whereas this was not the case with regards to the Δ 254 – 286 construct (lacking the RAD52-RPA binding region) (Ronson et al., 2023).

In summation, these data indicate that the toxicity created by Polθ loss in *Brca1*$^{C61G/C61G}$ *53bp1*$^{-/-}$ cells is due to the association between RPA and RAD52 as well as the RAD52-mediated interaction between MRE11 and ssDNA. Taken together, our data reveal that the suppression of RAD52/MRE11/RPA diminishes the toxicity of Polθ loss in *Brca1*$^{C61G/C61G}$ *53bp1*$^{-/-}$ cells.

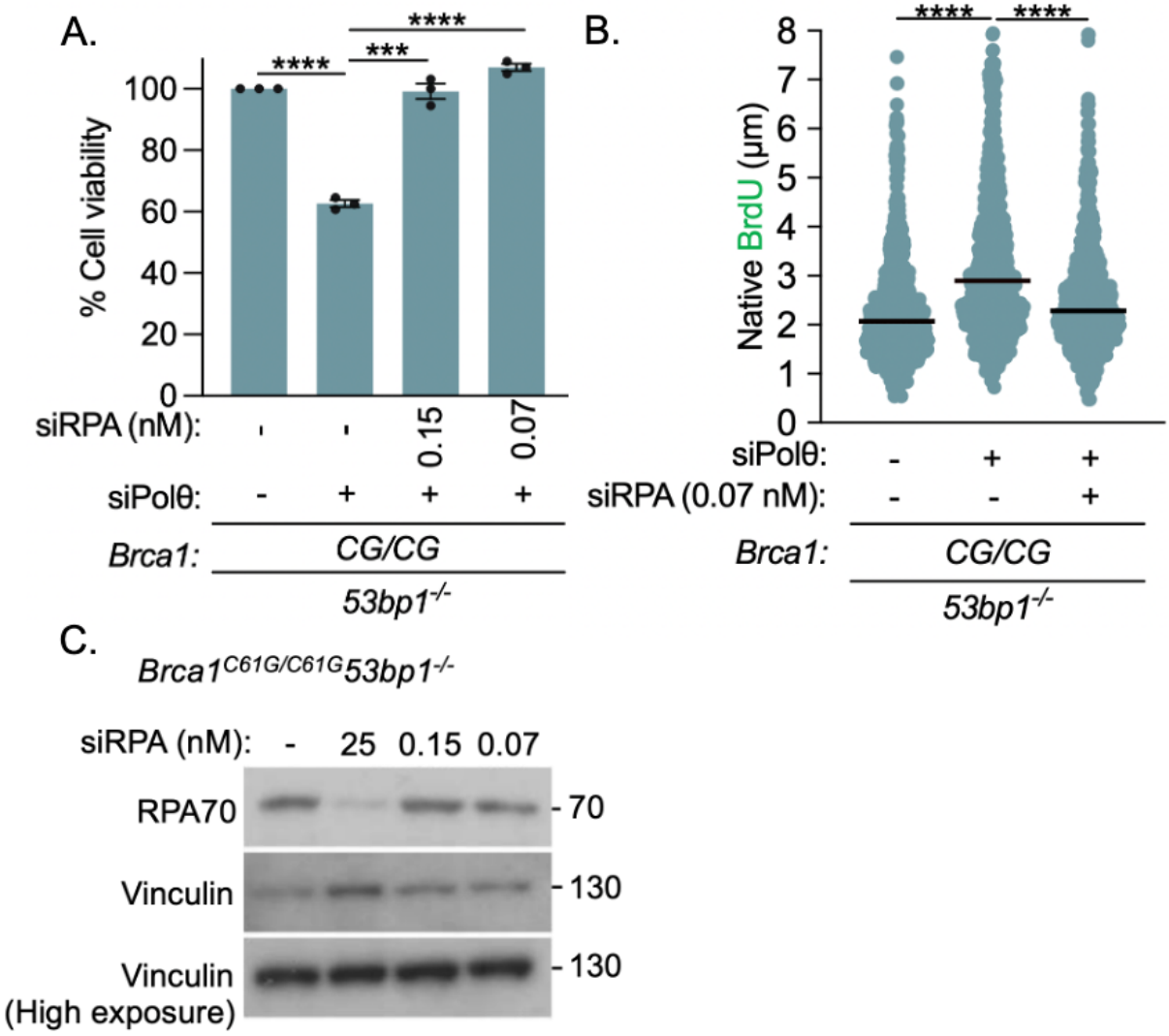

Figure 4.6. Reducing RPA improves cell viability in Polθ-depleted *Brca1*$^{C61G/C61G}$ *53bp1*$^{-/-}$ cells.

A. Colony survival of *Brca1*$^{C61G/C61G}$ *53bp1*$^{-/-}$ cells treated with NTC siRNA (-) and Polθ and/or RPA siRNA (+). N=3, data are mean ± SEM. Statistical analysis performed using a two-tailed Student's *t*-Test; ****= p≤0.0001; ***= p≤0.001.

B. Native BrdU tracts after control (-) or Polθ/RPA siRNA (+) for 72 h. n ≥ 750 tracks from 3 biological replicates. Data are median. Statistical analysis performed using Mann-Whitney test. ****= p≤0.0001.

C. Western blot analysis of RPA70 protein levels following NTC (-) or RPA70 targeting siRNA treatment with concentrations indicated. Vinculin was used as a loading control.

4.3.6. RAD52 contributes to the toxicity of Polθ inhibition in USP48-depleted cells

Throughout our observations we noted that *Brca1*$^{+/+}$ *53bp1*$^{-/-}$ cells present reduced sensitivity to Polθ loss and inhibition compared to *Brca1*$^{C61G/C61G}$ *53bp1*$^{-/-}$ MEFs, yet *Brca1*$^{+/+}$ *53bp1*$^{-/-}$ cells show increased susceptibility to Polθ inhibition compared to WT cells that are *53bp1*$^{+/+}$ (Chapter 3, Fig.3.3A). In Fig.4.3C we also saw that low concentrations of the RAD52 inhibitor 6-OHD could alleviate cell toxicity to Polθ inhibition by ART558 in *Brca1*$^{+/+}$ *53bp1*$^{-/-}$ cells, whereas low doses of 6-OHD could not suppress ART558-mediated cell death in *Brca1*$^{C61G/C61G}$ *53bp1*$^{-/-}$ MEFs (Fig.4.3B). Accordingly, *Brca1*$^{+/+}$ *53bp1*$^{-/-}$ cells harbouring fully functional BRCA1 and not the C61G-BRCA1 protein, show RAD52-mediated sensitivity to ART558.

The loss of 53BP1 enhances BRCA1-dependent DNA end resection (Bunting et al., 2010), hence we wanted to decipher whether alternative conditions of dysregulated resection is a vulnerability accommodating the relationship between Polθ and RAD52. The DUB USP48 antagonises BRCA1/BARD1-mediated ubiquitination of H2A at the C-terminus (K125/127/129) (Uckelmann et al., 2018). That being so, the depletion of USP48 potentiates long-range extended resection, promoting RAD52-mediated SSA (Uckelmann et al., 2018). USP48 loss promotes 53BP1 re-positioning to the periphery of the break site via the activation of SMARCAD1 (Fig.4.7A) (Uckelmann et al., 2018; Densham et al., 2016). We used WT cells treated with siRNA targeting USP48 as a model of alternative resection. We noted that USP48-depleted WT MEFs showed cell

sensitivity to the Polθ inhibitor ART558 compared to WT cells treated with non-targeting control siRNA (Fig.4.7C). Therefore, these data suggest that the depletion of USP48 renders cells vulnerable to Polθ inhibition.

We showed that USP48-depleted cells are sensitive to Polθ inhibition so we wanted to find out whether this toxicity could be reduced by suppressing RAD52. We treated USP48-depleted WT cells with 30 μM ART558 and low concentrations of the RAD52 inhibitor 6-OHD (0.15 – 1.2 μM). We discovered that 1.2 μM of 6-OHD could rescue the sensitivity of USP48-depleted cells to Polθ inhibition (Fig.4.7D). The rescue dose of 1.2 μM 6-OHD was interestingly the same concentration required to reduce cell toxicity in ART558-treated *Brca1*$^{+/+}$ *53bp1*$^{-/-}$ cells (Fig.4.3C). These data highlight that RAD52 mediated toxicity from Polθ inhibition takes place in USP48-depleted cells which create a situation of irregular extended resection.

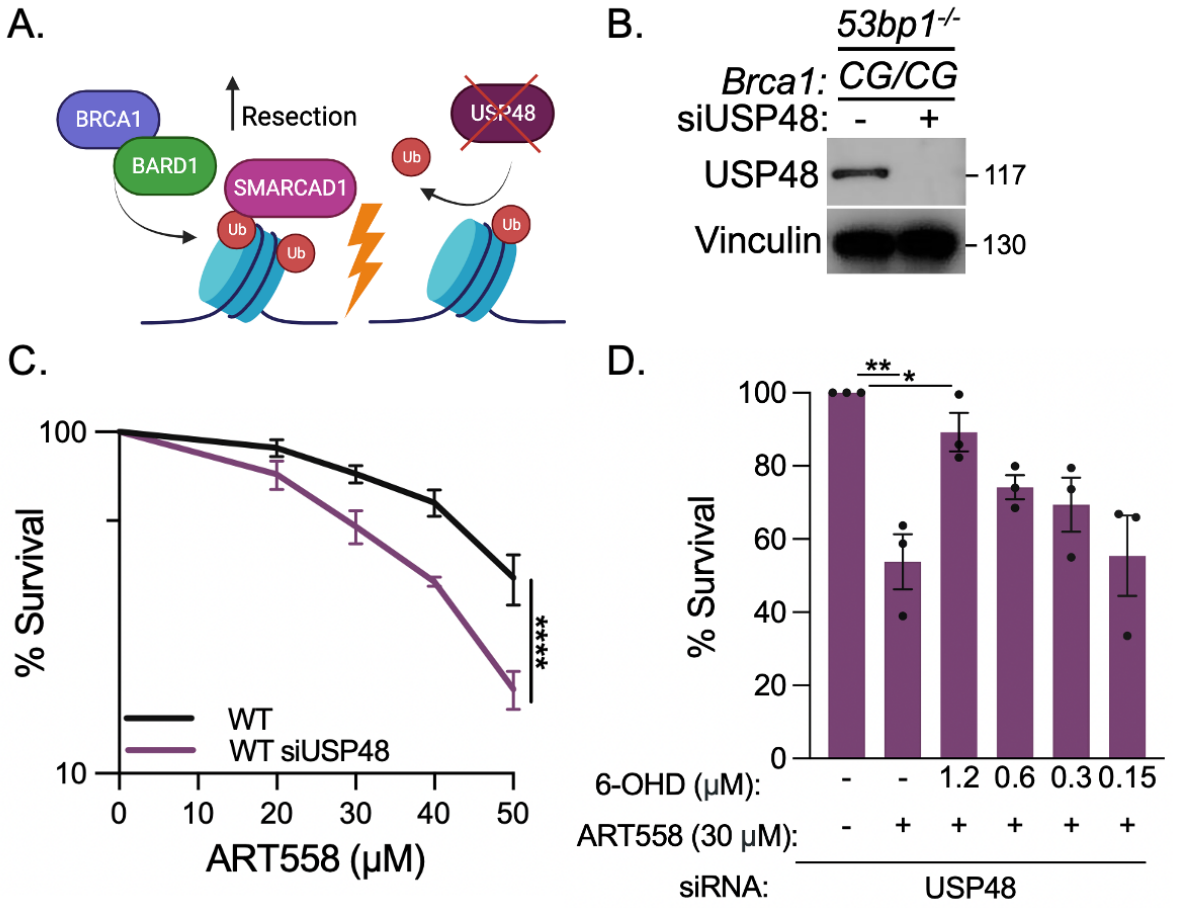

Figure 4.7. RAD52 contributes to the toxicity of Polθ inhibition in USP48-depleted cells.

A. Schematic showing that USP48 loss results in extended DNA end resection. Loss of USP48 leads to the unrestricted modification of H2A by BRCA1/BARD1 which increases SMARCAD1 nucleosome remodelling and elevated removal of 53BP1 from the break site. 53BP1 can no longer restrict end resection which increases RAD52-mediated single strand annealing (SSA).
B. Western blot analysis of USP48 protein levels following non-targeting control (−) or USP48 (+) targeting siRNA treatment. (Shown in *Brca1*$^{C61G/C61G}$ *53bp1*$^{-/-}$ MEFs instead of WT MEFs but confirms successful USP48 knockdown using siRNA targeting USP48).
C. Colony survival of WT cells treated with non-targeting control (NTC) or USP48 siRNA and increasing concentrations of the Polθ inhibitor ART558. n=3 biological repeats. Data are mean ± SEM. Statistical analyses performed using a two-way ANOVA; ****= p≤0.0001.
D. Colony survival of WT cells, treated with USP48 siRNA and 30 μM Polθ inhibitor ART558 with either DMSO or RAD52 inhibitor 6-OHD. n=3 biological repeats. Data are mean ± SEM. Statistical analyses performed using a two-tailed Student's *t*-Test; **= p≤0.01; *= p≤0.05.

4.3.7. Polθ prevents RAD52-mediated suppression of ssDNA gap filling in G2/M

So far, we have explained that Polθ acts to mitigate the toxic action of RAD52, however we have not identified the phenotype of interest for where this takes place. In Fig.4.5A we noted that although 0.15 μM of 6-OHD could rescue extended native BrdU lengths induced by Polθ loss in *Brca1*$^{C61G/C61G}$ *53bp1*$^{-/-}$ cells, 0.15 μM of 6-OHD alone stimulated extended ssDNA (Fig.4.5A). Therefore, increased ssDNA is not the feature modulating the relationship between RAD52 and Polθ in *Brca1*$^{C61G/C61G}$ *53bp1*$^{-/-}$ cells.

Previous findings have identified that Polθ-mediated TMEJ is prominent in G2/M and that *BRCA1/2*-deficient cells harbour MRE11-dependent ssDNA gaps in both S and G2, therefore we considered whether the relationship between Polθ and RAD52 acts in G2/M (Llorens-Agost et al., 2021; Carvajal-Garcia et al., 2021; Tirman et al., 2021b). Using the modified DNA fibre assay termed the PRR assay, we labelled nascent DNA with IdU for 1 hour, followed by treatment with nocodazole to arrest cells in G2/M and with the subsequent addition of CldU in the final 4 hours of nocodazole treatment (Tirman et al., 2021b). We counted the number of CldU dots, representing late DNA synthesis across IdU lengths, to calculate gap filling PRR events (Fig.4.8A) (Tirman et al., 2021b). First, we identified that WT cells depleted of BRCA1 showed a reduction in DNA synthesis fill-in events which has similarly been shown by others (Fig.4.8B) (Tirman et al., 2021b). Then we observed that *Brca1*$^{C61G/C61G}$ *53bp1*$^{-/-}$ cells exhibited reduced PRR density, which was depleted further upon treatment with siRNA to Polθ but could be rescued by co-treatment with 0.15 μM 6-OHD (Fig.4.8B), as seen in cell viability assays and SMART analysis. These results suggest that the suppression of RAD52 can rescue gap filling in Polθ-depleted *Brca1*$^{C61G/C61G}$ *53bp1*$^{-/-}$ cells.

Intriguingly, although reduced RAD52 could promote G2/M DNA synthesis fill-in in *Brca1*$^{C61G/C61G}$ *53bp1*$^{-/-}$ cells treated with Polθ siRNA, this was not the case in cells treated with the Polθ inhibitor ART558 (Ronson et al., 2023). *Brca1*$^{C61G/C61G}$ *53bp1*$^{-/-}$ cells treated with ART558 and low concentrations of the RAD52 inhibitor 6-OHD could not rescue cell survival (Fig.4.3B), nor promote G2/M DNA synthesis fill-in (Ronson et al., 2023). These data suggest that there is an alternative function with regards to Polθ polymerase inhibition compared to the loss of Polθ in *Brca1*$^{C61G/C61G}$ *53bp1*$^{-/-}$ cells.

Overall, we have shown that Polθ restricts the RAD52-mediated suppression of G2/M DNA synthesis gap fill-in.

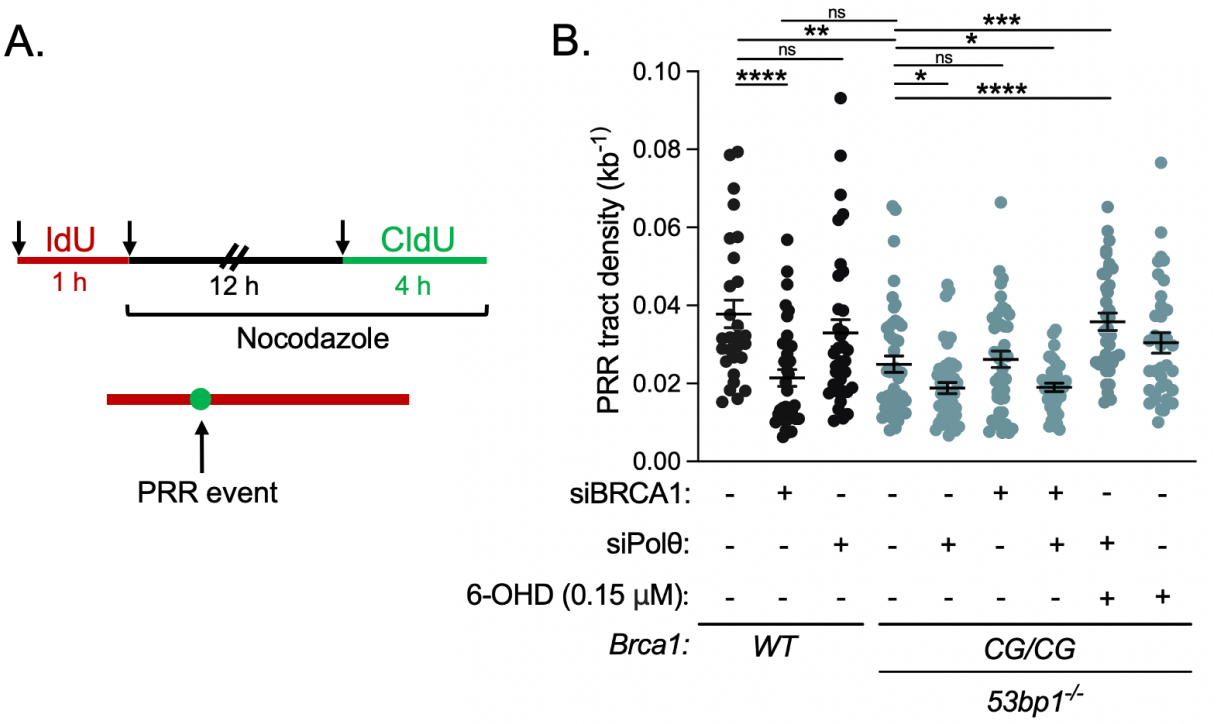

Figure 4.8. Polθ prevents RAD52-mediated suppression of ssDNA gap filling in G2/M.

A) Schematic showing the post-replicative repair (PRR) assay and an example of a PRR event (CldU) on DNA (IdU).

B) PRR assay in WT and *Brca1*$^{C61G/C61G}$ *53bp1*$^{-/-}$ cells treated with siRNA targeting BRCA1/Polθ or treated with the RAD52 inhibitor 6-OHD, n > 25 from 3 biological replicates. Data are mean ± SEM. Statistical analysis performed using a two-tailed Student's *t*-Test; ****= p≤0.0001; ***= p≤0.001; **= p≤0.01; *= p≤0.05; ns = not significant. (*With Katarzyna Starowicz).*

Taken together, we have identified that RAD52 is the factor modulating the toxicity created by Polθ depletion in *Brca1*$^{C61G/C61G}$ *53bp1*$^{-/-}$ cells, but also that RAD52 mediates the toxicity of Polθ inhibition in *Brca1*$^{+/+}$ *53bp1*$^{-/-}$ cells and USP48-depleted WT cells. RAD52 acts to suppress ssDNA gap filling and facilitates resection by promoting MRE11. Consequently, suppressing RAD52/RPA/MRE11 can alleviate the toxicities

associated with Polθ loss in *Brca1*$^{C61G/C61G}$ *53bp1*$^{-/-}$ cells. These data reveal the mechanism underlying the synthetic lethal relationship between *Brca1/53bp1* deficiencies and Polθ loss, and additionally demonstrates a genotype dependent context regarding Polθ inhibitor mechanisms.

4.4. Discussion

In summary, we have shown that *Brca1*$^{C61G/C61G}$ *53bp1*$^{-/-}$ cells rely on alternative DNA damage mechanisms involving proteins such as RNF168 and RAD52 for cell survival alongside the hypomorphic C61G-BRCA1 protein. More importantly, we revealed that Polθ depletion in *Brca1*$^{C61G/C61G}$ *53bp1*$^{-/-}$ cells resulted in elevated RAD52-mediated suppression of G2/M DNA synthesis gap fill-in. The suppression of RAD52 using the inhibitor 6-OHD could surprisingly limit toxic defects in Polθ-depleted *Brca1*$^{C61G/C61G}$ *53bp1*$^{-/-}$ cells such as preventing G2/M gap filling, cell death and extended ssDNA. Not only this but limiting the exonuclease activity of MRE11 and reducing RPA could equally improve cell viability and reduce excess ssDNA formation. However, low doses of RAD52 inhibition could no longer suppress ART558-mediated cell toxicity in *Brca1*$^{C61G/C61G}$ *53bp1*$^{-/-}$ cells but only in *Brca1*$^{+/+}$ *53bp1*$^{-/-}$ cells that harbour functional BRCA1. Therefore, a clear discrepancy between Polθ loss and inhibition can be seen between the different genotypes. We additionally noted that RAD52-mediated toxicity in the absence of Polθ takes place in alternative situations where resection is abnormally elongated, such as in cells depleted of USP48, generating BRCA1-dependent extended resection. Overall, our data show that the inappropriate engagement of RAD52 is detrimental to *Brca1*$^{C61G/C61G}$ *53bp1*$^{-/-}$ cells lacking Polθ and suppresses the fundamental ssDNA gap fill-in process during G2/M of the cell cycle.

Firstly, we wanted to determine whether RNF168 modulates the synthetic lethal relationship between Polθ and C61G-BRCA1. We identified that RNF168 is important for BARD1 foci formation and therefore the recruitment of BRCA1/BARD1 to sites of damage (Fig.4.1.B,C). Also, there was a significant reduction in BARD1 foci in *Brca1*$^{C61G/C61G}$ *53bp1*$^{-/-}$ cells compared to *Brca1*$^{+/+}$ *53bp1*$^{-/-}$ cells (Fig.4.1.B,C). Likewise, Krais *et al* (2021) revealed that RNF168-mediated BRCA1/BARD1 foci formation is reliant on the RING domain (Krais et al., 2021). Others have also shown that RNF168 loss reduces BRCA1 focal accumulation (Doil et al., 2009; Stewart et al., 2009; Luijsterburg et al., 2017), yet there have been reports where RNF168 depletion makes little change to BRCA1 foci numbers (Zong et al., 2019; Muñoz et al., 2012). The discrepancies could be due to method of quantification, cell lines used or potentially because RNF8, upstream of RNF168, facilitates BRCA1-A recruitment via RAP80 (Sobhian et al., 2007; Stewart et al., 2009).

RNF168 functions within the ubiquitylation cascade recruiting proteins such as 53BP1 and BRCA1 surrounding DSBs prior to resection but also promotes PALB2 loading post-resection during HR independently of BRCA1 (Luijsterburg et al., 2017; Zong et al., 2019; Doil et al., 2009; Mattiroli et al., 2012; Stewart et al., 2009). In association with this, my lab colleague found that depleting RNF168 in our *Brca1*$^{C61G/C61G}$ *53bp1*$^{-/-}$ cells reduced the number of HR DNA repair products, reinforcing that the hypomorphic C61G-BRCA1 protein requires RNF168 to perform HR efficiently and support cell survival (Ronson et al., 2023). When initially determining whether RNF168 was behind the cell toxicity in *Brca1*$^{C61G/C61G}$ *53bp1*$^{-/-}$ cells depleted of Polθ, we used low levels of siRNA to RNF168 alongside Polθ siRNA and witnessed that cell viability could not be rescued unlike low levels of RAD52 siRNA or RAD52 inhibitor 6-OHD (Ronson et al.,

2023). However, we did see that reduced RNF168 could bring RAD51 foci levels back down in *Brca1*$^{C61G/C61G}$ *53bp1*$^{-/-}$ cells treated with siRNA targeting Polθ (Ronson et al., 2023). Therefore, it appears that RNF168 supports HR in our *Brca1*$^{C61G/C61G}$ *53bp1*$^{-/-}$ cells but is not driving toxic defects due to Polθ loss.

The loss of Polθ and RAD52 are synthetic lethal in *BRCA1/2*-deficient cells, therefore complete inhibition of RAD52 results in cell death in *Brca1*$^{C61G/C61G}$ *53bp1*$^{-/-}$ cells, linking with the non-canonical requirement for RAD52 to support HR and SSA in HR-defective cells (Reddy et al., 1997; Ma et al., 2017b). Our data highlighted that RAD52 is the driver of cellular defects witnessed in Polθ-depleted *Brca1*$^{C61G/C61G}$ *53bp1*$^{-/-}$ cells, such as cell death, extended ssDNA and preventing G2/M DNA synthesis gap fill-in. We found that our C61G-BRCA1-mutated cells required the non-canonical support of RAD52 to support cell survival (Fig.4.2A), linking with work from my lab colleague demonstrating that RAD52 loss reduces HR efficiency in our *Brca1*$^{C61G/C61G}$ *53bp1*$^{-/-}$ cells (Ronson et al., 2023). Not only are our cells reliant on RAD52 for survival, but the loss of Polθ led to an accumulation of RAD52 (Fig.4.2D). Therefore, we deemed it possible that this increase in RAD52 is what is mediating cell toxicity in Polθ-depleted *Brca1*$^{C61G/C61G}$ *53bp1*$^{-/-}$ cells. Our data showed that reducing RAD52 concentrations in the absence of Polθ rescued cell viability, limited native BrdU lengths and restored PRR density in *Brca1*$^{C61G/C61G}$ *53bp1*$^{-/-}$ cells. The RAD52 inhibitor 6-OHD could have off-target effects, therefore we titrated RAD52 siRNA and confirmed that we could still rescue Polθ-depleted toxicity (Ronson et al., 2023). Taken together, it appears that Polθ restricts the toxic activity mediated by RAD52 accrual. In Ronson *et al* (2023), we demonstrated that in *Brca1*$^{+/+}$ *53bp1*$^{-/-}$ cells, neither the Polθ inhibitor nor Polθ itself are required for gap filling in G2/M, because they can be overcome by suppressing RAD52,

but that Polθ is fundamental for preventing the RAD52-mediated toxicity limiting functional PRR (Ronson et al., 2023). Tirman *et al* (2021) revealed that gap filling in G2/M is performed by the TLS polymerases REV1-POLζ stimulated by the mono-ubiquitination of PCNA by RAD18 (Tirman et al., 2021b). We have shown that Polθ, BRCA1 and resection limiters (MRE11/RPA) appear to restrict the inappropriate function of RAD52, and Llorens-Agost *et al* (2021) depicted a reversed relationship to us which is likely the other side to what we are seeing. They showed that Polθ-mediated TMEJ repair is regulated by RAD52, by preventing deregulated premature function of Polθ in S and G2 prior to mitosis in BRCA2 mutated cells (Llorens-Agost et al., 2021).

It has been proposed that MRE11 is essential for the processing of ssDNA gaps and that in *BRCA1/2*-deficient cells, the deregulated increase in MRE11-dependent nuclease digestion leads to elevated ssDNA gap accumulation and cell death (Tirman et al., 2021b; Dhoonmoon et al., 2022). Dias *et al* (2021) showed that *BRCA1*$^{-/-}$*53BP1*$^{-/-}$ cells exposed to PARPi depleted of Ligase III mediates the generation of MRE11-dependent ssDNA gaps so can enhance the efficacy of PARPi in the clinic (Paes Dias et al., 2021). Therefore, double deficient *BRCA1*$^{-/-}$*53BP1*$^{-/-}$ cells rely on Ligase III to suppress PARPi-induced ssDNA gaps (Paes Dias et al., 2021). Mann *et al* (2022) highlighted that the MRE11-NBS1-CtIP endonuclease cleaves ssDNA gaps left unprotected in the absence of Polθ, resulting in asymmetric single-ended DSBs (Mann et al., 2022; Belan et al., 2022; Schrempf et al., 2022). MRE11 extends ssDNA gaps bidirectionally in the 3’ to 5’ direction, which is typically suppressed by the action of BRCA1/2, subsequently leading to ssDNA gap cleavage by the endonuclease function of MRE11 forming DSBs (Hale et al., 2023). Our work suggests that MRE11 functions

downstream of RAD52, so if RAD52 is necessary for suppressing gap fill-in G2/M ssDNA gaps this is likely performed via the promotion of MRE11-dependent processing of ssDNA gaps (Ronson et al., 2023). In agreement with Tirman *et al* (2021) who showed that inhibiting the exonuclease activity of MRE11 can restore gap filling in S and G2 phase, with MRE11 activity usually being prevented by BRCA1/2 (Tirman et al., 2021b). Therefore, potentially in the absence of functional BRCA1/2 proteins, Polθ functions to prevent the RAD52-mediated action of MRE11, thus counteracting effective PRR activity.

Moreover, the activity of RAD52 has been shown to take place in complex with RPA (Park et al., 1996; Jackson et al., 2002; Deng et al., 2009), so both the RAD52-RPA complex and MRE11:ssDNA are necessary for RAD52-mediated toxicity in Polθ-depleted *Brca1*$^{C61G/C61G}$ *53bp1*$^{-/-}$ cells. As the helicase domain of Polθ removes RPA from ssDNA (Mateos-Gomez et al., 2017), it is possible that Polθ acts to remove the RAD52-RPA complex, however when Polθ is depleted, the RAD52-RPA complex accumulates in *Brca1*$^{C61G/C61G}$ *53bp1*$^{-/-}$ cells. Accordingly, we witnessed that depleting RPA limited extended ssDNA, likely because RPA stimulates nuclease activities, so we speculate that the association of RAD52 with RPA could further encourage the action of nucleases (Nimonkar et al., 2011; Chen et al., 2013). On that account, we cannot discount the possibility that RAD52 facilitates additional nucleases such as EXO1 or DNA2 or that reduced resection is the reason behind the suppression of RAD52 limiting MRE11 localisation.

In keeping with this, RPA hyperphosphorylation promotes the interaction between RAD52 and RAD51 to perform BRCA1/2-independent HR, and RAD51 has been shown to be essential for preventing ssDNA gaps by gap filling during S-phase (Carley

et al., 2022; Tirman et al., 2021b). Therefore, is it possible that RAD52 could be interacting with RAD51 to prevent RAD51-mediated ssDNA gap filling (Adar et al., 2009; Piberger et al., 2020; Tirman et al., 2021b). Yet, Tirman *et al* (2021) demonstrated that inactivating RAD51 did not impact gap filling during G2 only during S-phase, but could it be that RAD52 is already suppressing RAD51-mediated gap filling in G2/M. As it appears that the predominant factors facilitating gap filling during G2/M appear to be REV1-POLζ; we speculate that RAD52 prevents REV1-POLζ-mediated gap filling, yet the mechanism for this remains unclear. Additionally, it is possible that increased RAD52-RPA-ssDNA could lead to toxic recombination intermediates because reducing RAD52 limited Polθ-mediated accumulation of RAD51 (Ronson et al., 2023). Zhou *et al* (2021) also noted that inhibiting Polθ using Novobiocin led to elevated ssDNA intermediates and aberrant and non-functional RAD51 (Zhou et al., 2021). The loss of Polθ generated more micronuclei and DSBs, therefore it's likely that these DSBs are carried into G2/M of the cell cycle to be repaired by Polθ-mediated TMEJ, however depleting Polθ removes this possibility resulting in cell death (Llorens-Agost et al., 2021; Carvajal-Garcia et al., 2021; Gelot et al., 2023).

We observed a genotype-dependent rescue of Polθ inhibition by ART558 when suppressing RAD52, as *Brca1*$^{+/+}$ *53bp1*$^{-/-}$ cells treated with ART558 co-treated with low doses of the RAD52 inhibitor 6-OHD rescued cell viability however this was not the case in *Brca1*$^{C61G/C61G}$ *53bp1*$^{-/-}$ cells Fig.4.3. Work carried out by Zatreanu *et al* (2021) highlighted the possibility that ART558 is "trapped" onto DNA as treatment with ART558 in U2OS Flp-In Trex cells led to increased yellow fluorescent protein-tagged Polθ residence time at sites of laser-induced DNA damage (Zatreanu et al., 2021). In *Brca1*$^{+/+}$ *53bp1*$^{-/-}$ cells, low doses of RAD52 inhibition could alleviate defects in cell

survival, and G2/M DNA synthesis gap fill-in which was not the case in *Brca1*$^{C61G/C61G}$ *53bp1*$^{-/-}$ cells. These data imply that Polθ is engaged differently in cells with and without functional BRCA1.

We used WT cells depleted of USP48 to create a model of dysregulated resection and found increased sensitivity to the Polθ inhibitor ART558 (Fig.4.7C). ART558-mediated toxicity could be overcome by RAD52 suppression in WT cells depleted of USP48 which was also seen in *Brca1*$^{+/+}$ *53bp1*$^{-/-}$ cells but could not be replicated in *Brca1*$^{C61G/C61G}$ *53bp1*$^{-/-}$ cells further enhancing that the engagement of the Polθ inhibitor differs between cells with and without proficient BRCA1 function. Additionally, Zatreanu *et al* (2021) showed that Shieldin-deficient cancers are susceptible to Polθ inhibition unlike PARPi (Zatreanu et al., 2021). Therefore, it appears that abnormal resection encourages the engagement and reliance on Polθ, making Polθ targeting an effective treatment for HR and Shieldin/53BP1-deficient cancers. However, we should measure ssDNA lengths in WT cells depleted of USP48 treated with ART558. In future it would be interesting to use an alternative model of extended resection such as depleting REV7 and then determining whether these cells are sensitive to ART558 treatment and if this is the case, whether cell sensitivity can be reversed by suppressing RAD52-mediated toxicity.

In summary, we have demonstrated that *Brca1*$^{C61G/C61G}$ *53bp1*$^{-/-}$ cells are reliant on the non-canonical support of RNF168 and RAD52 to facilitate functional HR. Additionally, the loss of Polθ led to toxic accumulations of RAD52 which could be overcome by low doses of the RAD52 inhibitor 6-OHD. Yet, this toxicity could not be overcome in the context of Polθ inhibition by ART558 in *Brca1*$^{C61G/C61G}$ *53bp1*$^{-/-}$ cells but cell viability could be restored in *Brca1*$^{+/+}$ *53bp1*$^{-/-}$ cells that harbour the functional BRCA1 protein.

Other features of Polθ depleted toxicity could be overcome in *Brca1*$^{C61G/C61G}$ *53bp1*$^{-/-}$ cells, such as the reduction in extended native BrdU lengths and cell survival when reducing MRE11, RPA and RAD52. The exogenous expression of BARD1 and BRC4-RPA could curtail the toxicity that depleting RAD52 entirely can have on *Brca1*$^{C61G/C61G}$ *53bp1*$^{-/-}$ cells. Also, in the context of alternative extended resection generated by the depletion of USP48 in WT cells, ART558-mediated sensitivity could be reversed by low concentrations of RAD52 inhibition. Overall, we outline that RAD52 increases cell toxicity in the absence of Polθ in situations of abnormal resection, and supported by our recent publication that this is done by RAD52-mediated suppression of ssDNA gap filling in G2/M when Polθ is absent in *Brca1*$^{C61G/C61G}$ *53bp1*$^{-/-}$ cells (Fig.4.9).

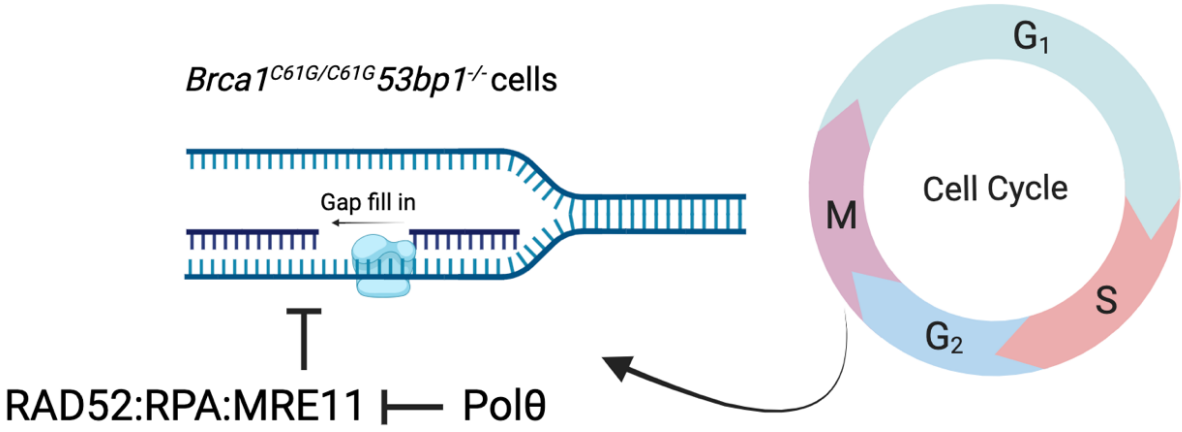

Figure 4.9. Working model: Polθ suppresses RAD52-facilitated toxicity in *Brca1*$^{C61G/C61G}$ *53bp1*$^{-/-}$ cells. RAD52 suppresses ssDNA DNA synthesis gap fill-in when Polθ is lost in *Brca1*$^{C61G/C61G}$ *53bp1*$^{-/-}$ cells. RAD52 promotes the formation of the RAD52-RPA complex and the association between MRE11:ssDNA to contribute to the toxicity of *Brca1*$^{C61G/C61G}$ *53bp1*$^{-/-}$ cells devoid of Polθ. Suppressing the action of RAD52:RPA:MRE11 can improve cell viability in the absence of Polθ in *Brca1*$^{C61G/C61G}$ *53bp1*$^{-/-}$ cells. Created using *BioRender.com.*

5. Characterisation of the R93E-Bard1 mutation

5.1. Introduction

We have discussed in depth the relationship between *Brca1/53bp1* deficiencies and Polθ loss and have revealed RAD52 as the driver of cell toxicity in our murine *Brca1*$^{C61G/C61G}$ *53bp1*$^{-/-}$ cell model depleted of Polθ. Now we want to further investigate the role of the BRCA1/BARD1 N-terminal RING domains, specifically regarding their E3 ubiquitin ligase function. BRCA1/BARD1 is a RING-type E3 ubiquitin ligase that was found to promote heterochromatin-mediated silencing of α-satellite DNA, which created a link between BRCA1/BARD1 ligase function, nucleosomal histone H2A, and the regulation of chromatin (Zhu et al., 2011; Witus et al., 2022). Subsequently, BRCA1/BARD1 was identified to specifically target H2A on the unstructured extreme C-terminal tail at K125/127/129 *in vitro* and *in vivo* (Kalb et al., 2014). BRCA1/BARD1 has also been found to ubiquitinate H2A isoforms, such as the histone variant MacroH2A1 (Kim et al., 2017a). Missense mutations associated with familial breast cancer have been identified within the RING domain of BARD1 that do not disrupt BRCA1/BARD1 heterodimer stability but have a reduced ability to bind to nucleosomes and modify H2A (Stewart et al., 2018; Morris et al., 2006). However, the association between BRCA1/BARD1 E3 ubiquitin ligase activity and tumour suppression remains controversial.

The ubiquitination of H2A by BRCA1/BARD1 has been implicated in the transcriptional regulation of oestrogen metabolism, which is abrogated in breast and ovarian cancers (Samavat and Kurzer, 2015; Mungenast and Thalhammer, 2014). BRCA1/BARD1-mediated ubiquitination of H2A has also been found to facilitate HR and DNA end

resection by recruiting the chromatin remodeller SMARCAD1 to displace 53BP1 from DSB sites (Densham et al., 2016). In addition, Sherker *et al* (2021) revealed that RAP80 functions redundantly alongside the BRCA1 N-terminal RING domain to promote recruitment of the BRCA1/BARD1 heterodimer to sites of damage (Sherker et al., 2021). The recruitment of the heterodimer to damage is complex and requires both recruitment by RAP80 and ABRAXAS to localise the BRCA1-A complex as well as the recognition of H2AK15-Ub by the BUDR domain of BARD1 (Sherker et al., 2021; Panagopoulos and Altmeyer, 2021). Sherker *et al* (2021) showed that *RAP80*-deficient cells were reliant on the N-terminal RING domain of BRCA1 for BRCA1/BARD1 recruitment as cells harbouring the I26A mutation, that disrupts its interaction with E2 enzymes, along with disrupted RAP80-mediated recruitment could no longer be localised to sites of damage, becoming sensitised to Olaparib (Sherker et al., 2021; Panagopoulos and Altmeyer, 2021).

However, several studies have shown results that do not associate E3 ligase activity with a role in HR (Nakamura et al., 2019; Krais et al., 2021). Originally, the I26A-*Brca1*-mutated mouse model, designed to be “ligase dead”, did not determine a correlation between E3 ligase activity and tumour suppression (Reid et al., 2008; Shakya et al., 2011). However, I26A-BRCA1 still retains a significant proportion of its E3 ligase activity and so the association between ligase activity and tumour prevention cannot be discounted (Stewart et al., 2017; Pruneda et al., 2012) Therefore, further investigation into whether there is an association between the BRCA1/BARD1 mediated ubiquitination of H2A and tumour suppression remains paramount.

More recently, a completely ligase-null triple BRCA1 mutant I26A/L63A plus the allosteric linchpin residue K65A (I26A/L63A/K65A) has been reported to entirely

abolish E3 ubiquitin ligase activity by removing its interaction with all of the E2 enzymes that associate with BRCA1 (Stewart et al., 2017; Wang et al., 2023). Wang *et al* (2023) suggest that BRCA1/BARD1 ligase activity facilitates an important role in the DNA damage response, promoting DNA end resection and facilitating late steps in HR (Wang et al., 2023). However, these results do not fully answer whether E3 ligase activity is required for tumour suppression. Interestingly, a pre-print by Salas-Lloret *et al* (2023) used a methodology termed Targets of Ubiquitin Ligases Identified by Proteomics (TULIP) for the revelation of E3-specific ubiquitination substrates and identified PCNA as a BRCA1/BARD1 specific substrate (Salas-Lloret et al., 2019, 2023). They suggested that BRCA1/BARD1 ubiquitinates PCNA in unperturbed conditions to prevent ssDNA gap accumulation, whereas the E3 ligase RAD18 performs PCNA ubiquitination in the presence of replication stress (Salas-Lloret et al., 2023). Similarly, Tian *et al* (2013) noted that MEFs expressing the I26A-BRCA1 mutation, an E3 ligase disruptive mutant, suppressed RAD18 foci formation and binding to chromatin, suggesting that BRCA1 has a role in DDT and TLS (Tian et al., 2013). Nonetheless, it should be noted that these two studies used the controversially debated I26A-BRCA1 mutation and should be taken with caution.

In more detail, our group carried out a mutational scan across BARD1 to identify a ubiquitin binding interface and revealed that substituting residue R99 to a glutamic acid (E) significantly reduced the interaction between the BRCA1/BARD1 heterodimer and the ubiquitin conjugating enzymes within the UBE2D family, whilst maintaining the interaction between BRCA1 and BARD1 (Densham et al., 2016). Whereas, substituting the R99 residue to a lysine (K) maintained a substantial interaction with conjugation proficient E2. Densham *et al* (2016) identified that R99-BARD1 is in contact with

ubiquitin and is in close proximity to the D32 side chain of ubiquitin (Densham et al., 2016; Densham and Morris, 2017). A D32R mutation was created within ubiquitin, and we discovered that the E3 ligase activity of the R99E-BARD1 mutant could be significantly improved, indicating that the contact between R99-BARD1 and ubiquitin is necessary for its catalytic activity. R99-BARD1 was shown to promote ubiquitin discharge from the E2 enzyme in contact with BRCA1 and for facilitating the interaction between the heterodimer and the ubiquitin~E2 thioester conjugate (Densham et al., 2016). HeLa cells expressing siRNA resistant R99E-BARD1 were sensitive to Olaparib, IR, camptothecin and etoposide but were resistant to the ICL agent cisplatin and the replication stress inducing agents HU and aphidicolin. BRCA1/BARD1-mediated modification of H2A was shown to promote DNA end resection and reposition 53BP1 by the chromatin remodeller SMARCAD1 via its ubiquitin-binding CUE domains (Densham et al., 2016; Densham and Morris, 2017).

In the following chapter we want to uncover more about the role for E3 ubiquitin ligase activity using a murine model system. We created a mouse model containing the R93E mutation (R99E in humans) to produce *Bard1*$^{R93E/R93E}$ mice and subsequently *Bard1*$^{R93E/R93E}$ immortalised MEFs. In this chapter we will begin to characterise the *R93E-Bard1* mutation and determine whether the mouse model could help elucidate the role of BRCA1/BARD1 E3 ubiquitin ligase.

5.2. Results

5.2.1. H2A ubiquitination is reduced in *Bard1*$^{R93E/R93E}$ cells

We generated *Bard1*$^{R93E/R93E}$ mice that were born at expected Mendelian ratios and did not require the loss of *53bp1* for embryonic development, unlike our *Brca1*$^{C61G/C61G}$

mutant mouse model (Fig.5.1A). Subsequently we derived *Bard1*$^{R93E/R93E}$ MEFs that were immortalised by SV40 large T antigen that we used for our study. Firstly, we wanted to determine whether BRCA1/BARD1 protein expression levels were altered in our *Bard1*$^{R93E/R93E}$ MEFs and discovered that there appeared to be no alteration to BRCA1 or BARD1 expression levels when comparing *Bard1*$^{+/+}$ (WT), *Bard1*$^{R93E/+}$ *(RE/+)* or *Bard1*$^{R93E/R93E}$ *(RE/RE)* MEFs (Fig.5.1B). However, more work will need to be done to evaluate the stability of the BRCA1/BARD1 heterodimer in *Bard1*$^{R93E/R93E}$ MEFs.

The BRCA1/BARD1 ubiquitination site on the C-terminal tail of H2A at K125/127/129 is well-established (Fig.5.1C) (Kalb et al., 2014; Nakamura et al., 2019; Becker et al., 2021; Densham et al., 2016). So, we wanted to assess the impact of the R93E mutation on overall ubiquityl-H2A at the C-terminus using the E6C5 H2A-Ub antibody. We compared H2A-Ub expression levels across our three genotypes. We determined that H2A-Ub is reduced more than 2-fold in our *Bard1*$^{R93E/R93E}$ MEFs compared to WT cells, with a larger reduction compared to *Bard1*$^{R93E/+}$ MEFs (Fig.5.1D). It appears that H2A ubiquitination is reduced in both heterozygous and homozygous MEFs, with a dramatic reduction in the *Bard1*$^{R93E/R93E}$ cells. Overall using western blot analysis, it appears that the *Bard1*$^{R93E/R93E}$ MEFs exhibit unimpacted BRCA1/BARD1 expression levels, albeit reduced H2A ubiquitination. These results corroborate with previous studies on the human R99E-BARD1 mutation showing that BRCA1/BARD1 heterodimer stability is maintained whilst E3 ubiquitin ligase activity is defective (Densham et al., 2016).

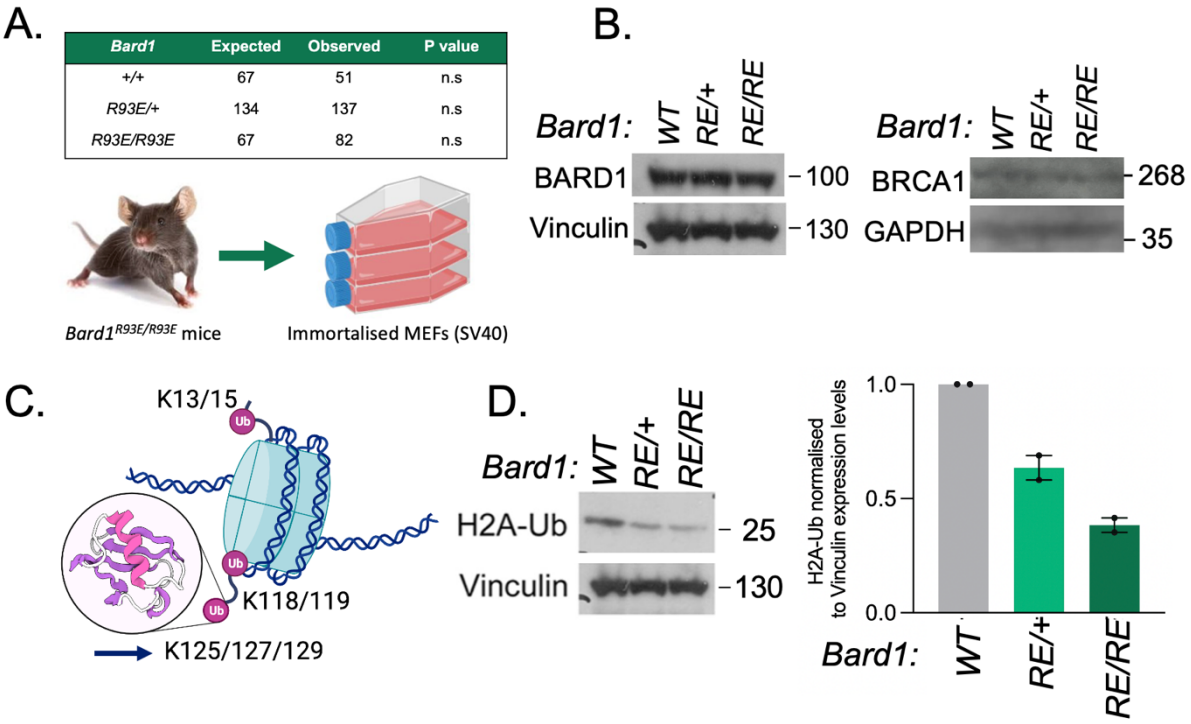

Figure 5.1. *Bard1*$^{R93E/R93E}$ MEFs exhibit unimpacted BRCA1/BARD1 expression and reduced H2A mono-ubiquitination.

A. The genotypes indicated were inter-crossed demonstrating the expected and observed numbers. A schematic showing the generation of SV40-generated immortalised MEFs from *Bard1*$^{R93E/R93E}$ mice.

B. Western blots of BARD1 and BRCA1 protein levels in the genotypes shown. Vinculin was used as a loading control for BARD1 and GAPDH as a loading control for BRCA1.

C. Sites of H2A ubiquitination by E3 ubiquitin ligases modifying H2A at lysine residues K13/15 (RNF168), K118/119 (RING1-BMI1), K125/127/129 (BRCA1/BARD1). Protein structure of ubiquitin is highlighted.

D. Western blot of H2A-Ub (E6C5 clone) and quantification of H2A-Ub normalised to vinculin expression levels (n=2 exposures).

5.2.2. *Bard1*$^{R93E/R93E}$ cells show proficient homologous recombination

Next, we wanted to shed light on whether *Bard1*$^{R93E/R93E}$ cells can form BARD1 foci and so whether recruitment is maintained. Figure 5.2A demonstrates that there was no significant difference in the number of BARD1 foci formed between WT and *Bard1*$^{R93E/R93E}$ cells (Fig.5.2A). To determine whether *Bard1*$^{R93E/R93E}$ cells show proficient HR, we looked at RAD51 foci generation, a marker for HR, as well as Olaparib sensitivity. We noted that RAD51 foci numbers did not change between WT and *Bard1*$^{R93E/R93E}$ cells (Fig.5.2B) and we identified that *Bard1*$^{R93E/R93E}$ cells were resistant to the PARPi Olaparib like that of WT cells (Fig.5.2C). So far, these data indicate that *Bard1*$^{R93E/R93E}$ cells show features of competent HR.

Therefore, my lab colleague measured HR proficiency using semi-quantitative PCR to measure HR outcome frequency, like that performed in Chapter 3 (Fig.3.1E). We noted that the HR-specific PCR products generated by both WT and *Bard1*$^{R93E/R93E}$ cells showed a similar HR frequency (Fig.5.2D). Overall, our data showed that *Bard1*$^{R93E/R93E}$ cells have functional BARD1 and RAD51 foci formation, proficient HR, unimpacted BRCA1/BARD1 protein expression but lowered H2A ubiquitination. So far, it appears that our *R93E-Bard1* mutant does not disrupt DSB repair by HR, nor does it disrupt the expression levels or localisation of BRCA1/BARD1. The only phenotype we have witnessed thus far is a reduction in H2A-ubiquitination. Nonetheless, a further investigation is required to confirm that these phenotypes are robust.

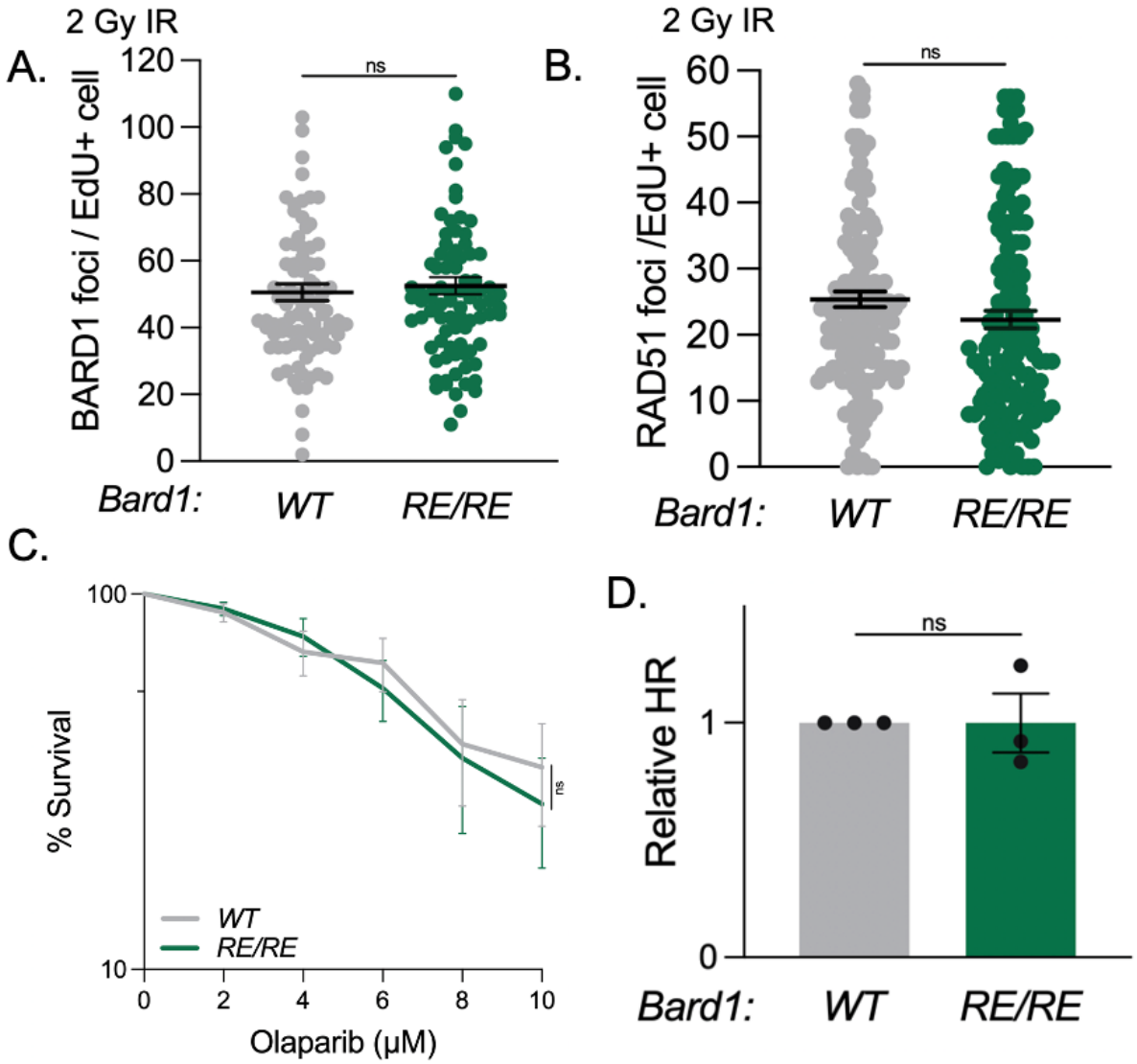

Figure 5.2. *Bard1*$^{R93E/R93E}$ cells appear proficient in homologous recombination.

A. Quantification of BARD1 foci 3 hr after 2 Gy IR in WT and *Bard1*$^{R93E/R93E}$ cells. N=90 cells from 3 biological replicates per condition. Statistical analysis performed using a two-tailed Student's *t*-Test; ns = not significant.

B. Quantification of RAD51 foci 3 hr after 2 Gy IR in WT and *Bard1*$^{R93E/R93E}$ cells. N=150 cells from 3 biological replicates per condition. Statistical analysis performed using a two-tailed Student's *t*-Test; ns = not significant.

C. Colony survival in MEFs of genotypes shown, treated with a dose range of Olaparib. MEFs were plated 24 hr prior to transfection, treated with Olaparib (2 – 10 μM) for 72 hours and re-plated into colonies and grown out for 7 days. N=5. Data are mean ± SEM. Statistical analysis performed using a two-way ANOVA; ns = not significant.

D. Relative PCR product intensity of HR-specific product in WT and *Bard1*$^{R93E/R93E}$ cells. n=3. Data are mean ± SEM. *George Ronson.*

5.2.3. The loss of RAP80 reduces BARD1 foci formation and sensitises *Bard1*$^{R93E/R93E}$ cells to Olaparib

Sherker *et al* (2021) revealed that RAP80 functions redundantly with the BRCA1 RING domain to localise BRCA1 to DNA damage sites. Whereby disrupting the E3 ligase activity by the I26A-BRCA1 mutation, in the absence of RAP80, could no longer promote BRCA1 recruitment to damage (Fig.5.3A) (Sherker et al., 2021). These data led us to question whether *Bard1*$^{R93E/R93E}$ cells can only maintain BRCA1/BARD1 recruitment via the RAP80-ABRAXAS axis, and whether depleting RAP80 could not only abrogate recruitment and BARD1 foci accrual but sensitise *Bard1*$^{R93E/R93E}$ cells to Olaparib.

We revisited the ability of *Bard1*$^{R93E/R93E}$ cells to form BARD1 foci, but now in the presence and absence of RAP80 (Fig.5.3C,D). We witnessed that BARD1 foci accumulation does not differ between WT and *Bard1*$^{R93E/R93E}$ cells (Fig.5.3C,D). Yet, when treated with siRNA to RAP80 we noted that our WT MEFs elicited no significant difference in BARD1 foci between RAP80 proficient or depleted cells (Fig.5.3C,D). Interestingly, and in line with data from Sherker *et al* (2021) we identified that *Bard1*$^{R93E/R93E}$ cells depleted of RAP80 formed fewer IR-induced BARD1 foci from an average of 53 foci per EdU+ cell in MEFs treated with the non-targeting control (NTC) to a mean of 35 foci per EdU+ cell in those devoid of RAP80 (Fig.5.3C,D). These data indicate that R93-BARD1 within the RING domain could be important for BARD1 foci formation in the absence of RAP80 and that the RING domain functions redundantly with RAP80 in the context of BARD1 damage localisation.

Additionally, we subjected *Bard1*$^{R93E/R93E}$ cells to Olaparib treatment and noted that the previously resistant homozygous R93E MEFs became sensitised to the PARPi upon depletion of RAP80, whereas the WT MEFs remained resistant to Olaparib (Fig.5.3E). However, there was no difference between WT and *Bard1*$^{R93E/R93E}$ cells treated with NTC siRNA and increasing concentrations of Olaparib (Fig.5.3E). In summary, these results highlight that BARD1 foci and therefore recruitment of BARD1 could require two redundant pathways involving the BRCA1 BRCT-RAP80 interaction and the catalytic activity of the RING domain with its cognate E2 conjugating enzymes. These results open up the possibility that the interaction between BARD1 and ubiquitin is likely disrupted in *Bard1*$^{R93E/R93E}$ cells, and that the catalytic activity is somehow important for BRCA1/BARD1 recruitment, but the reasoning remains to be elucidated.

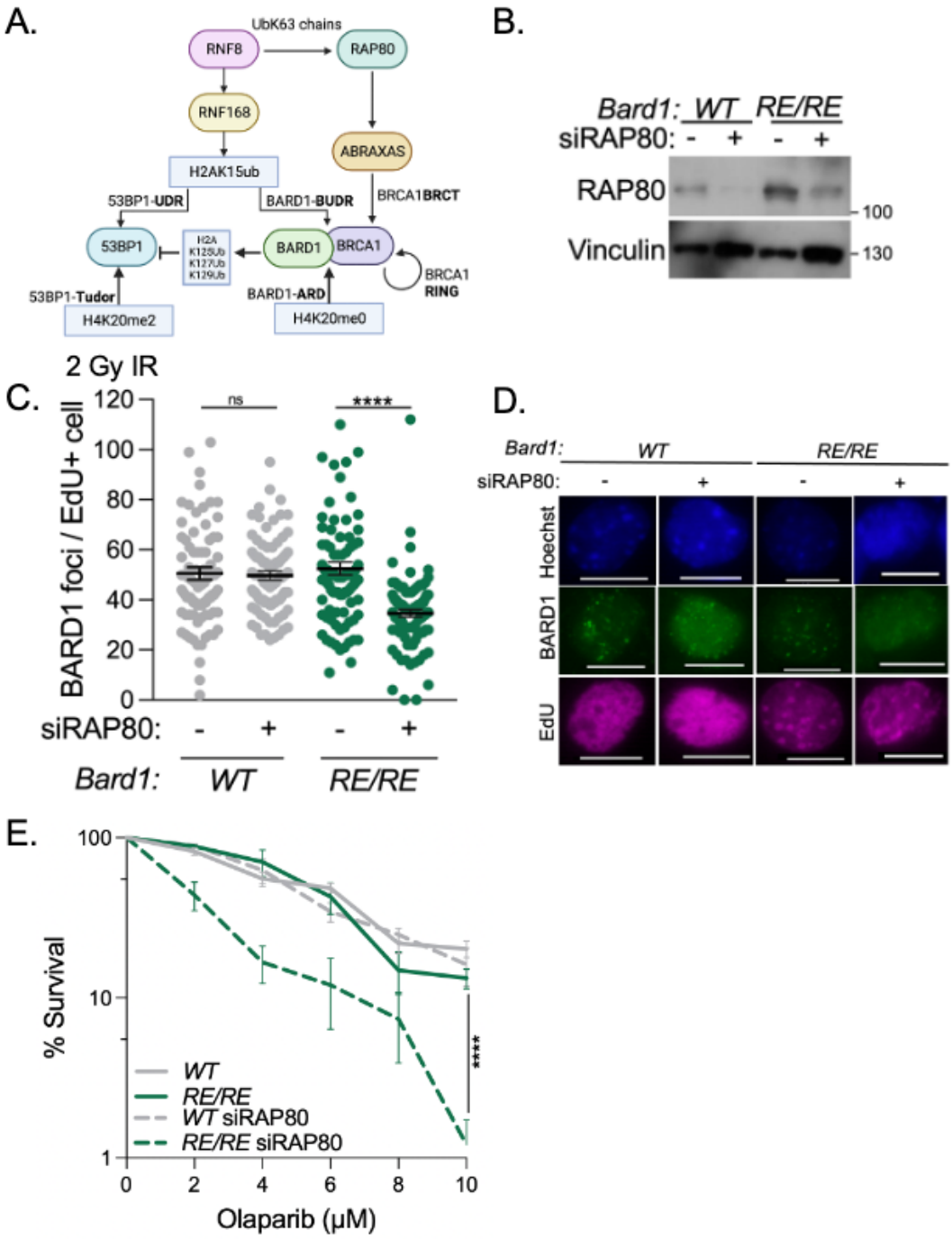

Figure 5.3. RAP80 acts redundantly in *Bard1*$^{R93E/R93E}$ cells to facilitate BRCA1/BARD1 recruitment.

A. Schematic of BRCA1 recruitment to DSBs via two redundant processes. The first pathway involves the recognition of RNF8-generated UbK63 chains by RAP80 which binds to the BRCT domain of BRCA1. The second mode is facilitated by the BUDR domain of BARD1 which recognises H2A-K13/15-Ub modified H4K20me0 nucleosomes. Based on Sherker *et al* (2021) and created using *BioRender.com*.

B. Western blot analysis of RAP80 expression levels treated with NTC (-) or RAP80 (+) siRNA and vinculin loading control.
C. Quantification of BARD1 foci 3 hr after 2 Gy IR in EdU + WT and *Bard1*$^{R93E/R93E}$ cells treated with siRNA targeting NTC (-) and RAP80 (+). N=90 cells from 3 biological replicates. Data are mean ± SEM. Statistical analysis performed using a two-tailed Student's *t*-Test; ****= p≤0.0001; ns = not significant.
D. Representative images of BARD1 foci 3 hr after 2 Gy IR in EdU + WT and *Bard1*$^{R93E/R93E}$ cells treated with siRNA targeting NTC (-) and RAP80 (+). Scale bar is 10 μm.
E. Colony survival in MEFs of genotypes shown, treated with a dose range of Olaparib following NTC (-) or RAP80 (+) targeting siRNA. MEFs were plated 24 hr prior to transfection, treated with Olaparib (2 – 10 μM) and NTC/RAP80 for 72 hr and re-plated into colonies and grown out for 7 days. N=3. Data are mean ± SEM. Statistical analysis performed using a two-way ANOVA; **** p≤0.0001.

5.2.4. *Bard1*$^{R93E/R93E}$ cells are resistant to HU but have increased replication fork velocity

So far, we have demonstrated that *Bard1*$^{R93E/R93E}$ MEFs are proficient in HR and are resistant to the PARPi Olaparib, in the presence of RAP80, and show reduced ubiquityl-H2A at the C-terminus. Schmid *et al* (2018) revealed that the mono-ubiquitination of H2A at K13/15 by RNF168 is necessary for efficient DNA replication during unperturbed S-phase (Schmid et al., 2018). On top of that, SMARCAD1, which binds to BRCA1/BARD1-mediated ubiquityl-H2A via its CUE domains, has been shown to have an HR-independent role in the maintenance of replication fork stability (Lo et al., 2021). Therefore, it is highly possible that the modification of H2A at K125/127/129 by BRCA1/BARD1 could have a role in DNA replication. So, we wanted to determine whether our *Bard1*$^{R93E/R93E}$ cells elicit proficient replication fork kinetics.

Firstly, we treated our cells with the ribonucleotide reductase inhibitor HU to deplete nucleotide pools and thus slow and stall replication forks. We noted that after treatment with HU for 16 hours prior to replating into colonies that there was little difference between WT and *Bard1*$^{R93E/R93E}$ MEFs (Fig.5.4A). We used WT cells subjected to siRNA to BRCA1 as a positive control and could see a sensitivity to HU treatment compared to WT and *Bard1*$^{R93E/R93E}$ cells (Fig.5.4A). However, there is a large margin of error surrounding these values due to the high toxicity that HU causes to cells and could require repetition with a shorter treatment or lower dose of HU to confirm these findings. Up to now, we can deduce that *Bard1*$^{R93E/R93E}$ cells are resistant to the replication stress agent HU.

BRCA1 is localised to ongoing and stalled replication forks with an important role in the protection of stalled replication forks from MRE11-dependent degradation by stabilising RAD51 (Hashimoto et al., 2010; Lomonosov et al., 2003; Schlacher et al., 2011, 2012; Sirbu et al., 2013). Consequently, we wanted to determine whether *Bard1*$^{R93E/R93E}$ cells harbour a replication fork protection defect. We pulse labelled both our WT and *Bard1*$^{R93E/R93E}$ cells with CldU for 20 minutes and IdU for 20 minutes followed by 5 mM HU treatment for 3 hours. We measured the ratio between the two labels and we witnessed that both WT and *Bard1*$^{R93E/R93E}$ cells elicited a ratio of almost 1 which is indicative of proficient fork protection (Fig.5.4B). It appears that *Bard1*$^{R93E/R93E}$ cells do not have a replication fork protection defect and so possibly the reduced ability to ubiquitinate H2A does not impact the ability of BRCA1/BARD1 to stabilise forks by RAD51 (Schlacher et al., 2012).

Subsequently, we used the DNA fibre assay to look at replication fork structures and dynamics in both the WT and *Bard1*$^{R93E/R93E}$ cells to determine whether there are

alternative replication dynamics between the MEFs. We pulse labelled our cells with the thymidine analogues CldU for 20 minutes followed by IdU for 20 minutes and visualised fork progression. The replication fork structures shown in Fig.5.4C, D reveal the different stages and processes of replication between WT and *Bard1*$^{R93E/R93E}$ cells (Fig.5.4C,D). We identified that there was no significant difference between WT and *Bard1*$^{R93E/R93E}$ cells when looking at ongoing forks, first and second label origins, and first and second label terminations, indicating that the stages of replication remain the same between the two cell lines (Fig.5.4D). Subsequently, we measured the rate of ongoing forks by analysing the lengths of IdU and CldU tracks to determine the speed of replication. Interestingly, *Bard1*$^{R93E/R93E}$ cells demonstrated significantly increased replication fork speeds compared to WT cells, with WT cells showing an average speed of 0.97 kb/min compared to 1.4 kb/min in *Bard1*$^{R93E/R93E}$ cells (Fig.5.4E, F).

An increase in fork speeds has been associated with elevated repriming by the primase-polymerase PRIMPOL in the presence of replication stress; but equally elevated fork speeds have been associated with defective fork reversal (Quinet et al., 2020; Bai et al., 2020; Mehta et al., 2022; Vujanovic et al., 2017). It remains unclear whether the enzymatic activity of BRCA1/BARD1 influences replisome associated processes but the unrestrained fork velocity in our *Bard1*$^{R93E/R93E}$ cells, designed to be ligase defective, has piqued our interest. That being the case, we wanted to investigate whether the elevated fork speeds are due to PRIMPOL-dependent repriming. Repriming is a DNA damage tolerance mechanism which authorises replication fork progression in the presence of replication barricades, whilst forming deleterious ssDNA gaps in the process (Piberger et al., 2020; Bai et al., 2020; Genois et al., 2021; Quinet et al., 2021; Kobayashi et al., 2016; Tirman et al., 2021a).

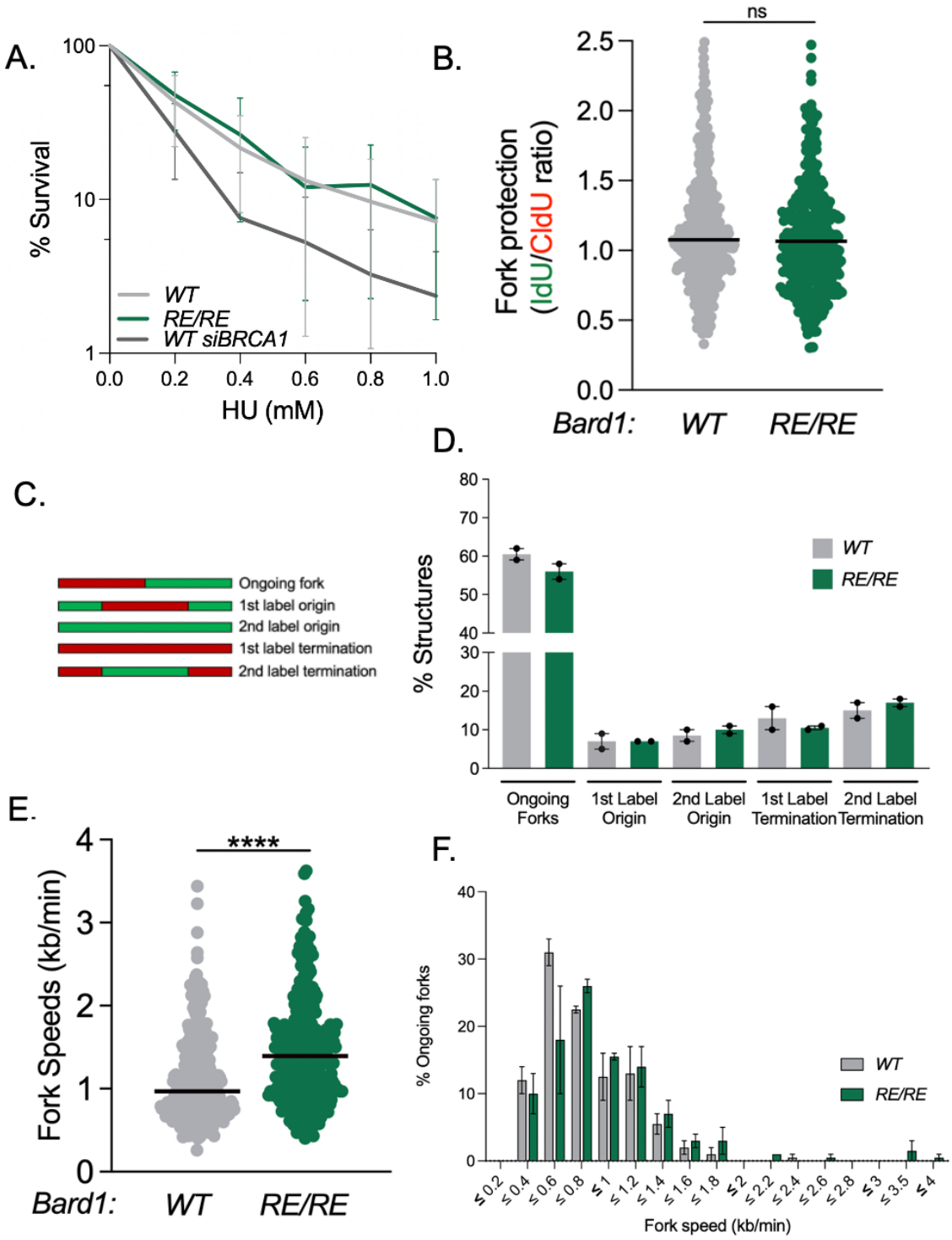

Figure 5.4. *Bard1*$^{R93E/R93E}$ cells have enhanced replication fork velocity.

A. Colony survival in MEFs of genotypes shown, treated with a dose range of HU. MEFs were plated 24 hr prior to transfection, treated HU for 16 hours and re-plated into colonies and grown out for 7 days. N=3. Data are mean ± SEM.

B. Fork protection fibres IdU/CldU ratios from WT and *Bard1*$^{R93E/R93E}$ cells. Cells treated with CldU and IdU for 20 mins and 5 mM HU for 3 hours prior to spreading. N ≥ 450 fibres from 4 biological replicates. Data are median. Statistical analysis was performed using a Mann–Whitney test; ns = not significant.
C. Schematic of replication fork structures. Ongoing fork, 1st label origin, 2nd label origin, 1st label termination, 2nd label termination.
D. Percentage of all DNA fibre structures compared between WT and *Bard1*$^{R93E/R93E}$ cells. Replication fork structures analysed included: ongoing fork, 1st label origin, 2nd label origin, 1st label termination, 2nd label termination.
E. DNA fibre speeds calculated by measuring CldU and IdU tract lengths of ongoing forks and determining the kb/min from the tract lengths. N ≥ 300 fibres from 2 biological replicates. Data are median. Statistical analysis was performed using a Mann–Whitney test; **** p≤0.0001.
F. Representative histogram of the percentage of ongoing forks. N ≥ 300 fibres from 2 biological replicates. Data are mean ± SEM.

5.2.5. *Bard1*$^{R93E/R93E}$ cells form PRIMPOL and SMUG1-dependent ssDNA gaps

Upon replication stress, ssDNA gaps can form and have been known to accumulate in *BRCA1/2*-deficient cells, and if left unrepaired ssDNA gaps can generate DSBs that require HR for repair (Tirman et al., 2021b; Cong et al., 2021). We explored ssDNA gap generation using the modified DNA fibre S1 nuclease assay in *Bard1*$^{R93E/R93E}$ cells. The S1 nuclease DNA fibre assay involves labelling with CldU for 20 minutes followed by IdU for 40 minutes and a 30-minute incubation at 37 °C with the ssDNA specific S1 nuclease. Remarkably, we saw that *Bard1*$^{R93E/R93E}$ cells generated significantly shortened IdU tract lengths compared to WT cells when treated with the S1 nuclease enzyme (Fig.5.5A). These data suggest that *Bard1*$^{R93E/R93E}$ cells show an alternative replication defect from fork protection.

Subsequently, we wanted to explore whether the endogenous ssDNA gaps formed in *Bard1*$^{R93E/R93E}$ cells are dependent on the primase-polymerase PRIMPOL. PRIMPOL bypasses replication lesions, forming ssDNA gaps, which could explain the elevated fork progression witnessed in Fig.5.4E (Guilliam and Doherty, 2017). We treated *Bard1*$^{R93E/R93E}$ cells with siRNA to PRIMPOL and discovered that the S1-dependent IdU tract lengths were rescued to lengths seen in cells not subjected to the S1 nuclease, suggesting that the ssDNA gaps formed required PRIMPOL function (Fig.5.5A).

As our *Bard1*$^{R93E/R93E}$ cells form endogenous PRIMPOL-dependent ssDNA gaps and *BRCA1*-deficient cells depleted of PRIMPOL elicit reduced cell survival (Quinet et al., 2020), we monitored cell survival in WT and *Bard1*$^{R93E/R93E}$ cells in the absence of PRIMPOL. Indeed, we witnessed a minor but not significant decrease in cell viability in *Bard1*$^{R93E/R93E}$ cells depleted of PRIMPOL compared to WT cells, indicative of a potential reliance on PRIMPOL for survival (Fig.5.5B). These data suggest that *Bard1*$^{R93E/R93E}$ MEFs require DNA damage tolerance mechanisms for efficient DNA replication and genome duplication.

PRIMPOL-dependent re-priming and ssDNA formation have been induced upon fork stalling due to abasic site generation by either base excision mediated by DNA glycosylases such as the uracil glycosylase SMUG1, or from the spontaneous loss of bases (García-Gómez et al., 2013; Kobayashi et al., 2016; Thompson and Cortez, 2020; Tirman et al., 2021b). SMUG1 creates abasic sites by hydrolysing 5-hydroxymethyluracil (5-hmU) sites originated from deamination of 5-hydroxymethyl-cytosine (5-hmC) or oxidative damage to thymine, which results in replication fork stalling and PRIMPOL-dependent re-priming leading to ssDNA accumulation (Fugger et al., 2021; Tirman et al., 2021b; Bordin et al., 2021; Raja and Van Houten, 2021). We

looked at S1 nuclease treated DNA fibre lengths in *Bard1*$^{R93E/R93E}$ cells treated with siRNA to SMUG1 and we witnessed that the fibre lengths showed no change in S1 treated and untreated conditions in cells depleted of SMUG1 (Fig.5.5A). It appears that the loss of SMUG1 reduces the formation of ssDNA gaps in *Bard1*$^{R93E/R93E}$ suggesting that SMUG1-generated abasic sites could stimulate PRIMPOL-dependent re-priming.

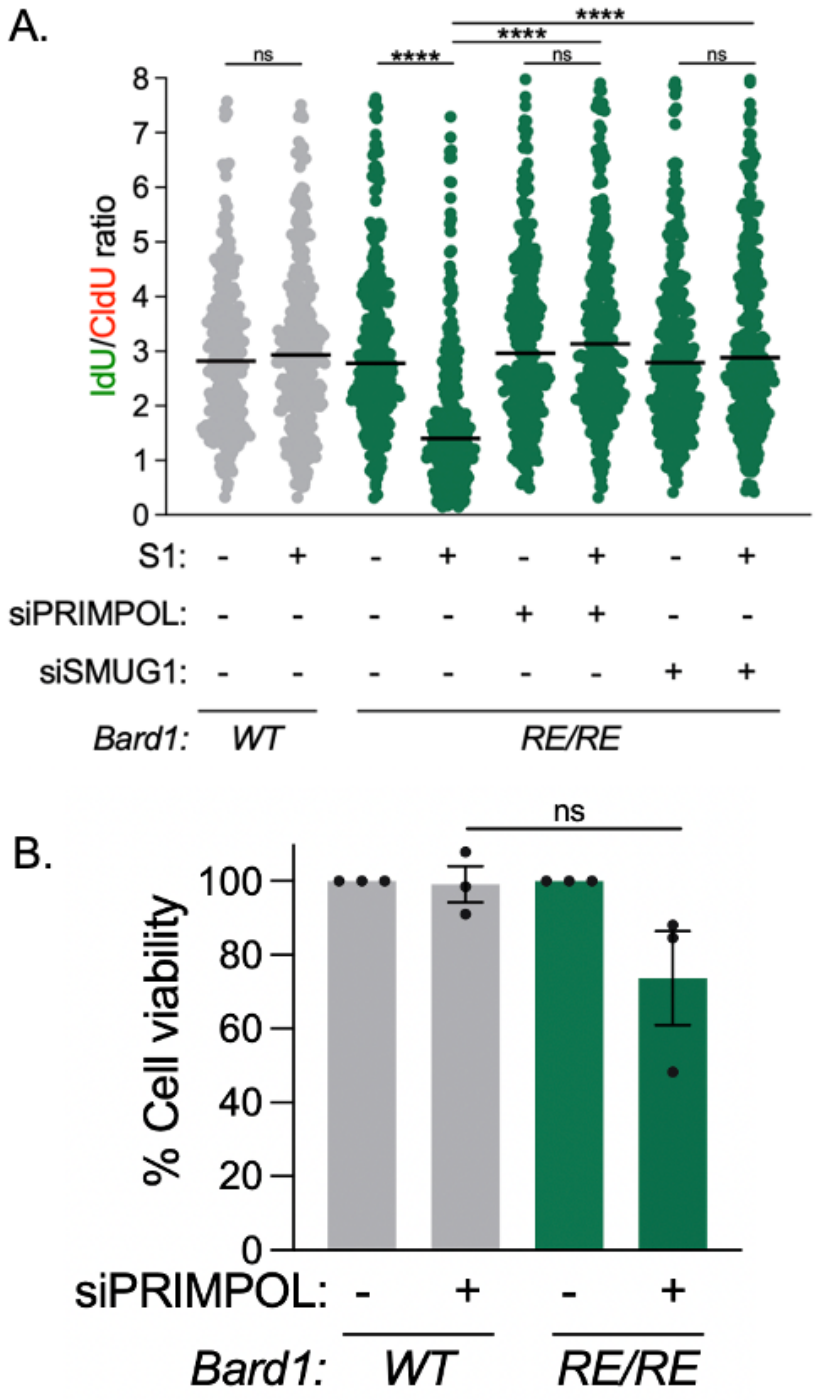

Figure 5.5. *Bard1*$^{R93E/R93E}$ cells form PRIMPOL and SMUG1-dependent ssDNA gaps.

A. S1 nuclease DNA fibre assay in WT and *Bard1*$^{R93E/R93E}$ cells treated with NTC (-), PRIMPOL (+) and SMUG1 (+) siRNA. n ≥ 300 tracks from 3 biological replicates. Data shown are median. Statistical analysis was performed using a Mann–Whitney test; ****= p≤0.0001; ns = not significant.
B. Colony survival in genotypes shown treated with siRNA to NTC (-) and PRIMPOL (+). N=3. Data are mean ± SEM. Statistical analysis performed using a two-tailed Student's *t*-Test; ns = not significant.

5.2.6. *Bard1*$^{R93E/R93E}$ cells are sensitive to Polθ inhibition which can be rescued by the suppression of RAD52

Polθ has been associated with the PRR of ssDNA gaps (Mann et al., 2022; Belan et al., 2022; Schrempf et al., 2021) and in Chapter 4 we determined that Polθ acts to repress RAD52-mediated suppression of ssDNA gaps at G2/M. So, we explored whether *Bard1*$^{R93E/R93E}$ MEFs rely on the non-canonical support of Polθ for survival. We treated both WT and *Bard1*$^{R93E/R93E}$ cells to increasing concentrations of the Polθ inhibitor ART558 and noted that the homozygous MEFs were significantly sensitive to Polθ inhibition compared to WT cells (Fig.5.6A).

Based on results from Chapter 4, we determined whether the sensitivity to ART558 treatment in *Bard1*$^{R93E/R93E}$ cells could be rescued by the suppression of RAD52. We treated *Bard1*$^{R93E/R93E}$ cells with 15 μM ART558 and low doses of the RAD52 inhibitor 6-OHD and carried out colony survival. Remarkably, we noted that ART558-mediated toxicity could be improved by low concentrations of 6-OHD. Concentrations between 0.15 - 1.2 μM 6-OHD could significantly improve cell viability in *Bard1*$^{R93E/R93E}$ cells treated with 15 μM ART558 (Fig.5.6B). These data provide information on the location of the toxic engagement of inhibited Polθ. ART558-mediated toxicity can be reversed

which indicates that there is a higher likelihood of the development of resistance to ART558 in *Bard1*$^{R93E/R93E}$ cells compared to *Brca1*$^{C61G/C61G}$ *53bp1*$^{-/-}$ cells (Chapter 3 and 4).

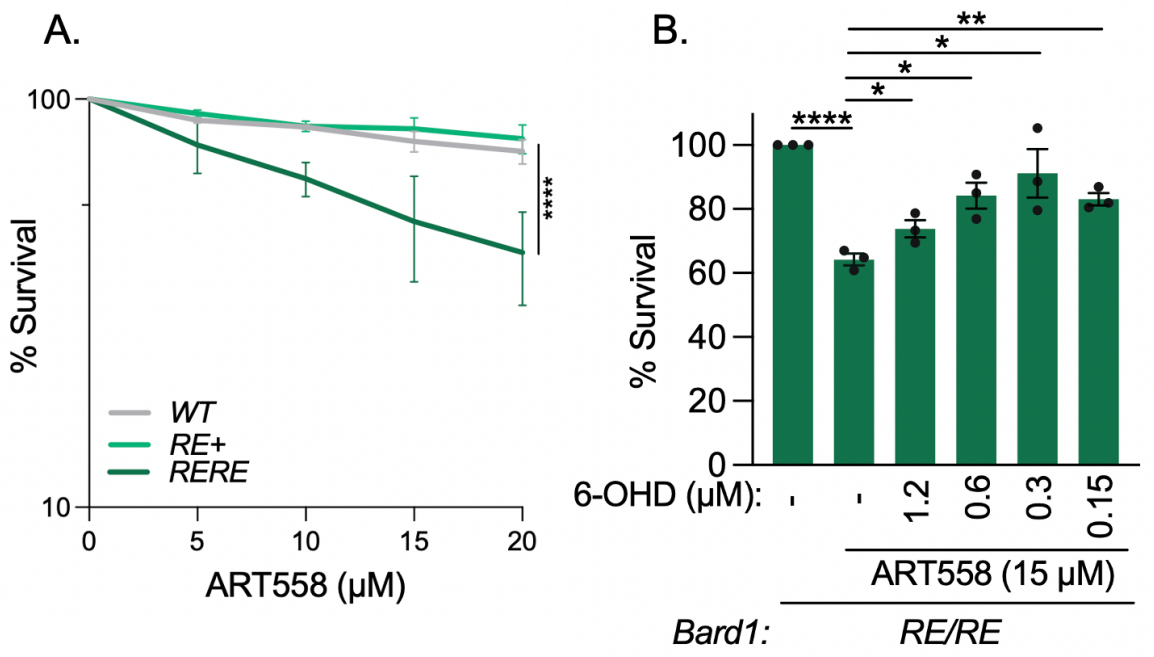

Figure 5.6. *Bard1*$^{R93E/R93E}$ cells are sensitive to Polθ inhibition by ART558 which can be overcome by RAD52 suppression.

A. Colony survival in MEFs of genotypes shown, treated with a dose range of ART558. MEFs were plated 24 hours prior to transfection, treated ART558 for 72 hr and re-plated into colonies and grown out for 7 days. N=3. Data are mean ± SEM. Statistical analysis performed using a two-way ANOVA; ****= p≤0.0001.

B. Colony survival of MEFs treated with DMSO (-) or ART558 (15 μM) and RAD52 inhibitor 6-OHD. N=3 biological repeats. Statistical analysis performed using a two-tailed Student's *t*-Test; ****= p≤0.0001; **= p≤0.01; *= p≤0.05.

In summation, we have generated WT, *Bard1*$^{R93E/+}$ and *Bard1*$^{R93E/R93E}$ MEFs based on original data exploring the R99E-BARD1 mutation in human cells (Densham et al., 2016). So far, we noted that the homozygous *Bard1*$^{R93E/R93E}$ MEFs show unimpacted BRCA1/BARD1 protein expression, produce near-normal RAD51 foci numbers,

proficient BARD1 foci numbers in the presence of RAP80 and exhibit HR frequencies like that of WT cells, and are resistant to the PARPi Olaparib and the replication stress agent HU. However, *Bard1*$^{R93E/R93E}$ cells show reduced H2A ubiquitination, increased replication fork velocity, form PRIMPOL-dependent ssDNA gaps, and reduced cell viability when Polθ is inhibited which can be rescued by low doses of the RAD52 inhibitor 6-OHD. Overall, these data give us a basic understanding of the murine R93E-*Bard1* mutation and how it doesn't appear to affect HR activity when the RAP80-ABRAXAS pathway is intact yet shows signs of defective replication.

5.3. Discussion

We initially evaluated the BRCA1/BARD1 expression levels in *Bard1*$^{R93E/R93E}$ cells and determined that there was no difference in expression between the WT, *Bard1*$^{R93E/+}$, and *Bard1*$^{R93E/R93E}$ cells (Fig.5.1B). However, to conclude that the heterodimer is not disrupted in these cells we would need to carry out a co-immunoprecipitation mass spectrometry and a co-localisation assay to determine the protein interactions. On first look, it appears that BRCA1/BARD1 expression is unaltered in *Bard1*$^{R93E/R93E}$ cells. We then went onto determine the H2A ubiquitination status of *Bard1*$^{R93E/R93E}$ cells compared to WT cells. We used the H2A-ubiquityl antibody (E6C5) and could see a significant reduction in the ubiquitination of H2A in *Bard1*$^{R93E/R93E}$ cells compared to *Bard1*$^{R93E/+}$ and WT cells (Fig.5.1D). Kalb *et al* (2014) noted that the BRCA1 site K125/127/129 does not affect the PRC1-mediated 118/119 site and that the H2A-Ub C-terminal E6C5 antibody can also detect K125/127/129 but this is masked by the 118/119 site (Kalb et al., 2014). However, there is currently no commercial antibody that targets the specific BRCA1/BARD1-mediated H2A-Ub site at K125/127/129.

Next, we determined whether *Bard1*$^{R93E/R93E}$ cells are proficient in DSB repair by HR. First, we looked BARD1 foci accumulation in untreated WT and *Bard1*$^{R93E/R93E}$ cells and did not witness a change in foci formation (Fig.5.2A). Therefore, it is likely that BRCA1/BARD1-mediated ubiquitination of H2A is not necessary for localisation of the heterodimer. Thereafter, we witnessed no significant alteration to the number of RAD51 foci and saw resistance to the PARPi Olaparib plus no change to HR frequency between WT and *Bard1*$^{R93E/R93E}$ cells (Fig.5.2B, C, D). These data suggest that *Bard1*$^{R93E/R93E}$ cells which only appear to be defective in their ability to modify H2A, perform functional HR activity. The results shown here are contradictory to work done by Densham *et al* (2016) denoting that the R99E-BARD1 human mutation and thus the E3 ligase mediated ubiquitination of H2A is important for HR (Densham et al., 2016; Densham and Morris, 2017). There are numerous possible reasons for this discrepancy, such as the different levels of RAP80/ABRAXAS within HeLa cells. Whereas, Nakamura *et al* (2019) highlighted, using the R99E-BARD1 mutation using a dergrON-based approach in HCT116 cells, that E3 ligase function is dispensable for HR (Nakamura et al., 2019). The latter results are in alignment with the following published literature (Drost et al., 2011; Reid et al., 2008; Shakya et al., 2011; Sherker et al., 2021). Yet, the (I26A/L63A/K65A) “ligase dead” BRCA1 mutation demonstrated that BRCA1/BARD1 ligase activity is required for HR, specifically DNA end resection and later stages of HR in Wang *et al* (2023) (Wang et al., 2023).

The controversy surrounding the role of E3 ubiquitin ligase activity and its role in tumour suppression and HR is due to the difficulty in assessing pathogenic BRCA1 RING domain mutations as they not only disrupt the binding to E2 conjugating enzymes but also abrogate the BRCA1/BARD1 heterodimer (Reid et al., 2008; Shakya

et al., 2011; Densham et al., 2016; Anantha et al., 2017; Nakamura et al., 2019; Becker et al., 2021). Wang *et al* (2023) comment that their triple BRCA1 mutation I26A/L63A/K65A completely eliminates ligase activity, but also comment that the BRCA1-I26A and BARD1-R99E mutations retain ligase activity and are not ligase-null mutations. They demonstrate that the ligase dead BRCA1/BARD1 is deficient in HR activity on a scale similar to the C61G-BRCA1 cancer predisposing mutation. However, their data highlights the significantly reduced catalytic activity of R99E-BARD1, which is lower than that of I26A-BRCA1 (Wang et al., 2023). These data do not evaluate the ability of BRCA1/BARD1 to ubiquitinate H2A at K125/127/129 nor do they demonstrate that ligase activity can suppress tumour formation. Overall, Wang *et al* (2023) do highlight that the R99E-BARD1 is clearly defective in its ability to function as an E3 ubiquitin ligase (Wang et al., 2023), and we reiterate that our murine R93E-BARD1 mouse model is used as a ligase defective not ligase null model.

It appears that BRCA1/BARD1 RING domain E3 ligase function could be important for BRCA1 recruitment to DSBs and works redundantly with RAP80/ABRAXAS (Sherker et al., 2021). Sherker *et al* (2021) demonstrated that BRCA1 cells harbouring the ligase defective I26A mutation in the absence of the RAP80/BRCA1-A recognition complex could no longer recruit BRCA1/BARD1 to DSBs (Sherker et al., 2021). Thus, we depleted our *Bard1*$^{R93E/R93E}$ cells of RAP80 and strikingly we saw a significant reduction in BARD1 focal accumulation as well as a susceptibility to Olaparib (Fig.5.3C,E). These results implied that the BRCA1/BARD1-mediated ubiquitination of H2A at K125/127/129 works redundantly with RAP80-mediated recruitment of the BRCA1-A complex. RAP80 alone is not necessary to promote BARD1 foci formation but likely works in conjunction with the catalytic activity of the RING domain. Nonetheless,

Sherker *et al* (2021) also determined that abolishing the interaction between BRCA1 and the nucleosome acidic patch mutating BRCA1 at K70A/R71A showed defective BRCA1 recruitment in *RAP80*$^{-/-}$ cells, albeit not to the extent of the I26A mutation (Sherker et al., 2021). Also, they demonstrated that RAP80-mediated recruitment of BRCA1/BARD1 becomes necessary when RNF168 is lost as RNF168 depletion reduces BRCA1 foci formation but the absence of both RNF8 (necessary for RAP80 activation) and RNF168 completely abolished BRCA1 focal accumulation (Sherker et al., 2021).

Sherker *et al* (2021) hypothesised that BRCA1/BARD1 ubiquitination of H2A at the C-terminus facilitates its own recruitment by the activation of the chromatin remodeller SMARCAD1 which mediates 53BP1 displacement from nucleosomes thereby permitting BRCA1/BARD1 binding to H2A-K13/15-Ub-bearing nucleosomes necessary for recruitment via BARD1-BUDR recognition of H2A-K13/15-Ub (Sherker et al., 2021; Densham et al., 2016). Recent structural advancements have highlighted that the BRCA1/BARD1 RING domains interact directly with the nucleosomal surface to position the E2 enzyme close to the intended H2A residues (Witus et al., 2021a; Hu et al., 2021). It would be interesting to observe whether this phenotype holds up using H2A-ubiquitin fusions or looking into cells co-depleted of SMARCAD1 and RAP80. Also, it is possible that BRCA1/BARD1 has an alternative ubiquitination target to H2A K125/127/129 causing this phenotype or that the ubiquitination of these lysine residues show crosstalk with H2A K13/15 which is leading to a recruitment defective phenotype in the absence of RAP80. However, future work is necessary to determine whether E3 ligase activity is important for BRCA1/BARD1 localisation in the absence of RAP80. Overall, these results imply that targeting RAP80 could re-sensitise potentially resistant

BRCA1/BARD1 RING domain cancers to PARPi such as Olaparib. It would be interesting to explore how the R93E-BARD1 mutation disrupts its ability to ubiquitinate H2A. It has been reported that the interactions between BRCA1/BARD1-UBE2D3 and the NCP advance its enzymatic activity and so influence the process of H2A ubiquitination at the C-terminus, so it would be important to evaluate how the R93E-BARD1 mutation impacts this protein-protein interaction structurally (Hu et al., 2021; Kalb et al., 2014).

Independently of HR function, we explored whether *Bard1*$^{R93E/R93E}$ cells were sensitive to the depletion of nucleotide pools by HU and noted that homozygous R93E MEFs were resistant to the replication stressing agent, unlike WT cells depleted of BRCA1 (Fig.5.4A). We elucidated that there was no fork protection defect in *Bard1*$^{R93E/R93E}$ cells, indicating that the function of BRCA1/2 to stabilise RAD51 and prevent MRE11-mediated degradation of nascent DNA remains unperturbed in *Bard1*$^{R93E/R93E}$ cells. BRCA1/BARD1 interacts with RAD51 which is essential for fork protection and this interaction is dependent on the activity of the phosphorylation-directed prolyl isomerase PIN1 (Daza-Martin et al., 2019). Isomerisation of BRCA1 by PIN1 enhances its interaction with BARD1 thus augmenting the BARD1-RAD51 interaction and promoting RAD51-mediated stabilisation of stalled replication forks (Daza-Martin et al., 2019). The AAE-BARD1 mutation disrupting the BARD1-RAD51 interaction impaired fork protection (Daza-Martin et al., 2019; Tye et al., 2020). Daza-Martin *et al* (2019) comment that R99E-BARD1 cannot rescue fork protection unlike AAE-BARD1, reinforcing the importance of the BARD1/RAD51 interacting region over its E3 ligase activity for sufficient protection of stalled replication forks (Daza-Martin et al., 2019).

Furthermore, we analysed replication fork kinetics and discovered that both WT and mutant cells did not vary in overall replication fork structures when analysing origin firing and termination (Fig.5.4D). Yet, an evident increase in replication fork velocity could be seen in *Bard1*$^{R93E/R93E}$ MEFs whilst there was no apparent increase in origin firing (Fig.5.4E, F). Unrestrained fork progression could be due to excessive PRIMPOL-dependent re-priming in the face of replication stress facilitating ssDNA gap formation leading to the activation of PRR pathways such as TLS or TS to prevent cell death (Thakar et al., 2020; Taglialatela et al., 2021; Tirman et al., 2021b; Cong et al., 2021; Thakar et al., 2022). TLS activation enables lesion bypass albeit this process is error prone and can accumulate point mutations (Yang and Gao, 2018) There is growing evidence for the PRR of ssDNA gaps by TLS polymerases, which could be heightened in *Bard1*$^{R93E/R93E}$ cells (Taglialatela et al., 2021; Tirman et al., 2021b). TS is less error-prone than TLS and requires a homologous template and mediates fork reversal or functions at post-replicative gaps behind the fork, but the decision making behind replication stress response pathway activation still remain unclear (Adar et al., 2009; Izhar et al., 2013; Neelsen and Lopes, 2015; Berti et al., 2020a).

Bard1$^{R93E/R93E}$ MEFs were unable to restrain replication fork progression unlike WT cells, which led us to investigate whether this was due to PRIMPOL-mediated repriming leading to lesion bypass and thus the generation of ssDNA gaps. Indeed, *Bard1*$^{R93E/R93E}$ cells showed significant shortening of IdU tract lengths after ssDNA-specific S1 treatment, however when depleted of PRIMPOL S1 treatment made no significant difference to IdU tract lengths (Fig.5.5A). Therefore, PRIMPOL-mediated repriming is likely a reason for the unrestrained fork velocity witnessed in *Bard1*$^{R93E/R93E}$ cells. Also, the depletion of PRIMPOL led to a slight but not significant reduction in cell

survival of *Bard1*$^{R93E/R93E}$ cells, indicative of a reliance on the DNA damage tolerance mechanism for cell viability (Fig.5.5B). A preprint by Salas-Lloret *et al* (2023) suggested that BRCA1/BARD1 E3 ligase activity and its ubiquitination of PCNA suppresses ssDNA gap formation, however they also noted that the ligase defective I26A-BRCA1 mutant was sensitive to HU and prevented BRCA1 S114 phosphorylation, important for isomerisation (Salas-Lloret et al., 2023). Yet, we saw no sensitivity to HU nor a fork protection defect in our *R93E-Bard1* murine model, which is in line with previous results from our group (Densham et al., 2016; Daza-Martin et al., 2019).

We then looked at whether *Bard1*$^{R93E/R93E}$ cells depleted of the uracil glycosylase SMUG1, which creates toxic abasic sites and hence ssDNA gaps, could rescue ssDNA gap generation and we confirmed this to be the case (Fugger et al., 2021; Raja and Van Houten, 2021; Taglialatela et al., 2021). SMUG1 removes uracil from U:A and U:G base pairs via the short-patch BER pathway (Akbari et al., 2004; Pettersen et al., 2007; Jang et al., 2023). A uracil moiety identified in DNA is 5-hydroxymethyl 2-deoxyuridine (5-hmdU), which is formed by the oxidation of thymine generated by methylcytosine dioxygenase (TET1)-mediated activity, oxidative stress, hydrogen peroxide or IR (Liu et al., 2013b; Pfaffeneder et al., 2014; Teebor et al., 1984; Djuric et al., 1993; Modrzejewska et al., 2016). SMUG1 functions to repair 5-hmdU and additional products of DNA-pyrimidine oxidation including 5-formyldeoyuridine (fdU) from DNA (Masaoka et al., 2003). Taglialatela *et al* (2021) showed that lesions created by SMUG1 induce fork stalling and PRIMPOL-dependent repriming and these gaps render cells that lack functional BRCA1-dependent HR and REV1-Polζ-mediated TLS susceptible to genotoxic agents (Taglialatela et al., 2021).

The presence of PRIMPOL and SMUG1-dependent ssDNA gaps in *Bard1*$^{R93E/R93E}$ cells made us investigate whether these cells are sensitive to Polθ inhibition by ART558. We noted a significant sensitivity to Polθ inhibition in *Bard1*$^{R93E/R93E}$ cells and remarkably was able to reverse cell toxicity to ART558 treatment by low doses of the RAD52 inhibitor 6-OHD (Fig.5.6A, B). It is therefore possible to remove ART558, which is thought to be potentially "trapped" onto DNA (Zatreanu et al., 2021), by suppressing potential RAD52-mediated toxicity present in ART558-treated *Bard1*$^{R93E/R93E}$ cells. Therefore, it is plausible that RAD52 is driving the toxicity associated with Polθ inhibition, so there could be a differential engagement of Polθ in cells with the R93E-BARD1 protein.

We surmise that the *Bard1*$^{R93E/R93E}$ cell model is defective in H2A ubiquitination and forms PRIMPOL and SMUG1-dependent ssDNA gaps, allowing us to ponder whether there is a correlative relationship between the two phenotypes. The proficient ability to repair DSBs by HR likely explains how the ssDNA gaps which could go onto form DSBs could be repaired in our *Bard1*$^{R93E/R93E}$ cells. Overall, in this chapter we have begun to characterise the murine *R93E-Bard1* mutation which could help us further understand the role of BRCA1/BARD1 E3 ligase activity.

Table 5.1. Phenotypes of the *R93E-Bard1* mutation.

Bard$^{R93E/R93E}$ cells	YES	NO
Reduced BRCA1/BARD1 expression		X
Reduced H2A-Ub expression	X	
Reduced BARD1 foci formation	X (- RAP80)	X
Reduced RAD51 foci formation		X
PARPi sensitivity	X (- RAP80)	X
HU sensitivity		X
ART558 sensitivity	X	
Increased fork speeds	X	
Fork protection defect		X
ssDNA gap formation	X	

6. Elucidating the role of USP1 in *Bard1*$^{R93E/R93E}$ cells

6.1. Introduction

Here, we introduce the DUB USP1 which forms a heterodimeric complex with UAF1 (WDR48), a WD40 repeat, to form the USP1-UAF1 complex which functions to maintain genomic stability by de-ubiquitinating proteins such as PCNA and FANCD2 involved in translesion synthesis and FA pathways respectively (Huang et al., 2006; Cohn et al., 2007). In this chapter we will be focusing on further understanding the synthetic lethal interaction between USP1 and BRCA1. The E3 ligase RAD18 monoubiquitinates PCNA at K164 to stimulate the transition from high to low fidelity DNA polymerases, which lack the intrinsic 3'-to-5' exonuclease domain and thus proof reading capability (Goodman, 2002; Yang, 2005). In addition, the Y family of TLS polymerases encompass a larger active site compared to replicative DNA polymerases, consequently permitting the entrance of large modified bases which can be bypassed leading to elevated mutation rates (Kannouche et al., 2004; Bienko et al., 2005; Prakash et al., 2005; Guo et al., 2006b).

The USP1-UAF1 complex localises to the replication fork to facilitate smooth DNA synthesis and Lim *et al* (2018) identified a role for USP1 in fork protection in *BRCA1*-deficient cells (Lim et al., 2018). USP1 and BRCA1 have a synthetic lethal relationship which can be overcome by the loss of the E3 ligase RAD18 and the TLS polymerase POLK, which accumulates in the absence of USP1 resulting in the elevated mono-ubiquitination of PCNA and excessive TLS (Lim et al., 2018). USP1 depletion has been associated with augmented ssDNA gaps and it's thought that the removal of USP1 in *BRCA1*-deficient cells could stimulate aberrant TLS activation and prohibit TLS-

mediated ssDNA gap fill-in (Simoneau et al., 2023a). In other cases, USP1 has been implicated in the expansion of ssDNA gaps by MRE11 and EXO1 during S-phase by preventing RAD18-mediated mono-ubiquitination of PCNA to repair ssDNA gaps (Nusawardhana et al., 2024). Inhibitors of USP1 are currently in Phase I/II clinical trials, such as KSQ-4279, which is a potent and selective inhibitor that elevates the mono-ubiquitination of USP1 substrates (Chen et al., 2021; Cadzow et al., 2022).

Interestingly, a novel role for 53BP1 has come to light which involves the coordination of replicative DNA damage bypass (Chen et al., 2022). In *BRCA1/2*-deficient DT40 cells, elevated mutation patterns induced by TLS polymerases such as insertion, deletion and base substitution mutations arise, and the depletion of 53BP1 can reduce TLS-mediated mutagenesis switching to the less erroneous TS pathway. In addition, it appears that 53BP1 plays a role in facilitating TLS in human cell extracts (Chen et al., 2022). In the current study, we are investigating whether *Bard1*$^{R93E/R93E}$ cells are reliant on USP1 and the factors that potentially regulate the function of USP1 in our cells such as POLK and 53BP1 in mediating elevated mono-ubiquitination of PCNA. We then go onto potentially show a link between the BRCA1/BARD1 modification of H2A at the C-terminus and the suppression of USP1 sensitivity.

6.2. Results

6.2.1. *Bard1*$^{R93E/R93E}$ cells are sensitive to the loss of USP1

USP1 is overexpressed in *BRCA1*-deficient tumours and is associated with poor prognosis (Koboldt et al., 2012; Lim et al., 2018; Sonego et al., 2019). Two well-established substrates of USP1 de-ubiquitination include PCNA and the FANCI-FANCD2 complex, important for TLS and ICL repair (Fig.6.1A) (Huang et al., 2006;

Nijman et al., 2005). USP1 loss is synthetic lethal in *BRCA1*-deficient cells (Lim et al., 2018), so we wanted to investigate whether *Bard1*$^{R93E/R93E}$ cells are reliant on USP1 for survival. We subjected WT and *Bard1*$^{R93E/R93E}$ cells to siRNA targeting USP1 and we noted that there was a significant reduction in cell viability in the absence of USP1 in *Bard1*$^{R93E/R93E}$ cells compared to WT cells, reducing the percentage of cell survival to 64% compared to 99% respectively (Fig.6.1B).

Next, we wanted to determine whether *Bard1*$^{R93E/R93E}$ cells were more sensitive to the USP1 inhibitor ML323, which is a potent, selective, allosteric inhibitor of the USP1/UAF1 complex (Liang et al., 2014; Coleman et al., 2022). We treated both WT and *Bard1*$^{R93E/R93E}$ cells with increasing concentrations of ML323 and witnessed that there was a noteworthy separation between the two cell lines, rendering *Bard1*$^{R93E/R93E}$ cells more sensitive to USP1 inhibition (Fig.6.1D).

In Chapter 5, we found that *Bard1*$^{R93E/R93E}$ cells were resistant to the PARPi Olaparib but recent reports have shown that USP1 and PARP inhibitors are synergistic in *BRCA1*-deficient cells (Simoneau et al., 2023a) so we wondered whether this would be the case when co-treating with ML323 and Olaparib in *Bard1*$^{R93E/R93E}$ cells. WT and *Bard1*$^{R93E/R93E}$ cells were treated with increasing doses of Olaparib and subjected to an additional low dose of 5 μM ML323. We noted that there was a striking sensitivity to the co-treatment of the USP1 inhibitor ML323 and Olaparib to *Bard1*$^{R93E/R93E}$ cells, whilst WT MEFs remained resistant (Fig.6.1E). Interestingly, we noted that ML323 treatment significantly increased USP1 expression levels, which has been seen by Coleman *et al* (2022) also (Coleman et al., 2022)(Fig.6.1F).

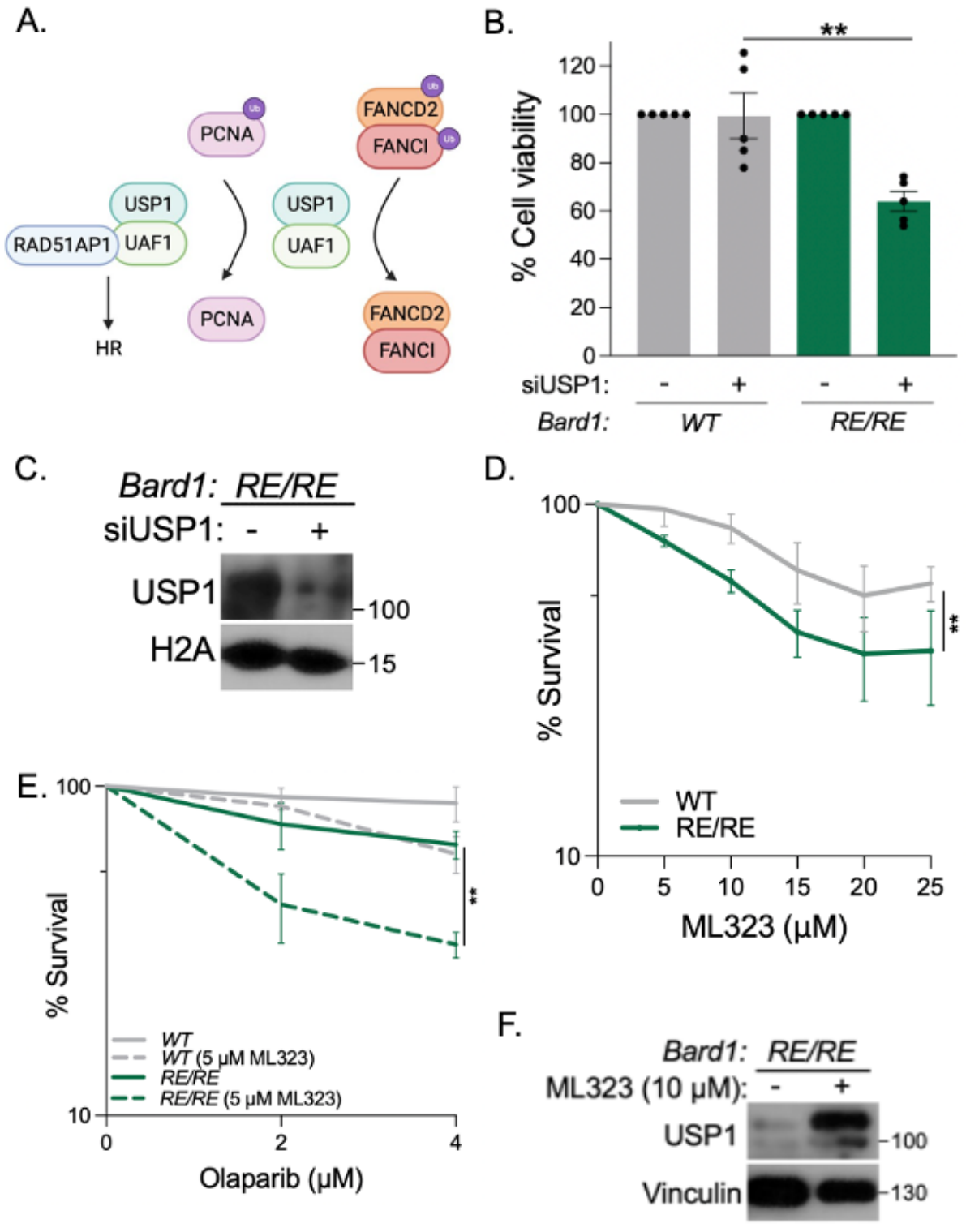

Figure 6.1. *Bard1*$^{R93E/R93E}$ cells are sensitive to the loss of USP1.

A. Schematic showing that USP1 de-ubiquitinates 1) the FANC2-FANCI complex to regulate the repair of interstrand cross-links (ICLs) and 2) PCNA to regulate DNA

damage bypass by translesion synthesis (TLS). 3) The USP1-UAF1 complex interacts with RAD51AP1 to promote homologous recombination (HR).

B. Colony survival of WT and *Bard1*$^{R93E/R93E}$ cells treated with non-targeting control (NTC) or siRNA to USP1. n=5 biological repeats. Statistical analyses performed using a two-tailed Student's *t*-Test; **= p≤0.01.
C. Western blot analysis of USP1 protein levels following non-targeting control (−) or USP1 (+) targeting siRNA treatment. H2A was used as a loading control.
D. Colony survival of WT and *Bard1*$^{R93E/R93E}$ cells treated with increasing concentrations of the USP1 inhibitor ML323. N=3 biological repeats. Statistical analyses performed using a two-way ANOVA; **= p≤0.01.
E. Colony survival of WT and *Bard1*$^{R93E/R93E}$ cells treated with increasing concentrations of Olaparib and 5 μM USP1 inhibitor ML323. N=3 biological repeats. Statistical analyses performed using a two-way ANOVA; **= p≤0.01.
F. Western blot analysis of USP1 protein levels following DMSO (−) or ML323 USP1 inhibitor (+) treatment. Vinculin was used as a loading control.

6.2.2. Depletion of the TLS polymerase POLK reversed the USP1-mediated loss of cell viability

USP1 is a de-ubiquitinase for PCNA which is a sliding DNA clamp fundamental for the recruitment of TLS polymerases for lesion bypass (Andersen et al., 2008). So, we wanted to look at the posttranslational modification of PCNA upon the loss of USP1 in *Bard1*$^{R93E/R93E}$ cells. Figure 6.2A demonstrates that PCNA ubiquitination was elevated in the homozygous MEFs with a further increase following USP1 loss, compared to WT cells (Fig.6.2A).

Lim *et al* (2018) deduced that USP1 is essential for replication fork protection in *BRCA1* but not *BRCA2*-mutated cancers by directly binding and stabilising the replication fork (Lim et al., 2018). For that reason, we investigated replication fork protection in WT and *Bard1*$^{R93E/R93E}$ cells treated with siRNA targeting NTC and USP1. In Chapter 5, we

observed that there was no fork protection defect in *Bard1*$^{R93E/R93E}$ cells (Chapter 5, Fig.5.4B). However, upon depletion of USP1, there was a defect in replication fork protection in *Bard1*$^{R93E/R93E}$ cells, with no defect to WT cells without USP1 (Fig.6.2B). Hence, USP1 could be necessary for the stabilisation of replication forks in the *R93E-Bard1* mutated MEFs.

Accordingly, these data led us to explore the TLS polymerase POLK which is among the Y family of TLS polymerases (including Pol eta, iota or REV1) (Bienko et al., 2005; Kannouche et al., 2004). Jones *et al* (2012) observed that atypical recruitment of POLK resulted in a USP1-mediated reduction in replication fork velocity (Jones et al., 2012). The co-depletion of USP1 and POLK could not only rescue diminished replication fork speed but the defect in replication fork protection and cell toxicity caused by USP1 loss in *BRCA1*-mutated cells (Lim et al., 2018; Jones et al., 2012). Knowing these results, we wanted to evaluate whether the loss of cell viability associated with the loss of USP1 in *Bard1*$^{R93E/R93E}$ cells could be rescued following co-depletion with POLK. We witnessed an improvement in cell survival when treating *Bard1*$^{R93E/R93E}$ cells with siRNA targeting USP1 and POLK, indicating that excess POLK could be contributing to the cell toxicity in the USP1-depleted MEFs (Fig.6.2C). That being so, we questioned whether the dependency on POLK in *Bard1*$^{R93E/R93E}$ cells devoid of USP1 is what is impacting replication fork protection seen in Fig.6.2B. We revisited the DNA fibre replication fork protection assay in WT and *Bard1*$^{R93E/R93E}$ cells and indeed determined that the co-depletion of USP1 and POLK was able to restore replication fork protection in R93E-*Bard1*-mutated cells (Fig.6.2B). These data elicit a potential role for POLK in mediating the toxicity shown in *Bard1*$^{R93E/R93E}$ cells lacking USP1-mediated protection of replication forks. We also looked at cell viability in the absence of POLK alone in WT

and *Bard1*$^{R93E/R93E}$ cells and there was no significant difference, although the data has high variability between repeats which could be due to knockdown efficiency and will require repetition in future (Fig.6.2D).

The enhanced mono-ubiquitination of PCNA upon depletion of USP1 might affect other factors involved in replication fork dynamics such as the nucleases and helicases MRE11 and DNA2. Hence, we did western blot analysis in WT and *Bard1*$^{R93E/R93E}$ MEFs depleted of USP1 but also USP1 and POLK in conjunction and discovered that co-depletion of both proteins could return PCNA ubiquitination levels back to untreated conditions (Fig.6.2A). In addition, we observed an increase in MRE11 and DNA2 expression in USP1-depleted *Bard1*$^{R93E/R93E}$ cells, but this was reduced upon co-treatment with siRNA to POLK (Fig.6.2A). These results suggest that the nucleases MRE11 and DNA2, both involved in the digestion of nascent DNA in unprotected replication forks, (Kolinjivadi et al., 2017b; Vujanovic et al., 2017; Lemaçon et al., 2017; Thangavel et al., 2015; Thakar et al., 2020; Schlacher et al., 2011) could be mediating replication fork de-protection in USP1-depleted *Bard1*$^{R93E/R93E}$ cells seen in Fig.6.2B.

Overall, the enhanced MRE11 AND DNA2 expression in USP1-depleted *Bard1*$^{R93E/R93E}$ cells but the reduction in MRE11 and DNA2 expression upon co-depletion with POLK siRNA aligns with the lack of fork protection which could be rescued by the loss of both USP1 and POLK seen in Fig.6.2B. However, future work is required to determine whether this is case, we would need to treat USP1-depleted *Bard1*$^{R93E/R93E}$ cells with the MRE11 inhibitor mirin and monitor fork protection.

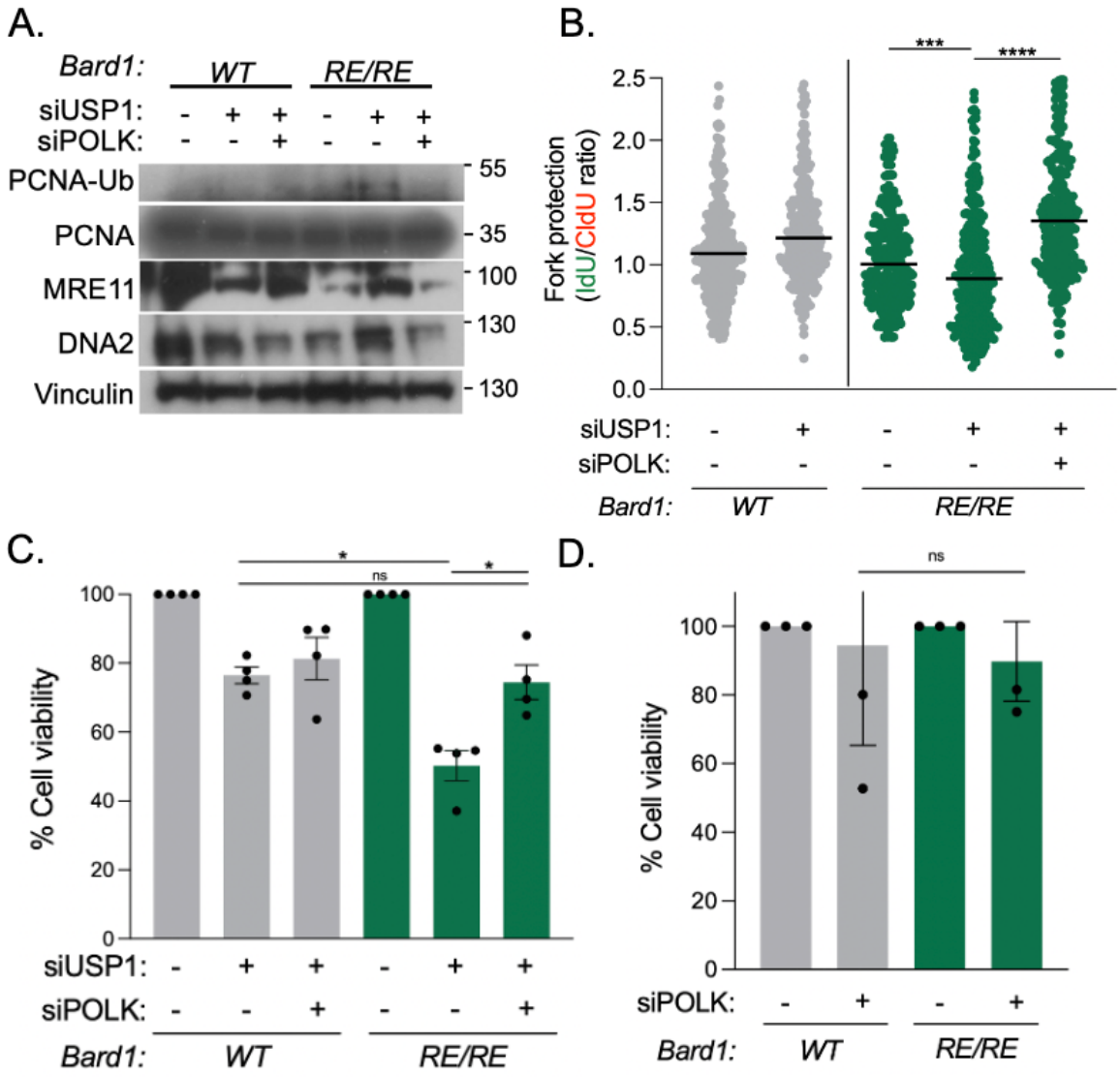

Figure 6.2. Depletion of the TLS polymerase POLK reversed the USP1-mediated loss of cell viability and replication fork defect in *Bard1*$^{R93E/R93E}$ MEFs.

A. Western blot analysis of PCNA-Ub, PCNA, MRE11, DNA2 protein levels following non-targeting control (−) or USP1/POLK (+) targeting siRNA treatment. Vinculin was used as a loading control.

B. Fork protection fibres IdU/CldU ratios from WT and *Bard1*$^{R93E/R93E}$ cells. Cells treated with CldU and IdU for 20 mins and 5 mM HU for 3 hr prior to spreading. Cells were treated with non-targeting control (NTC) or siRNA to USP1 and/or POLK. N ≥ 300 fibres from 3 biological replicates. Data shown are median. Statistical analysis was performed using a Mann–Whitney test; ****= p≤0.0001; ***= p≤0.001.

C. Colony survival of WT and *Bard1*$^{R93E/R93E}$ cells treated with non-targeting control (NTC) or siRNA to USP1 and/or POLK. n=3 biological repeats. Statistical analyses performed using a two-tailed Student's *t*-Test; *= p≤0.05; ns = not significant.
D. Colony survival of WT and *Bard1*$^{R93E/R93E}$ cells treated with non-targeting control (NTC) or siRNA to POLK. n=3 biological repeats. Statistical analyses performed using a two-tailed Student's *t*-Test; ns = not significant.

6.2.3. RAD18 foci formation is impaired in *Bard1*$^{R93E/R93E}$ cells.

In Fig.6.3A we quantified RAD18 expression levels (data not shown) and witnessed no difference to the PCNA E3 ligase RAD18 expression levels between WT and *Bard1*$^{R93E/R93E}$ cells and in cells treated with siRNA targeting NTC, USP1 or POLK (Fig.6.3A). Next, we investigated the ability of WT and *Bard1*$^{R93E/R93E}$ cells to form RAD18 foci. We observed a significant reduction in RAD18 foci formation in *Bard1*$^{R93E/R93E}$ cells at approximately 3 foci per cell compared to an average of 10 foci per cell in WT cells (Fig.6.3B). The data from Fig.6.3B indicates that RAD18 recruitment is impaired in *Bard1*$^{R93E/R93E}$ cells. WT cells treated with siRNA to USP1, or POLK led to increased RAD18 foci formation, which could be brought back down when co-depleting both USP1 and POLK (Fig.3.6B). When looking at RAD18 foci in *Bard1*$^{R93E/R93E}$ cells we noted a lower baseline of RAD18 foci which made a negligible increase upon the loss of USP1 and a larger one upon POLK depletion followed by a reduction in foci when co-depleting USP1 and POLK. The pattern of RAD18 foci in WT and *Bard1*$^{R93E/R93E}$ cells followed a similar trend, but foci formation was noticeably impaired in the latter. The reduced formation of RAD18 foci in *Bard1*$^{R93E/R93E}$ cells was surprising due to the increased baseline ubiquitination of PCNA seen in Fig.6.2A. It is possible that the modification of PCNA carried out in *Bard1*$^{R93E/R93E}$ cells is performed by an alternative E3 ubiquitin ligase or aberrantly by uncoordinated RAD18.

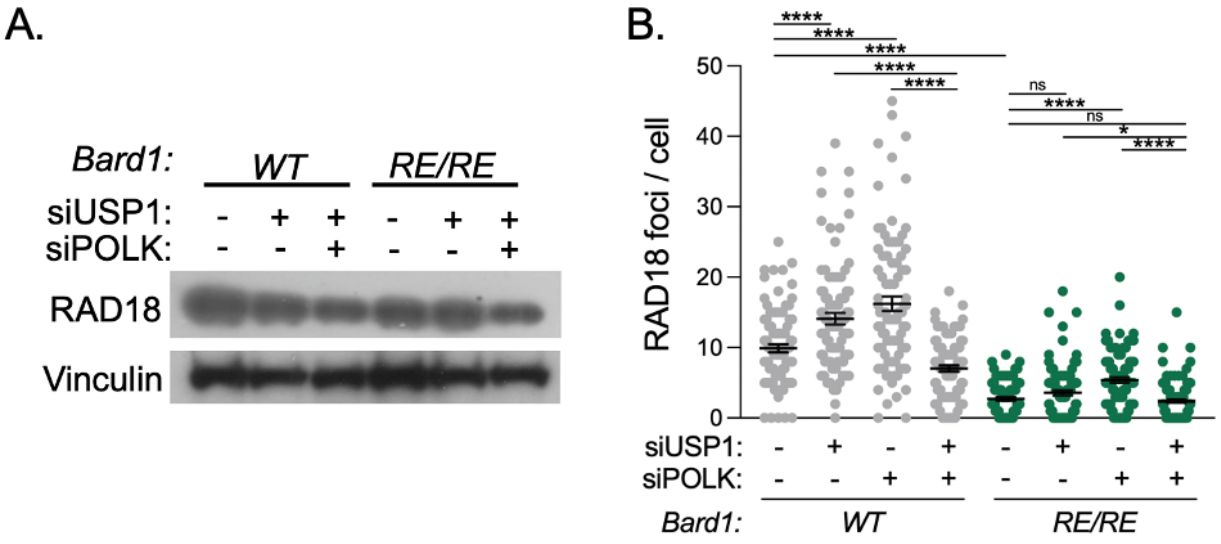

Figure 6.3. RAD18 foci formation is impaired in *Bard1*$^{R93E/R93E}$ cells.

A. Western blot analysis of RAD18 protein levels following non-targeting control (−) and USP1 and/or POLK (+) targeting siRNA treatment. Vinculin was used as a loading control.

B. Quantification of RAD18 foci in asynchronous cells with NTC siRNA (-) or siRNA to USP1 and/or POLK (+) siRNA. N=90 cells from 3 biological repeats. Statistical analyses performed using a two-tailed Student's *t*-Test; ****= p≤0.0001; *= p≤0.05; ns = not significant.

6.2.4. *Bard1*$^{R93E/R93E}$ cells are sensitive to the TLS inhibitor JH-RE-06.

So far, we have collated results suggesting that *Bard1*$^{R93E/R93E}$ cells could be adapted to hyperactivate TLS, as shown by the elevated mono-ubiquitination of PCNA, reliance on the de-ubiquitinase USP1, as well as the rescue of USP1-depleted toxicities upon the loss of the TLS polymerase POLK. There's a possibility that *Bard1*$^{R93E/R93E}$ cells are dependent on the surplus activation of TLS for survival. As well as POLK we wanted to evaluate alternative TLS polymerases, such as REV1, which functions as a scaffold protein by binding to PCNA and POLK, POLη, POLι Y-family polymerases or the REV7 component of the B-family Polζ complex (Guo et al., 2006a; De Groote et

al., 2011; Pozhidaeva et al., 2012; Liu et al., 2013a; Pustovalova et al., 2016). Mutagenesis witnessed in *BRCA1*-deficient cells has been linked to enhanced TLS-mediated generation of base substitutions (Chen et al., 2022). So, small molecule inhibitors that target TLS have been developed (Wojtaszek et al., 2019), including the REV1 inhibitor JH-RE-06 which abolishes the interaction between REV1 and REV7 by activating REV1 dimerisation, thus abrogating the REV1-REV7 association and averting the localisation of Polζ to the replication fork (Wojtaszek et al., 2019; Anand et al., 2023). REV1 is important for coordinating TLS by using one interface to recruit the insertion TLS polymerases such as POLK, and the second interface to recruit the Polζ complex (REV3L/REV7/POLD2/POLD3) via the REV7 component (Yamanaka et al., 2017). The REV1:REV7 interaction is an ideal target because it is important for mutagenic TLS and not accurate lesion bypass (Hashimoto et al., 2012; Wojtaszek et al., 2019).

We tested increasing concentrations of the REV1 TLS inhibitor JH-RE-06 on WT and *Bard1*$^{R93E/R93E}$ cells and demonstrated that JH-RE-06 is preferentially toxic to *Bard1*$^{R93E/R93E}$ cells (Fig.6.4A). The susceptibility of the R93E-*Bard1* mutated MEFs to JH-RE-06 suggest that they are reliant on TLS for survival. Next, we subjected both cell lines to increasing doses of JH-RE-06, but now with the treatment of siRNA to USP1 and observed that the sensitivity of *Bard1*$^{R93E/R93E}$ cells to JH-RE-06 was lost and cell viability was improved to a similar rate seen in WT cells (Fig.6.4B). USP1-depleted *Bard1*$^{R93E/R93E}$ cells can likely avoid aberrant TLS activation due to the inhibition of the REV1:REV7 interaction.

Taglialatela *et al* (2021) suggest that the toxicity towards JH-RE-06 treatment in *BRCA1*-deficient cells is due to the generation of PRIMPOL and SMUG1-dependent

ssDNA gaps (Taglialatela et al., 2021). In Chapter 5 Fig.5.5A we noted that *Bard1*$^{R93E/R93E}$ cells generate SMUG1 and PRIMPOL-dependent ssDNA gaps, whereas WT cells do not (Chapter 5, Fig.5.5A). In keeping with this, *BRCA1*-deficient cells devoid of USP1 have been associated with elevated ssDNA gap formation which can be reversed upon the loss of POLK (Lim et al., 2018). Taken together, we depleted WT and *Bard1*$^{R93E/R93E}$ cells with siRNA to USP1 followed by co-treatment with siRNA SMUG1 to determine whether the uracil glycosylase SMUG1 and thus the generation of abasic sites is driving the sensitivity to USP1 loss in *Bard1*$^{R93E/R93E}$ cells. Indeed, the loss of USP1 sensitised *Bard1*$^{R93E/R93E}$ and not WT cells, whereas the loss of SMUG1 made no difference to cell viability in either cell lines (Fig.6.4C). The co-depletion of USP1 and SMUG1 completely rescued cell survival back to untreated conditions in *Bard1*$^{R93E/R93E}$ cells (Fig.6.4C). These data suggest that the formation of abasic sites by SMUG1 is driving the USP1-depleted toxicity in *Bard1*$^{R93E/R93E}$ cells.

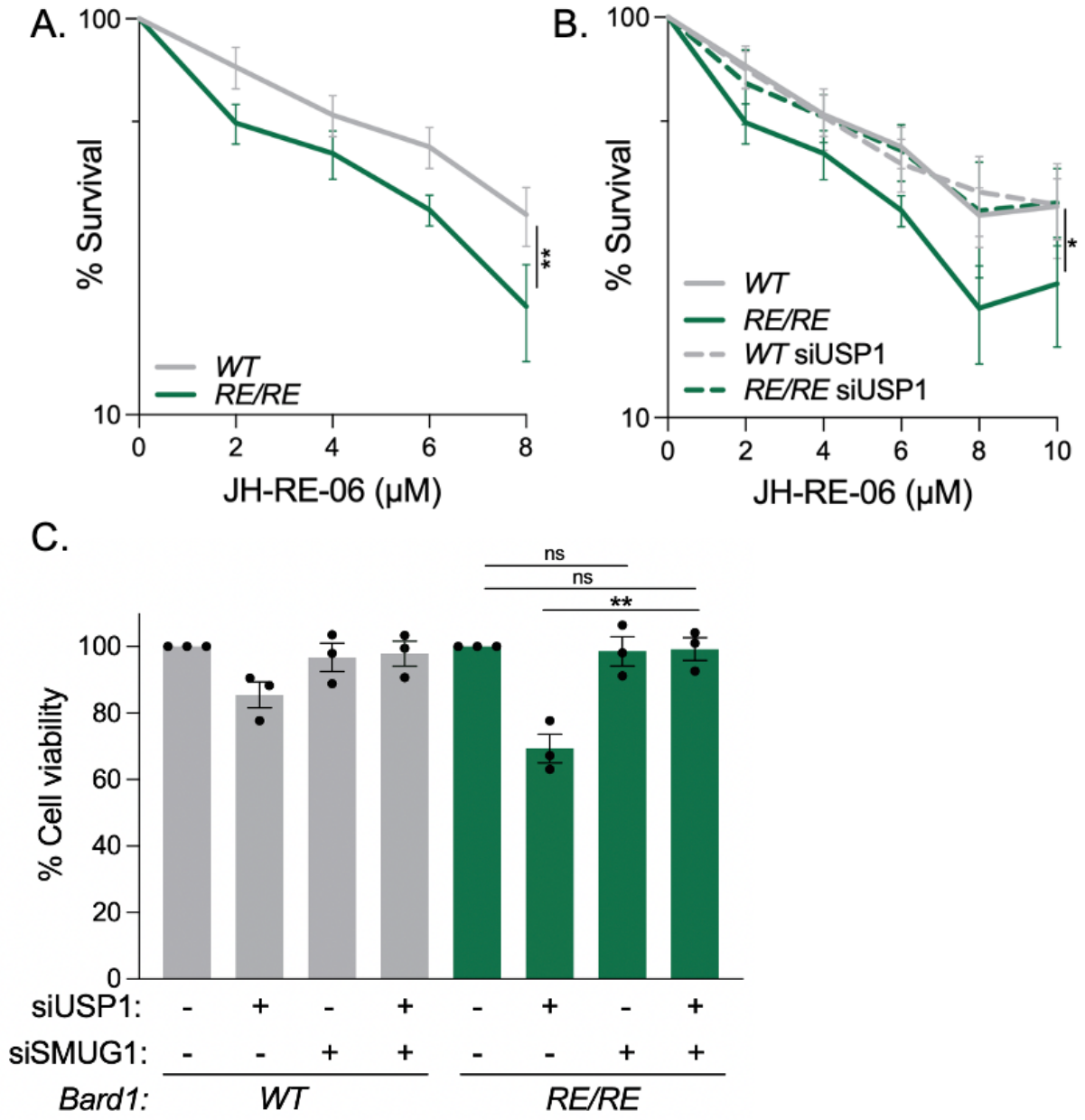

Figure 6.4. *Bard1*$^{R93E/R93E}$ cells are sensitive to the TLS inhibitor JH-RE-06.

A. Colony survival of WT and *Bard1*$^{R93E/R93E}$ cells treated with increasing concentrations of the TLS inhibitor JH-RE-06. N=3 biological repeats. Statistical analyses performed using a two-way ANOVA; **= p≤0.01.

B. Colony survival of WT and *Bard1*$^{R93E/R93E}$ cells treated with increasing concentrations of the TLS inhibitor JH-RE-06 and siRNA targeting USP1. N=3 biological repeats. Statistical analyses performed using a two-way ANOVA; *= p≤0.05.

C. Colony survival of WT and *Bard1*$^{R93E/R93E}$ cells treated with non-targeting control (NTC) or siRNA to USP1 and/or SMUG1. n=3 biological repeats. Statistical analyses performed using a two-tailed Student's *t*-Test; **= p≤0.01; ns = not significant.

6.2.5. USP1 sensitivity and fork protection defect can be rescued by the loss of 53BP1 in *Bard1*$^{R93E/R93E}$ MEFs

We wanted to investigate another factor that is driving cell toxicity in the absence of USP1. Chen *et al* (2022) have suggested that *BRCA1*-deficient DT40 cells have higher mutation rates with a significant proportion from TLS at replication stalling lesions; and that 53BP1 mediates TLS by preventing error-free DNA damage bypass by template switching (Chen et al., 2022). We therefore considered whether removing 53BP1 could alleviate the cellular defects associated with USP1 depletion in *Bard1*$^{R93E/R93E}$ MEFs. We treated the cells with siRNA to USP1 alone and co-depleted USP1 with 53BP1 and carried out colony survival assays. There was an improvement in cell viability in *Bard1*$^{R93E/R93E}$ cells treated with siRNA to both USP1 and 53BP1 compared to USP1 alone, indicating that 53BP1 is involved in mediating the toxic phenotypes in *Bard1*$^{R93E/R93E}$ cells lacking USP1 (Fig.6.5A).

These data led us to revisit the replication fork protection defect that we have seen in *Bard1*$^{R93E/R93E}$ cells devoid of USP1 (Fig.6.2B). Remarkably, co-depletion of USP1 and 53BP1 was able to restore replication fork protection, like that of removing POLK and USP1 (Fig.6.5B). Interestingly, on first observation the co-depletion of USP1 and 53BP1 appeared to reduce the ubiquitination of PCNA created from the loss of USP1 alone in *Bard1*$^{R93E/R93E}$ cells (Fig.6.5D). PCNA mono-ubiquitination was significantly reduced by depleting USP1 and 53BP1 compared to the co-depletion of USP1 and POLK (Fig.6.5D). The expression levels of 53BP1 were notably elevated in

Bard1$^{R93E/R93E}$ cells compared to WT cells, which could be important for the repair of endogenous damage albeit will require further investigation (Fig.6.5C). Overall, the removal of 53BP1 in USP1-depleted *Bard1*$^{R93E/R93E}$ cells restored cell survival and fork protection denoting that 53BP1 is likely a factor involved in the toxic phenotypes associated with USP1 loss.

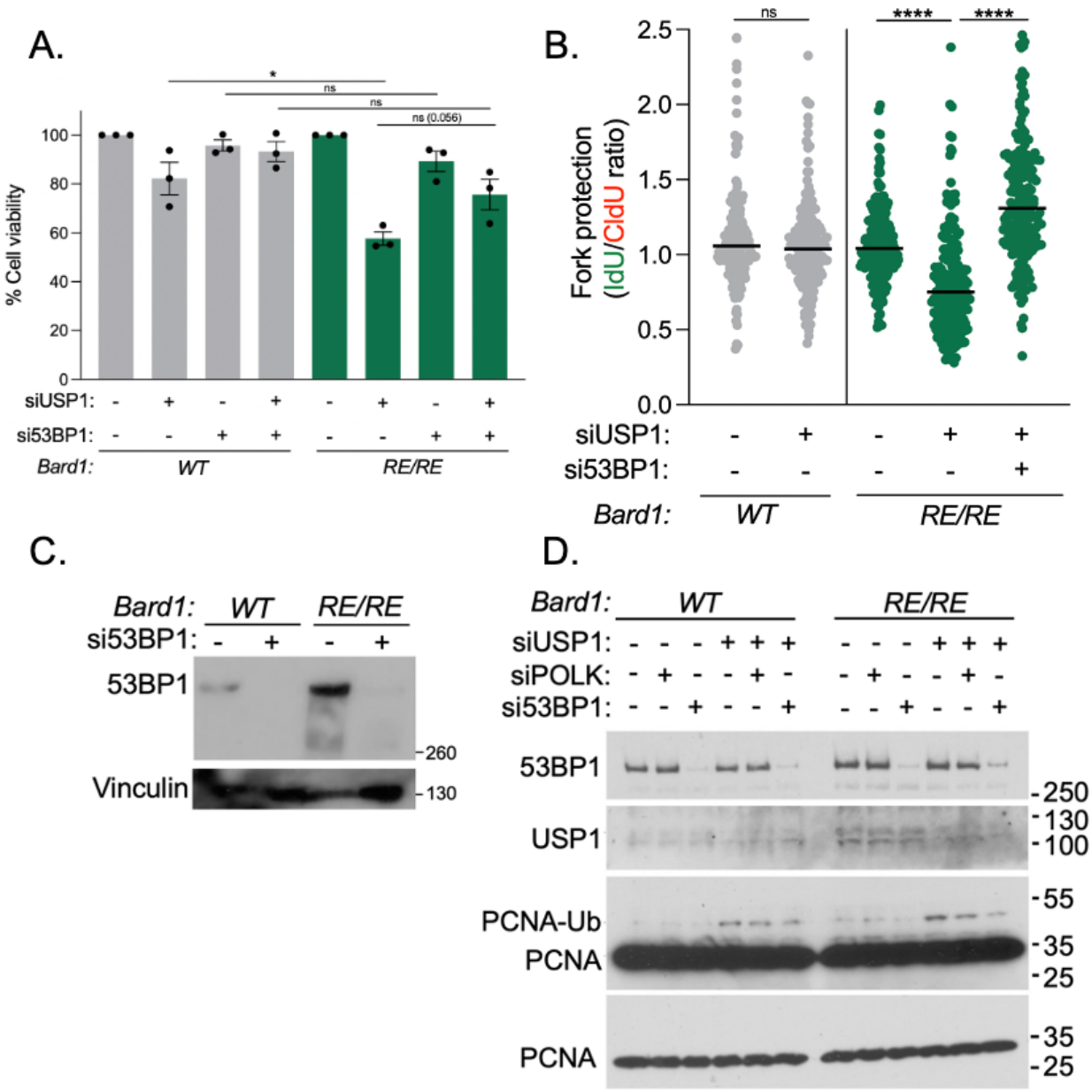

Figure 6.5. USP1 sensitivity and fork protection defect can be rescued by the loss of 53BP1 in *Bard1*$^{R93E/R93E}$ MEFs

A. Colony survival of WT and *Bard1*$^{R93E/R93E}$ cells treated with non-targeting control (NTC) or siRNA to USP1 and/or 53BP1. n=3 biological repeats. Statistical analyses performed using a two-tailed Student's t-Test; *= p≤0.05; ns = not significant.
B. Fork protection fibres IdU/CldU ratios from WT and *Bard1*$^{R93E/R93E}$ cells. Cells treated with CldU and IdU for 20 mins and 5 mM HU for 3 hr prior to spreading. Cells were treated with non-targeting control (NTC) or siRNA to USP1 and/or POLK. N ≥ 200 fibres from 2 biological replicates.
C. Western blot analysis of 53BP1 protein levels following non-targeting control (−) or 53BP1 (+) targeting siRNA treatment. Vinculin was used as a loading control.
D. Western blot analysis of 53BP1, USP1, PCNA-Ub, PCNA protein levels following non-targeting control (−) or USP1/POLK/53BP1 (+) targeting siRNA treatment. PCNA was used as a loading control. *Ruth Densham.*

6.2.6. SMARCAD1 likely plays an important role in *Bard1*$^{R93E/R93E}$ cells.

In Densham *et al* (2016) the chromatin remodeller SMARCAD1 was identified to play a role in binding to ubiquitinated H2A modified at the C-terminal tail at K125/127/129 by BRCA1/BARD1 (Densham and Morris, 2017; Densham et al., 2016). As well as HR, SMARCAD1 has been recognised for its role in replication where it regulates the levels of PCNA to retain genome integrity (Lo et al., 2021). The association between the role of BRCA1/BARD1 E3 ligase activity and the activation of SMARCAD1 in DSB repair and its localisation to unperturbed replication forks to interact with and coordinate levels of PCNA piqued our interest. This is because our *Bard1*$^{R93E/R93E}$ cells were designed as an E3 ligase defective model, and these cells exhibit increased modification of PCNA, so we wondered whether our MEFs rely on SMARCAD1 for survival.

We noted that SMARCAD1 expression levels were elevated in *Bard1*$^{R93E/R93E}$ cells compared to WT cells (Fig.6.6D). Next, we treated both WT and *Bard1*$^{R93E/R93E}$ cells with siRNA to SMARCAD1 and witnessed a significant reduction in cell viability in

Bard1$^{R93E/R93E}$ cells down to 53% survival compared to 82% survival in WT cells (Fig.6.6A). We then explored the co-treatment of siRNA to SMARCAD1 and USP1 and noticed that the loss of both proteins could improve cell toxicity to the loss of SMARCAD1 (Fig.6.6B). Therefore, it is possible that USP1 is taking part in the toxicity associated with the absence of SMARCAD1 in *Bard1*$^{R93E/R93E}$ cells and vice versa. Previous studies showed that SMARCAD1 is important for displacing 53BP1 from stalled replication forks, so the increase in SMARCAD1 and thereby the removal of 53BP1 could be relieving the stress associated with disallowing forks to restart (Lo et al., 2021). Also, upon treatment with 1 mM HU for 1 hour, SMARCAD1 is significantly elevated in both WT and *Bard1*$^{R93E/R93E}$ cells, albeit with considerably higher expression in *Bard1*$^{R93E/R93E}$ cells due to higher baseline levels of SMARCAD1 in the untreated cells (Fig.6.6C). In summation, these data infer that SMARCAD1 is essential for survival in *Bard1*$^{R93E/R93E}$ cells and could have a role in replication.

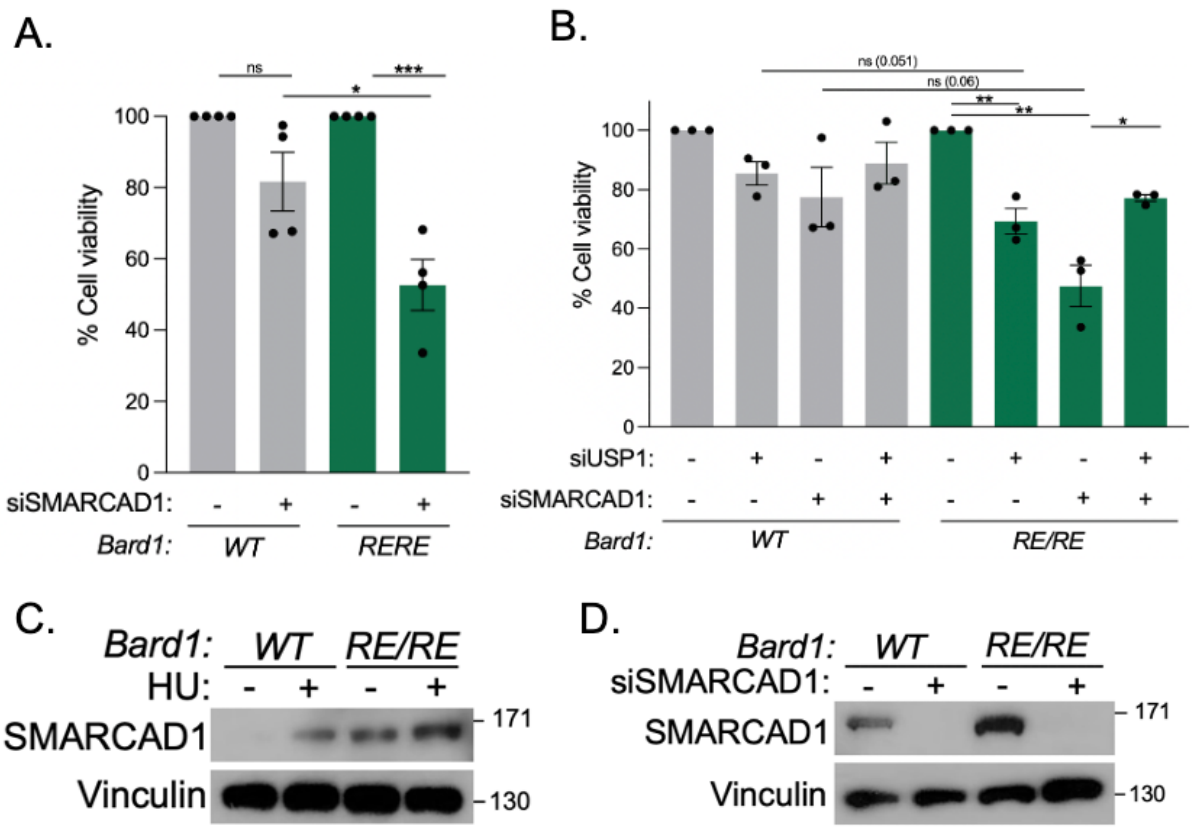

Figure.6.6. SMARCAD1 likely plays an important role in *Bard1*$^{R93E/R93E}$ cells.

A. Colony survival of WT and *Bard1*$^{R93E/R93E}$ cells treated with non-targeting control (NTC) or siRNA to SMARCAD1. n=4 biological repeats. Statistical analyses performed using a two-tailed Student's *t*-Test; ***= p≤0.001; ns = not significant.

B. Colony survival of WT and *Bard1*$^{R93E/R93E}$ cells treated with non-targeting control (NTC) or siRNA to SMARCAD1 and/or USP1. n=3 biological repeats. Statistical analyses performed using a two-tailed Student's *t*-Test; **= p≤0.01; *= p≤0.05; ns = not significant.

C. Western blot analysis of SMARCAD1 protein levels following 1 hr 1mM HU treatment (+). Vinculin was used as a loading control.

D. Western blot analysis of SMARCAD1 protein levels following non-targeting control (−) or SMARCAD1 (+) targeting siRNA treatment. Vinculin was used as a loading control.

6.2.7. USP48 is overexpressed in *Bard1*$^{R93E/R93E}$ cells.

Another DUB of interest in the context of BRCA1/BARD1 E3 ligase activity is USP48, which we explored briefly in Chapter 4. USP48 specifically de-ubiquitinates H2A at K125/127/129, counteracting its E3 ligase function and is essential to prevent extensive resection and SSA at DSBs (Uckelmann et al., 2018). Work carried out by Uckelmann *et al* (2018) highlighted that USP48 antagonises the activation of SMARCAD1 for the repositioning of 53BP1 from the break site and so restricts DNA end resection (Uckelmann et al., 2018). Surprisingly, we witnessed elevated USP48 expression levels in *Bard1*$^{R93E/R93E}$ cells compared to WT cells (Fig.6.7A). We also noted a slight cell sensitivity to the absence of USP48 in *Bard1*$^{R93E/R93E}$ cells compared to WT cells, although not significant and requires more repeats (Fig.6.7B). Fig.6.7A highlights that there could be a relationship between USP1 and USP48 as the loss of USP1 or POLK appears to reduce USP48 expression levels (Fig.6.7A). We have seen reduced USP48 expression upon the loss of USP1 on numerous occasions and could implicate USP48 in the network for TLS coordination. There is a possibility that USP48 has an alternative role within replication that requires further investigation.

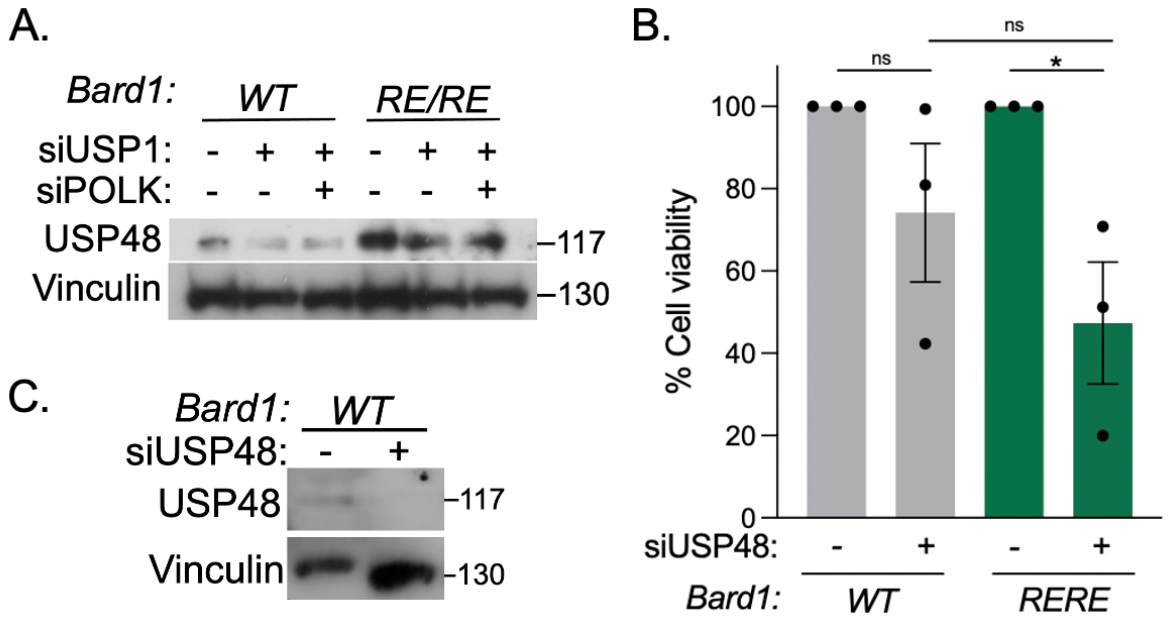

Figure. 6.7. USP48 is overexpressed in *Bard1*$^{R93E/R93E}$ cells.

A. Western blot analysis of USP48 protein levels following non-targeting control (−) or USP1 and/or POLK (+) targeting siRNA treatment. Vinculin was used as a loading control.
B. Colony survival of WT and *Bard1*$^{R93E/R93E}$ cells treated with non-targeting control (NTC) or siRNA to SMARCAD1. n=3 biological repeats. Statistical analyses performed using a two-tailed Student's *t*-Test; *= p≤0.05; ns = not significant.
C. Western blot analysis of USP48 protein levels in WT cells following non-targeting control (−) or USP48 (+) targeting siRNA treatment. Vinculin was used as a loading control.

6.2.8. Retroviral expression of H2A-Ub reduces cell sensitivity to USP1 loss in *Bard1*$^{R93E/R93E}$ cells.

So far, in Chapters 5 and 6 we have shown that *Bard1*$^{R93E/R93E}$ cells elicit reduced H2A ubiquitination, form ssDNA gaps, are sensitive to the loss of USP1 and SMARCAD1, with USP1-dependent toxicity partially reversed with the loss of POLK and 53BP1 and a complete rescue upon SMUG1 co-depletion, reduced RAD18 foci formation, are sensitive to the REV1 TLS inhibitor JH-RE-06, and a have potential reliance on USP48. These results suggest that the potentially defective modification of H2A at the C-terminal tail at K125/127/129 in *Bard1*$^{R93E/R93E}$ cells could have a role in the toxicity to USP1 removal.

Therefore, we generated H2A mutant -Ub fusion constructs which could be retrovirally expressed in *Bard1*$^{R93E/R93E}$ cells which have target lysines mutated to arginines in which ubiquitin has been fused to the C-terminus or both N- and C-termini to determine which position of modified H2A could be responsible for the phenotypes observed, such as USP1 dependency. The H2A fusion constructs include: WT-H2A, H2A bearing K-to-R substitution for all sites (K13/15/118/119/125/127/129R), H2A bearing K-to-R

substitution with ubiquitin or a blue fluorescent protein (BFP) (as a control for C-terminal protein fusion) fused to the C-terminus, H2A bearing the K-to-R alteration with ubiquitin fused to the N- and or C-terminus and one with the N- and C-terminus together (Fig.6.8A). However, due to time constraints only the following constructs were used for the following experiments: WT-H2A, H2A-Ub, Ub-H2A-Ub, H2A-BFP. In future, these experiments will be repeated using the entire set of H2A-Ub fusions. All the following H2A fusion constructs contained an HA tag, therefore we were able to visualise successful retroviral expression of the constructs in our *Bard1*$^{R93E/R93E}$ cells using an HA antibody (Fig.6.8B). Zhu *et al* (2011) demonstrated that the H2A-Ub fusion proteins can be incorporated into chromatin (Zhu et al., 2011).

We retrovirally infected *Bard1*$^{R93E/R93E}$ cells with the H2A fusion constructs shown in figure 6.8A (only the following constructs were used for the following experiment: WT-H2A, H2A-Ub, Ub-H2A-Ub, H2A-BFP) and treated the infected cells plus WT and *Bard1*$^{R93E/R93E}$ cells treated with empty vector with siRNA to USP1. On observation we noted that *Bard1*$^{R93E/R93E}$ cells treated with empty vector were sensitive to the loss of USP1 and that strikingly the loss of cell viability associated with USP1 depletion could be rescued to WT levels by the H2A-Ub C-terminal fusion construct (Fig.6.8C). Yet, the infection of WT-H2A, Ub-H2A-Ub, nor H2A-BFP could not rescue cell toxicity to USP1 depletion in *Bard1*$^{R93E/R93E}$ (Fig.6.8C). These data demonstrate that H2A with ubiquitin fused to the C-terminus, not by any alternative globular protein, could suppress cell sensitivity to USP1 loss in *Bard1*$^{R93E/R93E}$ cells. However, the effect of overexpressing the fusion constructs on cell viability on their own should be determined before we can come to a more definitive answer.

Another phenotype seen in *Bard1*$^{R93E/R93E}$ cells is the poor formation of RAD18 foci, so we wanted to determine whether the H2A-Ub C-terminal fusion construct, able to rescue cell sensitivity to USP1 loss, could rescue RAD18 foci numbers. We noted a decline in the percentage of cells with RAD18 foci in *Bard1*$^{R93E/R93E}$ cells to 22% compared to 63% in WT cells like we have seen previously in Fig.6.3B. The retroviral infection of *Bard1*$^{R93E/R93E}$ cells with H2A-Ub and Ub-H2A-Ub displayed a slight increase in the percentage of RAD18 foci at 39% and 34% respectively, with no or little change witnessed in H2A-WT and H2A-BFP treated cells (Fig.6.8D). However, H2A-Ub infection was not able to restore the percentage of cells containing RAD18 foci to the numbers seen in WT cells, unlike the USP1 sensitivity data. These results suggest that ubiquitin fused to the C-terminus of H2A could be important for RAD18 foci formation.

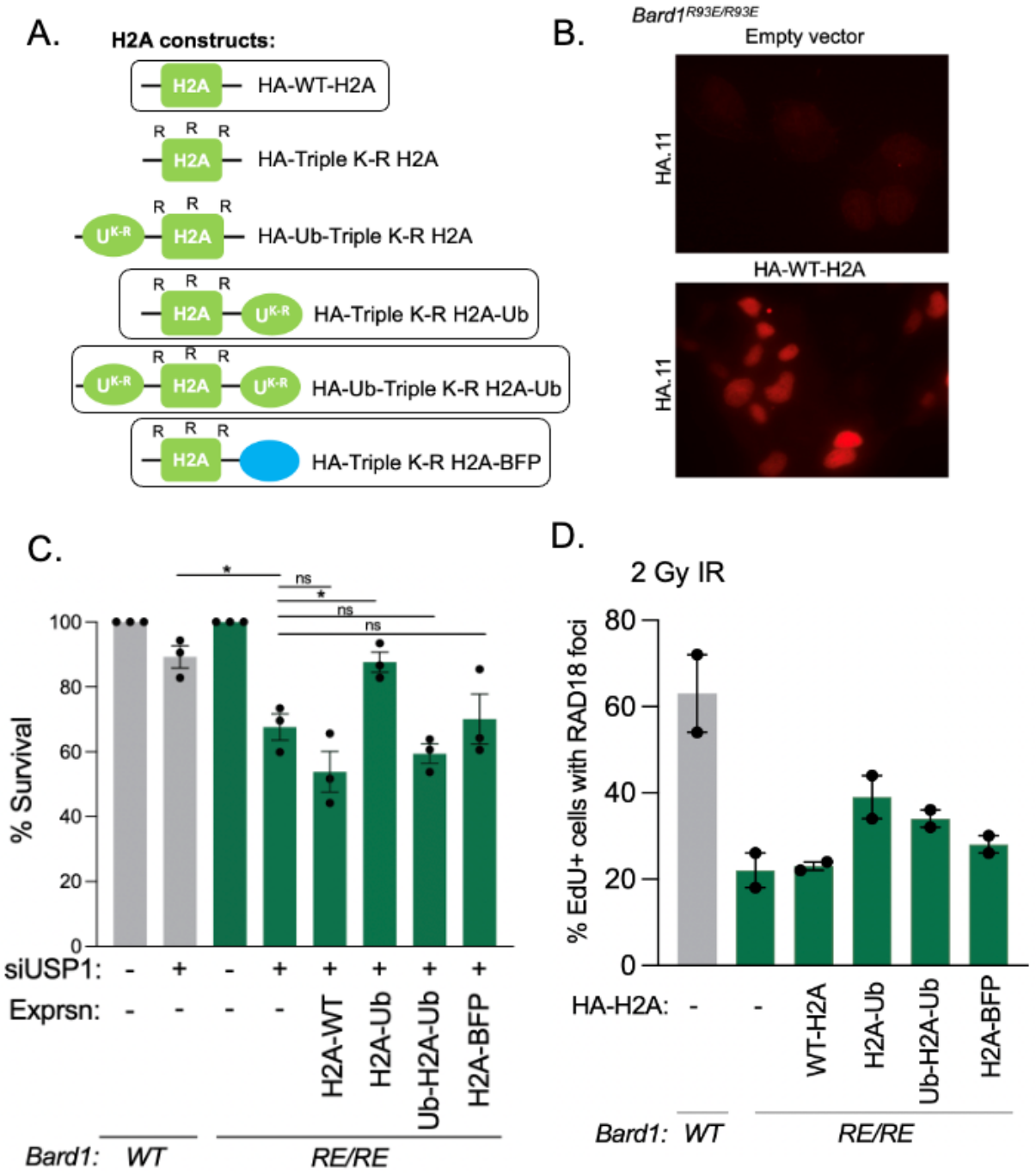

Figure. 6.8. Retroviral expression of H2A-Ub reduces cell sensitivity to USP1 loss in *Bard1*$^{R93E/R93E}$ cells.

A. Schematic showing the HA-tagged H2A fusion constructs and the modifications on the N/C-termini. (Those circled were used for the following experiments).
B. Representative image showing the retroviral transduction of WT-H2A into *Bard1*$^{R93E/R93E}$ cells using the HA.11 tag.

C. Colony survival in MEFs infected with empty vector (EV) or containing H2A fusion mutants treated with siRNA targeting USP1. n=3 biological repeats. Data are mean ± SEM. Statistics analysis performed using a two-tailed Student's *t*-Test; *= p≤0.5; ns = not significant.
D. Quantification of RAD18 foci post 3 hr 2 Gy IR in asynchronous *Bard1*$^{R93E/R93E}$ cells infected with empty vector (EV) or containing H2A fusion mutants. n=60 cells from 2 biological replicates per condition.

6.3. Discussion

In the current study, we have demonstrated that the DUB USP1 contributes to survival in *Bard1*$^{R93E/R93E}$ cells. In the absence of USP1, there is a significant reduction in cell viability, a loss of replication fork protection, increased expression of the nucleases MRE11 and DNA2, and enhanced susceptibility to Olaparib. Next, we wanted to identify what is driving the toxicity to the loss of USP1 in the homozygous MEFs. The loss of USP1 led to the persistent mono-ubiquitination of PCNA likely mediating aberrant recruitment of error-prone TLS polymerases such as POLK. Additionally, *Bard1*$^{R93E/R93E}$ cells showed a susceptibility to the TLS inhibitor JH-RE-06 which could be reversed upon USP1 loss. Co-depletion of USP1 and POLK could alleviate all the toxic features associated with USP1 loss in *Bard1*$^{R93E/R93E}$ cells. We also explored whether the removal of 53BP1, thought to potentially promote TLS (Chen et al., 2022), could relieve USP1-depleted toxicity. Indeed, the co-depletion of USP1 and 53BP1 was able to reduce USP1-depleted cell toxicity. Finally, the artificial fusion of ubiquitin onto H2A in *Bard1*$^{R93E/R93E}$ cells could suppress cell sensitivity to USP1 loss.

In *BRCA1*-deficient cells, USP1 is significantly upregulated to stabilise replication forks (Lim et al., 2018). The significant increase in USP1 expression and cell sensitivity to USP1 loss in *Bard1*$^{R93E/R93E}$ cells correlates with the overexpression of USP1 in

BRCA1-deficient breast and ovarian tumours (Koboldt et al., 2012; Lim et al., 2018). USP1 has been associated with the progression of numerous cancers including prostate cancer and glioma (Liu et al., 2016; Niu et al., 2020; Sonego et al., 2019). We noted that the USP1 inhibitor ML323 rendered *Bard1*$^{R93E/R93E}$ cells slightly more sensitive than WT cells (Fig.6.1F). The increased susceptibility will likely be due to aberrant PCNA mono-ubiquitination and error-prone TLS polymerase activation which we would expect to be higher in *Bard1*$^{R93E/R93E}$ cells.

Not only this, but we noted that treatment with the USP1 inhibitor ML323 resulted in increased USP1 expression (Fig.6.3F). In keeping with this, Coleman *et al* (2022) deduced that ML323 treatment retains full-length USP1 on DNA by preventing USP1 autocleavage, important for USP1 degradation and increased PCNA mono-ubiquitination, elevating cell cytotoxicity (Coleman et al., 2022). We can speculate that ML323 is potentially "trapping" USP1 onto DNA.

Remarkably, the inhibition of USP1 by ML323 and PARP by Olaparib are synergistic in *Bard1*$^{R93E/R93E}$ cells despite showing HR proficiency (Fig.6.3E). That being so, our data correlates with Simoneau *et al* (2023) as they demonstrated that the combined inhibition of USP1 and PARP sensitised not only *BRCA1/2*-mutated tumours but *BRCA1/2* WT cancers and *BRCA1/2*-mutated cells that retained RAD51 foci formation, a marker of HR proficiency (Simoneau et al., 2023a). Our results elicit that USP1 is a promising inhibitor for HR-proficient cancers, indicating that alternative DNA damage vulnerabilities such as dysregulated TLS or fork protection could render HR-proficient *BRCA1/2* WT cells vulnerable to USP1 loss (Lim et al., 2018; Simoneau et al., 2023a).

We have shown that there is elevated mono-ubiquitination of PCNA in *Bard1*$^{R93E/R93E}$ cells and this is enhanced further by the depletion of USP1 (Fig.6.2A). However, we have not identified whether the modification of PCNA is taking place at K164, the site known to be ubiquitinated by the E3 ligase RAD18. This could be the case because mono-ubiquitination at K164 is the site that promotes the switch to low-fidelity TLS polymerases (Choe and Moldovan, 2017; Leung et al., 2019; Hedglin and Benkovic, 2015). However, as the recruitment of RAD18 is likely impaired, it could be due to the modification at an alternative site on PCNA. It is also plausible that the mono-ubiquitination of PCNA is not important as it could just be a consequence of the loss of USP1. Another avenue that we need to explore is FANCD2 which is the other major target of USP1 de-ubiquitination.

DNA2/MRE11 expression was elevated in *Bard1*$^{R93E/R93E}$ cells depleted of USP1 (Fig.6.2A), which is in line with the loss of replication fork stability in the USP1-depleted MEFs. Similarly, Lim *et al* (2018) showed that replication fork instability could be rescued upon depletion of DNA2 and MRE11 in *BRCA1*-deficient cells treated with a USP1 inhibitor (Lim et al., 2018). Also, they showed that the knockdown of SMARCAL1, important for fork reversal (Kolinjivadi et al., 2017b), can rescue replication fork instability induced by USP1 inhibition in *BRCA1*-depleted cells (Lim et al., 2018), so it's possible that the co-depletion of USP1 and SMARCAL1 could rescue USP1-depleted fork de-protection phenotype in *Bard1*$^{R93E/R93E}$ cells. In contrast, Thakar *et al* (2020) demonstrated that the ubiquitination of PCNA protects stalled replication forks from degradation by DNA2 and its co-factor WRN (Thakar et al., 2020; Thangavel et al., 2015). These conflicting data indicate that the balance and coordination of PCNA mono-ubiquitination is important for replication fork stability.

The loss of fork protection and cell viability in the absence of USP1 could be improved upon the loss of the TLS polymerase POLK *Bard1*$^{R93E/R93E}$ cells (Fig.6.2B). Our results are in line with those from Lim *et al* (2018) who demonstrate that the loss of RAD18 can rescue the synthetic lethal relationship between BRCA1 and USP1 (Lim et al., 2018). The dysregulation of POLK to the replication fork has resulted in enhanced micronuclei and reduced replication fork speeds in a POLK-dependent manner (Pillaire et al., 2007; Jones et al., 2012). Interestingly, the increased interaction between PCNA and POLK, not dependent on its ubiquitin binding activity, can increase genomic instability (Jones et al., 2012). Whereas the elevated fork speed due to USP1 auto-cleavage is independent of POLK (Coleman et al., 2022). USP1 knock-out cells induced fork stalling, which could be reversed by depleting POLK, suggesting that aberrant retention of POLK is stimulating fork stalling (Coleman et al., 2022). An association between POLK and cancer development has been made in non-small cell lung cancer patients (O-Wang et al., 2001). However, it must be noted that POLK has roles beyond TLS such as the repair of UV damage by NER and in microsatellite stability (Ogi and Lehmann, 2006; Ogi et al., 2010; Hile and Eckert, 2008; Hile et al., 2012). It appears that the dysregulation of POLK in the absence of USP1 is driving replication fork instability in *Bard1*$^{R93E/R93E}$ cells.

RAD18 expression remains unchanged between WT and *Bard1*$^{R93E/R93E}$ cells (Fig.6.3A), regardless of USP1/POLK loss. However, we demonstrated that *Bard1*$^{R93E/R93E}$ cells cannot form high numbers of RAD18 foci, irrespective of USP1 loss or co-depletion with POLK (Fig.6.3B). Whereas WT MEFs formed RAD18 foci which were elevated further when treated with siRNA targeting USP1(Fig.6.3B). These results coincide with those from Tian *et al* (2013) who show that the percentage of

RAD18 foci are reduced in *BRCA1*-deficient cells and in cells mutated at the I26A-BRCA1 position (Tian et al., 2013). These data along with ours show that the E3 ligase activity of BRCA1/BARD1 is likely important for RAD18 recruitment. However, our *Bard1*$^{R93E/R93E}$ cells show elevated PCNA mono-ubiquitination compared to WT cells so could there be an alternative E3 ligase modifying PCNA. For example, *RAD18*-deficient cells retain residual PCNA mono-ubiquitination (Simpson et al., 2006; Leung et al., 2019; Huang et al., 2006; Arakawa et al., 2006).

There is the possibility that an alternative protein such as RFWD3 could be modifying PCNA in *Bard1*$^{R93E/R93E}$ cells. Gallina *et al* (2020) demonstrated that RFWD3 regulates TLS by poly-ubiquitinating PCNA to mediate gap filling DNA synthesis, which requires the RFWD3-RPA interaction which is also important for exchanging RPA with RAD51 for HR (Elia et al., 2015; Inano et al., 2017; Gallina et al., 2021). Also, RFWD3 promotes recruitment of the DNA translocase ZRANB3 to ubiquitinated targets that are substrates of USP1 for fork remodelling, and showing opposing roles for RFWD3 and USP1 regarding ZRANB3 (Moore et al., 2023). In addition, RNF8, Cullin-4-RING-ligase (CRL4)-Ddb1-Cdt2 (CRL4^{Cdt2}) and HLTF can mono-ubiquitinate PCNA, however their contribution is thought to be insignificant compared to RAD18 (Simpson et al., 2006; Leung et al., 2019; Huang et al., 2006; Arakawa et al., 2006; Lin et al., 2011).

The rescue of deleterious features associated with USP1 loss upon co-treatment with siRNA to POLK in *Bard1*$^{R93E/R93E}$ cells led us to explore whether our cells are dependent on TLS-mediated DNA damage bypass. Taglialatela *et al* (2021) investigated that the TLS inhibitor JH-RE-06 is cytotoxic in *BRCA1*-deficient cells which is dependent on PRIMPOL-dependent ssDNA gap formation (Taglialatela et al., 2021). Also, Taglialatela *et al* (2021) demonstrated that upon PRIMPOL depletion, the loss of

cell viability and reduced S1 nuclease-mediated tract shortening induced by JH-RE-06 were completely reversed. These results suggest that PRIMPOL-dependent ssDNA gaps generated in *BRCA1*-deficient cells are filled by the error-prone TLS REV1-Polζ complex resulting in spontaneous mutagenesis (Taglialatela et al., 2021; Vaisman and Woodgate, 2017; Waters et al., 2009). Likewise, the knockdown of the uracil deglycosylase SMUG1 suppressed cell sensitivity to JH-RE-06 and the co-depletion of PRIMPOL and SMUG1 did not generate additive effects indicating that they function in the same pathway (Taglialatela et al., 2021). We found that our *Bard1*$^{R93E/R93E}$ cells are more sensitive to the TLS inhibitor JH-RE-06 compared to WT MEFs and that cell sensitivity to USP1 loss could be reversed upon co-depletion with SMUG1 (Fig.6.4A,C). These data correlate with our findings that *Bard1*$^{R93E/R93E}$ cells show cell sensitivity to USP1 that can be reversed upon SMUG1 co-depletion and that these cells form PRIMPOL- and SMUG1-dependent ssDNA gaps, indicating that these gaps are likely repaired by the REV1-Polζ complex because they are sensitive to the REV1 inhibitor JH-RE-06. So, we need to look at the capability of PRR in *Bard1*$^{R93E/R93E}$ cells. Tirman *et al* (2021) show that REV1-Polζ are responsible for gap filling in both S and G2 phase of the cell cycle (Tirman et al., 2021b). Therefore, in future the PRR capability of *Bard1*$^{R93E/R93E}$ cells in G2/M should be evaluated. Additionally, it would be interesting to determine whether the loss of PRIMPOL or SMUG1 reverses JH-RE-06 inhibitor sensitivity, like the results shown by others (Taglialatela et al., 2021).

Previous findings have suggested that RAD18 facilitates the repair of ssDNA gaps by promoting gap filling by the REV1-Polζ complex, as the loss of RAD18 phenocopies JH-RE-06-mediated REV1-Polζ inhibition in *BRCA1/2*-deficient cells (Taglialatela et al., 2021). We have shown that our *Bard1*$^{R93E/R93E}$ cells demonstrate unaffected RAD18

expression, albeit compromised recruitment. Is it possible that *Bard1*$^{R93E/R93E}$ cells, that are HR-proficient and not entirely *BRCA1*-defective, like the cells used in Taglialatela *et al* (2021), could harbour reduced gap filling capabilities by REV1-Polζ due to impaired RAD18 recruitment. However, the hyperactivation of PCNA mono-ubiquitination and the fact that USP1 depletion is driving POLK-mediated toxicity indicates that TLS is still being activated. These results reiterate the requirement for analysis of the gap-filling capability of *Bard1*$^{R93E/R93E}$ cells.

We observed that loss of cell viability and the loss of fork protection in USP1-depleted *Bard1*$^{R93E/R93E}$ cells could be improved upon the loss of 53BP1 (Fig.6.5A,B). It appears that in *BRCA1*-deficient cells, 53BP1 is important for the regulation of TLS (Chen et al., 2022). Both BRCA1 and 53BP1 have been implicated in the contribution to the tolerance of DNA adducts and *53BP1*$^{-/-}$ cells are more sensitive to replication stalling adducts compared to DSBs which indicates that 53BP1 primarily functions in the regulation of lesion bypass (Chen et al., 2022). In the absence of SMARCAD1, the enrichment of 53BP1 at replication forks has been associated with the untimely removal of PCNA via ATAD5 which leads to increased ssDNA, fork stalling and inefficient fork restart (Lo et al., 2021). Recently it has been suggested that 53BP1 interacts with the RNA primer of Okazaki fragments and that the loss of 53BP1 disturbs the processing of lagging strands in unperturbed DNA replication, so could have a role in ssDNA gaps in *BRCA1*-deficient cells but this remains unknown (Leriche et al., 2023).

We identified that *Bard1*$^{R93E/R93E}$ cells are sensitive to the loss of SMARCAD1, show increased SMARCAD1 expression levels particularly when treated with HU, and that co-depletion of SMARCAD1 and USP1 can improved SMARCAD1-depleted toxicity

(Fig.6.6). Taken together, these results indicate that SMARCAD1 is important in *Bard1*$^{R93E/R93E}$ cells, particularly in situations of replication stress and drive a portion of cell toxicity in the absence of USP1. Lo *et al* (2021) revealed that SMARCAD1 is important for replication fork stability and is associated with active replication forks by interacting with PCNA and maintaining PCNA levels (Lo et al., 2021). Also, they hypothesise that SMARCAD1 is necessary for 53BP1 displacement from nucleosomes to suppress the 53BP1-ATAD5 complex (ATAD5 being the PCNA-unloader) from the untimely dissociation of PCNA resulting in defects such as inefficient fork restart, stalling and ssDNA gap formation (Lo et al., 2021). Further work into the role of SMARCAD1 in *Bard1*$^{R93E/R93E}$ cells with regards to replication is required.

Remarkably, USP48 expression was significantly increased in *Bard1*$^{R93E/R93E}$ cells and the loss of USP1 led to a reduction in USP48 expression in *Bard1*$^{R93E/R93E}$ cells, suggesting an epistatic relationship (Fig.6.7). USP48 has been associated with the FA pathway is synthetic viable in FA-defective cells, as the loss of USP48 reduced the sensitivity of FA-defective cells to ICL agents (Velimezi et al., 2018). This could tie in with USP1 which is a known de-ubiquitinase of FANCD2-FANCI important for regulating the repair of ICLs (Rennie et al., 2021).

H2A at K125/127/129 was identified as a ubiquitin ligase target of BRCA1/BARD1 (Kalb et al., 2014; Zhu et al., 2011; Mallery et al., 2002), so we generated artificial H2A mutant-Ub fusion proteins and infected *Bard1*$^{R93E/R93E}$ cells retrovirally. The H2A-Ub constructs were generated based on findings from our group in Densham *et al* (2016) to restore resection and HR in the BARD1-depleted human cells (Densham et al., 2016; Zhu et al., 2011). Zhu *et al* (2011) and Densham *et al* (2016) demonstrated that the H2A-Ub fusion proteins can be successfully incorporated into chromatin and

recapitulate the function of natural H2A-ubiquitin (Zhu et al., 2011; Densham et al., 2016). We wanted to determine whether the artificial fusion of ubiquitin to H2A on the C-terminus could improve cell sensitivity to USP1 loss. We transduced *Bard1*$^{R93E/R93E}$ cells with retrovirus expressing empty vector, WT-H2A, H2A-Ub, Ub-H2A-Ub and H2A-BFP and treated the cells with siRNA to USP1. The *Bard1*$^{R93E/R93E}$ cells expressing H2A-Ub was the only fusion construct to restore cell sensitivity to USP1 loss (Fig.6.8C). It would have been interesting to explore the Ub-H2A fusion on the N-terminus alone and the K-R mutant completely devolved of modifications, but due to time constraints this will be added in future. Also, it is imperative that we retrovirally infect WT cells to determine the toxicity regarding the overexpression of fusion constructs alone.

We also witnessed a slight increase in the percentage of RAD18 foci, indicating that the modification of H2A at the C-terminus could be involved in mediating RAD18 recruitment (Fig.6.8D). However, the data could be skewed due to the involvement of non-transformed cells so in future we should counter stain for H2A. There are caveats to the use of artificial H2A-Ub complementation as they can induce off target effects in cells as the modification of H2A is tightly regulated for cellular functions such as replication and transcription so can be toxic to cells (Higashi et al., 2010).

Overall, our results have demonstrated a reliance on USP1 in our *Bard1*$^{R93E/R93E}$ cells. The loss of USP1 created deleterious results such as the loss of fork protection, loss of cell viability and elevated PCNA-ubiquitination. These defects could be reduced by the co-depletion with the POLK and 53BP1. The cell sensitivity to USP1 loss in *Bard1*$^{R93E/R93E}$ cells appeared to be reversed upon the artificial addition of H2A modified at the C-terminal tail, indicating that the modification of H2A by BRCA1/BARD1 could be important for suppressing the reliance on USP1 for survival. The results from this

chapter are preliminary but give us an insight into the relationship between USP1 and BRCA1/BARD1.

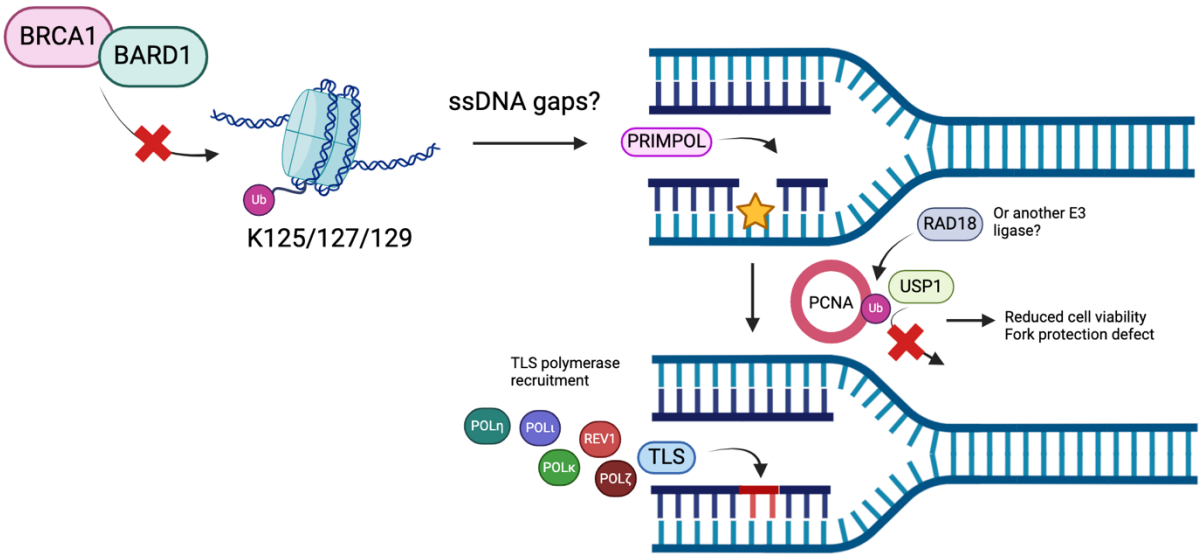

Figure 6.9. Working model: Could BRCA1/BARD1 E3 ligase activity have a role in DNA replication? *Bard1*$^{R93E/R93E}$ cells appear to have reduced H2A ubiquitination and present PRIMPOL dependent ssDNA gaps. Upon the depletion of USP1, *Bard1*$^{R93E/R93E}$ cells show reduced cell viability, increased PCNA mono-ubiquitination, a defect in fork protection, and are sensitive to the inhibition of TLS.

7. Overall Discussion and Future Perspectives

Overall, in this thesis we have identified that the sensitivity of *Brca1/53bp1*-mutated cells to Polθ loss and *53bp1*-deficient cells to Polθ inhibition require RAD52 and that the suppression of RAD52 could relieve these deleterious phenotypes. We have begun to characterise *Bard1*$^{R93E/R93E}$ MEFs in the hope of elucidating the role of the E3 ubiquitin ligase function of BRCA1/BARD1. Finally, we used *Bard1*$^{R93E/R93E}$ MEFs to further understand the synthetic lethal relationship between BRCA1 and USP1. The work in this thesis has helped uncover previously unanswered questions about survival pathways supporting BRCA1/BARD1 function and will likely be meaningful for the development of inhibitors in the clinic for patients harbouring *BRCA1/BARD1* mutations.

7.1. RAD51 is important to suppress ssDNA gap formation

In Chapters 3 and 4 we identified Polθ as a synthetic lethal target in *Brca1*$^{C61G/C61G}$ *53bp1*$^{-/-}$ cells and found that the Polθ inhibitor ART558 could specifically target *Brca1*$^{C61G/C61G}$ *53bp1*$^{-/-}$ cells over *Brca1*$^{+/+}$*53bp1*$^{-/-}$ cells. We wanted to elucidate whether we could overcome Polθ sensitivity by overexpressing the binding partner of BRCA1, BARD1. BARD1 overexpression could improve the localisation of C61G-BRCA1 and provide resistance to Polθ loss and inhibition. However, BARD1 overexpression could only rescue these phenotypes with the BARD1-RAD51 interaction intact. Disrupting the interaction using the BARD1-AAE mutant could no longer rescue cell susceptibility to Polθ loss nor reduce the accumulation of RAD52 foci mentioned in Chapter 4. The overexpression of BRCA2 BRC4-RPA, important for the exchange of RPA and RAD51 could overcome Polθ loss and inhibition. Therefore,

we can speculate that improving the recruitment of BRCA1/BARD1-RAD51 and BRCA2-RAD51 can overcome the need for Polθ. Tirman *et al* (2023) demonstrated the fundamentality of RAD51 for gap filling during S but not G2 phase (Tirman et al., 2021b) and Piberger *et al* (2021) highlighted a role for RAD51-mediated HR repair of ssDNA gaps generated by PRIMPOL re-priming (Piberger et al., 2020). Also, RAD51 is important for ssDNA gap prevention on the lagging strand and the depletion of RAD51 has been shown to increase the recruitment of Polθ to chromatin (Mann et al., 2022). Therefore, RAD51 is an important driver of ssDNA gap suppression when overexpressing BARD1 and BRC4-RPA in *Brca1*$^{C61G/C61G}$ *53bp1*$^{-/-}$ cells.

7.2. Where is the toxic engagement of Polθ taking place?

In this thesis we identified that in Chapter 4 Polθ limits RAD52-mediated suppression of ssDNA DNA synthesis gap fill-in during G2/M of the cell cycle. RAD52 contributes to the toxicity via its RAD52-RPA interaction and by promoting the association between MRE11:ssDNA. Suppressing the actions of RAD52:RPA;MRE11 improved cell viability in the absence of Polθ in *Brca1*$^{C61G/C61G}$ *53bp1*$^{-/-}$ cells. Whereas in Ronson *et al* (2023), ART558-mediated inhibition of Polθ in *Brca1*$^{C61G/C61G}$ *53bp1*$^{-/-}$ cells sustained the interaction between MRE11 and ssDNA regardless of RAD52 suppression, and DNA synthesis gap fill-in could take place in Polθ inhibited cells once RAD52 and Polθ are lost, indicating that there is a role regarding inhibited Polθ (Ronson et al., 2023). Also, in Chapter 3 we revealed that the overexpression of BARD1 and BRC4-RPA could suppress S1-sensitive nascent DNA and support G2/M DNA synthesis irrespective of whether Polθ was lost or inhibited in *Brca1*$^{C61G/C61G}$ *53bp1*$^{-/-}$ cells. Therefore, we cannot identify whether the ssDNA gaps reside at or behind the fork or later in G2/M for the toxic engagement of Polθ, either are possible.

It is likely that Polθ engagement is different at ssDNA G2/M gaps in the absence of appropriate RPA/RAD51 exchange and loading carried out by BRCA1/2. BRC4 has been found to be involved in the RAD51:Polα interaction and ssDNA gap suppression (Kolinjivadi et al., 2017b). It is plausible that the polymerase domain of Polθ could insert and carry out DNA synthesis opposite a toxic lesion and thus limit ssDNA gap formation at the fork (Yoon et al., 2014; Mann et al., 2022). Also, in the case that the Polθ polymerase is inhibited and there is a lack of RAD51 at the fork, Polθ could be "trapped" at junctions (Zatreanu et al., 2021). In other cases, the phosphorylation of Polθ by PLK1 activates Polθ recruitment during mitosis and mitotic cells treated with IR showed Polθ foci, suggesting that the role of Polθ is not restricted to S-phase and does not rule out the possibility of the involvement of Polθ in filling in ssDNA gaps post replication (Brambati et al., 2023; Gelot et al., 2023). As a consequence, a crucial question is to identify the location of the toxic engagement of Polθ.

7.3. What is the source of G2/M ssDNA gaps?

A fundamental question following this thesis is to elucidate the source of G2/M ssDNA gaps. From our data we can speculate that 53BP1 has a role in suppressing resection at ssDNA gaps in a similar process performed at DSBs (Setiaputra and Durocher, 2019), and therefore limiting the accumulation of RAD52 at resected DNA. In *BRCA1/2*-deficient cells ssDNA gaps can accumulate on the lagging strand in a PRIMPOL-independent manner due to Polα-dependent repriming (Guilliam and Yeeles, 2020; Taylor and Yeeles, 2018; Mehta et al., 2022). Mann *et al* (2022) suggested that a large fraction of RAD51 is bound to lagging strands at the replication fork, and that in the absence of RAD51, Polθ recruitment to chromatin is enhanced (Mann et al., 2022). ssDNA gaps can be repaired by HR-mediated mechanisms,

however *Brca1*$^{C61G/C61G}$ *53bp1*$^{-/-}$ cells exhibit competent yet sub-optimal HR and likely have to rely on error-prone TLS polymerases such as Polθ for gap filling in G2 (Tirman et al., 2021b; Piberger et al., 2020; Pilzecker et al., 2016). Tirman *et al* (2021) suggest that BRCA1/2 promote gap filling during both S and G2 phase by limiting MRE11 activity, whereas RAD51 acts solely in S-phase (Tirman et al., 2021b). REV1-POLζ polymerases act in G2 to support gap filling and so it would be interesting to measure PRR in the absence of the REV1-POLζ complex in *Brca1*$^{C61G/C61G}$ *53bp1*$^{-/-}$ cells. Proficient function of BRCA1/BRCA2-RAD51 could prevent MRE11-dependent gaps (Hashimoto et al., 2010; Kolinjivadi et al., 2017b; Tirman et al., 2021b), and RAD51 could promote Polα-mediated Okazaki fragment extension (Kolinjivadi et al., 2017b) or BRCA2/RAD51 bound to the lagging strand could contact the replisome component MCM10 to restrain fork progression to recouple the synthesis of leading and lagging strands (Kang et al., 2021). Overall, more work is required to identify the source of G2/M ssDNA gaps and to study how ssDNA gap sizes change upon inhibition of different TLS polymerases to compare the efficiency of gap filling. such as looking at the differences between Polθ and REV1-POLζ in G2.

7.4. Elucidating the role of Polθ in RAD52-mediated suppression of G2/M ssDNA gaps.

To further understand the role of Polθ regarding the limitation of RAD52-mediated suppression of G2/M ssDNA gap synthesis, we need to specifically evaluate the role of the domains of Polθ by using polymerase and helicase-dead mutants. The Polθ helicase domain removes RPA from ssDNA (Mateos-Gomez et al., 2017; Schaub et al., 2022), and therefore could limit the rise in RPA:RAD52 interactions. It would be

important to determine whether the Polθ inhibitor ART558, which acts by inhibiting the polymerase domain of Polθ, could reduce the activity of the helicase domain simultaneously, thereby accumulating toxic RPA:RAD52. In keeping with this, our analysis has been done using a Polθ polymerase domain inhibitor ART558, so it is fundamental that we look into Polθ inhibitors that target the helicase domain such as Novobiocin (Zhou et al., 2021). It would also be useful to compare our results using an alternative Polθ inhibitor that targets the polymerase domain, such as RP-6658 (Bubenik et al., 2022). In Ronson *et al* (2023) we used CAL51 human breast cancer epithelial cells to reinforce that DNA synthesis gap fill-in could be reduced by Polθ loss and reinstated with low concentrations of RAD52 inhibitor or siRNA in a human system (Ronson et al., 2023). Future work would require additional *BRCA1*-deficient human cell lines as well as the murine models.

RAD52 interacts with RPA and RPA enhances the function of nucleases, so we cannot discount the possibility that RAD52 can encourage interactions from nucleases additional to MRE11, such as EXO1 and DNA2. For example, *Brca1*$^{\Delta 11/\Delta 11}$*53bp1*$^{-/-}$cells are sensitive to ART558 treatment but this sensitivity can be suppressed upon EXO1 depletion (Zatreanu et al., 2021). It is a limitation that RAD52 could reduce the accumulation of MRE11 due to a reduction in resection. In keeping with this, toxicity associated with ART558 treatment in *Brca1*$^{C61G/C61G}$ *53bp1*$^{-/-}$ cells could not be reversed upon the suppression of RAD51:RPA:MRE11, yet others have shown that suppressing MRE11 can reverse Polθ inhibition by the “Polθ inhibitor” in *BRCA1/2*-depleted cells (Schrempf et al., 2022; Mann et al., 2022). We only witnessed a marginal increase in ssDNA gap generation when Polθ is inhibited (Ronson et al., 2023). Despite others having highlighted a more significant impact on Polθ inhibition and

ssDNA gap formation in *BRCA1/2*-defective cells (Schrempf et al., 2022; Belan et al., 2022; Mann et al., 2022). For example, Mann *et al* (2022) demonstrated significant S1 treated DNA fibre shortening in DLD1 BRCA2$^{-/-}$ cells treated with a Polθ inhibitor (Mann et al., 2022); Schrempf *et al* (2022) showed increased replication gap formation upon Polθ loss in RPE *BRCA1*$^{-/-}$*TP53*$^{-/-}$ cells (Schrempf et al., 2022) and Belan *et al* (2022) demonstrated increased ssDNA gaps in cells depleted of both BRCA2 and Polθ together but not alone (Belan et al., 2022). Interestingly the discrepancies between our minimal and their significant impact on S1-mediated tract shortening upon Polθ inhibition in *BRCA1/2*-mutated cell lines could be due to their use of single tract length measurements over our combined used of the IdU/CldU ratio. Using the single tract measurement loses a lot of information regarding the total fibre length which can drastically vary. Also, we are using *Brca1*$^{C61G/C61G}$ *53bp1*$^{-/-}$ cells which are not entirely HR-defective unlike cells completely devoid of BRCA1 function. We don't discount that there could be a role for inhibited Polθ in ssDNA gap exacerbation.

In Chapter 3 we found that *Brca1*$^{P62R/P62R}$ MEFs appeared to phenocopy *Brca1*$^{C61G/C61G}$ *53bp1*$^{-/-}$ cells. *Brca1*$^{P62R/P62R}$ mice were viable and did not require crossing on a *53bp1*$^{-/-}$ background. These data suggest that the C61G-BRCA1 mutation is more severe than P62R-BRCA1. C61 makes up part of Site II of the Zn^{2+} binding site which is fundamental for the macromolecular interactions forming the BRCA1//BARD1 heterodimer (Au and Henderson, 2005; Nelson and Holt, 2010), whereas P62 does not, which could play a role in its severity and the degree of destabilisation of the Zn^{2+} binding sites. It is interesting to note the severity of cell sensitivity to Polθ depletion in *Brca1*$^{P62R/P62R}$ MEFs compared to *Brca1*$^{C61G/C61G}$ *53bp1*$^{-/-}$ cells, but *Brca1*$^{P62R/P62R}$ MEFs are not on a *53bp1*$^{-/-}$ background which plays a part in ART558 sensitivity as shown by

others (Krais et al., 2023). It would be interesting to explore levels to which the BRCA1/BARD1 heterodimer is disrupted, E3 ligase activity, and sensitivity to ART558 in *Brca1*$^{P62R/P62R}$ cells for future experiments. It would also be important to cross *Brca1*$^{P62R/P62R}$ mice on a *53bp1*$^{-/-}$ background for comparison.

7.5. Identifying the role of ART558

It remains poorly understood why the inhibition of Polθ does not lead to the activation of alternative TLS polymerases to perform gap filling in its absence, could it be because Polθ contains a polymerase and a helicase domain which could be less error prone than other TLS DNA polymerases such as REV1-POLζ (Mann et al., 2022; Schrempf et al., 2022; Belan et al., 2022).

We observed that ART558-mediated toxicity could not be reversed by low doses of RAD52 inhibition in *Brca1*$^{C61G/C61G}$ *53bp1*$^{-/-}$ cells, whereas we could in *Brca1*$^{+/+}$ *53bp1*$^{-/-}$ cells. Strikingly, we also highlighted that ART558-mediated toxicity could be reversed by low doses of RAD52 inhibition in *Bard1*$^{R93E/R93E}$ cells. Chapters' 3 and 4 as well as work from our paper Ronson *et al* (2023) have showed that when Polθ is absent, RAD52 accumulations can suppress ssDNA gap filling in G2/M (Ronson et al., 2023). However, low doses of the RAD52 inhibitor 6-OHD could not rescue Polθ inhibition in BRCA1/53BP1-deficient cells but in those solely deprived of 53BP1 or USP48. So, in Chapter 5 the rescue of ART558 treatment by suppressing RAD52 in *Bard1*$^{R93E/R93E}$ cells allowed us to speculate how ART558-inhibited Polθ is differently deleterious in *Brca1*$^{C61G/C61G}$ *53bp1*$^{-/-}$ cells. In Chapter 3 we could reverse ssDNA gap generation and promote G2/M fill-in DNA synthesis by the exogenous expression of BARD1 or BRC4-RPA in *Brca1*$^{C61G/C61G}$ *53bp1*$^{-/-}$ cells so could the fact that *Bard1*$^{R93E/R93E}$ cells do not

show a defect in BARD1 and thus BRCA1 recruitment be important for this rescue. However, *Bard1*$^{R93E/R93E}$ cells still generate ssDNA gaps, which suggests that it is not this phenotype that is leading to the potential "trapping" of ART558. This lends us to speculate whether the R93E-BARD1 mutation somehow impacts the ability of RAD51 to promote gap filling in S phase (Tirman et al., 2021b). It is possible that Polθ is engaged differently at G2/M gaps, and therefore it is essential to determine the functionality of PRR in G2/M in *Bard1*$^{R93E/R93E}$ cells.

7.6. Exploring the relationship between BRCA1/BARD1 and USP1

In Chapter 6 we showed that *Brca1*$^{R93E/R93E}$ MEFs are sensitive to the loss of USP1. A recent publication has suggested that USP1 promotes the MRE11 and EXO1-mediated expansion of PRIMPOL-dependent ssDNA gaps. The upregulation of USP1 in *Brca1*$^{R93E/R93E}$ MEFs could go some way to explain the PRIMPOL-generated ssDNA gaps present (Nusawardhana et al., 2024). In reverse, the toxicity underlying the inhibition of USP1 in *BRCA1*-deficient cells is thought to be due to the accumulation of ssDNA gaps (Simoneau et al., 2023a; Da Costa et al., 2023). So, USP1 promotes ssDNA gap formation in cells overexpressing PRIMPOL, but in situations lacking BRCA1, the loss of USP1 can generate ssDNA gaps. Therefore, more work is required to improve our understanding of USP1, replication ssDNA gap generation and cell sensitivity.

We have demonstrated that *Bard1*$^{R93E/R93E}$ cells rely on USP1 for survival likely by promoting replication fork stability, which has been demonstrated in *BRCA1*-deficient tumour cells (Lim et al., 2018). However, this opens up questions as to what is making USP1 synthetic sick in cells that harbour the R93E-BARD1 protein. Our results suggest

that the loss of USP1 results in the toxic exacerbation of TLS polymerases, such as POLK and REV1 in *Bard1*$^{R93E/R93E}$ cells. It suggests that the R93E-BARD1 mutation disrupts the ability of cells to protect the replication fork from persistent TLS (Pathania et al., 2011; Tian et al., 2013). It appears that USP1-depleted *Bard1*$^{R93E/R93E}$ cells have destabilised forks which could be digested by nucleases such as MRE11 and DNA2. BRCA1 has been implicated in the promotion of DDT by directly interacting with RAD18, HLTF, Polη and REV1 (Tian et al., 2013), so could the R93E-BARD1 mutation disrupt any of these associations? A limitation of this work is that currently we are only using MEFs, so we should look at exploring R99E-BARD1 in a human system to determine whether the sensitivity to USP1 depletion can be reproduced. Also, we could mutate BRCA1 at I26A/L63A/K65A, suggested to be a "ligase dead" mutant of BRCA1, to decipher whether we can recapitulate the cell toxicity associated with USP1 depletion (Wang et al., 2023).

7.7. Is BRCA1/BARD1 modulating RAD18-mediated TLS?

In Chapter 6 we demonstrated that *Bard1*$^{R93E/R93E}$ cells, designed to be an E3 ligase defective mutant, elicit increased PCNA mono-ubiquitination, are sensitive to the loss of the DUB USP1 and the TLS inhibitor JH-RE-06. Also, the deleterious effects caused by USP1 loss in *Bard1*$^{R93E/R93E}$ cells can be reversed by the removal of the TLS polymerase POLK. The preprint Salas-Lloret *et al* (2023) denoted that BRCA1/BARD1 E3 ligase activity ubiquitinates PCNA at K164 at low levels in unperturbed conditions to prevent the accumulation of ssDNA gaps and promote smooth DNA replication, which is altered to RAD18-mediated ubiquitination of PCNA under conditions of replication stress (Salas-Lloret et al., 2023). They used a technique termed Targets of Ubiquitin Ligases Identified by Proteomics (TULIP) to identify ubiquitin E3-specific

targets (Salas-Lloret et al., 2019). Salas-Lloret *et al* (2023) generated BARD1-TULIP2 and surprisingly demonstrated that BARD1 preferentially directs the ubiquitination of alternative targets to BRCA1 and that BARD1-facilitated ubiquitination of PCNA is important for limiting ssDNA formation (Salas-Lloret et al., 2023). This is interesting because BRCA1/BARD1 ubiquitination of PCNA could be lost in our *Bard1*$^{R93E/R93E}$ cells, leading to ubiquitination by alternative and potentially more error prone E3 ligases. It is imperative to explore whether BRCA1/BARD1 modifies PCNA and whether this modification is lost in *Bard1*$^{R93E/R93E}$ cells.

It is possible that BRCA1/BARD1 ligase activity is regulating DDT pathways such as fork reversal, TLS, and repriming. *Bard1*$^{R93E/R93E}$ cells exhibit ssDNA gaps and defective RAD18 foci formation, and Salas-Lloret *et al* (2023) witnessed an increase in ssDNA gaps in the absence of functional BRCA1/BARD1 E3 ligase activity (Salas-Lloret et al., 2023). We speculate that defective BRCA1/BARD1 E3 ligase activity and the generation of ssDNA gaps is a consequence of the poor localisation of RAD18, somehow leading to uncoordinated and thus aberrant TLS activation. Salas-Lloret *et al* (2023) also indicate that RAD18 and BARD1 modify PCNA in alternative pathways, one under unperturbed and the other in perturbed conditions (Salas-Lloret et al., 2023). It is plausible that RAD18 could be poorly coordinated and causing aberrant mono-ubiquitination of PCNA or that there is an alternative E3 ligase modifying PCNA in *Bard1*$^{R93E/R93E}$ cells. Tian *et al* (2013) showed that the RING domain, specifically E3 ligase activity, is important for regulating RAD18 function and acts upstream of RAD18 for the regulation of PCNA mono-ubiquitination and TLS polymerase recruitment (Tian et al., 2013). Tian *et al* (2013) demonstrated that BRCA1 interacts with RAD18 via both the RING and BRCT domains of BRCA1, albeit more strongly via the RING domain

(Tian et al., 2013). Future work using an isolation of proteins on nascent DNA (iPOND) is imperative for the spatiotemporal analysis of proteins at replication forks or on chromatin post DNA replication, so we can identify protein recruitment and post-translational modifications at the fork in *Bard1*$^{R93E/R93E}$ cells (Sirbu et al., 2012).

7.8. BRCA1/BARD1 ubiquitination of H2A has a role in DSB repair but could also be implicated in DNA replication.

Altogether, using the results from Chapters 5 and 6 we can speculate a potential area of focus in *Bard1*$^{R93E/R93E}$ cells. BRCA1/BARD1-mediated ubiquitination of H2A at the C-terminus has been shown to activate the chromatin remodeller SMARCAD1 which binds to ubiquitinated H2A via its CUE domains (Densham et al., 2016). SMARCAD1 interacts with damage-proximal nucleosomes to mediate the repositioning of 53BP1 for the completion of resection (Densham et al., 2016; Densham and Morris, 2017). In terms of replication, SMARCAD1 has been implicated in regulating the levels of PCNA to reduce replication stress. SMARCAD1 localises to replication forks and removes 53BP1-associated nucleosomes to prevent the ill-timed accumulation of 53BP1-ATAD5 (Lo et al., 2021). ATAD5-RLC unloads PCNA from DNA after the termination of replication leading to increased fork stalling (Kang et al., 2019; Kubota et al., 2015; Kanellis et al., 2003; Mejlvang et al., 2014; Lo et al., 2021).

Moreover, SMARCAD1 is required for the stability of replication forks in *BRCA1*-mutated cells, as the loss of SMARCAD1 resulted in enriched 53BP1 and depleted PCNA levels at the fork (Lo et al., 2021). In our *Bard1*$^{R93E/R93E}$ cells we noted increased SMARCAD1 expression particularly upon HU treatment, a sensitivity to the loss of SMARCAD1, and an improvement in cell viability by co-treatment with siRNA to

SMARCAD1 and USP1. We can speculate that SMARCAD1 loss may increase the turnover of PCNA-ubiquitination thereby reducing the impact of USP1 loss. The loss of 53BP1 in *Bard1*$^{R93E/R93E}$ cells improved cell viability in the absence of USP1 and reduced the ubiquitination of PCNA, suggesting that the error-prone TLS pathway is no longer required in the absence of 53BP1. Future work should explore whether the SMARCAD1/53BP1/ATAD5/PCNA pathway is impacted by the reduced modification of H2A at the C-terminus in our *Bard1*$^{R93E/R93E}$ cells.

Chromatin Assembly Factor-1 (CAF-1) mediates replication-coupled nucleosome assembly which functions in a PCNA-dependent manner (Shibahara and Stillman, 1999; Zhang et al., 2000b). In *BRCA1/2*-deficient cells Polα-dependent ssDNA gaps form and retain PCNA-CAF-1 complexes, reducing their availability to be recycled and used at on-going forks and in turn leads to defects in nucleosome deposition (Thakar et al., 2022). The loss of PCNA ubiquitination can perturb Okazaki fragment ligation due to ssDNA gap accumulation which can restrict PCNA unloading by ATAD5 leading to defective nucleosome assembly by CAF-1, rendering replication forks susceptible to nucleolytic degradation by DNA2 (Thakar et al., 2020). It is possible that *Bard1*$^{R93E/R93E}$ cells upregulate PCNA-ubiquitination to prevent fork protection defects as a non-canonical mechanism in the absence of functional BRCA1/BARD1.

Watanabe *et al* (2009) identified that RAD18-mediated mono-ubiquitination of 53BP1 can retain 53BP1 at DSB sites (Watanabe et al., 2009). Yet, more recently RAD18 has been shown to bind NCP^{H2AK15ub} which explains the accumulation of RAD18 at DSBs and its displacement of 53BP1 from nucleosomes, but this has not been shown under physiological conditions. 53BP1 and RAD18 have antagonistic roles in DNA repair as RAD18 promotes HR by inhibiting the recruitment of 53BP1 to DSBs (Watanabe et al.,

2009; Helchowski et al., 2013; Hu et al., 2017). It is therefore possible that the poor localisation of RAD18 could be associated with the toxic activity associated with the potential accumulation of 53BP1 in USP1-depleted *Bard1*$^{R93E/R93E}$ cells.

An additional factor to place in this complex network is the DUB USP48 which is also involved in the H2A-Ub/SMARCAD1/53BP1 network regarding DSBs. USP48 cleaves the modification of H2A at the C-terminal tail (K125/127/129) which limits SMARCAD1 remodelling and limits 53BP1 re-positioning (Uckelmann et al., 2018). USP48 was significantly elevated in *Bard1*$^{R93E/R93E}$ cells which is unexpected as these cells have reduced H2A-ubiquitination, which implies that USP48 could have an alternative role within these cells as upon the loss of USP1 or POLK, USP48 expression appeared reduced. There is evidence for the potential role of USP48 in replication stress shown by an iPOND carried out by Lecona *et al* (2016) which identified that USP48 is upregulated around replisomes at sites of nascent chromatin (Lecona et al., 2016) and cell viability in A549 cells treated with shRNA to USP48 treated with 2mM HU was increased which is indicative of a role of USP48 in replication stress (Yuan et al., 2014).

Although there is limited association between H2A-ubiquitination at K125/127/129 and DNA replication, RNF168-dependent ubiquitination of H2A at K13/15 has been implicated in unperturbed DNA replication during S-phase (Schmid et al., 2018). Remarkably, RNF168 is localised to replication forks and can physically interact with PCNA and the loss of RNF168 can lead to reduced replication fork progression (Schmid et al., 2018). It is unknown whether there is crosstalk between the H2A-ubiquitin marks on the N- and C-terminus, and requires further investigation (Mattiroli and Penengo, 2021). RNF168 and BRCA1/BARD1 share a common E2 UbcH5c to target distinct regions of H2A on opposite sides by orienting UbcH5c to the N- ad C-

terminal tails (Hu et al., 2024). We can speculate that the modification of H2A by BRCA1/BARD1 could have a role in replication as well as DSB repair.

We used H2A-Ub fusion proteins to determine whether the modification of H2A at the C-terminal tail was suppressing cell sensitivity to USP1 loss in *Bard1*$^{R93E/R93E}$ cells. Our data has given us an indication that the fusion of ubiquitin on the C-terminus could relieve cell toxicity caused by USP1 depletion. However, we require the N-terminal fusion of ubiquitin to rule out of the possibility that this modification is important, and the fusions constructs should be overexpressed in WT cells to determine their toxicity alone. We must consider the drawbacks associated with the use of H2A-Ub fusion constructs as it is plausible that the overexpression of fusion constructs is inducing widespread disruption to chromatin and thus induce artifacts. However, it is currently challenging to analyse the modification of H2A at K125/127/129 by BRCA1/BARD1 due to the lack of a commercial antibody available and the very low basal cellular amount of H2A ubiquitination by BRCA1/BARD1. It is imperative that we determine whether H2A-ubiquitination at the C-terminus is disrupted in *Bard1*$^{R93E/R93E}$ cells using mass spectrometry, although the extreme C-terminus of H2A is lysine-rich which impedes the use of traditional mass spectrometry methods that use trypsin digestion which would form incredibly small peptide fragments (Witus et al., 2022).

The next question to answer is whether the expression of H2A-Ub can suppress ssDNA gap formation in *Bard1*$^{R93E/R93E}$ cells. These results would indicate whether BRCA1/BARD1 mono-ubiquitination of H2A could be important for the suppression of ssDNA gaps. In Chapter 5 we demonstrated that the loss of RAP80 reduced BARD1 foci formation and sensitised *Bard1*$^{R93E/R93E}$ cells to the PARPi Olaparib. Our results coincide with those from Sherker *et al* (2021) who speculate that BRCA1 recruitment

is controlled by the interaction between BRCA1 BRCT and RAP80 and the other via the BRCA1 RING domain and the RNF168-mediated ubiquitination of H2A K13/15 (Sherker et al., 2021). The latter potentially by the BRCA1/BARD1-mediated ubiquitination of H2A at K125/127/129 to facilitate self-recruitment by promoting the displacement of 53BP1 from nucleosomes to modulate the access of H2AK13/15-Ub modified nucleosomes to BRCA1/BARD1 or for the positioning of BARD1 to interact with H2AK13/15-Ub (Sherker et al., 2021; Panagopoulos and Altmeyer, 2021). Therefore, future work using the H2A-Ub fusion constructs could help us answer whether BRCA1/BARD1 E3 ligase activity is essential for the recruitment of BRCA1 to DSBs in the absence of RAP80. It would be imperative to design a H2A-Ub antibody that specifically targets the BRCA1/BARD1 site on H2A at K125/127/129 to monitor the modification of H2A at the C-terminal tail directly.

7.9. Summary

To summarise, the work from this thesis has increased our understanding of the role of survival pathways supporting BRCA1 function. We have demonstrated that BRCA1/2-RAD51 interactions suppress S1-sensitive nascent DNA gaps and promote ssDNA gap fill-in in *Brca1*$^{C61G/C61G}$ *53bp1*$^{-/-}$ cells treated with siRNA to Polθ or the Polθ inhibitor ART558 (Chapter 3). We have highlighted that Polθ reduces RAD52-mediated suppression of G2/M gap filling in *Brca1*$^{C61G/C61G}$ *53bp1*$^{-/-}$ cells (Chapter 4). Both Chapters 3 and 4 provide important information for the development of Polθ inhibitors and improving the understanding of patient stratification regarding Polθ inhibitors and the probability of developing resistance. We have also identified that *Bard1*$^{R93E/R93E}$ cells, designed to be a E3 ligase defective model, generate ssDNA gaps and that the inhibition of USP1 could be a synthetic lethal target in the HR proficient *Bard1*$^{R93E/R93E}$

cells (Chapters 5 and 6). Finally, we showed that the expression of the H2A-Ub fusion at the C-terminal tail in *Bard1*$^{R93E/R93E}$ cells can suppress cell sensitivity to USP1 loss, indicating that the modification of H2A could be important in the PCNA/TLS pathway (Chapter 6). Overall, these results highlight the complexity regarding BRCA1/BARD1 activity and the non-canonical support that prevents genome instability.

8. List of References

Abel, K.J., Xu, J., Yin, G.Y., et al. (1995) Mouse Brca1: Localization, sequence analysis and identification of evolutionarily conserved domains. *Human Molecular Genetics*, 4 (12). doi:10.1093/hmg/4.12.2265.

Achar, Y.J., Balogh, D. and Haracska, L. (2011) Coordinated protein and DNA remodeling by human HLTF on stalled replication fork. *Proceedings of the National Academy of Sciences of the United States of America*, 108 (34). doi:10.1073/pnas.1101951108.

Adam, S., Rossi, S.E., Moatti, N., et al. (2021) The CIP2A–TOPBP1 axis safeguards chromosome stability and is a synthetic lethal target for BRCA-mutated cancer. *Nature Cancer*, 2 (12). doi:10.1038/s43018-021-00266-w.

Adamovich, A.I., Banerjee, T., Wingo, M., et al. (2019) Functional analysis of BARD1 missense variants in homology-directed repair and damage sensitivity. *PLoS Genetics*, 15 (3). doi:10.1371/journal.pgen.1008049.

Adamowicz, M. (2018) Breaking up with ATM. *Journal of Immunological Sciences*, 2 (1). doi:10.29245/2578-3009/2018/1.1108.

Adar, S., Izhar, L., Hendel, A., et al. (2009) Repair of gaps opposite lesions by homologous recombination in mammalian cells. *Nucleic Acids Research*, 37 (17). doi:10.1093/nar/gkp632.

Ahrabi, S., Sarkar, S., Pfister, S.X., et al. (2016) A role for human homologous recombination factors in suppressing microhomology-mediated end joining. *Nucleic Acids Research*, 44 (12). doi:10.1093/nar/gkw326.

Akbari, M., Otterlei, M., Diaz-Peña, J., et al. (2004) Repair of U/G and U/A in DNA by UNG2-associated repair complexes takes place predominantly by short-patch repair both in proliferating and growth-arrested cells. *Nucleic Acids Research*, 32 (18). doi:10.1093/nar/gkh872.

Alabert, C. and Groth, A. (2012) Chromatin replication and epigenome maintenance. *Nature Reviews Molecular Cell Biology*. 13 (3). doi:10.1038/nrm3288.

Alagoz, M., Katsuki, Y., Ogiwara, H., et al. (2015) SETDB1, HP1 and SUV39 promote repositioning of 53BP1 to extend resection during homologous recombination in G2 cells. *Nucleic Acids Research*. doi:10.1093/nar/gkv722.

Alexandrov, L.B., Nik-Zainal, S., Wedge, D.C., et al. (2013) Signatures of mutational processes in human cancer. *Nature*. doi:10.1038/nature12477.

Altieri, A., Dell'Aquila, M., Pentimalli, F., et al. (2020) SMART (Single Molecule Analysis of Resection Tracks) Technique for Assessing DNA end-Resection in Response to DNA Damage. *Bio-protocol*, 10 (15). doi:10.21769/BioProtoc.3701.

Ameziane, N., May, P., Haitjema, A., et al. (2015) A novel Fanconi anaemia subtype associated with a dominant-negative mutation in RAD51. *Nature Communications*, 6. doi:10.1038/ncomms9829.

Ammazzalorso, F., Pirzio, L.M., Bignami, M., et al. (2010) ATR and ATM differently regulate WRN to prevent DSBs at stalled replication forks and promote replication fork recovery. *EMBO Journal*, 29 (18). doi:10.1038/emboj.2010.205.

Anand, J., Chiou, L., Sciandra, C., et al. (2023) Roles of trans-lesion synthesis (TLS) DNA polymerases in tumorigenesis and cancer therapy. *NAR Cancer*. 5 (1). doi:10.1093/narcan/zcad005.

Anand, R., Ranjha, L., Cannavo, E., et al. (2016) Phosphorylated CtIP Functions as a Co-factor of the MRE11-RAD50-NBS1 Endonuclease in DNA End Resection. *Molecular Cell*, 64 (5). doi:10.1016/j.molcel.2016.10.017.

Anantha, R.W., Simhadri, S., Foo, T.K., et al. (2017) Functional and mutational landscapes of BRCA1 for homology-directed repair and therapy resistance. *eLife*. doi:10.7554/eLife.21350.

Andersen, P.L., Xu, F. and Xiao, W. (2008) Eukaryotic DNA damage tolerance and translesion synthesis through covalent modifications of PCNA. *Cell Research*. 18 (1). doi:10.1038/cr.2007.114.

Arakawa, H. and Iliakis, G. (2015) Alternative okazaki fragment ligation pathway by dna ligase III. *Genes*. 6 (2). doi:10.3390/genes6020385.

Arakawa, H., Moldovan, G.L., Saribasak, H., et al. (2006) A role for PCNA ubiquitination in immunoglobulin hypermutation. *PLoS Biology*, 4 (11). doi:10.1371/journal.pbio.0040366.

Arbel, M., Choudhary, K., Tfilin, O., et al. (2021) PCNA loaders and unloaders—One ring that rules them all. *Genes*. 12 (11). doi:10.3390/genes12111812.

Au, W.W.Y. and Henderson, B.R. (2005) The BRCA1 RING and BRCT domains cooperate in targeting BRCA1 to ionizing radiation-induced nuclear foci. *Journal of*

Biological Chemistry, 280 (8). doi:10.1074/jbc.M408879200.

Audebert, M., Salles, B. and Calsou, P. (2004) Involvement of poly(ADP-ribose) polymerase-1 and XRCC1/DNA ligase III in an alternative route for DNA double-strand breaks rejoining. *Journal of Biological Chemistry*, 279 (53). doi:10.1074/jbc.M404524200.

Audeh, M.W., Carmichael, J., Penson, R.T., et al. (2010) Oral poly(ADP-ribose) polymerase inhibitor olaparib in patients with BRCA1 or BRCA2 mutations and recurrent ovarian cancer: A proof-of-concept trial. *The Lancet*, 376 (9737). doi:10.1016/S0140-6736(10)60893-8.

Azarm, K. and Smith, S. (2020) Nuclear PARPs and genome integrity. *Genes and Development*. 34 (5). doi:10.1101/gad.334730.119.

Aze, A. and Maiorano, D. (2018) Recent advances in understanding DNA replication: Cell type–specific adaptation of the DNA replication program [version 1; referees: 2 approved]. *F1000Research*. 7. doi:10.12688/f1000research.15408.1.

Bagchi, S., Fredriksson, R. and Wallén-Mackenzie, Å. (2015) In Situ Proximity Ligation Assay (PLA). *Methods in Molecular Biology*, 1318. doi:10.1007/978-1-4939-2742-5_15.

Bai, G., Kermi, C., Stoy, H., et al. (2020) HLTF Promotes Fork Reversal, Limiting Replication Stress Resistance and Preventing Multiple Mechanisms of Unrestrained DNA Synthesis. *Molecular Cell*, 78 (6). doi:10.1016/j.molcel.2020.04.031.

Bailey, L.J., Bianchi, J. and Doherty, A.J. (2019) PrimPol is required for the maintenance of efficient nuclear and mitochondrial DNA replication in human cells. *Nucleic Acids Research*, 47 (8). doi:10.1093/nar/gkz056.

Bailey, L.J., Teague, R., Kolesar, P., et al. (2021) PLK1 regulates the PrimPol damage tolerance pathway during the cell cycle. *Science Advances*, 7 (49). doi:10.1126/sciadv.abh1004.

Bainbridge, L.J., Teague, R. and Doherty, A.J. (2021) Repriming DNA synthesis: An intrinsic restart pathway that maintains efficient genome replication. *Nucleic Acids Research*. 49 (9). doi:10.1093/nar/gkab176.

Barazas, M., Annunziato, S., Pettitt, S.J., et al. (2018) The CST Complex Mediates End Protection at Double-Strand Breaks and Promotes PARP Inhibitor Sensitivity in BRCA1-Deficient Cells. *Cell Reports*. doi:10.1016/j.celrep.2018.04.046.

Barber, L.J., Sandhu, S., Chen, L., et al. (2013) Secondary mutations in BRCA2 associated with clinical resistance to a PARP inhibitor. *Journal of Pathology*, 229 (3). doi:10.1002/path.4140.

Bartkova, J., Rezaei, N., Liontos, M., et al. (2006) Oncogene-induced senescence is part of the tumorigenesis barrier imposed by DNA damage checkpoints. *Nature*, 444 (7119). doi:10.1038/nature05268.

Becker, J.R., Bonnet, C., Clifford, G., et al. (2020) BARD1 links histone H2A Lysine-15 ubiquitination to initiation of BRCA1-dependent homologous recombination. *bioRxiv*. doi:10.1101/2020.06.01.127951.

Becker, J.R., Clifford, G., Bonnet, C., et al. (2021) BARD1 reads H2A lysine 15 ubiquitination to direct homologous recombination. *Nature*, 596 (7872). doi:10.1038/s41586-021-03776-w.

Becker, J.R., Cuella-Martin, R., Barazas, M., et al. (2018) The ASCIZ-DYNLL1 axis promotes 53BP1-dependent non-homologous end joining and PARP inhibitor sensitivity. *Nature Communications*, 9 (1). doi:10.1038/s41467-018-07855-x.

Belan, O., Sebald, M., Adamowicz, M., et al. (2022) POLQ seals post-replicative ssDNA gaps to maintain genome stability in BRCA-deficient cancer cells. *Molecular Cell*, 82 (24). doi:10.1016/j.molcel.2022.11.008.

Belotserkovskaya, R., Raga Gil, E., Lawrence, N., et al. (2020) PALB2 chromatin recruitment restores homologous recombination in BRCA1-deficient cells depleted of 53BP1. *Nature Communications*. doi:10.1038/s41467-020-14563-y.

Bennardo, N., Cheng, A., Huang, N., et al. (2008) Alternative-NHEJ is a mechanistically distinct pathway of mammalian chromosome break repair. *PLoS Genetics*, 4 (6). doi:10.1371/journal.pgen.1000110.

Bernstein, K.A., Gangloff, S. and Rothstein, R. (2010) The RecQ DNA helicases in DNA repair. *Annual Review of Genetics*. 44. doi:10.1146/annurev-genet-102209-163602.

Bernstein, K.A., Shor, E., Sunjevaric, I., et al. (2009) Sgs1 function in the repair of DNA replication intermediates is separable from its role in homologous recombinational repair. *EMBO Journal*, 28 (7). doi:10.1038/emboj.2009.28.

Berti, M., Chaudhuri, A.R., Thangavel, S., et al. (2013) Human RECQ1 promotes restart of replication forks reversed by DNA topoisomerase I inhibition. *Nature*

Structural and Molecular Biology, 20 (3). doi:10.1038/nsmb.2501.

Berti, M., Cortez, D. and Lopes, M. (2020a) The plasticity of DNA replication forks in response to clinically relevant genotoxic stress. *Nature Reviews Molecular Cell Biology*. 21 (10). doi:10.1038/s41580-020-0257-5.

Berti, M., Teloni, F., Mijic, S., et al. (2020b) Sequential role of RAD51 paralog complexes in replication fork remodeling and restart. *Nature Communications*, 11 (1). doi:10.1038/s41467-020-17324-z.

Bétous, R., Mason, A.C., Rambo, R.P., et al. (2012) SMARCAL1 catalyzes fork regression and holliday junction migration to maintain genome stability during DNA replication. *Genes and Development*, 26 (2). doi:10.1101/gad.178459.111.

Bhargava, R., Onyango, D.O. and Stark, J.M. (2016) Regulation of Single-Strand Annealing and its Role in Genome Maintenance. *Trends in Genetics*. 32 (9). doi:10.1016/j.tig.2016.06.007.

Bhowmick, R., Minocherhomji, S. and Hickson, I.D. (2016) RAD52 Facilitates Mitotic DNA Synthesis Following Replication Stress. *Molecular Cell*. doi:10.1016/j.molcel.2016.10.037.

Bi, X. (2015) Mechanism of DNA damage tolerance. *World Journal of Biological Chemistry*, 6 (3). doi:10.4331/wjbc.v6.i3.48.

Bianchi, J., Rudd, S.G., Jozwiakowski, S.K., et al. (2013) Primpol bypasses UV photoproducts during eukaryotic chromosomal DNA replication. *Molecular Cell*, 52 (4). doi:10.1016/j.molcel.2013.10.035.

Bienko, M., Green, C.M., Crosetto, N., et al. (2005) Biochemistry: Ubiquitin-binding domains in Y-family polymerases regulate translesion synthesis. *Science*, 310 (5755). doi:10.1126/science.1120615.

Bienstock, R.J., Darden, T., Wiseman, R., et al. (1996) Molecular modeling of the amino-terminal zinc ring domain of BRCA1. *Cancer Research*, 56 (11).

Biertümpfel, C., Zhao, Y., Kondo, Y., et al. (2011) Erratum: Structure and mechanism of human DNA polymerase η. *Nature*, 476 (7360). doi:10.1038/nature10338.

Billing, D., Horiguchi, M., Wu-Baer, F., et al. (2018) The BRCT Domains of the BRCA1 and BARD1 Tumor Suppressors Differentially Regulate Homology-Directed Repair and Stalled Fork Protection. *Molecular Cell*, 72 (1). doi:10.1016/j.molcel.2018.08.016.

Biswas, K., Das, R., Alter, B.P., et al. (2011) Acomprehensive functional

characterization of BRCA2 variants associated with Fanconi anemia using mouse ES cell-based assay. *Blood*, 118 (9). doi:10.1182/blood-2010-12-324541.

Black, S.J., Ozdemir, A.Y., Kashkina, E., et al. (2019) Molecular basis of microhomology-mediated end-joining by purified full-length Polθ. *Nature Communications*, 10 (1). doi:10.1038/s41467-019-12272-9.

Blackford, A.N. and Jackson, S.P. (2017) ATM, ATR, and DNA-PK: The Trinity at the Heart of the DNA Damage Response. *Molecular Cell*. 66 (6). doi:10.1016/j.molcel.2017.05.015.

Blasiak, J. (2021) Single-strand annealing in cancer. *International Journal of Molecular Sciences*. 22 (4). doi:10.3390/ijms22042167.

Blow, J.J. and Gillespie, P.J. (2008) Replication licensing and cancer - A fatal entanglement? *Nature Reviews Cancer*. 8 (10). doi:10.1038/nrc2500.

Blow, J.J. and Laskey, R.A. (1988) A role for the nuclear envelope in controlling DNA replication within the cell cycle. *Nature*, 332 (6164). doi:10.1038/332546a0.

Boehm, E.M., Spies, M. and Washington, M.T. (2016) PCNA tool belts and polymerase bridges form during translesion synthesis. *Nucleic Acids Research*, 44 (17). doi:10.1093/nar/gkw563.

Bohgaki, M., Bohgaki, T., El Ghamrasni, S., et al. (2013) RNF168 ubiquitylates 53BP1 and controls its response to DNA double-strand breaks. *Proceedings of the National Academy of Sciences of the United States of America*, 110 (52). doi:10.1073/pnas.1320302111.

Bonilla, B., Hengel, S.R., Grundy, M.K., et al. (2020) RAD51 Gene Family Structure and Function. *Annual Review of Genetics*. 54. doi:10.1146/annurev-genet-021920-092410.

Boos, D., Sanchez-Pulido, L., Rappas, M., et al. (2011) Regulation of DNA replication through Sld3-Dpb11 interaction is conserved from yeast to humans. *Current Biology*, 21 (13). doi:10.1016/j.cub.2011.05.057.

Borden, K.L.B. and Freemont, P.S. (1996) The RING finger domain: A recent example of a sequence-structure family. *Current Opinion in Structural Biology*, 6 (3). doi:10.1016/S0959-440X(96)80060-1.

Bordin, D.L., Lirussi, L. and Nilsen, H. (2021) Cellular response to endogenous DNA damage: DNA base modifications in gene expression regulation. *DNA Repair*, 99.

doi:10.1016/j.dnarep.2021.103051.

van den Bosch, M., Bree, R.T. and Lowndes, N.F. (2003) The MRN complex: Coordinating and mediating the response to broken chromosomes. *EMBO Reports*. 4 (9). doi:10.1038/sj.embor.embor925.

Bostian, A.C.L., Maddukuri, L., Reed, M.R., et al. (2016) Kynurenine Signaling Increases DNA Polymerase Kappa Expression and Promotes Genomic Instability in Glioblastoma Cells. *Chemical Research in Toxicology*, 29 (1). doi:10.1021/acs.chemrestox.5b00452.

Botuyan, M.V., Lee, J., Ward, I.M., et al. (2006) Structural Basis for the Methylation State-Specific Recognition of Histone H4-K20 by 53BP1 and Crb2 in DNA Repair. *Cell*, 127 (7). doi:10.1016/j.cell.2006.10.043.

Boulton, S.J. and Jackson, S.P. (1996) Saccharomyces cerevisiae Ku70 potentiates illegitimate DNA double-strand break repair and serves as a barrier to error-prone DNA repair pathways. *EMBO Journal*, 15 (18). doi:10.1002/j.1460-2075.1996.tb00890.x.

Bouwman, P., Aly, A., Escandell, J.M., et al. (2010) 53BP1 loss rescues BRCA1 deficiency and is associated with triple-negative and BRCA-mutated breast cancers. *Nature Structural and Molecular Biology*. doi:10.1038/nsmb.1831.

Bouwman, P., van der Gulden, H., van der Heijden, I., et al. (2013) A high-throughput functional complementation assay for classification of BRCA1 missense variants. *Cancer Discovery*, 3 (10). doi:10.1158/2159-8290.CD-13-0094.

Bowman, G.D., O'Donnell, M. and Kuriyan, J. (2004) Structural analysis of a eukaryotic sliding DNA clamp-clamp loader complex. *Nature*, 429 (6993). doi:10.1038/nature02585.

Brambati, A., Barry, R.M. and Sfeir, A. (2020) DNA polymerase theta (Polθ) – an error-prone polymerase necessary for genome stability. *Current Opinion in Genetics and Development*. 60. doi:10.1016/j.gde.2020.02.017.

Brambati, A., Sacco, O., Porcella, S., et al. (2023) RHINO directs MMEJ to repair DNA breaks in mitosis. *Science (New York, N.Y.)*, 381 (6658). doi:10.1126/science.adh3694.

Branzei, D. (2011) Ubiquitin family modifications and template switching. *FEBS Letters*. 585 (18). doi:10.1016/j.febslet.2011.04.053.

Brough, R., Bajrami, I., Vatcheva, R., et al. (2012) APRIN is a cell cycle specific

BRCA2-interacting protein required for genome integrity and a predictor of outcome after chemotherapy in breast cancer. *EMBO Journal*, 31 (5). doi:10.1038/emboj.2011.490.

Bryant, H.E., Schultz, N., Thomas, H.D., et al. (2005) Specific killing of BRCA2-deficient tumours with inhibitors of poly(ADP-ribose) polymerase. *Nature*. doi:10.1038/nature03443.

Brzovic, P.S., Keeffe, J.R., Nishikawa, H., et al. (2003) Binding and recognition in the assembly of an active BRCA1/BARD1 ubiquitin-ligase complex. *Proceedings of the National Academy of Sciences of the United States of America*. doi:10.1073/pnas.0836054100.

Brzovic, P.S., Meza, J., King, M.C., et al. (1998) The cancer-predisposing mutation C61G disrupts homodimer formation in the NH2-terminal BRCA1 RING finger domain. *Journal of Biological Chemistry*, 273 (14). doi:10.1074/jbc.273.14.7795.

Brzovic, P.S., Meza, J.E., King, M.C., et al. (2001a) BRCA1 RING domain cancer-predisposing mutations. Structural consequences and effects on protein-protein interactions. *Journal of Biological Chemistry*, 276 (44). doi:10.1074/jbc.M106551200.

Brzovic, P.S., Rajagopal, P., Hoyt, D.W., et al. (2001b) Structure of a BRCA1-BARD1 heterodimeric RING-RING complex. *Nature Structural Biology*, 8 (10). doi:10.1038/nsb1001-833.

Bubenik, M., Mader, P., Mochirian, P., et al. (2022) Identification of RP-6685, an Orally Bioavailable Compound that Inhibits the DNA Polymerase Activity of Polθ. *Journal of Medicinal Chemistry*, 65 (19). doi:10.1021/acs.jmedchem.2c00998.

Bugreev, D. V., Rossi, M.J. and Mazin, A. V. (2011) Cooperation of RAD51 and RAD54 in regression of a model replication fork. *Nucleic Acids Research*, 39 (6). doi:10.1093/nar/gkq1139.

Buis, J., Stoneham, T., Spehalski, E., et al. (2012) Mre11 regulates CtIP-dependent double-strand break repair by interaction with CDK2. *Nature Structural and Molecular Biology*. doi:10.1038/nsmb.2212.

Bunting, S.F., Callén, E., Kozak, M.L., et al. (2012) BRCA1 Functions Independently of Homologous Recombination in DNA Interstrand Crosslink Repair. *Molecular Cell*. doi:10.1016/j.molcel.2012.02.015.

Bunting, S.F., Callén, E., Wong, N., et al. (2010) 53BP1 inhibits homologous

recombination in brca1-deficient cells by blocking resection of DNA breaks. *Cell*. doi:10.1016/j.cell.2010.03.012.

Burgers, P.M.J. and Kunkel, T.A. (2017) Eukaryotic DNA replication fork. *Annual Review of Biochemistry*. 86. doi:10.1146/annurev-biochem-061516-044709.

Burkovics, P., Sebesta, M., Balogh, D., et al. (2014) Strand invasion by HLTF as a mechanism for template switch in fork rescue. *Nucleic Acids Research*, 42 (3). doi:10.1093/nar/gkt1040.

Bylund, G.O. and Burgers, P.M.J. (2005) Replication Protein A-Directed Unloading of PCNA by the Ctf18 Cohesion Establishment Complex. *Molecular and Cellular Biology*, 25 (13). doi:10.1128/mcb.25.13.5445-5455.2005.

Cadzow, L., Tobin, E., Sullivan, P., et al. (2022) Abstract ND01: KSQ-4279: A first-in-class USP1 inhibitor for the treatment of cancers with homologous recombination deficiencies. *Cancer Research*, 82 (12_Supplement). doi:10.1158/1538-7445.am2022-nd01.

Cai, J., Uhlmann, F., Gibbs, E., et al. (1996) Reconstitution of human replication factor C from its five subunits in baculovirus-infected insect cells. *Proceedings of the National Academy of Sciences of the United States of America*, 93 (23). doi:10.1073/pnas.93.23.12896.

Caldecott, K.W. (2008) Single-strand break repair and genetic disease. *Nature Reviews Genetics*. 9 (8). doi:10.1038/nrg2380.

Callen, E., Zong, D., Wu, W., et al. (2020) 53BP1 Enforces Distinct Pre- and Post-resection Blocks on Homologous Recombination. *Molecular Cell*. doi:10.1016/j.molcel.2019.09.024.

Cannavo, E., Cejka, P. and Kowalczykowski, S.C. (2013) Relationship of DNA degradation by Saccharomyces cerevisiae Exonuclease 1 and its stimulation by RPA and Mre11-Rad50-Xrs2 to DNA end resection. *Proceedings of the National Academy of Sciences of the United States of America*, 110 (18). doi:10.1073/pnas.1305166110.

Cao, L., Kim, S., Xiao, C., et al. (2006) ATM-Chk2-p53 activation prevents tumorigenesis at an expense of organ homeostasis upon Brca1 deficiency. *EMBO Journal*. doi:10.1038/sj.emboj.7601115.

Cao, L., Xu, X., Bunting, S.F., et al. (2009) A Selective Requirement for 53BP1 in the Biological Response to Genomic Instability Induced by Brca1 Deficiency. *Molecular*

Cell. doi:10.1016/j.molcel.2009.06.037.

Carley, A.C., Jalan, M., Subramanyam, S., et al. (2022) Replication Protein A Phosphorylation Facilitates RAD52-Dependent Homologous Recombination in BRCA-Deficient Cells. *Molecular and Cellular Biology*, 42 (2). doi:10.1128/mcb.00524-21.

Carreira, A., Hilario, J., Amitani, I., et al. (2009) The BRC Repeats of BRCA2 Modulate the DNA-Binding Selectivity of RAD51. *Cell*, 136 (6). doi:10.1016/j.cell.2009.02.019.

Carreira, A. and Kowalczykowski, S.C. (2011) Two classes of BRC repeats in BRCA2 promote RAD51 nucleoprotein filament function by distinct mechanisms. *Proceedings of the National Academy of Sciences of the United States of America*, 108 (26). doi:10.1073/pnas.1106971108.

Carvajal-Garcia, J., Crown, K.N., Ramsden, D.A., et al. (2021) DNA polymerase theta suppresses mitotic crossing over. *PLoS Genetics*, 17 (3). doi:10.1371/journal.pgen.1009267.

Cary, R.B., Peterson, S.R., Wang, J., et al. (1997) DNA looping by Ku and the DNA-dependent protein kinase. *Proceedings of the National Academy of Sciences of the United States of America*, 94 (9). doi:10.1073/pnas.94.9.4267.

Castilla, L.H., Couch, F.J., Erdos, M.R., et al. (1994) Mutations in the BRCA1 gene in families with early-onset breast and ovarian cancer. *Nature Genetics*, 8 (4). doi:10.1038/ng1294-387.

Castillo, A., Paul, A., Sun, B., et al. (2014) The BRCA1-interacting protein Abraxas is required for genomic stability and tumor suppression. *Cell Reports*, 8 (3). doi:10.1016/j.celrep.2014.06.050.

Ceccaldi, R., Liu, J.C., Amunugama, R., et al. (2015) Homologous-recombination-deficient tumours are dependent on Polθ -mediated repair. *Nature*. doi:10.1038/nature14184.

Ceccaldi, R., Rondinelli, B. and D'Andrea, A.D. (2016) Repair Pathway Choices and Consequences at the Double-Strand Break. *Trends in Cell Biology*. 26 (1). doi:10.1016/j.tcb.2015.07.009.

Cejka, P., Plank, J.L., Bachrati, C.Z., et al. (2010) Rmi1 stimulates decatenation of double Holliday junctions during dissolution by Sgs1-Top3. *Nature Structural and Molecular Biology*, 17 (11). doi:10.1038/nsmb.1919.

Cejka, P., Plank, J.L., Dombrowski, C.C., et al. (2012) Decatenation of DNA by the S.

cerevisiae Sgs1-Top3-Rmi1 and RPA Complex: A Mechanism for Disentangling Chromosomes. *Molecular Cell*, 47 (6). doi:10.1016/j.molcel.2012.06.032.

Celeste, A., Fernandez-Capetillo, O., Kruhlak, M.J., et al. (2003) Histone H2AX phosphorylation is dispensable for the initial recognition of DNA breaks. *Nature Cell Biology*, 5 (7). doi:10.1038/ncb1004.

Chakraborty, P. and Hiom, K. (2021) DHX9-dependent recruitment of BRCA1 to RNA promotes DNA end resection in homologous recombination. *Nature Communications*, 12 (1). doi:10.1038/s41467-021-24341-z.

Chakraborty, S., Pandita, R.K., Hambarde, S., et al. (2018) SMARCAD1 Phosphorylation and Ubiquitination Are Required for Resection during DNA Double-Strand Break Repair. *iScience*. doi:10.1016/j.isci.2018.03.016.

Chan, S.H., Yu, A.M. and McVey, M. (2010) Dual roles for DNA polymerase theta in alternative end-joining repair of double-strand breaks in Drosophila. *PLoS Genetics*, 6 (7). doi:10.1371/journal.pgen.1001005.

Chandramouly, G., McDevitt, S., Sullivan, K., et al. (2015) Small-Molecule Disruption of RAD52 Rings as a Mechanism for Precision Medicine in BRCA-Deficient Cancers. *Chemistry and Biology*. doi:10.1016/j.chembiol.2015.10.003.

Chang, D.J. and Cimprich, K.A. (2009) DNA damage tolerance: When it's OK to make mistakes. *Nature Chemical Biology*. 5 (2). doi:10.1038/nchembio.139.

Chapman, J.R., Barral, P., Vannier, J.B., et al. (2013) RIF1 Is Essential for 53BP1-Dependent Nonhomologous End Joining and Suppression of DNA Double-Strand Break Resection. *Molecular Cell*. doi:10.1016/j.molcel.2013.01.002.

Chapman, J.R. and Jackson, S.P. (2008) Phospho-dependent interactions between NBS1 and MDC1 mediate chromatin retention of the MRN complex at sites of DNA damage. *EMBO Reports*, 9 (8). doi:10.1038/embor.2008.103.

Chaudhuri, A.R., Callen, E., Ding, X., et al. (2016) Replication fork stability confers chemoresistance in BRCA-deficient cells. *Nature*. doi:10.1038/nature18325.

Chen, C.C., Kass, E.M., Yen, W.F., et al. (2017) ATM loss leads to synthetic lethality in BRCA1 BRCT mutant mice associated with exacerbated defects in homology-directed repair. *Proceedings of the National Academy of Sciences of the United States of America*, 114 (29). doi:10.1073/pnas.1706392114.

Chen, D., Gervai, J.Z., Póti, Á., et al. (2022) BRCA1 deficiency specific base

substitution mutagenesis is dependent on translesion synthesis and regulated by 53BP1. *Nature Communications*, 13 (1). doi:10.1038/s41467-021-27872-7.

Chen, H., Lisby, M. and Symington, L.S. (2013) RPA Coordinates DNA End Resection and Prevents Formation of DNA Hairpins. *Molecular Cell*, 50 (4). doi:10.1016/j.molcel.2013.04.032.

Chen, J., Li, P., Song, L., et al. (2020) 53BP1 loss rescues embryonic lethality but not genomic instability of BRCA1 total knockout mice. *Cell Death and Differentiation*. doi:10.1038/s41418-020-0521-4.

Chen, L., Nievera, C.J., Lee, A.Y.L., et al. (2008) Cell cycle-dependent complex formation of BRCA1·CtIP·MRN is important for DNA double-strand break repair. *Journal of Biological Chemistry*, 283 (12). doi:10.1074/jbc.M710245200.

Chen, R. and Wold, M.S. (2014) Replication protein A: Single-stranded DNA's first responder: Dynamic DNA-interactions allow replication protein A to direct single-strand DNA intermediates into different pathways for synthesis or repair Prospects & Overviews R. Chen and M. S. Wold. *BioEssays*, 36 (12). doi:10.1002/bies.201400107.

Chen, S., Liu, Y. and Zhou, H. (2021) Advances in the development ubiquitin-specific peptidase (USP) inhibitors. *International Journal of Molecular Sciences*. 22 (9). doi:10.3390/ijms22094546.

Chen, X., Cui, D., Papusha, A., et al. (2012) The Fun30 nucleosome remodeller promotes resection of DNA double-strand break ends. *Nature*, 489 (7417). doi:10.1038/nature11355.

Chen, X., Niu, H., Yu, Y., et al. (2016) Enrichment of Cdk1-cyclins at DNA double-strand breaks stimulates Fun30 phosphorylation and DNA end resection. *Nucleic Acids Research*, 44 (6). doi:10.1093/nar/gkv1544.

Choe, K.N. and Moldovan, G.L. (2017) Forging Ahead through Darkness: PCNA, Still the Principal Conductor at the Replication Fork. *Molecular Cell*. doi:10.1016/j.molcel.2016.12.020.

Choudhary, R.K., Siddiqui, M.Q., Gadewal, N., et al. (2018) Biophysical evaluation to categorize pathogenicity of cancer-predisposing mutations identified in the BARD1 BRCT domain. *RSC Advances*, 8 (59). doi:10.1039/C8RA06524A.

Chun, C., Wu, Y., Lee, S.H., et al. (2016) The homologous recombination component EEPD1 is required for genome stability in response to developmental stress of

vertebrate embryogenesis. *Cell Cycle*, 15 (7). doi:10.1080/15384101.2016.1151585.
Chun, J., Buechelmaier, E.S. and Powell, S.N. (2013) Rad51 Paralog Complexes BCDX2 and CX3 Act at Different Stages in the BRCA1-BRCA2-Dependent Homologous Recombination Pathway. *Molecular and Cellular Biology*, 33 (2). doi:10.1128/mcb.00465-12.
Ciccia, A. and Elledge, S.J. (2010) The DNA Damage Response: Making It Safe to Play with Knives. *Molecular Cell*. 40 (2). doi:10.1016/j.molcel.2010.09.019.
Ciccia, A., Nimonkar, A. V., Hu, Y., et al. (2012) Polyubiquitinated PCNA Recruits the ZRANB3 Translocase to Maintain Genomic Integrity after Replication Stress. *Molecular Cell*, 47 (3). doi:10.1016/j.molcel.2012.05.024.
Clark, S.L., Rodriguez, A.M., Snyder, R.R., et al. (2012) Structure-function of the tumor suppressor BRCA1. *Computational and Structural Biotechnology Journal*. 1 (1). doi:10.5936/csbj.201204005.
Claussin, C. and Chang, M. (2016) Multiple Rad52-Mediated Homology-Directed Repair Mechanisms Are Required to Prevent Telomere Attrition-Induced Senescence in Saccharomyces cerevisiae. *PLoS Genetics*, 12 (7). doi:10.1371/journal.pgen.1006176.
Cleaver, J.E. (1968) Defective repair replication of DNA in xeroderma pigmentosum. *Nature*, 218 (5142). doi:10.1038/218652a0.
Clement, K., Rees, H., Canver, M.C., et al. (2019) CRISPResso2 provides accurate and rapid genome editing sequence analysis. *Nature Biotechnology*. 37 (3). doi:10.1038/s41587-019-0032-3.
Cohn, M.A., Kowal, P., Yang, K., et al. (2007) A UAF1-Containing Multisubunit Protein Complex Regulates the Fanconi Anemia Pathway. *Molecular Cell*, 28 (5). doi:10.1016/j.molcel.2007.09.031.
Cole, D.J., Janecek, M., Stokes, J.E., et al. (2017) Computationally-guided optimization of small-molecule inhibitors of the Aurora A kinase-TPX2 protein-protein interaction. *Chemical Communications*, 53 (67). doi:10.1039/c7cc05379g.
Coleman, K.E., Yin, Y., Lui, S.K.L., et al. (2022) USP1-trapping lesions as a source of DNA replication stress and genomic instability. *Nature Communications*, 13 (1). doi:10.1038/s41467-022-29369-3.
Cong, K., Peng, M., Kousholt, A.N., et al. (2021) Replication gaps are a key

determinant of PARP inhibitor synthetic lethality with BRCA deficiency. *Molecular Cell*, 81 (15). doi:10.1016/j.molcel.2021.06.011.

Cooper, M.P., Machwe, A., Orren, D.K., et al. (2000) Ku complex interacts with and stimulates the Werner protein. *Genes and Development*, 14 (8). doi:10.1101/gad.14.8.907.

Cortez, D., Wang, Y., Qin, J., et al. (1999) Requirement of ATM-dependent phosphorylation of Brca1 in the DNA damage response to double-strand breaks. *Science*, 286 (5442). doi:10.1126/science.286.5442.1162.

Da Costa, A.A.B.A., Bose, A., Martignetti, D., et al. (2023) Abstract 5725: The USP1 inhibitor I-138 kills BRCA1-deficient tumor cells and overcomes PARP inhibitor resistance. *Cancer Research*, 83 (7_Supplement). doi:10.1158/1538-7445.am2023-5725.

Costelloe, T., Louge, R., Tomimatsu, N., et al. (2012) The yeast Fun30 and human SMARCAD1 chromatin remodellers promote DNA end resection. *Nature*, 489 (7417). doi:10.1038/nature11353.

Crackower, M.A., Scherer, S.W., Rommens, J.M., et al. (1996) Characterization of the split hand/split foot malformation locus SHFM1 at 7q21.3-q22.1 and analysis of a candidate gene for its expression during limb development. *Human Molecular Genetics*, 5 (5). doi:10.1093/hmg/5.5.571.

Cramer-Morales, K., Nieborowska-Skorska, M., Scheibner, K., et al. (2013) Personalized synthetic lethality induced by targeting RAD52 in leukemias identified by gene mutation and expression profile. *Blood*. doi:10.1182/blood-2013-05-501072.

Cressman, V.L., Backlund, D.C., Avrutskaya, A. V., et al. (1999) Growth Retardation, DNA Repair Defects, and Lack of Spermatogenesis in BRCA1-Deficient Mice. *Molecular and Cellular Biology*, 19 (10). doi:10.1128/mcb.19.10.7061.

Cruz-García, A., López-Saavedra, A. and Huertas, P. (2014) BRCA1 accelerates CtIP-ediated DNA-end resection. *Cell Reports*, 9 (2). doi:10.1016/j.celrep.2014.08.076.

D'Andrea, A.D. (2018) Mechanisms of PARP inhibitor sensitivity and resistance. *DNA Repair*. 71. doi:10.1016/j.dnarep.2018.08.021.

Dai, L., Dai, Y., Han, J., et al. (2021) Structural insight into BRCA1-BARD1 complex recruitment to damaged chromatin. *Molecular Cell*, 81 (13). doi:10.1016/j.molcel.2021.05.010.

Daley, J.M., Gaines, W.A., Kwon, Y., et al. (2014) Regulation of DNA Pairing in Homologous Recombination. *Cold Spring Harbor Perspectives in Biology*, 6 (11). doi:10.1101/cshperspect.a017954.

Daley, J.M., Vander Laan, R.L., Suresh, A., et al. (2005) DNA joint dependence of Pol X family polymerase action in nonhomologous end joining. *Journal of Biological Chemistry*, 280 (32). doi:10.1074/jbc.M505277200.

Daley, J.M., Niu, H., Miller, A.S., et al. (2015) Biochemical mechanism of DSB end resection and its regulation. *DNA Repair*, 32. doi:10.1016/j.dnarep.2015.04.015.

Daley, J.M. and Sung, P. (2014) 53BP1, BRCA1, and the Choice between Recombination and End Joining at DNA Double-Strand Breaks. *Molecular and Cellular Biology*. doi:10.1128/mcb.01639-13.

Dantzer, F., De La Rubia, G., Ménissier-De Murcia, J., et al. (2000) Base excision repair is impaired in mammalian cells lacking poly(ADP- ribose) polymerase-1. *Biochemistry*, 39 (25). doi:10.1021/bi0003442.

Dantzer, F., Schreiber, V., Niedergang, C., et al. (1999) Involvement of poly(ADP-ribose) polymerase in base excision repair. *Biochimie*, 81 (1–2). doi:10.1016/S0300-9084(99)80040-6.

Davies, O.R. and Pellegrini, L. (2007) Interaction with the BRCA2 C terminus protects RAD51-DNA filaments from disassembly by BRC repeats. *Nature Structural and Molecular Biology*, 14 (6). doi:10.1038/nsmb1251.

Davis, A.J. and Chen, D.J. (2013) DNA double strand break repair via non-homologous end-joining. *Translational Cancer Research*. 2 (3). doi:10.3978/j.issn.2218-676X.2013.04.02.

Davis, A.J., Chi, L., So, S., et al. (2014) BRCA1 modulates the autophosphorylation status of DNA-PKcs in S phase of the cell cycle. *Nucleic Acids Research*, 42 (18). doi:10.1093/nar/gku824.

Daza-Martin, M., Starowicz, K., Jamshad, M., et al. (2019) Isomerization of BRCA1–BARD1 promotes replication fork protection. *Nature*, 571 (7766). doi:10.1038/s41586-019-1363-4.

Dedes, K.J., Wilkerson, P.M., Wetterskog, D., et al. (2011) Synthetic lethality of PARP inhibition in cancers lacking BRCA1 and BRCA2 mutations. *Cell Cycle*. 10 (8). doi:10.4161/cc.10.8.15273.

Deng, S.K., Gibb, B., De Almeida, M.J., et al. (2014) RPA antagonizes microhomology-mediated repair of DNA double-strand breaks. *Nature Structural and Molecular Biology*, 21 (4). doi:10.1038/nsmb.2786.

Deng, X., Prakash, A., Dhar, K., et al. (2009) Human replication protein A-Rad52-single-stranded DNA complex: Stoichiometry and evidence for strand transfer regulation by phosphorylation. *Biochemistry*, 48 (28). doi:10.1021/bi900564k.

Densham, R.M., Garvin, A.J., Stone, H.R., et al. (2016) Human BRCA1-BARD1 ubiquitin ligase activity counteracts chromatin barriers to DNA resection. *Nature Structural and Molecular Biology*. doi:10.1038/nsmb.3236.

Densham, R.M. and Morris, J.R. (2017) The BRCA1 Ubiquitin ligase function sets a new trend for remodelling in DNA repair. *Nucleus*. doi:10.1080/19491034.2016.1267092.

Densham, R.M. and Morris, J.R. (2019) Moving Mountains—The BRCA1 Promotion of DNA Resection. *Frontiers in Molecular Biosciences*. doi:10.3389/fmolb.2019.00079.

Dev, H., Chiang, T.W.W., Lescale, C., et al. (2018) Shieldin complex promotes DNA end-joining and counters homologous recombination in BRCA1-null cells. *Nature Cell Biology*. doi:10.1038/s41556-018-0140-1.

Dexheimer, T.S., Rosenthal, A.S., Liang, Q., et al. (2010) *Discovery of ML323 as a Novel Inhibitor of the USP1/UAF1 Deubiquitinase Complex*.

Dhoonmoon, A., Nicolae, C.M. and Moldovan, G.L. (2022) The KU-PARP14 axis differentially regulates DNA resection at stalled replication forks by MRE11 and EXO1. *Nature Communications*, 13 (1). doi:10.1038/s41467-022-32756-5.

Diaz-Cruz, E.S., Cabrera, M.C., Nakles, R., et al. (2010) BRCA1 deficient mouse models to study pathogenesis and therapy of triple negative breast cancer. *Breast Disease*, 32 (1–2). doi:10.3233/BD-2010-0308.

Díaz-Talavera, A., Montero-Conde, C., Leandro-García, L.J., et al. (2022) PrimPol: A Breakthrough among DNA Replication Enzymes and a Potential New Target for Cancer Therapy. *Biomolecules*. 12 (2). doi:10.3390/biom12020248.

Dine, J. and Deng, C.X. (2013) Mouse models of BRCA1 and their application to breast cancer research. *Cancer and Metastasis Reviews*, 32 (1–2). doi:10.1007/s10555-012-9403-7.

Djuric, Z., Everett, C.K. and Luongo, D.A. (1993) Toxicity, single-strand breaks, and 5-

hydroxymethyl-2′-deoxyuridine formation in human breast epithelial cells treated with hydrogen peroxide. *Free Radical Biology and Medicine*, 14 (5). doi:10.1016/0891-5849(93)90111-7.

Dodson, G.E., Shi, Y. and Tibbetts, R.S. (2004) DNA replication defects, spontaneous DNA damage, and ATM-dependent checkpoint activation in replication protein A-deficient cells. *Journal of Biological Chemistry*, 279 (32). doi:10.1074/jbc.C400242200.

Doil, C., Mailand, N., Bekker-Jensen, S., et al. (2009) RNF168 Binds and Amplifies Ubiquitin Conjugates on Damaged Chromosomes to Allow Accumulation of Repair Proteins. *Cell*, 136 (3). doi:10.1016/j.cell.2008.12.041.

Dray, E., Etchin, J., Wiese, C., et al. (2010) Enhancement of RAD51 recombinase activity by the tumor suppressor PALB2. *Nature Structural and Molecular Biology*, 17 (10). doi:10.1038/nsmb.1916.

Drost, R., Bouwman, P., Rottenberg, S., et al. (2011) BRCA1 RING function is essential for tumor suppression but dispensable for therapy resistance. *Cancer Cell*. doi:10.1016/j.ccr.2011.11.014.

Drost, R., Dhillon, K.K., Van Der Gulden, H., et al. (2016) BRCA1185delAG tumors may acquire therapy resistance through expression of RING-less BRCA1. *Journal of Clinical Investigation*. doi:10.1172/JCI70196.

Drost, R. and Jonkers, J. (2014) Opportunities and hurdles in the treatment of BRCA1-related breast cancer. *Oncogene*. 33 (29). doi:10.1038/onc.2013.329.

Duan, H. and Pathania, S. (2020) RPA, RFWD3 and BRCA2 at stalled forks: a balancing act. *Molecular and Cellular Oncology*. 7 (6). doi:10.1080/23723556.2020.1801089.

Edmunds, C.E., Simpson, L.J. and Sale, J.E. (2008) PCNA Ubiquitination and REV1 Define Temporally Distinct Mechanisms for Controlling Translesion Synthesis in the Avian Cell Line DT40. *Molecular Cell*, 30 (4). doi:10.1016/j.molcel.2008.03.024.

Elia, A.E.H. and Elledge, S.J. (2012) BRCA1 as tumor suppressor: Lord without its RING? *Breast Cancer Research*. 14 (2). doi:10.1186/bcr3118.

Elia, A.E.H., Wang, D.C., Willis, N.A., et al. (2015) RFWD3-Dependent Ubiquitination of RPA Regulates Repair at Stalled Replication Forks. *Molecular Cell*. doi:10.1016/j.molcel.2015.09.011.

Ellison, V. and Stillman, B. (2003) Biochemical characterization of DNA damage

checkpoint complexes: Clamp loader and clamp complexes with specificity for 5′ recessed DNA. *PLoS Biology*, 1 (2). doi:10.1371/journal.pbio.0000033.

Esashi, F., Christ, N., Cannon, J., et al. (2005) CDK-dependent phosphorylation of BRCA2 as a regulatory mechanism for recombinational repair. *Nature*, 434 (7033). doi:10.1038/nature03404.

Esashi, F., Galkin, V.E., Yu, X., et al. (2007) Stabilization of RAD51 nucleoprotein filaments by the C-terminal region of BRCA2. *Nature Structural and Molecular Biology*, 14 (6). doi:10.1038/nsmb1245.

Escribano-Díaz, C., Orthwein, A., Fradet-Turcotte, A., et al. (2013) A Cell Cycle-Dependent Regulatory Circuit Composed of 53BP1-RIF1 and BRCA1-CtIP Controls DNA Repair Pathway Choice. *Molecular Cell*, 49 (5). doi:10.1016/j.molcel.2013.01.001.

Eyfjord, J.E. and Bodvarsdottir, S.K. (2005) “Genomic instability and cancer: Networks involved in response to DNA damage.” In *Mutation Research - Fundamental and Molecular Mechanisms of Mutagenesis*. 2005. doi:10.1016/j.mrfmmm.2005.05.010.

Fabbro, M., Rodriguez, J.A., Baer, R., et al. (2002) BARD1 induces BRCA1 intranuclear foci formation by increasing RING-dependent BRCA1 nuclear import and inhibiting BRCA1 nuclear export. *Journal of Biological Chemistry*, 277 (24). doi:10.1074/jbc.M200769200.

Faesen, A.C., Luna-Vargas, M.P.A., Geurink, P.P., et al. (2011) The differential modulation of USP activity by internal regulatory domains, interactors and eight ubiquitin chain types. *Chemistry and Biology*, 18 (12). doi:10.1016/j.chembiol.2011.10.017.

Falbo, K.B., Alabert, C., Katou, Y., et al. (2009) Involvement of a chromatin remodeling complex in damage tolerance during DNA replication. *Nature Structural and Molecular Biology*, 16 (11). doi:10.1038/nsmb.1686.

Falck, J., Coates, J. and Jackson, S.P. (2005) Conserved modes of recruitment of ATM, ATR and DNA-PKcs to sites of DNA damage. *Nature*, 434 (7033). doi:10.1038/nature03442.

Farmer, H., McCabe, H., Lord, C.J., et al. (2005) Targeting the DNA repair defect in BRCA mutant cells as a therapeutic strategy. *Nature*, 434 (7035). doi:10.1038/nature03445.

Feng, L., Fong, K.W., Wang, J., et al. (2013) RIF1 counteracts BRCA1-mediated end resection during DNA repair. *Journal of Biological Chemistry*, 288 (16). doi:10.1074/jbc.M113.457440.

Feng, L., Huang, T. and Chen, J. (2009) MERIT40 facilitates BRCA1 localization and DNA damage repair. *Genes and Development*, 23 (6). doi:10.1101/gad.1770609.

Feng, W. and Jasin, M. (2017) Homologous Recombination and Replication Fork Protection: BRCA2 and More! *Cold Spring Harbor symposia on quantitative biology*, 82. doi:10.1101/sqb.2017.82.035006.

Feng, W., Simpson, D.A., Carvajal-Garcia, J., et al. (2019) Genetic determinants of cellular addiction to DNA polymerase theta. *Nature Communications*, 10 (1). doi:10.1038/s41467-019-12234-1.

Feng, Z., Scott, S.P., Bussen, W., et al. (2011) Rad52 inactivation is synthetically lethal with BRCA2 deficiency. *Proceedings of the National Academy of Sciences of the United States of America*, 108 (2). doi:10.1073/pnas.1010959107.

Findlay, G.M., Daza, R.M., Martin, B., et al. (2018) Accurate classification of BRCA1 variants with saturation genome editing. *Nature*, 562 (7726). doi:10.1038/s41586-018-0461-z.

Fong, P.C., Yap, T.A., Boss, D.S., et al. (2010) Poly(ADP)-ribose polymerase inhibition: Frequent durable responses in BRCA carrier ovarian cancer correlating with platinum-free interval. *Journal of Clinical Oncology*, 28 (15). doi:10.1200/JCO.2009.26.9589.

Foulkes, W.D. (2008) Inherited Susceptibility to Common Cancers. *New England Journal of Medicine*, 359 (20). doi:10.1056/nejmra0802968.

Fowler, F.C. and Tyler, J.K. (2022) A Proximity Ligation Method to Detect Proteins Bound to Single-Stranded DNA after DNA End Resection at DNA Double-Strand Breaks. *Methods and Protocols*, 5 (1). doi:10.3390/mps5010003.

Fradet-Turcotte, A., Canny, M.D., Escribano-Díaz, C., et al. (2013) 53BP1 is a reader of the DNA-damage-induced H2A Lys 15 ubiquitin mark. *Nature*, 499 (7456). doi:10.1038/nature12318.

Fragkos, M., Ganier, O., Coulombe, P., et al. (2015) DNA replication origin activation in space and time. *Nature Reviews Molecular Cell Biology*. 16 (6). doi:10.1038/nrm4002.

Friedberg, E.C., Wagner, R. and Radman, M. (2002) Specialized DNA polymerases, cellular survival, and the genesis of mutations. *Science*. 296 (5573). doi:10.1126/science.1070236.

Fu, T.J., Tse-Dinh, Y.C. and Seeman, N.C. (1994) Holliday junction crossover topology. *Journal of Molecular Biology*, 236 (1). doi:10.1006/jmbi.1994.1121.

Fu, Y. V., Yardimci, H., Long, D.T., et al. (2011) Selective bypass of a lagging strand roadblock by the eukaryotic replicative DNA helicase. *Cell*, 146 (6). doi:10.1016/j.cell.2011.07.045.

Fugger, K., Bajrami, I., Dos Santos, M.S., et al. (2021) Targeting the nucleotide salvage factor DNPH1 sensitizes BRCA-deficient cells to PARP inhibitors. *Science*, 372 (6538). doi:10.1126/science.abb4542.

Fugger, K., Mistrik, M., Neelsen, K.J., et al. (2015) FBH1 catalyzes regression of stalled replication forks. *Cell Reports*, 10 (10). doi:10.1016/j.celrep.2015.02.028.

Gallina, I., Hendriks, I.A., Hoffmann, S., et al. (2021) The ubiquitin ligase RFWD3 is required for translesion DNA synthesis. *Molecular Cell*, 81 (3). doi:10.1016/j.molcel.2020.11.029.

Gao, S., Feng, S., Ning, S., et al. (2018) An OB-fold complex controls the repair pathways for DNA double-strand breaks. *Nature Communications*. doi:10.1038/s41467-018-06407-7.

García-Gómez, S., Reyes, A., Martínez-Jiménez, M.I., et al. (2013) PrimPol, an Archaic Primase/Polymerase Operating in Human Cells. *Molecular Cell*, 52 (4). doi:10.1016/j.molcel.2013.09.025.

García-Muse, T. and Aguilera, A. (2016) Transcription-replication conflicts: How they occur and how they are resolved. *Nature Reviews Molecular Cell Biology*. 17 (9). doi:10.1038/nrm.2016.88.

Garcin, E.B., Gon, S., Sullivan, M.R., et al. (2019) Differential requirements for the RAD51 paralogs in genome repair and maintenance in human cells. *PLoS Genetics*, 15 (10). doi:10.1371/journal.pgen.1008355.

Gatti, M., Pinato, S., Maspero, E., et al. (2012) A novel ubiquitin mark at the N-terminal tail of histone H2As targeted by RNF168 ubiquitin ligase. *Cell Cycle*, 11 (13). doi:10.4161/cc.20919.

Gelot, C., Kovacs, M.T., Miron, S., et al. (2023) Polθ is phosphorylated by Polo-like

kinase 1 (PLK1) to enable repair of DNA double strand breaks in mitosis. *bioRxiv*.
Genois, M.M., Gagné, J.P., Yasuhara, T., et al. (2021) CARM1 regulates replication fork speed and stress response by stimulating PARP1. *Molecular Cell*, 81 (4). doi:10.1016/j.molcel.2020.12.010.
Georgescu, R.E., Yao, N., Indiani, C., et al. (2014) Replisome mechanics: Lagging strand events that influence speed and processivity. *Nucleic Acids Research*, 42 (10). doi:10.1093/nar/gku257.
Ghezraoui, H., Oliveira, C., Becker, J.R., et al. (2018) 53BP1 cooperation with the REV7–shieldin complex underpins DNA structure-specific NHEJ. *Nature*, 560 (7716). doi:10.1038/s41586-018-0362-1.
Ghimenti, C., Sensi, E., Presciuttini, S., et al. (2002) Germline mutations of the BRCA1-associated ring domain (BARD1) gene in breast and breast/ovarian families negative for BRCA1 and BRCA2 alterations. *Genes Chromosomes and Cancer*, 33 (3). doi:10.1002/gcc.1223.
Giannattasio, M., Zwicky, K., Follonier, C., et al. (2014) Visualization of recombination-mediated damage bypass by template switching. *Nature Structural and Molecular Biology*, 21 (10). doi:10.1038/nsmb.2888.
Giordano, C.N., Yew, Y.W., Spivak, G., et al. (2016) Understanding photodermatoses associated with defective DNA repair: Syndromes with cancer predisposition. *Journal of the American Academy of Dermatology*. 75 (5). doi:10.1016/j.jaad.2016.03.045.
Goldberg, M., Stucki, M., Falck, J., et al. (2003) MDC1 is required for the intra-S-phase DNA damage checkpoint. *Nature*, 421 (6926). doi:10.1038/nature01445.
Gong, Z., Kim, J.E., Leung, C.C.Y., et al. (2010) BACH1/FANCJ Acts with TopBP1 and Participates Early in DNA Replication Checkpoint Control. *Molecular Cell*, 37 (3). doi:10.1016/j.molcel.2010.01.002.
González-Acosta, D., Blanco-Romero, E., Ubieto-Capella, P., et al. (2021) PrimPol-mediated repriming facilitates replication traverse of DNA interstrand crosslinks. *The EMBO Journal*, 40 (14). doi:10.15252/embj.2020106355.
Goodman, M.F. (2002) Error-prone repair DNA polymerases in prokaryotes and eukaryotes. *Annual Review of Biochemistry*. 71. doi:10.1146/annurev.biochem.71.083101.124707.
Gornstein, E.L., Sandefur, S., Chung, J.H., et al. (2018) BRCA2 Reversion Mutation

Associated With Acquired Resistance to Olaparib in Estrogen Receptor-positive Breast Cancer Detected by Genomic Profiling of Tissue and Liquid Biopsy. *Clinical Breast Cancer*, 18 (2). doi:10.1016/j.clbc.2017.12.010.

Gottifredi, V. and Wiesmüller, L. (2020) Current understanding of RAD52 functions: Fundamental and therapeutic insights. *Cancers*. 12 (3). doi:10.3390/cancers12030705.

Gottlieb, T.M. and Jackson, S.P. (1993) The DNA-dependent protein kinase: Requirement for DNA ends and association with Ku antigen. *Cell*, 72 (1). doi:10.1016/0092-8674(93)90057-W.

Gowen, L.C., Johnson, B.L., Latour, A.M., et al. (1996) Brca1 deficiency results in early embryonic lethality characterized by neuroepithelial abnormalities. *Nature Genetics*, 12 (2). doi:10.1038/ng0296-191.

Graham, W.J., Putnam, C.D. and Kolodner, R.D. (2018) “DNA mismatch repair: Mechanisms and cancer genetics.” In *Encyclopedia of Cancer*. doi:10.1016/B978-0-12-801238-3.96130-0.

Grawunder, U., Wilm, M., Wu, X., et al. (1997) Activity of DNA ligase IV stimulated by complex formation with XRCC4 protein in mammalian cells. *Nature*, 388 (6641). doi:10.1038/41358.

Greenberg, R.A., Sobhian, B., Pathania, S., et al. (2006) Multifactorial contributions to an acute DNA damage response by BRCA1/BARD1-containing complexes. *Genes and Development*, 20 (1). doi:10.1101/gad.1381306.

Greenman, J., Mohammed, S., Ellis, D., et al. (1998) Identification of missense and truncating mutations in the BRCA1 gene in sporadic and familial breast and ovarian cancer. *Genes Chromosomes and Cancer*, 21 (3). doi:10.1002/(sici)1098-2264(199803)21:3<244::aid-gcc9>3.0.co;2-%23.

Grimme, J.M., Honda, M., Wright, R., et al. (2010) Human Rad52 binds and wraps single-stranded DNA and mediates annealing via two hRad52-ssDNA complexes. *Nucleic Acids Research*, 38 (9). doi:10.1093/nar/gkp1249.

De Groote, F.H., Jansen, J.G., Masuda, Y., et al. (2011) The Rev1 translesion synthesis polymerase has multiple distinct DNA binding modes. *DNA Repair*, 10 (9). doi:10.1016/j.dnarep.2011.04.033.

Grundy, G.J., Rulten, S.L., Zeng, Z., et al. (2013) APLF promotes the assembly and

activity of non-homologous end joining protein complexes. *EMBO Journal*, 32 (1). doi:10.1038/emboj.2012.304.

Gu, J., Lu, H., Tippin, B., et al. (2007) XRCC4:DNA ligase IV can ligate incompatible DNA ends and can ligate across gaps. *EMBO Journal*, 26 (4). doi:10.1038/sj.emboj.7601559.

Gudmundsdottir, K., Lord, C.J., Witt, E., et al. (2004) DSS1 is required for RAD51 focus formation and genomic stability in mammalian cells. *EMBO Reports*, 5 (10). doi:10.1038/sj.embor.7400255.

Guh, C.-L., Lei, K.-H., Chen, Y.-A., et al. (2023) RAD51 paralogs synergize with RAD51 to protect reversed forks from cellular nucleases. *Nucleic Acids Research*, 51 (21): 11717–11731. doi:10.1093/nar/gkad856.

Guilliam, T.A. (2021) Mechanisms for Maintaining Eukaryotic Replisome Progression in the Presence of DNA Damage. *Frontiers in Molecular Biosciences*. 8. doi:10.3389/fmolb.2021.712971.

Guilliam, T.A., Brissett, N.C., Ehlinger, A., et al. (2017) Molecular basis for PrimPol recruitment to replication forks by RPA. *Nature Communications*, 8. doi:10.1038/ncomms15222.

Guilliam, T.A. and Doherty, A.J. (2017) Primpol—prime time to reprime. *Genes*. 8 (1). doi:10.3390/genes8010020.

Guilliam, T.A. and Yeeles, J.T.P. (2020) Reconstitution of translesion synthesis reveals a mechanism of eukaryotic DNA replication restart. *Nature Structural and Molecular Biology*, 27 (5). doi:10.1038/s41594-020-0418-4.

Gulbis, J.M., Kelman, Z., Hurwitz, J., et al. (1996) Structure of the C-terminal region of p21(WAF1/CIP1) complexed with human PCNA. *Cell*, 87 (2). doi:10.1016/S0092-8674(00)81347-1.

Guo, C., Kosarek-Stancel, J.N., Tang, T.S., et al. (2009) Y-family DNA polymerases in mammalian cells. *Cellular and Molecular Life Sciences*. 66 (14). doi:10.1007/s00018-009-0024-4.

Guo, C., Sonoda, E., Tang, T.S., et al. (2006a) REV1 Protein Interacts with PCNA: Significance of the REV1 BRCT Domain In Vitro and In Vivo. *Molecular Cell*, 23 (2). doi:10.1016/j.molcel.2006.05.038.

Guo, C., Tang, T.-S., Bienko, M., et al. (2006b) Ubiquitin-Binding Motifs in REV1

Protein Are Required for Its Role in the Tolerance of DNA Damage. *Molecular and Cellular Biology*, 26 (23). doi:10.1128/mcb.01118-06.

Gupta, A., Hunt, C.R., Chakraborty, S., et al. (2014) Role of 53BP1 in the regulation of DNA double-strand break repair pathway choice. *Radiation Research*. 181 (1). doi:10.1667/RR13572.1.

Haas, K.T., Lee, M.Y., Esposito, A., et al. (2018) Single-molecule localization microscopy reveals molecular transactions during RAD51 filament assembly at cellular DNA damage sites. *Nucleic Acids Research*, 46 (5). doi:10.1093/nar/gkx1303.

Hakem, R., De la Pompa, J.L., Elia, A., et al. (1997) Partial rescue of Brca15-6 early embryonic lethality by p53 or p21 null mutation. *Nature Genetics*, 16 (3). doi:10.1038/ng0797-298.

Hakem, R., De La Pompa, J.L., Sirard, C., et al. (1996) The tumor suppressor gene Brca1 is required for embryonic cellular proliferation in the mouse. *Cell*. doi:10.1016/S0092-8674(00)81302-1.

Hale, A., Dhoonmoon, A., Straka, J., et al. (2023) Multi-step processing of replication stress-derived nascent strand DNA gaps by MRE11 and EXO1 nucleases. *Nature Communications*, 14 (1): 6265. doi:10.1038/s41467-023-42011-0.

Hammel, M., Yu, Y., Fang, S., et al. (2010) XLF Regulates Filament Architecture of the XRCC4·Ligase IV Complex. *Structure*, 18 (11). doi:10.1016/j.str.2010.09.009.

Hanamshet, K. and Mazin, A. V. (2020) The function of RAD52 N-terminal domain is essential for viability of BRCA-deficient cells. *Nucleic Acids Research*, 48 (22). doi:10.1093/nar/gkaa1145.

Hanamshet, K., Mazina, O.M. and Mazin, A. V. (2016) Reappearance from obscurity: Mammalian Rad52 in homologous recombination. *Genes*. doi:10.3390/genes7090063.

Hanzlikova, H. and Caldecott, K.W. (2019) Perspectives on PARPs in S Phase. *Trends in Genetics*. 35 (6). doi:10.1016/j.tig.2019.03.008.

Hanzlikova, H., Kalasova, I., Demin, A.A., et al. (2018) The Importance of Poly(ADP-Ribose) Polymerase as a Sensor of Unligated Okazaki Fragments during DNA Replication. *Molecular Cell*, 71 (2). doi:10.1016/j.molcel.2018.06.004.

Hashimoto, K., Cho, Y., Yang, I.Y., et al. (2012) The vital role of polymerase ζ and REV1 in mutagenic, but not correct, DNA synthesis across Benzo[a]pyrene-dG and

recruitment of polymerase ζ by REV1 to replication-stalled site. *Journal of Biological Chemistry*, 287 (12). doi:10.1074/jbc.M111.331728.

Hashimoto, Y., Chaudhuri, A.R., Lopes, M., et al. (2010) Rad51 protects nascent DNA from Mre11-dependent degradation and promotes continuous DNA synthesis. *Nature Structural and Molecular Biology*. doi:10.1038/nsmb.1927.

Hashimoto, Y. and Takisawa, H. (2003) Xenopus Cut5 is essential for a CDK-dependent process in the initiation of DNA replication. *EMBO Journal*, 22 (10). doi:10.1093/emboj/cdg238.

Hashizume, R., Fukuda, M., Maeda, I., et al. (2001) The RING Heterodimer BRCA1-BARD1 Is a Ubiquitin Ligase Inactivated by a Breast Cancer-derived Mutation. *Journal of Biological Chemistry*, 276 (18). doi:10.1074/jbc.C000881200.

Van Hatten, R.A., Tutter, A. V., Holway, A.H., et al. (2002) The Xenopus Xmus101 protein is required for the recruitment of Cdc45 to origins of DNA replication. *Journal of Cell Biology*, 159 (4). doi:10.1083/jcb.200207090.

Hayner, J.N., Douma, L.G. and Bloom, L.B. (2014) The interplay of primer-template DNA phosphorylation status and single-stranded DNA binding proteins in directing clamp loaders to the appropriate polarity of DNA. *Nucleic Acids Research*, 42 (16). doi:10.1093/nar/gku774.

He, Y.J., Meghani, K., Caron, M.C., et al. (2018) DYNLL1 binds to MRE11 to limit DNA end resection in BRCA1-deficient cells. *Nature*, 563 (7732). doi:10.1038/s41586-018-0670-5.

Hedglin, M. and Benkovic, S.J. (2015) Regulation of Rad6/Rad18 Activity during DNA Damage Tolerance. *Annual Review of Biophysics*, 44. doi:10.1146/annurev-biophys-060414-033841.

Van der heijden, T., Seidel, R., Modesti, M., et al. (2007) Real-time assembly and disassembly of human RAD51 filaments on individual DNA molecules. *Nucleic Acids Research*, 35 (17). doi:10.1093/nar/gkm629.

Heinen, C.D. (2016) Mismatch repair defects and Lynch syndrome: The role of the basic scientist in the battle against cancer. *DNA Repair*. 38. doi:10.1016/j.dnarep.2015.11.025.

Helchowski, C.M., Skow, L.F., Roberts, K.H., et al. (2013) A small ubiquitin binding domain inhibits ubiquitin-dependent protein recruitment to DNA repair foci. *Cell Cycle*,

12 (24). doi:10.4161/cc.26640.

Helleday, T. (2011) The underlying mechanism for the PARP and BRCA synthetic lethality: Clearing up the misunderstandings. *Molecular Oncology*. 5 (4). doi:10.1016/j.molonc.2011.07.001.

Heller, R.C., Kang, S., Lam, W.M., et al. (2011) Eukaryotic origin-dependent DNA replication in vitro reveals sequential action of DDK and S-CDK kinases. *Cell*, 146 (1). doi:10.1016/j.cell.2011.06.012.

Hershko, A. and Ciechanover, A. (1998) The ubiquitin system. *Annual Review of Biochemistry*. 67. doi:10.1146/annurev.biochem.67.1.425.

Heyer, W.D., Ehmsen, K.T. and Liu, J. (2010) Regulation of homologous recombination in eukaryotes. *Annual Review of Genetics*. 44. doi:10.1146/annurev-genet-051710-150955.

Higashi, M., Inoue, S. and Ito, T. (2010) Core histone H2A ubiquitylation and transcriptional regulation. *Experimental Cell Research*. 316 (17). doi:10.1016/j.yexcr.2010.05.028.

Higgins, G.S., Prevo, R., Lee, Y.F., et al. (2010) A small interfering RNA screen of genes involved in DNA repair identifies tumor-specific radiosensitization by POLQ knockdown. *Cancer Research*, 70 (7). doi:10.1158/0008-5472.CAN-09-4040.

Higgins, S.A., Frenkel, K., Cummings, A., et al. (1987) Definitive Characterization of Human Thymine Glycol N-Glycosylase Activity. *Biochemistry*, 26 (6). doi:10.1021/bi00380a029.

Hile, S.E. and Eckert, K.A. (2008) DNA polymerase kappa produces interrupted mutations and displays polar pausing within mononucleotide microsatellite sequences. *Nucleic Acids Research*, 36 (2). doi:10.1093/nar/gkm1089.

Hile, S.E., Wang, X., Lee, M.Y.W.T., et al. (2012) Beyond translesion synthesis: Polymerase κ fidelity as a potential determinant of microsatellite stability. *Nucleic Acids Research*, 40 (4). doi:10.1093/nar/gkr889.

Hoege, C., Pfander, B., Moldovan, G.L., et al. (2002) RAD6-dependent DNA repair is linked to modification of PCNA by ubiquitin and SUMO. *Nature*, 419 (6903). doi:10.1038/nature00991.

Hoeijmakers, J.H.J. (2001) Genome maintenance mechanisms for preventing cancer. *Nature*. 411 (6835). doi:10.1038/35077232.

Hogg, M., Sauer-Eriksson, A.E. and Johansson, E. (2012) Promiscuous DNA synthesis by human DNA polymerase θ. *Nucleic Acids Research*, 40 (6). doi:10.1093/nar/gkr1102.

Hogg, M., Seki, M., Wood, R.D., et al. (2011) Lesion bypass activity of DNA polymerase θ (POLQ) is an intrinsic property of the pol domain and depends on unique sequence inserts. *Journal of Molecular Biology*, 405 (3). doi:10.1016/j.jmb.2010.10.041.

Hohenstein, P., Kielman, M.F., Breukel, C., et al. (2001) A targeted mouse Brca1 mutation removing the last BRCT repeat results in apoptosis and embryonic lethality at the headfold stage. *Oncogene*, 20 (20). doi:10.1038/sj.onc.1204363.

Hromas, R., Kim, H.S., Sidhu, G., et al. (2017) The endonuclease EEPD1 mediates synthetic lethality in RAD52-depleted BRCA1 mutant breast cancer cells. *Breast Cancer Research*. doi:10.1186/s13058-017-0912-8.

Hu, Q., Botuyan, M.V., Cui, G., et al. (2017) Mechanisms of Ubiquitin-Nucleosome Recognition and Regulation of 53BP1 Chromatin Recruitment by RNF168/169 and RAD18. *Molecular Cell*, 66 (4). doi:10.1016/j.molcel.2017.04.009.

Hu, Q., Botuyan, M.V., Zhao, D., et al. (2021) Mechanisms of BRCA1–BARD1 nucleosome recognition and ubiquitylation. *Nature*, 596 (7872). doi:10.1038/s41586-021-03716-8.

Hu, Q., Zhao, D., Cui, G., et al. (2024) Mechanisms of RNF168 nucleosome recognition and ubiquitylation. *Molecular Cell*. doi:https://doi.org/10.1016/j.molcel.2023.12.036.

Hu, X., Kim, J.A., Castillo, A., et al. (2011) NBA1/MERIT40 and BRE interaction is required for the integrity of two distinct deubiquitinating enzyme BRCC36-containing complexes. *Journal of Biological Chemistry*, 286 (13). doi:10.1074/jbc.M110.200857.

Huang, F., Goyal, N., Sullivan, K., et al. (2016) Targeting BRCA1-and BRCA2-deficient cells with RAD52 small molecule inhibitors. *Nucleic Acids Research*, 44 (9). doi:10.1093/nar/gkw087.

Huang, T.T., Nijman, S.M.B., Mirchandani, K.D., et al. (2006) Regulation of monoubiquitinated PCNA by DUB autocleavage. *Nature Cell Biology*, 8 (4). doi:10.1038/ncb1378.

Huang, X., Kolbanovskiy, A., Wu, X., et al. (2003) Effects of base sequence context on

translesion synthesis past a bulky (+)-trans-anti-B[a]P-N2-dG lesion catalyzed by the Y-family polymerase pol κ. *Biochemistry*, 42 (8). doi:10.1021/bi026912q.

Huber, L.J., Yang, T.W., Sarkisian, C.J., et al. (2001) Impaired DNA Damage Response in Cells Expressing an Exon 11-Deleted Murine Brca1 Variant That Localizes to Nuclear Foci. *Molecular and Cellular Biology*. doi:10.1128/mcb.21.12.4005-4015.2001.

Huen, M.S.Y., Sy, S.M.H. and Chen, J. (2010) BRCA1 and its toolbox for the maintenance of genome integrity. *Nature Reviews Molecular Cell Biology*. 11 (2). doi:10.1038/nrm2831.

Huertas, P. and Jackason, S.P. (2009) Human CtIP mediates cell cycle control of DNA end resection and double strand break repair. *Journal of Biological Chemistry*, 284 (14). doi:10.1074/jbc.M808906200.

Hyrien, O. (2016) How MCM loading and spreading specify eukaryotic DNA replication initiation sites [version 1; referees: 4 approved]. *F1000Research*. 5. doi:10.12688/F1000RESEARCH.9008.1.

Ignatius, J., Knuutila, S., Scherer, S.W., et al. (1996) Split hand/split foot malformation, deafness, and mental retardation with a complex cytogenetic rearrangement involving 7q21.3. *Journal of Medical Genetics*, 33 (6). doi:10.1136/jmg.33.6.507.

Ilves, I., Petojevic, T., Pesavento, J.J., et al. (2010) Activation of the MCM2-7 Helicase by Association with Cdc45 and GINS Proteins. *Molecular Cell*, 37 (2). doi:10.1016/j.molcel.2009.12.030.

Inano, S., Sato, K., Katsuki, Y., et al. (2017) RFWD3-Mediated Ubiquitination Promotes Timely Removal of Both RPA and RAD51 from DNA Damage Sites to Facilitate Homologous Recombination. *Molecular Cell*. 66 (5). doi:10.1016/j.molcel.2017.04.022.

Ira, G. and Haber, J.E. (2002) Characterization of RAD51 -Independent Break-Induced Replication That Acts Preferentially with Short Homologous Sequences . *Molecular and Cellular Biology*, 22 (18). doi:10.1128/mcb.22.18.6384-6392.2002.

Irminger-Finger, I. and Jefford, C.E. (2006) Is there more to BARD1 than BRCA1? *Nature Reviews Cancer*. 6 (5). doi:10.1038/nrc1878.

Ishitobi, M., Miyoshi, Y., Hasegawa, S., et al. (2003) Mutational analysis of BARD1 in familial breast cancer patients in Japan. *Cancer Letters*, 200 (1). doi:10.1016/S0304-

3835(03)00387-2.

Izhar, L., Ziv, O., Cohen, I.S., et al. (2013) Genomic assay reveals tolerance of DNA damage by both translesion DNA synthesis and homology-dependent repair in mammalian cells. *Proceedings of the National Academy of Sciences of the United States of America*, 110 (16). doi:10.1073/pnas.1216894110.

Jachimowicz, R.D., Beleggia, F., Isensee, J., et al. (2019) UBQLN4 Represses Homologous Recombination and Is Overexpressed in Aggressive Tumors. *Cell*, 176 (3). doi:10.1016/j.cell.2018.11.024.

Jackson, D., Dhar, K., Wahl, J.K., et al. (2002) Analysis of the human replication protein A:Rad52 complex: Evidence for crosstalk between RPA32, RPA70, Rad52 and DNA. *Journal of Molecular Biology*, 321 (1). doi:10.1016/S0022-2836(02)00541-7.

Jackson, S.P. and Bartek, J. (2009) The DNA-damage response in human biology and disease. *Nature*. 461 (7267). doi:10.1038/nature08467.

Jalan, M., Olsen, K.S. and Powell, S.N. (2019) Emerging roles of RAD52 in genome maintenance. *Cancers*. 11 (7). doi:10.3390/cancers11071038.

Jang, S., Raja, S.J., Roginskaya, V., et al. (2023) UV-DDB stimulates the activity of SMUG1 during base excision repair of 5-hydroxymethyl-2'-deoxyuridine moieties. *Nucleic Acids Research*, 51 (10). doi:10.1093/nar/gkad206.

Jasin, M. and Rothstein, R. (2013) Repair of strand breaks by homologous recombination. *Cold Spring Harbor Perspectives in Biology*, 5 (11). doi:10.1101/cshperspect.a012740.

Jaspers, J.E., Kersbergen, A., Boon, U., et al. (2013) Loss of 53BP1 causes PARP inhibitor resistance in BRCA1-mutated mouse mammary tumors. *Cancer Discovery*, 3 (1). doi:10.1158/2159-8290.CD-12-0049.

Jeggo, P.A., Geuting, V. and Löbrich, M. (2011) The role of homologous recombination in radiation-induced double-strand break repair. *Radiotherapy and Oncology*. 101 (1). doi:10.1016/j.radonc.2011.06.019.

Jensen, R.B., Carreira, A. and Kowalczykowski, S.C. (2010) Purified human BRCA2 stimulates RAD51-mediated recombination. *Nature*, 467 (7316). doi:10.1038/nature09399.

Jin, Y., Xu, X.L., Yang, M.C.W., et al. (1997) Cell cycle-dependent colocalization of BARD1 and BRCA1 proteins in discrete nuclear domains. *Proceedings of the National*

Academy of Sciences of the United States of America, 94 (22). doi:10.1073/pnas.94.22.12075.

Jones, M.J.K., Colnaghi, L. and Huang, T.T. (2012) Dysregulation of DNA polymerase κ recruitment to replication forks results in genomic instability. *EMBO Journal*, 31 (4). doi:10.1038/emboj.2011.457.

Joseph, S.A., Taglialatela, A., Leuzzi, G., et al. (2020) Time for remodeling: SNF2-family DNA translocases in replication fork metabolism and human disease. *DNA Repair*, 95. doi:10.1016/j.dnarep.2020.102943.

Kabotyanski, E.B., Gomelsky, L., Han, J.O., et al. (1998) Double-strand break repair in Ku86- and XRCC4-deficient cells. *Nucleic Acids Research*, 26 (23). doi:10.1093/nar/26.23.5333.

Kadyrov, F.A., Genschel, J., Fang, Y., et al. (2009) A possible mechanism for exonuclease 1-independent eukaryotic mismatch repair. *Proceedings of the National Academy of Sciences of the United States of America*, 106 (21). doi:10.1073/pnas.0903654106.

Kaelin, W.G. (2005) The concept of synthetic lethality in the context of anticancer therapy. *Nature Reviews Cancer*. 5 (9). doi:10.1038/nrc1691.

Kais, Z., Rondinelli, B., Holmes, A., et al. (2016) FANCD2 Maintains Fork Stability in BRCA1/2-Deficient Tumors and Promotes Alternative End-Joining DNA Repair. *Cell Reports*. doi:10.1016/j.celrep.2016.05.031.

Kakarougkas, A., Ismail, A., Katsuki, Y., et al. (2013a) Co-operation of BRCA1 and POH1 relieves the barriers posed by 53BP1 and RAP80 to resection. *Nucleic Acids Research*. doi:10.1093/nar/gkt802.

Kakarougkas, A., Ismail, A., Klement, K., et al. (2013b) Opposing roles for 53BP1 during homologous recombination. *Nucleic Acids Research*, 41 (21). doi:10.1093/nar/gkt729.

Kalb, R., Mallery, D.L., Larkin, C., et al. (2014) BRCA1 is a histone-H2A-specific ubiquitin ligase. *Cell Reports*, 8 (4). doi:10.1016/j.celrep.2014.07.025.

Kanellis, P., Agyei, R. and Durocher, D. (2003) Elg1 forms an alternative PCNA-interacting RFC complex required to maintain genome stability. *Current Biology*, 13 (18). doi:10.1016/S0960-9822(03)00578-5.

Kang, M.S., Ryu, E., Lee, S.W., et al. (2019) Regulation of PCNA cycling on replicating

DNA by RFC and RFC-like complexes. *Nature Communications*, 10 (1). doi:10.1038/s41467-019-10376-w.

Kang, S., Warner, M.D. and Bell, S.P. (2014) Multiple Functions for Mcm2-7 ATPase Motifs during Replication Initiation. *Molecular Cell*, 55 (5). doi:10.1016/j.molcel.2014.06.033.

Kang, Z., Fu, P., Alcivar, A.L., et al. (2021) BRCA2 associates with MCM10 to suppress PRIMPOL-mediated repriming and single-stranded gap formation after DNA damage. *Nature Communications*, 12 (1). doi:10.1038/s41467-021-26227-6.

Kanno, S.I., Kuzuoka, H., Sasao, S., et al. (2007) A novel human AP endonuclease with conserved zinc-finger-like motifs involved in DNA strand break responses. *EMBO Journal*, 26 (8). doi:10.1038/sj.emboj.7601663.

Kannouche, P.L., Wing, J. and Lehmann, A.R. (2004) Interaction of human DNA polymerase η with monoubiquitinated PCNA: A possible mechanism for the polymerase switch in response to DNA damage. *Molecular Cell*, 14 (4). doi:10.1016/S1097-2765(04)00259-X.

Karras, G.I., Fumasoni, M., Sienski, G., et al. (2013) Noncanonical Role of the 9-1-1 Clamp in the Error-Free DNA Damage Tolerance Pathway. *Molecular Cell*, 49 (3). doi:10.1016/j.molcel.2012.11.016.

Keen, B.A., Jozwiakowski, S.K., Bailey, L.J., et al. (2014) Molecular dissection of the domain architecture and catalytic activities of human PrimPol. *Nucleic Acids Research*, 42 (9). doi:10.1093/nar/gku214.

Kelch, B.A. (2016) Review: The lord of the rings: Structure and mechanism of the sliding clamp loader. *Biopolymers*. 105 (8). doi:10.1002/bip.22827.

Kelso, A.A., Lopezcolorado, F.W., Bhargava, R., et al. (2019) Distinct roles of RAD52 and POLQ in chromosomal break repair and replication stress response. *PLoS Genetics*. doi:10.1371/journal.pgen.1008319.

Kent, T., Chandramouly, G., Mcdevitt, S.M., et al. (2015a) Mechanism of Microhomology-Mediated End-Joining Promoted by Human DNA Polymerase Theta HHS Public Access Author manuscript. *Nat Struct Mol Biol*, 22 (3).

Kent, T., Chandramouly, G., Mcdevitt, S.M., et al. (2015b) Mechanism of microhomology-mediated end-joining promoted by human DNA polymerase θ. *Nature Structural and Molecular Biology*. doi:10.1038/nsmb.2961.

Kent, T., Mateos-Gomez, P.A., Sfeir, A., et al. (2016) Polymerase θ is a robust terminal transferase that oscillates between three different mechanisms during end-joining. *eLife*, 5 (JUN2016). doi:10.7554/eLife.13740.

Kim, B.J., Chan, D.W., Jung, S.Y., et al. (2017a) The Histone Variant MacroH2A1 Is a BRCA1 Ubiquitin Ligase Substrate. *Cell Reports*, 19 (9). doi:10.1016/j.celrep.2017.05.027.

Kim, H., Chen, J. and Yu, X. (2007a) Ubiquitin-binding protein RAP80 mediates BRCA1-dependent DNA damage response. *Science*. doi:10.1126/science.1139621.

Kim, H., Huang, J. and Chen, J. (2007b) CCDC98 is a BRCA1-BRCT domain-binding protein involved in the DNA damage response. *Nature Structural and Molecular Biology*, 14 (8). doi:10.1038/nsmb1277.

Kim, H.S., Nickoloff, J.A., Wu, Y., et al. (2017b) Endonuclease EEPD1 Is a gatekeeper for repair of stressed replication forks. *Journal of Biological Chemistry*. doi:10.1074/jbc.M116.758235.

Kim, P.M., Allen, C., Wagener, B.M., et al. (2001) Overexpression of human RAD51 and RAD52 reduces double-strand break-induced homologous recombination in mammalian cells. *Nucleic Acids Research*, 29 (21). doi:10.1093/nar/29.21.4352.

Kim, S.S., Cao, L., Baek, H.J., et al. (2009) Impaired skin and mammary gland development and increased γ-irradiation-induced tumorigenesis in mice carrying a mutation of S1152-ATM phosphorylation site in Brca1. *Cancer Research*. doi:10.1158/0008-5472.CAN-09-2418.

Kim, S.S., Cao, L., Li, C., et al. (2004) Uterus Hyperplasia and Increased Carcinogen-Induced Tumorigenesis in Mice Carrying a Targeted Mutation of the Chk2 Phosphorylation Site in Brca1. *Molecular and Cellular Biology*. doi:10.1128/mcb.24.21.9498-9507.2004.

King, M.C., Marks, J.H. and Mandell, J.B. (2003) Breast and Ovarian Cancer Risks Due to Inherited Mutations in BRCA1 and BRCA2. *Science*, 302 (5645). doi:10.1126/science.1088759.

Kinner, A., Wu, W., Staudt, C., et al. (2008) Gamma-H2AX in recognition and signaling of DNA double-strand breaks in the context of chromatin. *Nucleic acids research*. 36 (17). doi:10.1093/nar/gkn550.

Kleczkowska, H.E., Marra, G., Lettieri, T., et al. (2001) hMSH3 and hMSH6 interact

with PCNA and colocalize with it to replication foci. *Genes and Development*, 15 (6). doi:10.1101/gad.191201.

Kobayashi, K., Guilliam, T.A., Tsuda, M., et al. (2016) Repriming by PrimPol is critical for DNA replication restart downstream of lesions and chain-terminating nucleosides. *Cell Cycle*, 15 (15). doi:10.1080/15384101.2016.1191711.

Koboldt, D.C., Fulton, R.S., McLellan, M.D., et al. (2012) Comprehensive molecular portraits of human breast tumours. *Nature*, 490 (7418). doi:10.1038/nature11412.

Kojic, M., Yang, H., Kostrub, C.F., et al. (2003) The BRCA2-interacting protein DSS1 is vital for DNA repair, recombination, and genome stability in Ustilago maydis. *Molecular Cell*, 12 (4). doi:10.1016/S1097-2765(03)00367-8.

Kolas, N.K., Chapman, J.R., Nakada, S., et al. (2007) Orchestration of the DNA-damage response by the RNF8 ubiquitin ligase. *Science*, 318 (5856). doi:10.1126/science.1150034.

Kolinjivadi, A.M., Sannino, V., de Antoni, A., et al. (2017a) Moonlighting at replication forks – a new life for homologous recombination proteins BRCA1, BRCA2 and RAD51. *FEBS Letters*. 591 (8). doi:10.1002/1873-3468.12556.

Kolinjivadi, A.M., Sannino, V., De Antoni, A., et al. (2017b) Smarcal1-Mediated Fork Reversal Triggers Mre11-Dependent Degradation of Nascent DNA in the Absence of Brca2 and Stable Rad51 Nucleofilaments. *Molecular Cell*, 67 (5). doi:10.1016/j.molcel.2017.07.001.

Kondrashova, O., Nguyen, M., Shield-Artin, K., et al. (2017) Secondary somatic mutations restoring RAD51C and RAD51D associated with acquired resistance to the PARP inhibitor rucaparib in high-grade ovarian carcinoma. *Cancer Discovery*, 7 (9). doi:10.1158/2159-8290.CD-17-0419.

Koole, W., Van Schendel, R., Karambelas, A.E., et al. (2014) A polymerase theta-dependent repair pathway suppresses extensive genomic instability at endogenous G4 DNA sites. *Nature Communications*, 5. doi:10.1038/ncomms4216.

Kottemann, M.C., Conti, B.A., Lach, F.P., et al. (2018) Removal of RTF2 from Stalled Replisomes Promotes Maintenance of Genome Integrity. *Molecular Cell*, 69 (1). doi:10.1016/j.molcel.2017.11.035.

Krais, J.J., Glass, D.J., Chudoba, I., et al. (2023) Genetic separation of Brca1 functions reveal mutation-dependent Polθ vulnerabilities. *Nature Communications*, 14 (1): 7714.

doi:10.1038/s41467-023-43446-1.

Krais, J.J. and Johnson, N. (2021) BRCA1 mutations in cancer: Coordinating deficiencies in homologous recombination with tumorigenesis. *Cancer Research*. 80 (21). doi:10.1158/0008-5472.CAN-20-1830.

Krais, J.J., Wang, Y., Bernhardy, A.J., et al. (2020) RNF168-mediated ubiquitin signaling inhibits the viability of BRCA1 null cancers. *Cancer Research*. doi:10.1158/0008-5472.can-19-3033.

Krais, J.J., Wang, Y., Patel, P., et al. (2021) RNF168-mediated localization of BARD1 recruits the BRCA1-PALB2 complex to DNA damage. *Nature Communications*, 12 (1). doi:10.1038/s41467-021-25346-4.

Krishna, T.S.R., Kong, X.P., Gary, S., et al. (1994) Crystal structure of the eukaryotic DNA polymerase processivity factor PCNA. *Cell*, 79 (7). doi:10.1016/0092-8674(94)90014-0.

Krokan, H.E. and Bjørås, M. (2013) Base excision repair. *Cold Spring Harbor Perspectives in Biology*, 5 (4). doi:10.1101/cshperspect.a012583.

Kubota, T., Katou, Y., Nakato, R., et al. (2015) Replication-Coupled PCNA Unloading by the Elg1 Complex Occurs Genome-wide and Requires Okazaki Fragment Ligation. *Cell Reports*, 12 (5). doi:10.1016/j.celrep.2015.06.066.

Kumagai, A., Shevchenko, A., Shevchenko, A., et al. (2010) Treslin Collaborates with TopBP1 in Triggering the Initiation of DNA Replication. *Cell*, 140 (3). doi:10.1016/j.cell.2009.12.049.

Kumamoto, S., Nishiyama, A., Chiba, Y., et al. (2021) HPF1-dependent PARP activation promotes LIG3-XRCC1-mediated backup pathway of Okazaki fragment ligation. *Nucleic Acids Research*, 49 (9). doi:10.1093/nar/gkab269.

Kumar, A., Purohit, S. and Sharma, N.K. (2016) Aberrant DNA Double-strand Break Repair Threads in Breast Carcinoma: Orchestrating Genomic Insult Survival. *Journal of Cancer Prevention*, 21 (4). doi:10.15430/jcp.2016.21.4.227.

Kumaraswamy, E. and Shiekhattar, R. (2007) Activation of BRCA1/BRCA2-Associated Helicase BACH1 Is Required for Timely Progression through S Phase. *Molecular and Cellular Biology*, 27 (19). doi:10.1128/mcb.00961-07.

Kunkel, T.A. (2009) “Evolving views of DNA replication (in)fidelity.” In *Cold Spring Harbor Symposia on Quantitative Biology*. 2009. doi:10.1101/sqb.2009.74.027.

Kunkel, T.A. and Burgers, P.M. (2008) Dividing the workload at a eukaryotic replication fork. *Trends in Cell Biology*. 18 (11). doi:10.1016/j.tcb.2008.08.005.

Kusumoto, R., Dawut, L., Marchetti, C., et al. (2008) Werner protein cooperates with the XRCC4-DNA ligase IV complex in end-processing. *Biochemistry*, 47 (28). doi:10.1021/bi702325t.

Kwon, Y., Rösner, H., Zhao, W., et al. (2023) DNA binding and RAD51 engagement by the BRCA2 C-terminus orchestrate DNA repair and replication fork preservation. *Nature Communications*, 14 (1). doi:10.1038/s41467-023-36211-x.

Kwon, Y. and Sung, P. (2017) Rad52, Maestro of Inverse Strand Exchange. *Molecular Cell*. 67 (1). doi:10.1016/j.molcel.2017.06.015.

Lamarche, B.J., Orazio, N.I. and Weitzman, M.D. (2010) The MRN complex in double-strand break repair and telomere maintenance. *FEBS Letters*. 584 (17). doi:10.1016/j.febslet.2010.07.029.

Lane, T.F., Deng, C., Elson, A., et al. (1995) Expression of Brca1 is associated with terminal differentiation of ectodermally and mesodermally derived tissues in mice. *Genes and Development*, 9 (21). doi:10.1101/gad.9.21.2712.

Laufer, M., Nandula, S. V., Modi, A.P., et al. (2007) Structural requirements for the BARD1 tumor suppressor in chromosomal stability and homology-directed DNA repair. *Journal of Biological Chemistry*, 282 (47). doi:10.1074/jbc.M705198200.

Lecona, E., Rodriguez-Acebes, S., Specks, J., et al. (2016) USP7 is a SUMO deubiquitinase essential for DNA replication. *Nature Structural and Molecular Biology*. doi:10.1038/nsmb.3185.

Lee, C., Banerjee, T., Gillespie, J., et al. (2015) Functional Analysis of BARD1 Missense Variants in Homology-Directed Repair of DNA Double Strand Breaks. *Human Mutation*, 36 (12). doi:10.1002/humu.22902.

Lee, J.H. and Paull, T.T. (2005) ATM activation by DNA double-strand breaks through the Mre11-Rad50-Nbs1 complex. *Science*, 308 (5721). doi:10.1126/science.1108297.

Lehmann, A.R., Niimi, A., Ogi, T., et al. (2007) Translesion synthesis: Y-family polymerases and the polymerase switch. *DNA Repair*, 6 (7). doi:10.1016/j.dnarep.2007.02.003.

Leimbacher, P.A., Jones, S.E., Shorrocks, A.M.K., et al. (2019) MDC1 Interacts with TOPBP1 to Maintain Chromosomal Stability during Mitosis. *Molecular Cell*, 74 (3).

doi:10.1016/j.molcel.2019.02.014.
Lemaçon, D., Jackson, J., Quinet, A., et al. (2017) MRE11 and EXO1 nucleases degrade reversed forks and elicit MUS81-dependent fork rescue in BRCA2-deficient cells. *Nature Communications*, 8 (1). doi:10.1038/s41467-017-01180-5.
Lemée, F., Bergoglio, V., Fernandez-Vidal, A., et al. (2010) DNA polymerase θ up-regulation is associated with poor survival in breast cancer, perturbs DNA replication, and promotes genetic instability. *Proceedings of the National Academy of Sciences of the United States of America*, 107 (30). doi:10.1073/pnas.0910759107.
Leppard, J.B., Dong, Z., Mackey, Z.B., et al. (2003) Physical and Functional Interaction between DNA Ligase IIIα and Poly(ADP-Ribose) Polymerase 1 in DNA Single-Strand Break Repair. *Molecular and Cellular Biology*, 23 (16). doi:10.1128/mcb.23.16.5919-5927.2003.
Ler, A.A.L. and Carty, M.P. (2022) DNA Damage Tolerance Pathways in Human Cells: A Potential Therapeutic Target. *Frontiers in Oncology*. 11. doi:10.3389/fonc.2021.822500.
Leriche, M., Bonnet, C., Jana, J., et al. (2023) 53BP1 interacts with the RNA primer from Okazaki fragments to support their processing during unperturbed DNA replication. *Cell Reports*, 42 (11): 113412. doi:10.1016/j.celrep.2023.113412.
Leung, C.C.Y. and Glover, J.N.M. (2011) BRCT domains: Easy as one, two, three. *Cell Cycle*. 10 (15). doi:10.4161/cc.10.15.16312.
Leung, W., Baxley, R.M., Moldovan, G.L., et al. (2019) Mechanisms of DNA damage tolerance: post-translational regulation of PCNA. *Genes*. 10 (1). doi:10.3390/genes10010010.
Levikova, M., Pinto, C. and Cejka, P. (2017) The motor activity of dna2 functions as an ssdna translocase to promote dna end resection. *Genes and Development*, 31 (5). doi:10.1101/gad.295196.116.
Li, H. (2018) Minimap2: Pairwise alignment for nucleotide sequences. *Bioinformatics*, 34 (18). doi:10.1093/bioinformatics/bty191.
Li, M., Cole, F., Patel, D.S., et al. (2016) 53 BP 1 ablation rescues genomic instability in mice expressing ‘ RING -less’ BRCA 1 . *EMBO reports*. doi:10.15252/embr.201642497.
Li, M. and Yu, X. (2013) Function of BRCA1 in the DNA Damage Response Is Mediated

by ADP-Ribosylation. *Cancer Cell*, 23 (5). doi:10.1016/j.ccr.2013.03.025.
Li, S., Silvestri, V., Leslie, G., et al. (2022) Cancer Risks Associated With BRCA1 and BRCA2 Pathogenic Variants. *Journal of Clinical Oncology*, 40 (14). doi:10.1200/JCO.21.02112.
Li, S., Topatana, W., Juengpanich, S., et al. (2020a) Development of synthetic lethality in cancer: molecular and cellular classification. *Signal Transduction and Targeted Therapy*. 5 (1). doi:10.1038/s41392-020-00358-6.
Li, Y., Roberts, N.D., Wala, J.A., et al. (2020b) Patterns of somatic structural variation in human cancer genomes. *Nature*, 578 (7793). doi:10.1038/s41586-019-1913-9.
Li, Y., Wu, J., Liu, J., et al. (2023) Abstract 502: ISM3091, a novel selective USP1 inhibitor as a targeted anticancer therapy. *Cancer Research*, 83 (7_Supplement). doi:10.1158/1538-7445.am2023-502.
Liang, L., Deng, L., Chen, Y., et al. (2005) Modulation of DNA end joining by nuclear proteins. *Journal of Biological Chemistry*, 280 (36). doi:10.1074/jbc.M503776200.
Liang, L., Deng, L., Nguyen, S.C., et al. (2008) Human DNA ligases I and III, but not ligase IV, are required for microhomology-mediated end joining of DNA double-strand breaks. *Nucleic Acids Research*, 36 (10). doi:10.1093/nar/gkn184.
Liang, Q., Dexheimer, T.S., Zhang, P., et al. (2014) A selective USP1-UAF1 inhibitor links deubiquitination to DNA damage responses. *Nature Chemical Biology*, 10 (4). doi:10.1038/nchembio.1455.
Liao, H., Ji, F., Helleday, T., et al. (2018) Mechanisms for stalled replication fork stabilization: new targets for synthetic lethality strategies in cancer treatments. *EMBO reports*, 19 (9). doi:10.15252/embr.201846263.
Lieber, M.R. (2008) The mechanism of human nonhomologous DNA End joining. *Journal of Biological Chemistry*. 283 (1). doi:10.1074/jbc.R700039200.
Lieber, M.R., Gu, J., Lu, H., et al. (2014) Nonhomologous DNA end joining (NHEJ) and chromosomal translocations in humans. *Subcellular Biochemistry*, 50. doi:10.1007/978-90-481-3471-7_14.
Lim, K.S., Li, H., Roberts, E.A., et al. (2018) USP1 Is Required for Replication Fork Protection in BRCA1-Deficient Tumors. *Molecular Cell*. doi:10.1016/j.molcel.2018.10.045.
Lim, P.X., Zaman, M. and Jasin, M. (2023) BRCA2 promotes genomic integrity and

therapy resistance primarily through its role in homology-directed repair. *bioRxiv : the preprint server for biology*. doi:10.1101/2023.04.11.536470.

Lin, J.R., Zeman, M.K., Chen, J.Y., et al. (2011) SHPRH and HLTF Act in a Damage-Specific Manner to Coordinate Different Forms of Postreplication Repair and Prevent Mutagenesis. *Molecular Cell*, 42 (2). doi:10.1016/j.molcel.2011.02.026.

Lindahl, T. (1993) Instability and decay of the primary structure of DNA. *Nature*. 362 (6422). doi:10.1038/362709a0.

Liptay, M., Barbosa, J.S. and Rottenberg, S. (2020) Replication Fork Remodeling and Therapy Escape in DNA Damage Response-Deficient Cancers. *Frontiers in Oncology*. 10. doi:10.3389/fonc.2020.00670.

Liu, C.Y., Flesken-Nikitin, A., Li, S., et al. (1996) Inactivation of the mouse Brca1 gene leads to failure in the morphogenesis of the egg cylinder in early postimplantation development. *Genes and Development*, 10 (14). doi:10.1101/gad.10.14.1835.

Liu, D., Ryu, K.S., Ko, J., et al. (2013a) Insights into the regulation of human Rev1 for translesion synthesis polymerases revealed by the structural studies on its polymerase-interacting domain. *Journal of Molecular Cell Biology*. 5 (3). doi:10.1093/jmcb/mjs061.

Liu, J., Doty, T., Gibson, B., et al. (2010) Human BRCA2 protein promotes RAD51 filament formation on RPA-covered single-stranded DNA. *Nature Structural and Molecular Biology*, 17 (10). doi:10.1038/nsmb.1904.

Liu, J. and Heyer, W.D. (2011) Who's who in human recombination: BRCA2 and RAD52. *Proceedings of the National Academy of Sciences of the United States of America*. 108 (2). doi:10.1073/pnas.1016614108.

Liu, J., Zhu, H., Zhong, N., et al. (2016) Gene silencing of USP1 by lentivirus effectively inhibits proliferation and invasion of human osteosarcoma cells. *International Journal of Oncology*, 49 (6). doi:10.3892/ijo.2016.3752.

Liu, Q., Guntuku, S., Cui, X.S., et al. (2000) Chk1 is an essential kinase that is regulated by Atr and required for the G2/M DNA damage checkpoint. *Genes and Development*, 14 (12). doi:10.1101/gad.14.12.1448.

Liu, S., Opiyo, S.O., Manthey, K., et al. (2012) Distinct roles for DNA-PK, ATM and ATR in RPA phosphorylation and checkpoint activation in response to replication stress. *Nucleic Acids Research*, 40 (21). doi:10.1093/nar/gks849.

Liu, S., Wang, J., Su, Y., et al. (2013b) Quantitative assessment of Tet-induced oxidation products of 5-methylcytosine in cellular and tissue DNA. *Nucleic Acids Research*, 41 (13). doi:10.1093/nar/gkt360.

Liu, W., Saito, Y., Jackson, J., et al. (2023) RAD51 bypasses the CMG helicase to promote replication fork reversal. *Science*, 380 (6643). doi:10.1126/science.add7328.

Liu, Y. and Lu, L.Y. (2020) BRCA1 and homologous recombination: Implications from mouse embryonic development. *Cell and Bioscience*. doi:10.1186/s13578-020-00412-4.

Liu, Z., Wu, J. and Yu, X. (2007) CCDC98 targets BRCA1 to DNA damage sites. *Nature Structural and Molecular Biology*, 14 (8). doi:10.1038/nsmb1279.

Livneh, Z., Ziv, O. and Shachar, S. (2010) Multiple two-polymerase mechanisms in mammalian translesion DNA synthesis. *Cell Cycle*. 9 (4). doi:10.4161/cc.9.4.10727.

Llorens-Agost, M., Ensminger, M., Le, H.P., et al. (2021) POLθ-mediated end joining is restricted by RAD52 and BRCA2 until the onset of mitosis. *Nature Cell Biology*, 23 (10). doi:10.1038/s41556-021-00764-0.

Lloyd, J.A., McGrew, D.A. and Knight, K.L. (2005) Identification of residues important for DNA binding in the full-length human Rad52 protein. *Journal of Molecular Biology*, 345 (2). doi:10.1016/j.jmb.2004.10.065.

Lo, C.S.Y., van Toorn, M., Gaggioli, V., et al. (2021) SMARCAD1-mediated active replication fork stability maintains genome integrity. *Science Advances*, 7 (19). doi:10.1126/sciadv.abe7804.

Loeb, L.A. and Preston, B.D. (1986) Mutagenesis by apurinic/apyrimidinic sites. *Annual review of genetics*. 20. doi:10.1146/annurev.ge.20.120186.001221.

Lok, B.H., Carley, A.C., Tchang, B., et al. (2013) RAD52 inactivation is synthetically lethal with deficiencies in BRCA1 and PALB2 in addition to BRCA2 through RAD51-mediated homologous recombination. *Oncogene*. doi:10.1038/onc.2012.391.

Lomonosov, M., Anand, S., Sangrithi, M., et al. (2003) Stabilization of stalled DNA replication forks by the BRCA2 breast cancer susceptibility protein. *Genes and Development*, 17 (24). doi:10.1101/gad.279003.

Longo, M.A., Roy, S., Chen, Y., et al. (2023) RAD51C-XRCC3 structure and cancer patient mutations define DNA replication roles. *Nature Communications*, 14 (1). doi:10.1038/s41467-023-40096-1.

Lord, C.J. and Ashworth, A. (2012) The DNA damage response and cancer therapy. *Nature*. 481 (7381). doi:10.1038/nature10760.

Lord, C.J. and Ashworth, A. (2013) Mechanisms of resistance to therapies targeting BRCA-mutant cancers. *Nature Medicine*. doi:10.1038/nm.3369.

Lord, C.J. and Ashworth, A. (2017) PARP inhibitors: Synthetic lethality in the clinic. *Science*. 355 (6330). doi:10.1126/science.aam7344.

Lu, C., Xie, M., Wendl, M.C., et al. (2015) Patterns and functional implications of rare germline variants across 12 cancer types. *Nature Communications*, 6. doi:10.1038/ncomms10086.

Lu, G., Duan, J., Shu, S., et al. (2016) Ligase I and ligase III mediate the DNA double-strand break ligation in alternative end-joining. *Proceedings of the National Academy of Sciences of the United States of America*, 113 (5). doi:10.1073/pnas.1521597113.

Lu, H., Pannicke, U., Schwarz, K., et al. (2007) Length-dependent binding of human XLF to DNA and stimulation of XRCC4·DNA ligase IV activity. *Journal of Biological Chemistry*, 282 (15). doi:10.1074/jbc.M609904200.

Ludwig, T., Chapman, D.L., Papaioannou, V.E., et al. (1997) Targeted mutations of breast cancer susceptibility gene homologs in mice: Lethal phenotypes of Brca1, Brca2, Brca1/Brca2, Brca1/p53, and Brca2/p53 nullizygous embryos. *Genes and Development*, 11 (10). doi:10.1101/gad.11.10.1226.

Ludwig, T., Fisher, P., Ganesan, S., et al. (2001) Tumorigenesis in mice carrying a truncating Brca1 mutation. *Genes and Development*, 15 (10). doi:10.1101/gad.879201.

Luijsterburg, M.S., Typas, D., Caron, M.C., et al. (2017) A PALB2-interacting domain in RNF168 couples homologous recombination to DNA break-induced chromatin ubiquitylation. *eLife*, 6. doi:10.7554/eLife.20922.

Ma, C.J., Gibb, B., Kwon, Y., et al. (2017a) Protein dynamics of human RPA and RAD51 on ssDNA during assembly and disassembly of the RAD51 filament. *Nucleic Acids Research*, 45 (2). doi:10.1093/nar/gkw1125.

Ma, C.J., Kwon, Y., Sung, P., et al. (2017b) Human RAD52 interactions with replication protein a and the RAD51 presynaptic complex. *Journal of Biological Chemistry*. doi:10.1074/jbc.M117.794545.

Ma, X., Tang, T.S. and Guo, C. (2020) Regulation of translesion DNA synthesis in

mammalian cells. *Environmental and Molecular Mutagenesis*. 61 (7). doi:10.1002/em.22359.

Ma, Y., Pannicke, U., Schwarz, K., et al. (2002) Hairpin opening and overhang processing by an Artemis/DNA-dependent protein kinase complex in nonhomologous end joining and V(D)J recombination. *Cell*, 108 (6). doi:10.1016/S0092-8674(02)00671-2.

Ma, Y.Y., Lin, H., Chang, F.M., et al. (2013) Identification of the deleted in split hand/split foot 1 protein as a novel biomarker for human cervical cancer. *Carcinogenesis*, 34 (1). doi:10.1093/carcin/bgs279.

Machwe, A., Xiao, L., Groden, J., et al. (2006) The Werner and Bloom syndrome proteins catalyze regression of a model replication fork. *Biochemistry*, 45 (47). doi:10.1021/bi0615487.

Mah, L.J., El-Osta, A. and Karagiannis, T.C. (2010) γh2AX: A sensitive molecular marker of DNA damage and repair. *Leukemia*. 24 (4). doi:10.1038/leu.2010.6.

Mailand, N., Bekker-Jensen, S., Faustrup, H., et al. (2007) RNF8 Ubiquitylates Histones at DNA Double-Strand Breaks and Promotes Assembly of Repair Proteins. *Cell*, 131 (5). doi:10.1016/j.cell.2007.09.040.

Maiorano, D., Rul, W. and Méchali, M. (2004) Cell cycle regulation of the licensing activity of Cdt1 in Xenopus laevis. *Experimental Cell Research*, 295 (1). doi:10.1016/j.yexcr.2003.11.018.

Mak, W.B. and Fix, D. (2008) DNA sequence context affects UV-induced mutagenesis in Escherichia coli. *Mutation Research - Fundamental and Molecular Mechanisms of Mutagenesis*, 638 (1–2). doi:10.1016/j.mrfmmm.2007.10.001.

Malacaria, E., Pugliese, G.M., Honda, M., et al. (2019) Rad52 prevents excessive replication fork reversal and protects from nascent strand degradation. *Nature Communications*. doi:10.1038/s41467-019-09196-9.

Malivert, L., Ropars, V., Nunez, M., et al. (2010) Delineation of the Xrcc4-interacting region in the globular head domain of cernunnos/XLF. *Journal of Biological Chemistry*, 285 (34). doi:10.1074/jbc.M110.138156.

Mallery, D.L., Vandenberg, C.J. and Hiom, K. (2002) Activation of the E3 ligase function of the BRCA1/BARD1 complex by polyubiquitin chains. *EMBO Journal*, 21 (24). doi:10.1093/emboj/cdf691.

Manke, I.A., Lowery, D.M., Nguyen, A., et al. (2003) BRCT Repeats As Phosphopeptide-Binding Modules Involved in Protein Targeting. *Science*, 302 (5645). doi:10.1126/science.1088877.

Mann, A., Ramirez-Otero, M.A., De Antoni, A., et al. (2022) POLθ prevents MRE11-NBS1-CtIP-dependent fork breakage in the absence of BRCA2/RAD51 by filling lagging-strand gaps. *Molecular Cell*, 82 (22). doi:10.1016/j.molcel.2022.09.013.

Mansour, W.Y., Rhein, T. and Dahm-Daphi, J. (2010) The alternative end-joining pathway for repair of DNA double-strand breaks requires PARP1 but is not dependent upon microhomologies. *Nucleic Acids Research*, 38 (18). doi:10.1093/nar/gkq387.

Mao, Z., Bozzella, M., Seluanov, A., et al. (2008) DNA repair by nonhomologous end joining and homologous recombination during cell cycle in human cells. *Cell Cycle*, 7 (18). doi:10.4161/cc.7.18.6679.

De Marco Zompit, M., Esteban, M.T., Mooser, C., et al. (2022) The CIP2A-TOPBP1 complex safeguards chromosomal stability during mitosis. *Nature Communications*, 13 (1). doi:10.1038/s41467-022-31865-5.

Marheineke, K. and Hyrien, O. (2004) Control of replication origin density and firing time in Xenopus egg extracts. Role of a caffeine-sensitive, ATR-dependent checkpoint. *Journal of Biological Chemistry*, 279 (27). doi:10.1074/jbc.M401574200.

Mari, P.O., Florea, B.I., Persengiev, S.P., et al. (2006) Dynamic assembly of end-joining complexes requires interaction between Ku70/80 and XRCC4. *Proceedings of the National Academy of Sciences of the United States of America*, 103 (49). doi:10.1073/pnas.0609061103.

Marteijn, J.A., Lans, H., Vermeulen, W., et al. (2014) Understanding nucleotide excision repair and its roles in cancer and ageing. *Nature Reviews Molecular Cell Biology*. 15 (7). doi:10.1038/nrm3822.

Martins, D.J., Tirman, S., Quinet, A., et al. (2022) Detection of Post-Replicative Gaps Accumulation and Repair in Human Cells using the DNA Fiber Assay. *Journal of Visualized Experiments*, 2022 (180). doi:10.3791/63448.

Masai, H., Matsumoto, S., You, Z., et al. (2010) Eukaryotic chromosome DNA replication: Where, when, and how? *Annual Review of Biochemistry*. 79. doi:10.1146/annurev.biochem.052308.103205.

Masaoka, A., Matsubara, M., Hasegawa, R., et al. (2003) Mammalian 5-formyluracil-

DNA glycosylase. 2. Role of SMUG1 uracil-DNA glycosylase in repair of 5-formyluracil and other oxidized and deaminated base lesions. *Biochemistry*, 42 (17). doi:10.1021/bi0273213.

Mason, J.M., Chan, Y.L., Weichselbaum, R.W., et al. (2019) Non-enzymatic roles of human RAD51 at stalled replication forks. *Nature Communications*, 10 (1). doi:10.1038/s41467-019-12297-0.

Masson, J.Y., Stasiak, A.Z., Stasiak, A., et al. (2001a) Complex formation by the human RAD51C and XRCC3 recombination repair proteins. *Proceedings of the National Academy of Sciences of the United States of America*, 98 (15). doi:10.1073/pnas.111005698.

Masson, J.Y., Tarsounas, M.C., Stasiak, A.Z., et al. (2001b) Identification and purification of two distinct complexes containing the five RAD51 paralogs. *Genes and Development*, 15 (24). doi:10.1101/gad.947001.

Masutani, C. (2000) Mechanisms of accurate translesion synthesis by human DNA polymerase eta. *The EMBO Journal*, 19 (12). doi:10.1093/emboj/19.12.3100.

Masutani, C., Araki, M., Yamada, A., et al. (1999) Xeroderma pigmentosum variant (XP-V) correcting protein from HeLa cells has a thymine dimer bypass DNA polymerase activity. *EMBO Journal*, 18 (12). doi:10.1093/emboj/18.12.3491.

Mateo, J., Lord, C.J., Serra, V., et al. (2019) A decade of clinical development of PARP inhibitors in perspective. *Annals of Oncology*, 30 (9). doi:10.1093/annonc/mdz192.

Mateos-Gomez, P.A., Gong, F., Nair, N., et al. (2015) Mammalian polymerase θ promotes alternative NHEJ and suppresses recombination. *Nature*. doi:10.1038/nature14157.

Mateos-Gomez, P.A., Kent, T., Deng, S.K., et al. (2017) The helicase domain of Polθ counteracts RPA to promote alt-NHEJ. *Nature Structural and Molecular Biology*, 24 (12). doi:10.1038/nsmb.3494.

Matsuoka, S., Huang, M. and Elledge, S.J. (1998) Linkage of ATM to cell cycle regulation by the Chk2 protein kinase. *Science*, 282 (5395). doi:10.1126/science.282.5395.1893.

Mattiroli, F. and Penengo, L. (2021) Histone Ubiquitination: An Integrative Signaling Platform in Genome Stability. *Trends in Genetics*. 37 (6). doi:10.1016/j.tig.2020.12.005.

Mattiroli, F., Vissers, J.H.A., Van Dijk, W.J., et al. (2012) RNF168 ubiquitinates K13-15 on H2A/H2AX to drive DNA damage signaling. *Cell*, 150 (6). doi:10.1016/j.cell.2012.08.005.

Maya-Mendoza, A., Moudry, P., Merchut-Maya, J.M., et al. (2018) High speed of fork progression induces DNA replication stress and genomic instability. *Nature*, 559 (7713). doi:10.1038/s41586-018-0261-5.

Mazina, O.M., Keskin, H., Hanamshet, K., et al. (2017) Rad52 Inverse Strand Exchange Drives RNA-Templated DNA Double-Strand Break Repair. *Molecular Cell*, 67 (1). doi:10.1016/j.molcel.2017.05.019.

McCarthy, A., Savage, K., Gabriel, A., et al. (2007) A mouse model of basal-like breast carcinoma with metaplastic elements. *Journal of Pathology*, 211 (4). doi:10.1002/path.2124.

McCarthy, E.E., Celebi, J.T., Baer, R., et al. (2003) Loss of Bard1, the Heterodimeric Partner of the Brca1 Tumor Suppressor, Results in Early Embryonic Lethality and Chromosomal Instability. *Molecular and Cellular Biology*, 23 (14). doi:10.1128/mcb.23.14.5056-5063.2003.

McCulloch, S.D. and Kunkel, T.A. (2008) The fidelity of DNA synthesis by eukaryotic replicative and translesion synthesis polymerases. *Cell Research*. 18 (1). doi:10.1038/cr.2008.4.

McIlwraith, M.J., Van Dyck, E., Masson, J.Y., et al. (2000) Reconstitution of the strand invasion step of double-strand break repair using human Rad51 Rad52 and RPA proteins. *Journal of Molecular Biology*, 304 (2). doi:10.1006/jmbi.2000.4180.

Mehta, K.P.M., Thada, V., Zhao, R., et al. (2022) CHK1 phosphorylates PRIMPOL to promote replication stress tolerance. *Science Advances*, 8 (13). doi:10.1126/sciadv.abm0314.

Mejlvang, J., Feng, Y., Alabert, C., et al. (2014) New histone supply regulates replication fork speed and PCNA unloading. *Journal of Cell Biology*, 204 (1). doi:10.1083/jcb.201305017.

Melander, F., Bekker-Jensen, S., Falck, J., et al. (2008) Phosphorylation of SDT repeats in the MDC1 N terminus triggers retention of NBS1 at the DNA damage-modified chromatin. *Journal of Cell Biology*, 181 (2). doi:10.1083/jcb.200708210.

Meng, D. and Li, D. (2022) Ubiquitin-specific protease 1 overexpression indicates poor

prognosis and promotes proliferation, migration, and invasion of gastric cancer cells. *Tissue and Cell*, 74. doi:10.1016/j.tice.2021.101723.

Ménissier De Murcia, J., Niedergang, C., Trucco, C., et al. (1997) Requirement of poly(ADP-ribose) polymerase in recovery from DNA damage in mice and in cells. *Proceedings of the National Academy of Sciences of the United States of America*, 94 (14). doi:10.1073/pnas.94.14.7303.

Meza, J.E., Brzovic, P.S., King, M.C., et al. (1999) Mapping the functional domains of BRCA1. Interaction of the ring finger domains of BRCA1 and BARD1. *Journal of Biological Chemistry*, 274 (9). doi:10.1074/jbc.274.9.5659.

Mgbemena, V.E., Signer, R.A.J., Wijayatunge, R., et al. (2017) Distinct Brca1 Mutations Differentially Reduce Hematopoietic Stem Cell Function. *Cell Reports*. doi:10.1016/j.celrep.2016.12.075.

Michelena, J., Lezaja, A., Teloni, F., et al. (2018) Analysis of PARP inhibitor toxicity by multidimensional fluorescence microscopy reveals mechanisms of sensitivity and resistance. *Nature Communications*, 9 (1). doi:10.1038/s41467-018-05031-9.

Mijic, S., Zellweger, R., Chappidi, N., et al. (2017) Replication fork reversal triggers fork degradation in BRCA2-defective cells. *Nature Communications*, 8 (1). doi:10.1038/s41467-017-01164-5.

Miki, Y., Swensen, J., Shattuck-Eidens, D., et al. (1994) A strong candidate for the breast and ovarian cancer susceptibility gene BRCA1. *Science*, 266 (5182). doi:10.1126/science.7545954.

Mishra, A.P., Hartford, S.A., Sahu, S., et al. (2022) BRCA2-DSS1 interaction is dispensable for RAD51 recruitment at replication-induced and meiotic DNA double strand breaks. *Nature Communications*, 13 (1). doi:10.1038/s41467-022-29409-y.

Modrzejewska, M., Gawronski, M., Skonieczna, M., et al. (2016) Vitamin C enhances substantially formation of 5-hydroxymethyluracil in cellular DNA. *Free Radical Biology and Medicine*, 101. doi:10.1016/j.freeradbiomed.2016.10.535.

Moon, A.F., Garcia-Diaz, M., Batra, V.K., et al. (2007) The X family portrait: Structural insights into biological functions of X family polymerases. *DNA Repair*. 6 (12). doi:10.1016/j.dnarep.2007.05.009.

Moore, C.E., Yalcindag, S.E., Czeladko, H., et al. (2023) RFWD3 promotes ZRANB3 recruitment to regulate the remodeling of stalled replication forks. *Journal of Cell*

Biology, 222 (5). doi:10.1083/jcb.202106022.

Morita, S., Kojima, T. and Kitamura, T. (2000) Plat-E: An efficient and stable system for transient packaging of retroviruses. *Gene Therapy*, 7 (12). doi:10.1038/sj.gt.3301206.

Morris, J.R., Keep, N.H. and Solomon, E. (2002) Identification of residues required for the interaction of BARD1 with BRCA1. *Journal of Biological Chemistry*, 277 (11). doi:10.1074/jbc.M109249200.

Morris, J.R., Pangon, L., Boutell, C., et al. (2006) Genetic analysis of BRCA1 ubiquitin ligase activity and its relationship to breast cancer susceptibility. *Human Molecular Genetics*, 15 (4). doi:10.1093/hmg/ddi476.

Mortensen, U.H., Bendixen, C., Sunjevaric, I., et al. (1996) DNA strand annealing is promoted by the yeast RaD52 protein. *Proceedings of the National Academy of Sciences of the United States of America*, 93 (20). doi:10.1073/pnas.93.20.10729.

Motegi, A., Liaw, H.J., Lee, K.Y., et al. (2008) Polyubiquitination of proliferating cell nuclear antigen by HLTF and SHPRH prevents genomic instability from stalled replication forks. *Proceedings of the National Academy of Sciences of the United States of America*, 105 (34). doi:10.1073/pnas.0805685105.

Motycka, T.A., Bessho, T., Post, S.M., et al. (2004) Physical and Functional Interaction between the XPF/ERCC1 Endonuclease and hRad52. *Journal of Biological Chemistry*, 279 (14). doi:10.1074/jbc.M313779200.

Mourón, S., Rodriguez-Acebes, S., Martínez-Jiménez, M.I., et al. (2013) Repriming of DNA synthesis at stalled replication forks by human PrimPol. *Nature Structural and Molecular Biology*, 20 (12). doi:10.1038/nsmb.2719.

Moynahan, M.E., Chiu, J.W., Koller, B.H., et al. (1999) Brca1 controls homology-directed DNA repair. *Molecular Cell*, 4 (4). doi:10.1016/S1097-2765(00)80202-6.

Moynahan, M.E. and Jasin, M. (2010) Mitotic homologous recombination maintains genomic stability and suppresses tumorigenesis. *Nature Reviews Molecular Cell Biology*. doi:10.1038/nrm2851.

Mungenast, F. and Thalhammer, T. (2014) Estrogen biosynthesis and action in ovarian cancer. *Frontiers in Endocrinology*, 5 (NOV). doi:10.3389/fendo.2014.00192.

Muñoz, M.C., Laulier, C., Gunn, A., et al. (2012) Ring finger nuclear factor RNF168 is important for defects in homologous recombination caused by loss of the breast cancer

susceptibility factor BRCA1. *Journal of Biological Chemistry*, 287 (48). doi:10.1074/jbc.M112.410951.

Murfuni, I., Basile, G., Subramanyam, S., et al. (2013) Survival of the Replication Checkpoint Deficient Cells Requires MUS81-RAD52 Function. *PLoS Genetics*, 9 (10). doi:10.1371/journal.pgen.1003910.

Murfuni, I., De Santis, A., Federico, M., et al. (2012) Perturbed replication induced genome wide or at common fragile sites is differently managed in the absence of WRN. *Carcinogenesis*, 33 (9). doi:10.1093/carcin/bgs206.

Murphy, A.K., Fitzgerald, M., Ro, T., et al. (2014) Phosphorylated RPA recruits PALB2 to stalled DNA replication forks to facilitate fork recovery. *Journal of Cell Biology*, 206 (4). doi:10.1083/jcb.201404111.

Mylavarapu, S., Das, A. and Roy, M. (2018) Role of BRCA mutations in the modulation of response to platinum therapy. *Frontiers in Oncology*. doi:10.3389/fonc.2018.00016.

Nacson, J., Krais, J.J., Bernhardy, A.J., et al. (2018) BRCA1 Mutation-Specific Responses to 53BP1 Loss-Induced Homologous Recombination and PARP Inhibitor Resistance. *Cell Reports*. doi:10.1016/j.celrep.2018.08.086.

Nagaraju, G., Hartlerode, A., Kwok, A., et al. (2009) XRCC2 and XRCC3 Regulate the Balance between Short- and Long-Tract Gene Conversions between Sister Chromatids. *Molecular and Cellular Biology*, 29 (15). doi:10.1128/mcb.01406-08.

Nagaraju, G., Odate, S., Xie, A., et al. (2006) Differential Regulation of Short- and Long-Tract Gene Conversion between Sister Chromatids by Rad51C. *Molecular and Cellular Biology*, 26 (21). doi:10.1128/mcb.01235-06.

Nakamura, K., Saredi, G., Becker, J.R., et al. (2019) H4K20me0 recognition by BRCA1–BARD1 directs homologous recombination to sister chromatids. *Nature Cell Biology*. 21 (3). doi:10.1038/s41556-019-0282-9.

Nayak, S., Calvo, J.A. and Cantor, S.B. (2021) Targeting translesion synthesis (TLS) to expose replication gaps, a unique cancer vulnerability. *Expert Opinion on Therapeutic Targets*. 25 (1). doi:10.1080/14728222.2021.1864321.

Nayak, S., Calvo, J.A., Cong, K., et al. (2020) Inhibition of the translesion synthesis polymerase REV1 exploits replication gaps as a cancer vulnerability. *Science Advances*, 6 (24). doi:10.1126/sciadv.aaz7808.

Nayak, S., Sullivan, P., Mishina, Y., et al. (2023) Abstract 2771: KSQ-4279 mediated

USP1 inhibition induces replication associated DNA gaps that contribute to cell death. *Cancer Research*, 83 (7_Supplement). doi:10.1158/1538-7445.am2023-2771.

Neelsen, K.J. and Lopes, M. (2015) Replication fork reversal in eukaryotes: From dead end to dynamic response. *Nature Reviews Molecular Cell Biology*. 16 (4). doi:10.1038/nrm3935.

Nelson, A.C. and Holt, J.T. (2010) Impact of RING and BRCT domain mutations on BRCA1 protein stability, localization and recruitment to DNA damage. *Radiation Research*, 174 (1). doi:10.1667/RR1290.1.

Newman, J.A., Cooper, C.D.O., Aitkenhead, H., et al. (2015) Structure of the Helicase Domain of DNA Polymerase Theta Reveals a Possible Role in the Microhomology-Mediated End-Joining Pathway. *Structure*, 23 (12). doi:10.1016/j.str.2015.10.014.

Nick McElhinny, S.A., Snowden, C.M., McCarville, J., et al. (2000) Ku Recruits the XRCC4-Ligase IV Complex to DNA Ends. *Molecular and Cellular Biology*, 20 (9). doi:10.1128/mcb.20.9.2996-3003.2000.

Nijman, S.M.B., Huang, T.T., Dirac, A.M.G., et al. (2005) The deubiquitinating enzyme USP1 regulates the fanconi anemia pathway. *Molecular Cell*. doi:10.1016/j.molcel.2005.01.008.

Nimonkar, A. V., Genschel, J., Kinoshita, E., et al. (2011) BLM-DNA2-RPA-MRN and EXO1-BLM-RPA-MRN constitute two DNA end resection machineries for human DNA break repair. *Genes and Development*, 25 (4). doi:10.1101/gad.2003811.

Nishikawa, H., Ooka, S., Sato, K., et al. (2004) Mass Spectrometric and Mutational Analyses Reveal Lys-6-linked Polyubiquitin Chains Catalyzed by BRCA1-BARD1 Ubiquitin Ligase. *Journal of Biological Chemistry*, 279 (6). doi:10.1074/jbc.M308540200.

Niu, Z., Li, X., Feng, S., et al. (2020) The deubiquitinating enzyme USP1 modulates ERα and modulates breast cancer progression. *Journal of Cancer*, 11 (23). doi:10.7150/JCA.50477.

Noordermeer, S.M., Adam, S., Setiaputra, D., et al. (2018) The shieldin complex mediates 53BP1-dependent DNA repair. *Nature*. doi:10.1038/s41586-018-0340-7.

Noordermeer, S.M. and van Attikum, H. (2019) PARP Inhibitor Resistance: A Tug-of-War in BRCA-Mutated Cells. *Trends in Cell Biology*. 29 (10). doi:10.1016/j.tcb.2019.07.008.

Nowicka, U., Zhang, D., Walker, O., et al. (2015) DNA-damage-inducible 1 protein (Ddi1) contains an uncharacteristic ubiquitin-like domain that binds ubiquitin. *Structure*, 23 (3). doi:10.1016/j.str.2015.01.010.

Nowsheen, S., Aziz, K., Aziz, A., et al. (2018) L3MBTL2 orchestrates ubiquitin signalling by dictating the sequential recruitment of RNF8 and RNF168 after DNA damage. *Nature Cell Biology*, 20 (4). doi:10.1038/s41556-018-0071-x.

Nusawardhana, A., Pale, L.M., Nicolae, C.M., et al. (2024) USP1-dependent nucleolytic expansion of PRIMPOL-generated nascent DNA strand discontinuities during replication stress. *Nucleic Acids Research*. doi:10.1093/nar/gkad1237.

O-Wang, J., Kawamura, K., Tada, Y., et al. (2001) DNA polymerase κ, implicated in spontaneous and DNA damage-induced mutagenesis, is overexpressed in lung cancer. *Cancer Research*, 61 (14).

O'Neil, N.J., Bailey, M.L. and Hieter, P. (2017) Synthetic lethality and cancer. *Nature Reviews Genetics*. 18 (10). doi:10.1038/nrg.2017.47.

Ogi, T. and Lehmann, A.R. (2006) The Y-family DNA polymerase κ (pol κ) functions in mammalian nucleotide-excision repair. *Nature Cell Biology*, 8 (6). doi:10.1038/ncb1417.

Ogi, T., Limsirichaikul, S., Overmeer, R.M., et al. (2010) Three DNA Polymerases, Recruited by Different Mechanisms, Carry Out NER Repair Synthesis in Human Cells. *Molecular Cell*, 37 (5). doi:10.1016/j.molcel.2010.02.009.

Okazaki, R., Okazaki, T., Sakabe, K., et al. (1968) Mechanism of DNA chain growth. I. Possible discontinuity and unusual secondary structure of newly synthesized chains. *Proceedings of the National Academy of Sciences of the United States of America*, 59 (2). doi:10.1073/pnas.59.2.598.

Oliver, A.W., Swift, S., Lord, C.J., et al. (2009) Structural basis for recruitment of BRCA2 by PALB2. *EMBO Reports*, 10 (9). doi:10.1038/embor.2009.126.

Orhan, E., Velazquez, C., Tabet, I., et al. (2021) Regulation of rad51 at the transcriptional and functional levels: What prospects for cancer therapy? *Cancers*. 13 (12). doi:10.3390/cancers13122930.

Orthwein, A., Noordermeer, S.M., Wilson, M.D., et al. (2015) A mechanism for the suppression of homologous recombination in G1 cells. *Nature*, 528 (7582). doi:10.1038/nature16142.

Ozdemir, A.Y., Rusanov, T., Kent, T., et al. (2018) Polymerase θ-helicase efficiently unwinds DNA and RNA-DNA hybrids. *Journal of Biological Chemistry*, 293 (14). doi:10.1074/jbc.RA117.000565.

Paes Dias, M., Tripathi, V., van der Heijden, I., et al. (2021) Loss of nuclear DNA ligase III reverts PARP inhibitor resistance in BRCA1/53BP1 double-deficient cells by exposing ssDNA gaps. *Molecular Cell*, 81 (22). doi:10.1016/j.molcel.2021.09.005.

Panagopoulos, A. and Altmeyer, M. (2021) When the RAP (80) fades out, you can hear BRCA1 RING. *EMBO reports*, 22 (12). doi:10.15252/embr.202154116.

Pang, D., Yoo, S., Dynan, W.S., et al. (1997) Ku proteins join DNA fragments as shown by atomic force microscopy. *Cancer Research*, 57 (8).

Panzarino, N.J., Krais, J.J., Cong, K., et al. (2021) Replication gaps underlie BRCA deficiency and therapy response. *Cancer Research*, 81 (5). doi:10.1158/0008-5472.CAN-20-1602.

Park, D., Bergin, S.M., Jones, D., et al. (2020) Ablation of the Brca1-Palb2 interaction phenocopies fanconi anemia in mice. *Cancer Research*, 80 (19). doi:10.1158/0008-5472.CAN-20-0486.

Park, J.Y., Singh, T.R., Nassar, N., et al. (2014) Breast cancer-associated missense mutants of the PALB2 WD40 domain, which directly binds RAD51C, RAD51 and BRCA2, disrupt DNA repair. *Oncogene*, 33 (40). doi:10.1038/onc.2013.421.

Park, M.S., Ludwig, D.L., Stigger, E., et al. (1996) Physical interaction between human RAD52 and RPA is required for homologous recombination in mammalian cells. *Journal of Biological Chemistry*, 271 (31). doi:10.1074/jbc.271.31.18996.

Park, S.H., Kang, N., Song, E., et al. (2019) ATAD5 promotes replication restart by regulating RAD51 and PCNA in response to replication stress. *Nature Communications*, 10 (1). doi:10.1038/s41467-019-13667-4.

Patel, P.S., Abraham, K.J., Guturi, K.K.N., et al. (2021a) RNF168 regulates R-loop resolution and genomic stability in BRCA1/2-deficient tumors. *Journal of Clinical Investigation*, 131 (3). doi:10.1172/JCI140105.

Patel, P.S., Algouneh, A. and Hakem, R. (2021b) Exploiting synthetic lethality to target BRCA1/2-deficient tumors: where we stand. *Oncogene*. 40 (17). doi:10.1038/s41388-021-01744-2.

Pathania, S., Nguyen, J., Hill, S.J., et al. (2011) BRCA1 is required for postreplication

repair after UV-induced DNA damage. *Molecular Cell*, 44 (2). doi:10.1016/j.molcel.2011.09.002.

Peng, C., Chen, Z., Wang, S., et al. (2016) The error-prone DNA polymerase k promotes temozolomide resistance in glioblastoma through Rad17-dependent activation of ATR-Chk1 signaling. *Cancer Research*, 76 (8). doi:10.1158/0008-5472.CAN-15-1884.

Pereira, P.D., Serra-Caetano, A., Cabrita, M., et al. (2017) Quantification of cell cycle kinetics by EdU (5-ethynyl-2'- deoxyuridine)-coupled-fluorescence-intensity analysis. *Oncotarget*, 8 (25). doi:10.18632/oncotarget.17121.

Petermann, E., Woodcock, M. and Helleday, T. (2010) Chk1 promotes replication fork progression by controlling replication initiation. *Proceedings of the National Academy of Sciences of the United States of America*, 107 (37). doi:10.1073/pnas.1005031107.

Petrucelli, N., Daly, M.B. and Feldman, G.L. (2017) BRCA1 and BRCA2 Hereditary Breast and Ovarian Cancer. *GeneReviews® [Internet]*, 00 (00).

Pettersen, H.S., Sundheim, O., Gilljam, K.M., et al. (2007) Uracil-DNA glycosylases SMUG1 and UNG2 coordinate the initial steps of base excision repair by distinct mechanisms. *Nucleic Acids Research*, 35 (12). doi:10.1093/nar/gkm372.

Pettijohn, D. and Hanawalt, P. (1964) Evidence for repair-replication of ultraviolet damaged DNA in bacteria. *Journal of Molecular Biology*, 9 (2). doi:10.1016/S0022-2836(64)80216-3.

Pettitt, S.J., Krastev, D.B., Brandsma, I., et al. (2018) Genome-wide and high-density CRISPR-Cas9 screens identify point mutations in PARP1 causing PARP inhibitor resistance. *Nature Communications*, 9 (1). doi:10.1038/s41467-018-03917-2.

Pfaffeneder, T., Spada, F., Wagner, M., et al. (2014) Tet oxidizes thymine to 5-hydroxymethyluracil in mouse embryonic stem cell DNA. *Nature Chemical Biology*, 10 (7). doi:10.1038/nchembio.1532.

Piberger, A.L., Bowry, A., Kelly, R.D.W., et al. (2020) PrimPol-dependent single-stranded gap formation mediates homologous recombination at bulky DNA adducts. *Nature Communications*, 11 (1). doi:10.1038/s41467-020-19570-7.

Pickart, C.M. and Eddins, M.J. (2004) Ubiquitin: Structures, functions, mechanisms. *Biochimica et Biophysica Acta - Molecular Cell Research*. 1695 (1–3). doi:10.1016/j.bbamcr.2004.09.019.

Pillaire, M.J., Betous, R., Conti, C., et al. (2007) Upregulation of error-prone DNA polymerases β and κ slows down fork progression without activating the replication checkpoint. *Cell Cycle*, 6 (4). doi:10.4161/cc.6.4.3857.

Pilzecker, B., Buoninfante, O.A., Pritchard, C., et al. (2016) PrimPol prevents APOBEC/AID family mediated DNA mutagenesis. *Nucleic Acids Research*, 44 (10). doi:10.1093/nar/gkw123.

Pinato, S., Scandiuzzi, C., Arnaudo, N., et al. (2009) RNF168, a new RING finger, MIU-containing protein that modifies chromatin by ubiquitination of histones H2A and H2AX. *BMC Molecular Biology*, 10. doi:10.1186/1471-2199-10-55.

Pino, M.S., Mino-Kenudson, M., Wildemore, B.M., et al. (2009) Deficient DNA mismatch repair is common in Lynch syndrome-associated colorectal adenomas. *Journal of Molecular Diagnostics*, 11 (3). doi:10.2353/jmoldx.2009.080142.

Pinto, C., Kasaciunaite, K., Seidel, R., et al. (2016) Human DNA2 possesses a cryptic DNA unwinding activity that functionally integrates with BLM or WRN helicases. *eLife*, 5 (September). doi:10.7554/eLife.18574.

Plank, J.L., Wu, J. and Hsieh, T.S. (2006) Topoisomerase IIIα and Bloom's helicase can resolve a mobile double Holliday junction substrate through convergent branch migration. *Proceedings of the National Academy of Sciences of the United States of America*, 103 (30). doi:10.1073/pnas.0604873103.

Pleschke, J.M., Kleczkowska, H.E., Strohm, M., et al. (2000) Poly(ADP-ribose) binds to specific domains in DNA damage checkpoint proteins. *Journal of Biological Chemistry*, 275 (52). doi:10.1074/jbc.M006520200.

Pommier, Y., Huang, S.H., Das, B.B., et al. (2012) 284 Differential Trapping of PARP1 and PARP2 by Clinical PARP Inhibitors. *European Journal of Cancer*, 48. doi:10.1016/s0959-8049(12)72082-8.

Povirk, L.F., Zhou, T., Zhou, R., et al. (2007) Processing of 3′-phosphoglycolate-terminated DNA double strand breaks by artemis nuclease. *Journal of Biological Chemistry*, 282 (6). doi:10.1074/jbc.M607745200.

Powers, K.T. and Washington, M.T. (2018) Eukaryotic translesion synthesis: Choosing the right tool for the job. *DNA Repair*. 71. doi:10.1016/j.dnarep.2018.08.016.

Pozhidaeva, A., Pustovalova, Y., D'Souza, S., et al. (2012) NMR structure and dynamics of the C-Terminal domain from human Rev1 and its complex with Rev1

interacting region of DNA polymerase η. *Biochemistry*, 51 (27). doi:10.1021/bi300566z.

Prakash, R., Zhang, Y., Feng, W., et al. (2015) Homologous recombination and human health: The roles of BRCA1, BRCA2, and associated proteins. *Cold Spring Harbor Perspectives in Biology*. doi:10.1101/cshperspect.a016600.

Prakash, S., Johnson, R.E. and Prakash, L. (2005) Eukaryotic translesion synthesis DNA polymerases: Specificity of structure and function. *Annual Review of Biochemistry*. 74. doi:10.1146/annurev.biochem.74.082803.133250.

Pruneda, J.N., Littlefield, P.J., Soss, S.E., et al. (2012) Structure of an E3:E2~Ub Complex Reveals an Allosteric Mechanism Shared among RING/U-box Ligases. *Molecular Cell*, 47 (6). doi:10.1016/j.molcel.2012.07.001.

Pulver, E.M., Mukherjee, C., van de Kamp, G., et al. (2021) A BRCA1 Coiled-Coil Domain Variant Disrupting PALB2 Interaction Promotes the Development of Mammary Tumors and Confers a Targetable Defect in Homologous Recombination Repair. *Cancer Research*, 81 (24). doi:10.1158/0008-5472.CAN-21-1415.

Pustovalova, Y., Maclejewski, M.W. and Korzhnev, D.M. (2013) NMR mapping of PCNA interaction with translesion synthesis DNA polymerase Rev1 mediated by Rev1-BRCT domain. *Journal of Molecular Biology*, 425 (17). doi:10.1016/j.jmb.2013.05.029.

Pustovalova, Y., Magalhães, M.T.Q., D'Souza, S., et al. (2016) Interaction between the Rev1 C-Terminal Domain and the PolD3 Subunit of Polζ Suggests a Mechanism of Polymerase Exchange upon Rev1/Polζ-Dependent Translesion Synthesis. *Biochemistry*, 55 (13). doi:10.1021/acs.biochem.5b01282.

Quinet, A., Carvajal-Maldonado, D., Lemacon, D., et al. (2017) "DNA Fiber Analysis: Mind the Gap!" In *Methods in Enzymology*. doi:10.1016/bs.mie.2017.03.019.

Quinet, A., Lerner, L.K., Martins, D.J., et al. (2018) Filling gaps in translesion DNA synthesis in human cells. *Mutation Research - Genetic Toxicology and Environmental Mutagenesis*. 836. doi:10.1016/j.mrgentox.2018.02.004.

Quinet, A., Tirman, S., Cybulla, E., et al. (2021) To skip or not to skip: choosing repriming to tolerate DNA damage. *Molecular Cell*. 81 (4). doi:10.1016/j.molcel.2021.01.012.

Quinet, A., Tirman, S., Jackson, J., et al. (2020) PRIMPOL-Mediated Adaptive Response Suppresses Replication Fork Reversal in BRCA-Deficient Cells. *Molecular*

Cell, 77 (3). doi:10.1016/j.molcel.2019.10.008.

Quinet, A. and Vindigni, A. (2018) Superfast DNA replication causes damage in cancer cells. *Nature*. 559 (7713). doi:10.1038/d41586-018-05501-6.

Rahman, N. and Stratton, M.R. (1998) The genetics of breast cancer susceptibility. *Annual Review of Genetics*. 32. doi:10.1146/annurev.genet.32.1.95.

Raja, S. and Van Houten, B. (2021) The multiple cellular roles of smug1 in genome maintenance and cancer. *International Journal of Molecular Sciences*. 22 (4). doi:10.3390/ijms22041981.

Rasmussen, R.E. and Painter, R.B. (1964) Evidence for repair of ultra-violet damaged deoxyribonucleic acid in cultured mammalian cells. *Nature*, 203 (4952). doi:10.1038/2031360a0.

Rass, U. (2013) Resolving branched DNA intermediates with structure-specific nucleases during replication in eukaryotes. *Chromosoma*. 122 (6). doi:10.1007/s00412-013-0431-z.

Ratajska, M., Antoszewska, E., Piskorz, A., et al. (2012) Cancer predisposing BARD1 mutations in breast-ovarian cancer families. *Breast Cancer Research and Treatment*, 131 (1). doi:10.1007/s10549-011-1403-8.

Ray Chaudhuri, A. and Nussenzweig, A. (2017) The multifaceted roles of PARP1 in DNA repair and chromatin remodelling. *Nature Reviews Molecular Cell Biology*. 18 (10). doi:10.1038/nrm.2017.53.

Reczek, C.R., Szabolcs, M., Stark, J.M., et al. (2013) The interaction between CtIP and BRCA1 is not essential for resection-mediated DNA repair or tumor suppression. *Journal of Cell Biology*, 201 (5). doi:10.1083/jcb.201302145.

Reddy, G., Golub, E.I. and Radding, C.M. (1997) Human Rad52 protein promotes single-strand DNA annealing followed by branch migration. *Mutation Research - Fundamental and Molecular Mechanisms of Mutagenesis*, 377 (1). doi:10.1016/S0027-5107(97)00057-2.

Reid, L.J., Shakya, R., Modi, A.P., et al. (2008) E3 ligase activity of BRCA1 is not essential for mammalian cell viability or homology-directed repair of double-strand DNA breaks. *Proceedings of the National Academy of Sciences of the United States of America*. doi:10.1073/pnas.0811203106.

Reinhardt, H.C., Aslanian, A.S., Lees, J.A., et al. (2007) p53-Deficient Cells Rely on

ATM- and ATR-Mediated Checkpoint Signaling through the p38MAPK/MK2 Pathway for Survival after DNA Damage. *Cancer Cell*, 11 (2). doi:10.1016/j.ccr.2006.11.024.

Remus, D., Beuron, F., Tolun, G., et al. (2009) Concerted Loading of Mcm2-7 Double Hexamers around DNA during DNA Replication Origin Licensing. *Cell*, 139 (4). doi:10.1016/j.cell.2009.10.015.

Rennie, M.L., Arkinson, C., Chaugule, V.K., et al. (2021) Structural basis of FANCD2 deubiquitination by USP1−UAF1. *Nature Structural and Molecular Biology*, 28 (4). doi:10.1038/s41594-021-00576-8.

Rennie, M.L., Arkinson, C., Chaugule, V.K., et al. (2022) Cryo-EM reveals a mechanism of USP1 inhibition through a cryptic binding site. *Science Advances*, 8 (39). doi:10.1126/sciadv.abq6353.

Rezano, A., Kuwahara, K., Yamamoto-Ibusuki, M., et al. (2013) Breast cancers with high DSS1 expression that potentially maintains BRCA2 stability have poor prognosis in the relapse-free survival. *BMC Cancer*, 13. doi:10.1186/1471-2407-13-562.

Rijkers, T., Van Den Ouweland, J., Morolli, B., et al. (1998) Targeted Inactivation of Mouse RAD52 Reduces Homologous Recombination but Not Resistance to Ionizing Radiation . *Molecular and Cellular Biology*, 18 (11). doi:10.1128/mcb.18.11.6423.

Robertson, A.B., Klungland, A., Rognes, T., et al. (2009) Base excision repair: The long and short of it. *Cellular and Molecular Life Sciences*. 66 (6). doi:10.1007/s00018-009-8736-z.

Robu, M., Shah, R.G. and Shah, G.M. (2020) Methods to Study Intracellular Movement and Localization of the Nucleotide Excision Repair Proteins at the DNA Lesions in Mammalian Cells. *Frontiers in Cell and Developmental Biology*, 8. doi:10.3389/fcell.2020.590242.

Rodriguez, M., Yu, X., Chen, J., et al. (2003) Phosphopeptide Binding Specificities of BRCA1 COOH-terminal (BRCT) Domains. *Journal of Biological Chemistry*, 278 (52). doi:10.1074/jbc.C300407200.

Rogakou, E.P., Boon, C., Redon, C., et al. (1999) Megabase chromatin domains involved in DNA double-strand breaks in vivo. *Journal of Cell Biology*, 146 (5). doi:10.1083/jcb.146.5.905.

Rogakou, E.P., Pilch, D.R., Orr, A.H., et al. (1998) DNA double-stranded breaks induce histone H2AX phosphorylation on serine 139. *Journal of Biological Chemistry*, 273

(10). doi:10.1074/jbc.273.10.5858.
Ronson, G.E., Starowicz, K., Anthony, E.J., et al. (2023) Mechanisms of synthetic lethality between BRCA1/2 and 53BP1 deficiencies and DNA polymerase theta targeting. *Nature Communications*, 14 (1): 7834. doi:10.1038/s41467-023-43677-2.
Rose, M., Burgess, J.T., O'Byrne, K., et al. (2020) PARP Inhibitors: Clinical Relevance, Mechanisms of Action and Tumor Resistance. *Frontiers in Cell and Developmental Biology*. 8. doi:10.3389/fcell.2020.564601.
Rosen, E.M. (2013) BRCA1 in the DNA damage response and at telomeres. *Frontiers in Genetics*. doi:10.3389/fgene.2013.00085.
Rothenberg, E., Grimme, J.M., Spies, M., et al. (2008) Human Rad52-mediated homology search and annealing occurs by continuous interactions between overlapping nucleoprotein complexes. *Proceedings of the National Academy of Sciences of the United States of America*, 105 (51). doi:10.1073/pnas.0810317106.
Rottenberg, S., Jaspers, J.E., Kersbergen, A., et al. (2008) High sensitivity of BRCA1-deficient mammary tumors to the PARP inhibitor AZD2281 alone and in combination with platinum drugs. *Proceedings of the National Academy of Sciences of the United States of America*, 105 (44). doi:10.1073/pnas.0806092105.
Rottenberg, S., Nygren, A.O.H., Pajic, M., et al. (2007) Selective induction of chemotherapy resistance of mammary tumors in a conditional mouse model for hereditary breast cancer. *Proceedings of the National Academy of Sciences of the United States of America*, 104 (29). doi:10.1073/pnas.0702955104.
Roy, R., Chun, J. and Powell, S.N. (2012) BRCA1 and BRCA2: Different roles in a common pathway of genome protection. *Nature Reviews Cancer*. doi:10.1038/nrc3181.
Ruffner, H., Joazeiro, C.A.P., Hemmati, D., et al. (2001) Cancer-predisposing mutations within the RING domain of BRCA1: Loss of ubiquitin protein ligase activity and protection from radiation hypersensitivity. *Proceedings of the National Academy of Sciences of the United States of America*, 98 (9). doi:10.1073/pnas.081068398.
Sabatinos, S.A. and Forsburg, S.L. (2015) Managing single-stranded DNA during replication stress in fission yeast. *Biomolecules*. 5 (3). doi:10.3390/biom5032123.
Saeki, H., Siaud, N., Christ, N., et al. (2006) Suppression of the DNA repair defects of BRCA2-deficient cells with heterologous protein fusions. *Proceedings of the National*

Academy of Sciences of the United States of America, 103 (23). doi:10.1073/pnas.0600298103.

Salas-Lloret, D., Agabitini, G. and González-Prieto, R. (2019) TULIP2: An Improved Method for the Identification of Ubiquitin E3-Specific Targets. *Frontiers in Chemistry*, 7. doi:10.3389/fchem.2019.00802.

Salas-Lloret, D., García-Rodríguez, N., Giebel, L., et al. (2023) BRCA1/BARD1 ubiquitinates PCNA in unperturbed conditions to promote replication fork stability and continuous DNA synthesis. *bioRxiv*, p. 2023.01.12.523782. doi:10.1101/2023.01.12.523782.

Saldanha, J., Rageul, J., Patel, J.A., et al. (2023) The Adaptive Mechanisms and Checkpoint Responses to a Stressed DNA Replication Fork. *International Journal of Molecular Sciences*. 24 (13). doi:10.3390/ijms241310488.

Sale, J.E., Lehmann, A.R. and Woodgate, R. (2012) Y-family DNA polymerases and their role in tolerance of cellular DNA damage. *Nature Reviews Molecular Cell Biology*. 13 (3). doi:10.1038/nrm3289.

Sallmyr, A. and Tomkinson, A.E. (2018) Repair of DNA double-strand breaks by mammalian alternative end-joining pathways. *Journal of Biological Chemistry*. 293 (27). doi:10.1074/jbc.TM117.000375.

Samavat, H. and Kurzer, M.S. (2015) Estrogen metabolism and breast cancer. *Cancer Letters*. 356 (2). doi:10.1016/j.canlet.2014.04.018.

Sancar, A. (2016) Mechanisms of DNA Repair by Photolyase and Excision Nuclease (Nobel Lecture). *Angewandte Chemie - International Edition*. 55 (30). doi:10.1002/anie.201601524.

Saredi, G., Huang, H., Hammond, C.M., et al. (2016) H4K20me0 marks post-replicative chromatin and recruits the TONSL-MMS22L DNA repair complex. *Nature*, 534 (7609). doi:10.1038/nature18312.

Sato, K., Shimomuki, M., Katsuki, Y., et al. (2016) FANCI-FANCD2 stabilizes the RAD51-DNA complex by binding RAD51 and protects the 5'-DNA end. *Nucleic Acids Research*, 44 (22). doi:10.1093/nar/gkw876.

Savage, K.I., Gorski, J.J., Barros, E.M., et al. (2014) Identification of a BRCA1-mRNA Splicing Complex Required for Efficient DNA Repair and Maintenance of Genomic Stability. *Molecular Cell*, 54 (3). doi:10.1016/j.molcel.2014.03.021.

Savage, K.I. and Harkin, D.P. (2015) BRCA1, a “complex” protein involved in the maintenance of genomic stability. *FEBS Journal*. 282 (4). doi:10.1111/febs.13150.

Saxena, S., Dixit, S., Somyajit, K., et al. (2019) ATR Signaling Uncouples the Role of RAD51 Paralogs in Homologous Recombination and Replication Stress Response. *Cell Reports*, 29 (3). doi:10.1016/j.celrep.2019.09.008.

Saxena, S., Somyajit, K. and Nagaraju, G. (2018) XRCC2 Regulates Replication Fork Progression during dNTP Alterations. *Cell Reports*, 25 (12). doi:10.1016/j.celrep.2018.11.085.

Schaub, J.M., Soniat, M.M. and Finkelstein, I.J. (2022) Polymerase theta-helicase promotes end joining by stripping single-stranded DNA-binding proteins and bridging DNA ends. *Nucleic Acids Research*, 50 (7). doi:10.1093/nar/gkac119.

Schimmel, J., van Schendel, R., den Dunnen, J.T., et al. (2019) Templated Insertions: A Smoking Gun for Polymerase Theta-Mediated End Joining. *Trends in Genetics*. doi:10.1016/j.tig.2019.06.001.

Schlacher, K., Christ, N., Siaud, N., et al. (2011) Double-strand break repair-independent role for BRCA2 in blocking stalled replication fork degradation by MRE11. *Cell*. doi:10.1016/j.cell.2011.03.041.

Schlacher, K., Wu, H. and Jasin, M. (2012) A Distinct Replication Fork Protection Pathway Connects Fanconi Anemia Tumor Suppressors to RAD51-BRCA1/2. *Cancer Cell*. doi:10.1016/j.ccr.2012.05.015.

Schmid, J.A., Berti, M., Walser, F., et al. (2018) Histone Ubiquitination by the DNA Damage Response Is Required for Efficient DNA Replication in Unperturbed S Phase. *Molecular Cell*, 71 (6). doi:10.1016/j.molcel.2018.07.011.

Schrempf, A., Bernardo, S., Arasa Verge, E.A., et al. (2022) POLθ processes ssDNA gaps and promotes replication fork progression in BRCA1-deficient cells. *Cell Reports*, 41 (9). doi:10.1016/j.celrep.2022.111716.

Schrempf, A., Slyskova, J. and Loizou, J.I. (2021) Targeting the DNA Repair Enzyme Polymerase θ in Cancer Therapy. *Trends in Cancer*. 7 (2). doi:10.1016/j.trecan.2020.09.007.

Schwartz, E.K. and Heyer, W.D. (2011) Processing of joint molecule intermediates by structure-selective endonucleases during homologous recombination in eukaryotes. *Chromosoma*. 120 (2). doi:10.1007/s00412-010-0304-7.

Scott, D.E., Francis-Newton, N.J., Marsh, M.E., et al. (2021) A small-molecule inhibitor of the BRCA2-RAD51 interaction modulates RAD51 assembly and potentiates DNA damage-induced cell death. *Cell Chemical Biology*, 28 (6). doi:10.1016/j.chembiol.2021.02.006.

Scully, R., Chen, J., Ochs, R.L., et al. (1997) Dynamic changes of BRCA1 subnuclear location and phosphorylation state are initiated by DNA damage. *Cell*, 90 (3). doi:10.1016/S0092-8674(00)80503-6.

Scully, R., Elango, R., Panday, A., et al. (2021) Recombination and restart at blocked replication forks. *Current Opinion in Genetics and Development*. 71. doi:10.1016/j.gde.2021.08.003.

Scully, R., Panday, A., Elango, R., et al. (2019) DNA double-strand break repair-pathway choice in somatic mammalian cells. *Nature Reviews Molecular Cell Biology*. 20 (11). doi:10.1038/s41580-019-0152-0.

Seki, M., Marini, F. and Wood, R.D. (2003) POLQ (Pol θ), a DNA polymerase and DNA-dependent ATPase in human cells. *Nucleic Acids Research*, 31 (21). doi:10.1093/nar/gkg814.

Seki, M., Masutani, C., Yang, L.W., et al. (2004) High-efficiency bypass of DNA damage by human DNA polymerase Q. *EMBO Journal*, 23 (22). doi:10.1038/sj.emboj.7600424.

Sergey, Koren, Brian, P., et al. (2017) Canu: scalable and accurate long-read assembly via adaptive k-mer weighting and repeat separation. *Genome research*.

Serra, H., Da Ines, O., Degroote, F., et al. (2013) Roles of XRCC2, RAD51B and RAD51D in RAD51-Independent SSA Recombination. *PLoS Genetics*, 9 (11). doi:10.1371/journal.pgen.1003971.

Setiaputra, D. and Durocher, D. (2019) Shieldin – the protector of DNA ends . *EMBO reports*, 20 (5). doi:10.15252/embr.201847560.

Sfeir, A. and Symington, L.S. (2015) Microhomology-Mediated End Joining: A Back-up Survival Mechanism or Dedicated Pathway? *Trends in Biochemical Sciences*. doi:10.1016/j.tibs.2015.08.006.

Shadfar, S., Parakh, S., Jamali, M.S., et al. (2023) Redox dysregulation as a driver for DNA damage and its relationship to neurodegenerative diseases. *Translational Neurodegeneration*. 12 (1). doi:10.1186/s40035-023-00350-4.

Shakya, R., Reid, L.J., Reczek, C.R., et al. (2011) BRCA1 tumor suppression depends on BRCT phosphoprotein binding, but not its E3 ligase activity. *Science*. doi:10.1126/science.1209909.

Shakya, R., Szabolcs, M., McCarthy, E., et al. (2008) The basal-like mammary carcinomas induced by Brca1 or Bard1 inactivation implicate the BRCA1/BARD1 heterodimer in tumor suppression. *Proceedings of the National Academy of Sciences of the United States of America*, 105 (19). doi:10.1073/pnas.0711032105.

Sharma, S., Javadekar, S.M., Pandey, M., et al. (2015) Homology and enzymatic requirements of microhomology-dependent alternative end joining. *Cell death & disease*, 6. doi:10.1038/cddis.2015.58.

Sharma, S., Stumpo, D.J., Balajee, A.S., et al. (2007) RECQL, a Member of the RecQ Family of DNA Helicases, Suppresses Chromosomal Instability. *Molecular and Cellular Biology*, 27 (5). doi:10.1128/mcb.01620-06.

Shechter, D., Costanzo, V. and Gautier, J. (2004) ATR and ATM regulate the timing of DNA replication origin firing. *Nature Cell Biology*, 6 (7). doi:10.1038/ncb1145.

Shen, S.X., Weaver, Z., Xu, X., et al. (1998) A targeted disruption of the murine Brca1 gene causes γ-irradiation hypersensitivity and genetic instability. *Oncogene*, 17 (24). doi:10.1038/sj.onc.1202243.

Shen, Z., Cloud, K.G., Chen, D.J., et al. (1996) Specific interactions between the human RAD51 and RAD52 proteins. *Journal of Biological Chemistry*, 271 (1). doi:10.1074/jbc.271.1.148.

Sherker, A., Chaudhary, N., Adam, S., et al. (2021) Two redundant ubiquitin-dependent pathways of BRCA1 localization to DNA damage sites. *EMBO reports*, 22 (12). doi:10.15252/embr.202153679.

Shibahara, K.I. and Stillman, B. (1999) Replication-dependent marking of DNA by PCNA facilitates CAF-1-coupled inheritance of chromatin. *Cell*, 96 (4). doi:10.1016/S0092-8674(00)80661-3.

Shibata, A., Conrad, S., Birraux, J., et al. (2011) Factors determining DNA double-strand break repair pathway choice in G2 phase. *EMBO Journal*, 30 (6). doi:10.1038/emboj.2011.27.

Shim, E.Y., Chung, W.H., Nicolette, M.L., et al. (2010) Saccharomyces cerevisiae Mre11/Rad50/Xrs2 and Ku proteins regulate association of Exo1 and Dna2 with DNA

breaks. *EMBO Journal*, 29 (19). doi:10.1038/emboj.2010.219.

Shinohara, A., Shinohara, M., Ohta, T., et al. (1998) Rad52 forms ring structures and co-operates with RPA in single-strand DNA annealing. *Genes to Cells*, 3 (3). doi:10.1046/j.1365-2443.1998.00176.x.

Shiozaki, E.N., Gu, L., Yan, N., et al. (2004) Structure of the BRCT repeats of BRCA1 bound to a BACH1 phosphopeptide: Implications for signaling. *Molecular Cell*, 14 (3). doi:10.1016/S1097-2765(04)00238-2.

Shreeram, S. and Blow, J.J. (2003) The role of the replication licensing system in cell proliferation and cancer. *Progress in cell cycle research*. 5.

Simoneau, A., Engel, J.L., Bandi, M., et al. (2023a) Ubiquitinated PCNA Drives USP1 Synthetic Lethality in Cancer. *Molecular Cancer Therapeutics*, 22 (2). doi:10.1158/1535-7163.MCT-22-0409.

Simoneau, A., Wu, H.-J., Bandi, M., et al. (2023b) Abstract 4968: Characterization of the clinical development candidate TNG348 as a potent and selective inhibitor of USP1 for the treatment of BRCA1/2mut cancers. *Cancer Research*, 83 (7_Supplement). doi:10.1158/1538-7445.am2023-4968.

Simoneau, A., Xiong, R. and Zou, L. (2021) The trans cell cycle effects of PARP inhibitors underlie their selectivity toward BRCA1/2-deficient cells. *Genes and Development*, 35 (17–18). doi:10.1101/GAD.348479.121.

Simpson, L.J., Ross, A.L., Szüts, D., et al. (2006) RAD18-independent ubiquitination of proliferating-cell nuclear antigen in the avian cell line DT40. *EMBO Reports*, 7 (9). doi:10.1038/sj.embor.7400777.

Sims, A.E., Spiteri, E., Sims, R.J., et al. (2007) FANCI is a second monoubiquitinated member of the Fanconi anemia pathway. *Nature Structural and Molecular Biology*, 14 (6). doi:10.1038/nsmb1252.

Simsek, D., Brunet, E., Wong, S.Y.W., et al. (2011) DNA ligase III promotes alternative nonhomologous end-joining during chromosomal translocation formation. *PLoS Genetics*, 7 (6). doi:10.1371/journal.pgen.1002080.

Sirbu, B.M., Couch, F.B. and Cortez, D. (2012) Monitoring the spatiotemporal dynamics of proteins at replication forks and in assembled chromatin using isolation of proteins on nascent DNA. *Nature Protocols*, 7 (3). doi:10.1038/nprot.2012.010.

Sirbu, B.M., McDonald, W.H., Dungrawala, H., et al. (2013) Identification of proteins at

active, stalled, and collapsed replication forks using isolation of proteins on nascent DNA (iPOND) coupled with mass spectrometry. *Journal of Biological Chemistry*, 288 (44). doi:10.1074/jbc.M113.511337.

Sobhian, B., Shao, G., Lilli, D.R., et al. (2007) RAP80 targets BRCA1 to specific ubiquitin structures at DNA damage sites. *Science*, 316 (5828). doi:10.1126/science.1139516.

Somyajit, K., Basavaraju, S., Scully, R., et al. (2013) ATM- and ATR-Mediated Phosphorylation of XRCC3 Regulates DNA Double-Strand Break-Induced Checkpoint Activation and Repair. *Molecular and Cellular Biology*, 33 (9). doi:10.1128/mcb.01521-12.

Somyajit, K., Saxena, S., Babu, S., et al. (2015) Mammalian RAD51 paralogs protect nascent DNA at stalled forks and mediate replication restart. *Nucleic Acids Research*, 43 (20). doi:10.1093/nar/gkv880.

Somyajit, K., Spies, J., Coscia, F., et al. (2021) Homology-directed repair protects the replicating genome from metabolic assaults. *Developmental Cell*, 56 (4). doi:10.1016/j.devcel.2021.01.011.

Sonego, M., Pellarin, I., Costa, A., et al. (2019) USP1 links platinum resistance to cancer cell dissemination by regulating Snail stability. *Science Advances*, 5 (5). doi:10.1126/sciadv.aav3235.

Song, B., Jiang, Y., Jiang, Y., et al. (2022) ML323 suppresses the progression of ovarian cancer via regulating USP1-mediated cell cycle. *Frontiers in Genetics*, 13. doi:10.3389/fgene.2022.917481.

Sotiriou, S.K., Kamileri, I., Lugli, N., et al. (2016) Mammalian RAD52 Functions in Break-Induced Replication Repair of Collapsed DNA Replication Forks. *Molecular Cell*. doi:10.1016/j.molcel.2016.10.038.

Spurdle, A.B., Healey, S., Devereau, A., et al. (2012) ENIGMA-evidence-based network for the interpretation of germline mutant alleles: An international initiative to evaluate risk and clinical significance associated with sequence variation in BRCA1 and BRCA2 genes. *Human Mutation*, 33 (1). doi:10.1002/humu.21628.

Spycher, C., Miller, E.S., Townsend, K., et al. (2008) Constitutive phosphorylation of MDC1 physically links the MRE11-RAD50-NBS1 complex to damaged chromatin. *Journal of Cell Biology*, 181 (2). doi:10.1083/jcb.200709008.

Stark, J.M., Pierce, A.J., Oh, J., et al. (2004) Genetic Steps of Mammalian Homologous Repair with Distinct Mutagenic Consequences. *Molecular and Cellular Biology*, 24 (21). doi:10.1128/mcb.24.21.9305-9316.2004.

Stasiak, A.Z., Larquet, E., Stasiak, A., et al. (2000) The human Rad52 protein exists as a heptameric ring. *Current Biology*, 10 (6). doi:10.1016/S0960-9822(00)00385-7.

Stefanovie, B., Hengel, S.R., MIcouskova, J., et al. (2020) DSS1 interacts with and stimulates RAD52 to promote the repair of DSBs. *Nucleic Acids Research*, 48 (2). doi:10.1093/nar/gkz1052.

Stelter, P. and Ulrich, H.D. (2003) Control of spontaneous and damage-induced mutagenesis by SUMO and ubiquitin conjugation. *Nature*. 425 (6954). doi:10.1038/nature01965.

Stewart, G.S., Panier, S., Townsend, K., et al. (2009) The RIDDLE Syndrome Protein Mediates a Ubiquitin-Dependent Signaling Cascade at Sites of DNA Damage. *Cell*, 136 (3). doi:10.1016/j.cell.2008.12.042.

Stewart, M.D., Duncan, E.D., Coronado, E., et al. (2017) Tuning BRCA1 and BARD1 activity to investigate RING ubiquitin ligase mechanisms. *Protein Science*, 26 (3). doi:10.1002/pro.3091.

Stewart, M.D., Zelin, E., Dhall, A., et al. (2018) BARD1 is necessary for ubiquitylation of nucleosomal histone H2A and for transcriptional regulation of estrogen metabolism genes. *Proceedings of the National Academy of Sciences of the United States of America*, 115 (6). doi:10.1073/pnas.1715467115.

Stiff, T., O'Driscoll, M., Rief, N., et al. (2004) ATM and DNA-PK Function Redundantly to Phosphorylate H2AX after Exposure to Ionizing Radiation. *Cancer Research*, 64 (7). doi:10.1158/0008-5472.CAN-03-3207.

Stucki, M., Clapperton, J.A., Mohammad, D., et al. (2005) MDC1 directly binds phosphorylated histone H2AX to regulate cellular responses to DNA double-strand breaks. *Cell*, 123 (7). doi:10.1016/j.cell.2005.09.038.

Sturzenegger, A., Burdova, K., Kanagaraj, R., et al. (2014) DNA2 cooperates with the WRN and BLM RecQ helicases to mediate long-range DNA end resection in human cells. *Journal of Biological Chemistry*, 289 (39). doi:10.1074/jbc.M114.578823.

Su, X., Bernal, J.A. and Venkitaraman, A.R. (2008) Cell-cycle coordination between DNA replication and recombination revealed by a vertebrate N-end rule degron-Rad51.

Nature Structural and Molecular Biology, 15 (10). doi:10.1038/nsmb.1490.

Sugawara, N., Goldfarb, T., Studamire, B., et al. (2004) Heteroduplex rejection during single-strand annealing requires Sgs1 helicase and mismatch repair proteins Msh2 and Msh6 but not Pms1. *Proceedings of the National Academy of Sciences of the United States of America*, 101 (25). doi:10.1073/pnas.0305749101.

Sugiyama, T., New, J.H. and Kowalczykowski, S.C. (1998) DNA annealing by Rad52 protein is stimulated by specific interaction with the complex of replication protein A and single-stranded DNA. *Proceedings of the National Academy of Sciences of the United States of America*, 95 (11). doi:10.1073/pnas.95.11.6049.

Sugiyama, T., Zaitseva, E.M. and Kowalczykowski, S.C. (1997) A single-stranded DNA-binding protein is needed for efficient presynaptic complex formation by the Saccharomyces cerevisiae Rad51 protein. *Journal of Biological Chemistry*, 272 (12). doi:10.1074/jbc.272.12.7940.

Sullivan-Reed, K., Bolton-Gillespie, E., Dasgupta, Y., et al. (2018) Simultaneous Targeting of PARP1 and RAD52 Triggers Dual Synthetic Lethality in BRCA-Deficient Tumor Cells. *Cell Reports*. doi:10.1016/j.celrep.2018.05.034.

Sung, P., Krejci, L., Van Komen, S., et al. (2003) Rad51 Recombinase and Recombination Mediators. *Journal of Biological Chemistry*. 278 (44). doi:10.1074/jbc.R300027200.

Suwaki, N., Klare, K. and Tarsounas, M. (2011) RAD51 paralogs: Roles in DNA damage signalling, recombinational repair and tumorigenesis. *Seminars in Cell and Developmental Biology*. 22 (8). doi:10.1016/j.semcdb.2011.07.019.

Suzuki, K., Kodama, S. and Watanabe, M. (1999) Recruitment of ATM protein to double strand DNA irradiated with ionizing radiation. *Journal of Biological Chemistry*, 274 (36). doi:10.1074/jbc.274.36.25571.

Sy, S.M.H., Huen, M.S.Y. and Chen, J. (2009a) PALB2 is an integral component of the BRCA complex required for homologous recombination repair. *Proceedings of the National Academy of Sciences of the United States of America*, 106 (17). doi:10.1073/pnas.0811159106.

Sy, S.M.H., Huen, M.S.Y., Zhu, Y., et al. (2009b) PALB2 regulates recombinational repair through chromatin association and oligomerization. *Journal of Biological Chemistry*, 284 (27). doi:10.1074/jbc.M109.016717.

Symington, L.S. (2002) Role of RAD52 Epistasis Group Genes in Homologous Recombination and Double-Strand Break Repair . *Microbiology and Molecular Biology Reviews*, 66 (4). doi:10.1128/mmbr.66.4.630-670.2002.

Symington, L.S. (2016) Mechanism and regulation of DNA end resection in eukaryotes. *Critical Reviews in Biochemistry and Molecular Biology*. 51 (3). doi:10.3109/10409238.2016.1172552.

Taglialatela, A., Alvarez, S., Leuzzi, G., et al. (2017) Restoration of Replication Fork Stability in BRCA1- and BRCA2-Deficient Cells by Inactivation of SNF2-Family Fork Remodelers. *Molecular Cell*. doi:10.1016/j.molcel.2017.09.036.

Taglialatela, A., Leuzzi, G., Sannino, V., et al. (2021) REV1-Polζ maintains the viability of homologous recombination-deficient cancer cells through mutagenic repair of PRIMPOL-dependent ssDNA gaps. *Molecular Cell*, 81 (19). doi:10.1016/j.molcel.2021.08.016.

Tanaka, S. and Diffley, J.F.X. (2002) Interdependent nuclear accumulation of budding yeast Cdt1 and Mcm2-7 during G1 phase. *Nature Cell Biology*, 4 (3). doi:10.1038/ncb757.

Tanaka, S., Umemori, T., Hirai, K., et al. (2007) CDK-dependent phosphorylation of Sld2 and Sld3 initiates DNA replication in budding yeast. *Nature*, 445 (7125). doi:10.1038/nature05465.

Tarsounas, M. and Sung, P. (2020) The antitumorigenic roles of BRCA1–BARD1 in DNA repair and replication. *Nature Reviews Molecular Cell Biology*. 21 (5). doi:10.1038/s41580-020-0218-z.

Taylor, M.R.G. and Yeeles, J.T.P. (2018) The Initial Response of a Eukaryotic Replisome to DNA Damage. *Molecular Cell*, 70 (6). doi:10.1016/j.molcel.2018.04.022.

Teebor, G.W., Frenkel, K. and Goldstein, M.S. (1984) Ionizing radiation and tritium transmutation both cause formation of 5-hydroxymethyl-2'-deoxyuridine in cellular DNA. *Proceedings of the National Academy of Sciences of the United States of America*, 81 (2 I). doi:10.1073/pnas.81.2.318.

Temprine, K., Campbell, N.R., Huang, R., et al. (2020) Regulation of the error-prone DNA polymerase Polκ by oncogenic signaling and its contribution to drug resistance. *Science Signaling*, 13 (629). doi:10.1126/scisignal.aau1453.

Thai, T.H., Du, F., Tsan, J.T., et al. (1998) Mutations in the BRCA1-associated RING

domain (BARD1) gene in primary breast, ovarian and uterine cancers. *Human Molecular Genetics*, 7 (2). doi:10.1093/hmg/7.2.195.

Thakar, T., Dhoonmoon, A., Straka, J., et al. (2022) Lagging strand gap suppression connects BRCA-mediated fork protection to nucleosome assembly through PCNA-dependent CAF-1 recycling. *Nature Communications*, 13 (1). doi:10.1038/s41467-022-33028-y.

Thakar, T., Leung, W., Nicolae, C.M., et al. (2020) Ubiquitinated-PCNA protects replication forks from DNA2-mediated degradation by regulating Okazaki fragment maturation and chromatin assembly. *Nature Communications*, 11 (1). doi:10.1038/s41467-020-16096-w.

Thangavel, S., Berti, M., Levikova, M., et al. (2015) DNA2 drives processing and restart of reversed replication forks in human cells. *Journal of Cell Biology*, 208 (5). doi:10.1083/jcb.201406100.

Thangavel, S., Mendoza-Maldonado, R., Tissino, E., et al. (2010) Human RECQ1 and RECQ4 Helicases Play Distinct Roles in DNA Replication Initiation. *Molecular and Cellular Biology*, 30 (6). doi:10.1128/mcb.01290-09.

Thompson, P.S. and Cortez, D. (2020) New insights into abasic site repair and tolerance. *DNA Repair*, 90. doi:10.1016/j.dnarep.2020.102866.

Thorslund, T., Ripplinger, A., Hoffmann, S., et al. (2015) Histone H1 couples initiation and amplification of ubiquitin signalling after DNA damage. *Nature*, 527 (7578). doi:10.1038/nature15401.

Thorslund, T. and West, S.C. (2007) BRCA2: A universal recombinase regulator. *Oncogene*. 26 (56). doi:10.1038/sj.onc.1210870.

Tian, F., Sharma, S., Zou, J., et al. (2013) BRCA1 promotes the ubiquitination of PCNA and recruitment of translesion polymerases in response to replication blockade. *Proceedings of the National Academy of Sciences of the United States of America*, 110 (33). doi:10.1073/pnas.1306534110.

Tirman, S., Cybulla, E., Quinet, A., et al. (2021a) PRIMPOL ready, set, reprime! *Critical Reviews in Biochemistry and Molecular Biology*. 56 (1). doi:10.1080/10409238.2020.1841089.

Tirman, S., Quinet, A., Wood, M., et al. (2021b) Temporally distinct post-replicative repair mechanisms fill PRIMPOL-dependent ssDNA gaps in human cells. *Molecular*

Cell, 81 (19). doi:10.1016/j.molcel.2021.09.013.
Toma, M., Sullivan-Reed, K., Śliwiński, T., et al. (2019) RAD52 as a potential target for synthetic lethality-based anticancer therapies. *Cancers*. doi:10.3390/cancers11101561.
Topatana, W., Juengpanich, S., Li, S., et al. (2020) Advances in synthetic lethality for cancer therapy: Cellular mechanism and clinical translation. *Journal of Hematology and Oncology*. 13 (1). doi:10.1186/s13045-020-00956-5.
Traven, A. and Heierhorst, J. (2005) SQ/TQ cluster domains: Concentrated ATM/ATR kinase phosphorylation site regions in DNA-damage-response proteins. *BioEssays*. 27 (4). doi:10.1002/bies.20204.
Trenner, A. and Sartori, A.A. (2019) Harnessing DNA Double-Strand Break Repair for Cancer Treatment. *Frontiers in Oncology*. doi:10.3389/fonc.2019.01388.
Truong, L.N., Li, Y., Shi, L.Z., et al. (2013) Microhomology-mediated End Joining and Homologous Recombination share the initial end resection step to repair DNA double-strand breaks in mammalian cells. *Proceedings of the National Academy of Sciences of the United States of America*, 110 (19). doi:10.1073/pnas.1213431110.
Tye, S., Ronson, G.E. and Morris, J.R. (2020) A fork in the road: Where homologous recombination and stalled replication fork protection part ways. *Seminars in Cell and Developmental Biology*. doi:10.1016/j.semcdb.2020.07.004.
Uckelmann, M., Densham, R.M., Baas, R., et al. (2018) USP48 restrains resection by site-specific cleavage of the BRCA1 ubiquitin mark from H2A. *Nature Communications*. doi:10.1038/s41467-017-02653-3.
Ünsal-Kaçmaz, K., Makhov, A.M., Griffith, J.D., et al. (2002) Preferential binding of ATR protein to UV-damaged DNA. *Proceedings of the National Academy of Sciences of the United States of America*, 99 (10). doi:10.1073/pnas.102167799.
Uziel, T., Lerenthal, Y., Moyal, L., et al. (2003) Requirement of the MRN complex for ATM activation by DNA damage. *EMBO Journal*, 22 (20). doi:10.1093/emboj/cdg541.
Vaisman, A. and Woodgate, R. (2017) Translesion DNA polymerases in eukaryotes: what makes them tick? *Critical Reviews in Biochemistry and Molecular Biology*. 52 (3). doi:10.1080/10409238.2017.1291576.
Vanoli, F., Fumasoni, M., Szakal, B., et al. (2010) Replication and recombination factors contributing to recombination-dependent bypass of DNA lesions by template

switch. *PLoS Genetics*, 6 (11). doi:10.1371/journal.pgen.1001205.

Vassin, V.M., Wold, M.S. and Borowiec, J.A. (2004) Replication Protein A (RPA) Phosphorylation Prevents RPA Association with Replication Centers. *Molecular and Cellular Biology*, 24 (5). doi:10.1128/mcb.24.5.1930-1943.2004.

Velimezi, G., Robinson-Garcia, L., Muñoz-Martínez, F., et al. (2018) Map of synthetic rescue interactions for the Fanconi anemia DNA repair pathway identifies USP48. *Nature Communications*, 9 (1). doi:10.1038/s41467-018-04649-z.

Verma, P., Dilley, R.L., Zhang, T., et al. (2019) RAD52 and SLX4 act nonepistatically to ensure telomere stability during alternative telomere lengthening. *Genes and Development*, 33 (3–4). doi:10.1101/gad.319723.118.

Vujanovic, M., Krietsch, J., Raso, M.C., et al. (2017) Replication Fork Slowing and Reversal upon DNA Damage Require PCNA Polyubiquitination and ZRANB3 DNA Translocase Activity. *Molecular Cell*, 67 (5). doi:10.1016/j.molcel.2017.08.010.

Wakefield, M.J., Nesic, K., Kondrashova, O., et al. (2019) Diverse mechanisms of PARP inhibitor resistance in ovarian cancer. *Biochimica et Biophysica Acta - Reviews on Cancer*. 1872 (2). doi:10.1016/j.bbcan.2019.08.002.

Wan, L., Lou, J., Xia, Y., et al. (2013) HPrimpol1/CCDC111 is a human DNA primase-polymerase required for the maintenance of genome integrity. *EMBO Reports*, 14 (12). doi:10.1038/embor.2013.159.

Wang, B., Hurov, K., Hofmann, K., et al. (2009) NBA1, a new player in the Brcal A complex, is required for DNA damage resistance and checkpoint control. *Genes and Development*, 23 (6). doi:10.1101/gad.1770309.

Wang, B., Matsuoka, S., Ballif, B.A., et al. (2007) Abraxas and RAP80 form a BRCA1 protein complex required for the DNA damage response. *Science*, 316 (5828). doi:10.1126/science.1139476.

Wang, J., Aroumougame, A., Lobrich, M., et al. (2014) PTIP associates with artemis to dictate DNA repair pathway choice. *Genes and Development*, 28 (24). doi:10.1101/gad.252478.114.

Wang, M., Li, W., Tomimatsu, N., et al. (2023) Crucial roles of the BRCA1-BARD1 E3 ubiquitin ligase activity in homology-directed DNA repair. *Molecular Cell*, 83 (20): 3679-3691.e8. doi:10.1016/j.molcel.2023.09.015.

Wang, M., Wu, W., Wu, W., et al. (2006) PARP-1 and Ku compete for repair of DNA

double strand breaks by distinct NHEJ pathways. *Nucleic Acids Research*, 34 (21). doi:10.1093/nar/gkl840.

Wang, Z., Song, Y., Li, S., et al. (2019) DNA polymerase (POLQ) is important for repair of DNA double-strand breaks caused by fork collapse. *Journal of Biological Chemistry*. doi:10.1074/jbc.RA118.005188.

Wang, Z.Q., Stingl, L., Morrison, C., et al. (1997) PARP is important for genomic stability but dispensable in apoptosis. *Genes and Development*, 11 (18). doi:10.1101/gad.11.18.2347.

Wassing, I.E. and Esashi, F. (2021) RAD51: Beyond the break. *Seminars in Cell and Developmental Biology*. 113. doi:10.1016/j.semcdb.2020.08.010.

Watanabe, K., Iwabuchi, K., Sun, J., et al. (2009) RAD18 promotes DNA double-strand break repair during G1 phase through chromatin retention of 53BP1. *Nucleic Acids Research*, 37 (7). doi:10.1093/nar/gkp082.

Waters, L.S., Minesinger, B.K., Wiltrout, M.E., et al. (2009) Eukaryotic Translesion Polymerases and Their Roles and Regulation in DNA Damage Tolerance. *Microbiology and Molecular Biology Reviews*, 73 (1). doi:10.1128/mmbr.00034-08.

West, K.L., Kelliher, J.L., Xu, Z., et al. (2019) LC8/DYNLL1 is a 53BP1 effector and regulates checkpoint activation. *Nucleic Acids Research*, 47 (12). doi:10.1093/NAR/GKZ263.

West, S.C. (2003) Molecular views of recombination proteins and their control. *Nature Reviews Molecular Cell Biology*. 4 (6). doi:10.1038/nrm1127.

Weterings, E. and Van Gent, D.C. (2004) The mechanism of non-homologous end-joining: A synopsis of synapsis. *DNA Repair*. 3 (11). doi:10.1016/j.dnarep.2004.06.003.

Wiese, C., Dray, E., Groesser, T., et al. (2007) Promotion of Homologous Recombination and Genomic Stability by RAD51AP1 via RAD51 Recombinase Enhancement. *Molecular Cell*, 28 (3). doi:10.1016/j.molcel.2007.08.027.

van Wietmarschen, N. and Nussenzweig, A. (2018) Mechanism for Synthetic Lethality in BRCA-Deficient Cancers: No Longer Lagging Behind. *Molecular Cell*. 71 (6). doi:10.1016/j.molcel.2018.08.045.

Williams, R.S., Green, R. and Glover, J.N.M. (2001) Crystal structure of the BRCT repeat region from the breast cancer-associated protein BRCA1. *Nature Structural*

Biology, 8 (10). doi:10.1038/nsb1001-838.

Witus, S.R., Burrell, A.L., Farrell, D.P., et al. (2021a) BRCA1/BARD1 site-specific ubiquitylation of nucleosomal H2A is directed by BARD1. *Nature Structural and Molecular Biology*, 28 (3). doi:10.1038/s41594-020-00556-4.

Witus, S.R., Stewart, M.D. and Klevit, R.E. (2021b) The BRCA1/BARD1 ubiquitin ligase and its substrates. *The Biochemical journal*. 478 (18). doi:10.1042/BCJ20200864.

Witus, S.R., Zhao, W., Brzovic, P.S., et al. (2022) BRCA1/BARD1 is a nucleosome reader and writer. *Trends in Biochemical Sciences*. 47 (7). doi:10.1016/j.tibs.2022.03.001.

Wojtaszek, J.L., Chatterjee, N., Najeeb, J., et al. (2019) A Small Molecule Targeting Mutagenic Translesion Synthesis Improves Chemotherapy. *Cell*, 178 (1). doi:10.1016/j.cell.2019.05.028.

Wold, M.S. (1997) Replication protein A: A heterotrimeric, single-stranded DNA-binding protein required for eukaryotic DNA metabolism. *Annual Review of Biochemistry*. 66. doi:10.1146/annurev.biochem.66.1.61.

Wong, A.K.C., Ormonde, P.A., Pero, R., et al. (1998) Characterization of a carboxy-terminal BRCA1 interacting protein. *Oncogene*, 17 (18). doi:10.1038/sj.onc.1202150.

Wong, A.K.C., Pero, R., Ormonde, P.A., et al. (1997) RAD51 interacts with the evolutionarily conserved BRC motifs in the human breast cancer susceptibility gene brca2. *Journal of Biological Chemistry*, 272 (51). doi:10.1074/jbc.272.51.31941.

Wood, R.D. and Doublié, S. (2016) DNA polymerase θ (POLQ), double-strand break repair, and cancer. *DNA Repair*. doi:10.1016/j.dnarep.2016.05.003.

Wright, W.D., Shah, S.S. and Heyer, W.D. (2018) Homologous recombination and the repair of DNA double-strand breaks. *Journal of Biological Chemistry*. 293 (27). doi:10.1074/jbc.TM118.000372.

Wu, L., Chan, K.L., Ralf, C., et al. (2005) The HRDC domain of BLM is required for the dissolution of double Holliday junctions. *EMBO Journal*, 24 (14). doi:10.1038/sj.emboj.7600740.

Wu, L. and Hickson, I.O. (2003) The Bloom's syndrome helicase suppresses crossing over during homologous recombination. *Nature*, 426 (6968). doi:10.1038/nature02253.

Wu, L., Luo, K., Lou, Z., et al. (2008a) MDC1 regulates intra-S-phase checkpoint by

targeting NBS1 to DNA double-strand breaks. *Proceedings of the National Academy of Sciences of the United States of America*, 105 (32). doi:10.1073/pnas.0802885105.

Wu, L.C., Wang, Z.W., Tsan, J.T., et al. (1996) Identification of a RING protein that can interact in vivo with the BRCA1 gene product. *Nature Genetics*, 14 (4). doi:10.1038/ng1296-430.

Wu, Q., Jubb, H. and Blundell, T.L. (2015a) Phosphopeptide interactions with BRCA1 BRCT domains: More than just a motif. *Progress in Biophysics and Molecular Biology*. 117 (2–3). doi:10.1016/j.pbiomolbio.2015.02.003.

Wu, W., Koike, A., Takeshita, T., et al. (2008b) The ubiquitin E3 ligase activity of BRCA1 and its biological functions. *Cell Division*. doi:10.1186/1747-1028-3-1.

Wu, Y., Lee, S.H., Williamson, E.A., et al. (2015b) EEPD1 Rescues Stressed Replication Forks and Maintains Genome Stability by Promoting End Resection and Homologous Recombination Repair. *PLoS Genetics*, 11 (12). doi:10.1371/journal.pgen.1005675.

Wyatt, D.W., Feng, W., Conlin, M.P., et al. (2016) Essential Roles for Polymerase θ-Mediated End Joining in the Repair of Chromosome Breaks. *Molecular Cell*, 63 (4). doi:10.1016/j.molcel.2016.06.020.

Xia, B., Sheng, Q., Nakanishi, K., et al. (2006) Control of BRCA2 Cellular and Clinical Functions by a Nuclear Partner, PALB2. *Molecular Cell*, 22 (6). doi:10.1016/j.molcel.2006.05.022.

Xia, Y., Pao, G.M., Chen, H.W., et al. (2003) Enhancement of BRCA1 E3 ubiquitin ligase activity through direct interaction with the BARD1 protein. *Journal of Biological Chemistry*, 278 (7). doi:10.1074/jbc.M204591200.

Xu, B., O'Donnell, A.H., Kim, S.T., et al. (2002) Phosphorylation of serine 1387 in Brca1 is specifically required for the Atm-mediated S-phase checkpoint after ionizing irradiation. *Cancer Research*, 62 (16).

Xu, X., Blackwell, S., Lin, A., et al. (2015) Error-free DNA-damage tolerance in Saccharomyces cerevisiae. *Mutation Research - Reviews in Mutation Research*. 764. doi:10.1016/j.mrrev.2015.02.001.

Xu, X., Li, S., Cui, X., et al. (2019) Inhibition of Ubiquitin Specific Protease 1 Sensitizes Colorectal Cancer Cells to DNA-Damaging Chemotherapeutics. *Frontiers in Oncology*, 9. doi:10.3389/fonc.2019.01406.

Xu, X., Wagner, K.U., Larson, D., et al. (1999) Conditional mutation of Brca 1 in mammary epithelial cells results in blunted ductal morphogenesis and tumour formation. *Nature Genetics*, 22 (1). doi:10.1038/8743.

Yamanaka, K., Chatterjee, N., Hemann, M.T., et al. (2017) Inhibition of mutagenic translesion synthesis: A possible strategy for improving chemotherapy? *PLoS Genetics*, 13 (8). doi:10.1371/journal.pgen.1006842.

Yan, J., Kim, Y.S., Yang, X.P., et al. (2007) The ubiquitin-interacting motif-containing protein RAP80 interacts with BRCA1 and functions in DNA damage repair response. *Cancer Research*, 67 (14). doi:10.1158/0008-5472.CAN-07-0924.

Yan, Z., Delannoy, M., Ling, C., et al. (2010) A Histone-Fold Complex and FANCM Form a Conserved DNA-Remodeling Complex to Maintain Genome Stability. *Molecular Cell*, 37 (6). doi:10.1016/j.molcel.2010.01.039.

Yang, D., Khan, S., Sun, Y., et al. (2011) Association of BRCA1 and BRCA2 mutations with survival, chemotherapy sensitivity, and gene mutator phenotype in patients with ovarian cancer. *JAMA - Journal of the American Medical Association*, 306 (14). doi:10.1001/jama.2011.1456.

Yang, H., Jeffrey, P.D., Miller, J., et al. (2002) BRCA2 function in DNA binding and recombination from a BRCA2-DSS1-ssDNA structure. *Science*, 297 (5588). doi:10.1126/science.297.5588.1837.

Yang, W. (2005) “Portraits of a Y-family DNA polymerase.” In *FEBS Letters*. 2005. doi:10.1016/j.febslet.2004.11.047.

Yang, W. and Gao, Y. (2018) Translesion and Repair DNA Polymerases: Diverse Structure and Mechanism. *Annual Review of Biochemistry*. 87. doi:10.1146/annurev-biochem-062917-012405.

Yano, K.I., Morotomi-Yano, K., Adachi, N., et al. (2009) Molecular mechanism of protein assembly on dna double-strand breaks in the non-homologous end-joining pathway. *Journal of Radiation Research*. 50 (2). doi:10.1269/jrr.08119.

Yarden, R.I., Pardo-Reoyo, S., Sgagias, M., et al. (2002) BRCA1 regulates the G2/M checkpoint by activating Chk1 kinase upon DNA damage. *Nature Genetics*, 30 (3). doi:10.1038/ng837.

Yazinski, S.A., Comaills, V., Buisson, R., et al. (2017) ATR inhibition disrupts rewired homologous recombination and fork protection pathways in PARP inhibitor-resistant

BRCA-deficient cancer cells. *Genes and Development*. doi:10.1101/gad.290957.116.

Yeeles, J.T.P., Deegan, T.D., Janska, A., et al. (2015) Regulated eukaryotic DNA replication origin firing with purified proteins. *Nature*, 519 (7544). doi:10.1038/nature14285.

Yi, M., Dong, B., Qin, S., et al. (2019) Advances and perspectives of PARP inhibitors. *Experimental Hematology and Oncology*. 8 (1). doi:10.1186/s40164-019-0154-9.

Ying, S., Hamdy, F.C. and Helleday, T. (2012) Mre11-dependent degradation of stalled DNA replication forks is prevented by BRCA2 and PARP1. *Cancer Research*, 72 (11). doi:10.1158/0008-5472.CAN-11-3417.

Yokoyama, H., Sarai, N., Kagawa, W., et al. (2004) Preferential binding to branched DNA strands and strand-annealing activity of the human Rad51B, Rad51C, Rad51D and Xrcc2 protein complex. *Nucleic Acids Research*, 32 (8). doi:10.1093/nar/gkh578.

Yoon, J.H., Choudhury, J.R., Park, J., et al. (2014) A role for DNA polymerase θ in promoting replication through oxidative DNA lesion, thymine glycol, in human cells. *Journal of Biological Chemistry*, 289 (19). doi:10.1074/jbc.M114.556977.

Yoon, J.H., Lee, C.S., O'Connor, T.R., et al. (2000) The DNA damage spectrum produced by simulated sunlight. *Journal of Molecular Biology*, 299 (3). doi:10.1006/jmbi.2000.3771.

Yoon, J.H., McArthur, M.J., Park, J., et al. (2019) Error-Prone Replication through UV Lesions by DNA Polymerase θ Protects against Skin Cancers. *Cell*, 176 (6). doi:10.1016/j.cell.2019.01.023.

You, Y.H., Lee, D.H., Yoon, J.H., et al. (2001) Cyclobutane Pyrimidine Dimers Are Responsible for the Vast Majority of Mutations Induced by UVB Irradiation in Mammalian Cells. *Journal of Biological Chemistry*, 276 (48). doi:10.1074/jbc.M107696200.

Yousefzadeh, M.J., Wyatt, D.W., Takata, K. ichi, et al. (2014) Mechanism of Suppression of Chromosomal Instability by DNA Polymerase POLQ. *PLoS Genetics*, 10 (10). doi:10.1371/journal.pgen.1004654.

Yu, X. and Baer, R. (2000) Nuclear localization and cell cycle-specific expression of CtIP, a protein that associates with the BRCA1 tumor suppressor. *Journal of Biological Chemistry*, 275 (24). doi:10.1074/jbc.M909494199.

Yu, X. and Chen, J. (2004) DNA Damage-Induced Cell Cycle Checkpoint Control

Requires CtIP, a Phosphorylation-Dependent Binding Partner of BRCA1 C-Terminal Domains. *Molecular and Cellular Biology*, 24 (21). doi:10.1128/mcb.24.21.9478-9486.2004.

Yu, X., Chini, C.C.S., He, M., et al. (2003) The BRCT Domain Is a Phospho-Protein Binding Domain. *Science*, 302 (5645). doi:10.1126/science.1088753.

Yu, X., Wu, L.C., Bowcock, A.M., et al. (1998) The C-terminal (BRCT) domains of BRCA1 interact in vive with CtIP, a protein implicated in the CtBP pathway of transcriptional repression. *Journal of Biological Chemistry*, 273 (39). doi:10.1074/jbc.273.39.25388.

Yuan, J., Luo, K., Deng, M., et al. (2014) HERC2-USP20 axis regulates DNA damage checkpoint through Claspin. *Nucleic Acids Research*, 42 (21). doi:10.1093/nar/gku1034.

Yueh, W.-T., Glass, D.J. and Johnson, N. (2024) Brca1 Mouse Models: Functional Insights and Therapeutic Opportunities. *Journal of Molecular Biology*, 436 (1): 168372. doi:10.1016/j.jmb.2023.168372.

Yun, M.H. and Hiom, K. (2009) CtIP-BRCA1 modulates the choice of DNA double-strand-break repair pathway throughout the cell cycle. *Nature*. doi:10.1038/nature07955.

Zadorozhny, K., Sannino, V., Beláň, O., et al. (2017) Fanconi-Anemia-Associated Mutations Destabilize RAD51 Filaments and Impair Replication Fork Protection. *Cell Reports*, 21 (2). doi:10.1016/j.celrep.2017.09.062.

Zatreanu, D., Robinson, H.M.R., Alkhatib, O., et al. (2021) Polθ inhibitors elicit BRCA-gene synthetic lethality and target PARP inhibitor resistance. *Nature Communications*, 12 (1). doi:10.1038/s41467-021-23463-8.

Zellweger, R., Dalcher, D., Mutreja, K., et al. (2015) Rad51-mediated replication fork reversal is a global response to genotoxic treatments in human cells. *Journal of Cell Biology*, 208 (5). doi:10.1083/jcb.201406099.

Zeman, M.K. and Cimprich, K.A. (2014) Causes and consequences of replication stress. *Nature Cell Biology*. 16 (1). doi:10.1038/ncb2897.

Zhang, F., Bick, G., Park, J.Y., et al. (2012) MDC1 and RNF8 function in a pathway that directs BRCA1-dependent localization of PALB2 required for homologous recombination. *Journal of Cell Science*, 125 (24). doi:10.1242/jcs.111872.

Zhang, F., Fan, Q., Ren, K., et al. (2009a) PALB2 functionally connects the breast cancer susceptibility proteins BRCA1 and BRCA2. *Molecular Cancer Research*, 7 (7). doi:10.1158/1541-7786.MCR-09-0123.

Zhang, F., Ma, J., Wu, J., et al. (2009b) PALB2 Links BRCA1 and BRCA2 in the DNA-Damage Response. *Current Biology*, 19 (6). doi:10.1016/j.cub.2009.02.018.

Zhang, H. and Lawrence, C.W. (2005) The error-free component of the RAD6/RAD18 DNA damage tolerance pathway of budding yeast employs sister-strand recombination. *Proceedings of the National Academy of Sciences of the United States of America*, 102 (44). doi:10.1073/pnas.0504586102.

Zhang, H., Liu, H., Chen, Y., et al. (2016) A cell cycle-dependent BRCA1-UHRF1 cascade regulates DNA double-strand break repair pathway choice. *Nature Communications*. doi:10.1038/ncomms10201.

Zhang, J.M., Yadav, T., Ouyang, J., et al. (2019) Alternative Lengthening of Telomeres through Two Distinct Break-Induced Replication Pathways. *Cell Reports*, 26 (4). doi:10.1016/j.celrep.2018.12.102.

Zhang, Y., Yuan, F., Wu, X., et al. (2000a) Error-free and error-prone lesion bypass by human DNA polymerase κ in vitro. *Nucleic Acids Research*, 28 (21). doi:10.1093/nar/28.21.4138.

Zhang, Z., Shibahara, K.I. and Stillman, B. (2000b) PCNA connects DNA replication to epigenetic inheritance in yeast. *Nature*, 408 (6809). doi:10.1038/35041601.

Zhao, F., Kim, W., Kloeber, J.A., et al. (2020) DNA end resection and its role in DNA replication and DSB repair choice in mammalian cells. *Experimental and Molecular Medicine*. 52 (10). doi:10.1038/s12276-020-00519-1.

Zhao, W., Steinfeld, J.B., Liang, F., et al. (2017a) BRCA1-BARD1 promotes RAD51-mediated homologous DNA pairing. *Nature*, 550 (7676). doi:10.1038/nature24060.

Zhao, W., Steinfeld, J.B., Liang, F., et al. (2017b) Promotion of RAD51-mediated homologous DNA pairing by BRCA1-BARD1. *Nature.*, 47 (3).

Zhao, W., Vaithiyalingam, S., San Filippo, J., et al. (2015) Promotion of BRCA2-Dependent Homologous Recombination by DSS1 via RPA Targeting and DNA Mimicry. *Molecular Cell*, 59 (2). doi:10.1016/j.molcel.2015.05.032.

Zhao, W., Wiese, C., Kwon, Y., et al. (2019) The BRCA tumor suppressor network in chromosome damage repair by homologous recombination. *Annual Review of*

Biochemistry. 88. doi:10.1146/annurev-biochem-013118-111058.

Zhao, Y., Biertümpfel, C., Gregory, M.T., et al. (2012) Structural basis of human DNA polymerase η-mediated chemoresistance to cisplatin. *Proceedings of the National Academy of Sciences of the United States of America*, 109 (19). doi:10.1073/pnas.1202681109.

Zhou, C., Pourmal, S. and Pavletich, N.P. (2015) Dna2 nuclease-helicase structure, mechanism and regulation by Rpa. *eLife*, 4 (OCTOBER2015). doi:10.7554/eLife.09832.

Zhou, J., Gelot, C., Pantelidou, C., et al. (2021) A first-in-class polymerase theta inhibitor selectively targets homologous-recombination-deficient tumors. *Nature Cancer*, 2 (6). doi:10.1038/s43018-021-00203-x.

Zhou, W., Chen, Y.W., Liu, X., et al. (2013) Expression of DNA translesion synthesis polymerase η in head and neck squamous cell cancer predicts resistance to gemcitabine and cisplatin-based chemotherapy. *PLoS ONE*, 8 (12). doi:10.1371/journal.pone.0083978.

Zhu, Q., Pao, G.M., Huynh, A.M., et al. (2011) BRCA1 tumour suppression occurs via heterochromatin-mediated silencing. *Nature*, 477 (7363). doi:10.1038/nature10371.

Zimmermann, M. and De Lange, T. (2014) 53BP1: Pro choice in DNA repair. *Trends in Cell Biology*. 24 (2). doi:10.1016/j.tcb.2013.09.003.

Zimmermann, M., Lottersberger, F., Buonomo, S.B., et al. (2013) 53BP1 regulates DSB repair using Rif1 to control 5′ end resection. *Science*. doi:10.1126/science.1231573.

Zong, D., Adam, S., Wang, Y., et al. (2019) BRCA1 Haploinsufficiency Is Masked by RNF168-Mediated Chromatin Ubiquitylation. *Molecular Cell*. doi:10.1016/j.molcel.2018.12.010.

Zou, Y., Liu, Y., Wu, X., et al. (2006) Functions of human replication protein A (RPA): From DNA replication to DNA damage and stress responses. *Journal of Cellular Physiology*, 208 (2). doi:10.1002/jcp.20622.